VAN VETERINARY JOURNAL

Year: 2026 / Volume: 37 / Issue: 1

ISSN : 2149-3359
e-ISSN : 2149-8644

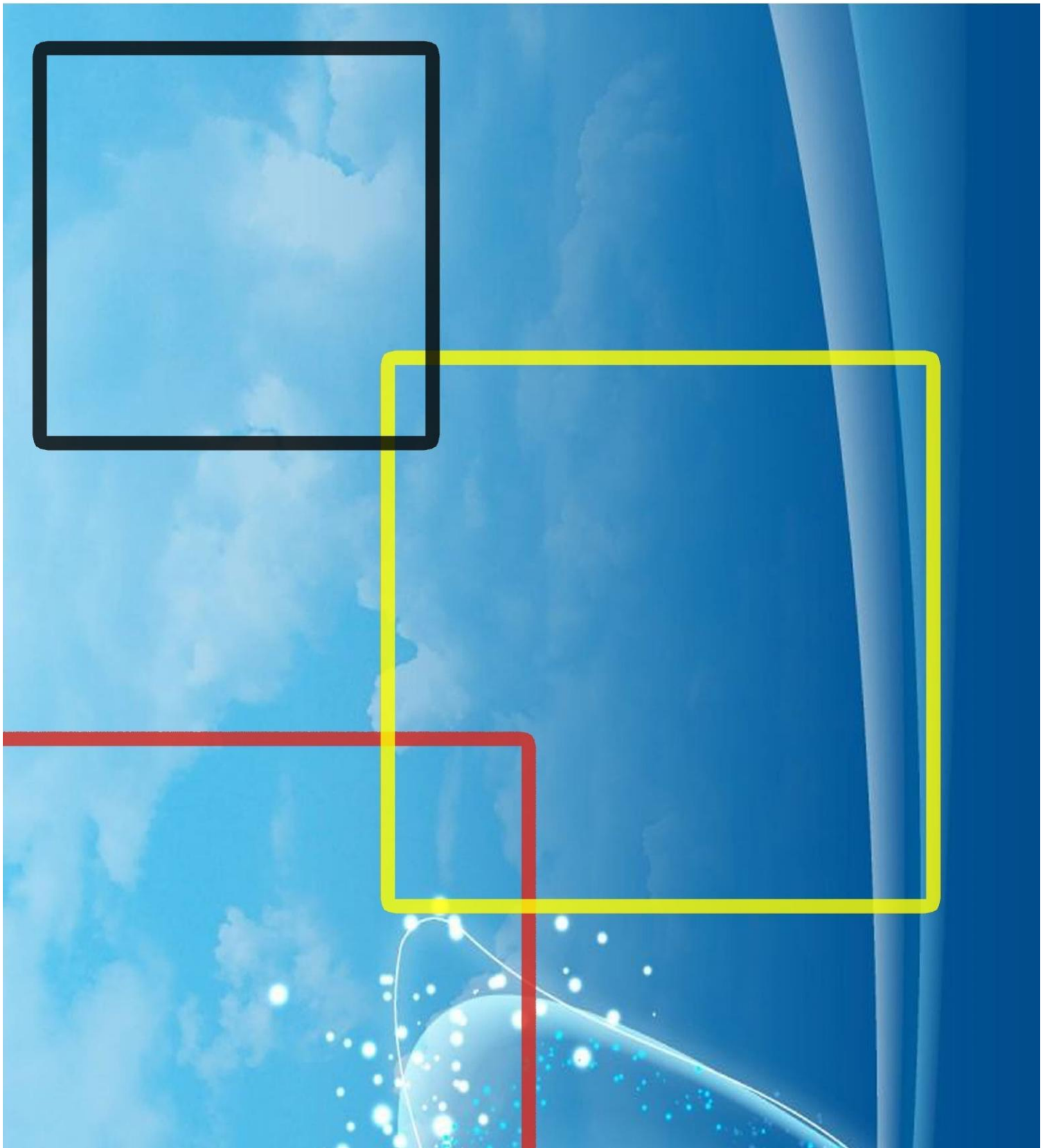

March - 2026

VAN VETERINARY JOURNAL

This journal previously published as: **Yüzüncü Yıl Üniversitesi Veteriner Fakültesi Dergisi**

ISSN: 2149-3359 E-ISSN: 2149-8644

This journal is published three times a year. Journal Tittle Abbreviation: Van Vet J
All articles in this journal are available free of charge from https://dergipark.org.tr/tr/pub/vanvetj

Year	Volume	Issue
2026	**37**	**1**

This journal indexed / abstracted in Asos Index, CAB Abstracts, EBSCOhost, Google Scholar, Index Copernicus, Sobiad, TR Dizin and Türkiye Atıf Dizini

March - 2026

VAN VETERINARY JOURNAL

This journal previously published as: **Yüzüncü Yıl Üniversitesi Veteriner Fakültesi Dergisi**

ISSN: 2149-3359 E-ISSN: 2149-8644

Reviewers of This Issue

Prof. Dr. Aliye GÜLMEZ SAĞLAM (Kafkas University)
Prof. Dr. Betül APAYDIN YILDIRIM (Atatürk University)
Prof. Dr. Burcu ONUK (Ondokuz Mayis University)
Prof. Dr. Cenk YARDIMCI (Ondokuz Mayis University)
Prof. Dr. Cihan GÜNAY (Firat University)
Prof. Dr. Cüneyt ÇAĞLAYAN (Bilecik Seyh Edebali University)
Prof. Dr. Duygu BAKİ ACAR (Afyon Kocatepe University)
Prof. Dr. Ergün Ömer GÖKSOY (Aydin Adnan Menderes University)
Prof. Dr. Hüseyin ERDEM (Selcuk University)
Prof. Dr. Kadir BOZUKLUHAN (Kafkas University)
Prof. Dr. Loğman ASLAN (Van Yuzuncu Yil University)
Prof. Dr. Mehmet Borga TIRPAN (Ankara University)
Prof. Dr. Mehmet Erdem AKBALIK (Dicle University)
Prof. Dr. Mehmet HALIGÜR (Cukurova University)
Prof. Dr. Mukadderat GÖKMEN (Aksaray University)
Prof. Dr. Özgür KAYNAR (Kastamonu University)
Prof. Dr. Recep KARA (Afyon Kocatepe University)
Prof. Dr. Semra KAYA (Kafkas University)
Prof. Dr. Tahir KAHRAMAN (Karabuk University)
Assoc. Prof. Dr. Alper KOÇYIĞIT (Ondokuz Mayis University)
Assoc. Prof. Dr. Beste DEMİRCİ (Kastamonu University)
Assoc. Prof. Dr. Emine ÇATALKAYA (Dicle University)
Assoc. Prof. Dr. Gamze EVKURAN DAL (Istanbul University-Cerrahpasa)
Assoc. Prof. Dr. Hüseyin Serkan EROL (Balikesir University)
Assoc. Prof. Dr. İrem ERGİN (Ankara University)
Assoc. Prof. Dr. Kadri KULUALP (Dokuz Eylül University)
Assoc. Prof. Dr. Mehmet Emin AYDEMİR (Harran University)
Assoc. Prof. Dr. Muhammet Bahaeddin DÖRTBUDAK (Harran University)
Assoc. Prof. Dr. Onur CEYLAN (Selcuk University)
Assoc. Prof. Dr. Sefa KÜÇÜKLER (Atatürk University)
Assoc. Prof. Dr. Serkan İrfan KÖSE (Hatay Mustafa Kemal University)
Assoc. Prof. Dr. Tunahan SANCAK (Sivas Cumhuriyet University)
Assoc. Prof. Dr. Volkan GELEN (Kafkas University)
Assist. Prof. Dr. Ayfer Güllü YÜCETEPE (Harran University)
Assist. Prof. Dr. Aysel ERASLAN ŞAKAR (Hatay Mustafa Kemal University)
Assist. Prof. Dr. Baran ERDEM (Hatay Mustafa Kemal University)
Assist. Prof. Dr. Behzat TEBRİZİ (Dicle University)
Assist. Prof. Dr. Elif EKİNCİ (Dicle University)
Assist. Prof. Dr. Gülüzar ŞENGÜL (Bingol University)
Assist. Prof. Dr. Hakan SANCAK (Bitlis Eren University)
Assist. Prof. Dr. Muhammed Ahmed SELÇUK (Siirt University)
Assist. Prof. Dr. Muhammet Hanifi SELVİ (Necmettin Erbakan University)
Assist. Prof. Dr. Ömer Tarık ORHUN (Necmettin Erbakan University)
Assist. Prof. Dr. Pelin KOÇAK KIZANLIK (Aydin Adnan Menderes University)
Assist. Prof. Dr. Yavuzkan PAKSOY (Cukurova University)
Res. Asst. Dr. Gizem KIRMIZIOĞLU (Istanbul University-Cerrahpasa)

This journal is published three times a year. Journal Tittle Abbreviation: Van Vet J

All articles in this journal are available free of charge from https://dergipark.org.tr/tr/pub/vanveti

Year	Volume	Issue
2026	37	1

This journal indexed / abstracted in Asos Index, CAB Abstracts, EBSCOhost, Google Scholar, Index Copernicus, Sobiad, TR Dizin and Türkiye Atıf Dizini

VAN VETERINARY JOURNAL

CONTENTS

Page

Original Articles

VAN VETERINARY JOURNAL

CONTENTS

Page

Original Articles

VAN VETERINARY JOURNAL

CONTENTS

Page

Van Veterinary Journal

https://dergipark.org.tr/tr/pub/vanvetj

Cite this article as: **Çubukçu M, Yaman T (2026).** Investigation of the Antidiabetic Effects of Bee Bread (Perga) in Diabetic Rats: A Histopathological, Immunohistochemical, and Biochemical Study. *Van Vet J*, 37(1), 1-6. DOI: https://doi.org/10.36483/vanvetj.1734940

ISSN: 2149-3359 **Original Article** e-ISSN: 2149-8644

Investigation of the Antidiabetic Effects of Bee Bread (Perga) in Diabetic Rats: A Histopathological, Immunohistochemical, and Biochemical Study

Mehmet ÇUBUKÇU[1] Turan YAMAN[2,*]

[1] *Van Yüzüncü Yıl University, Institute of Health Sciences, 65040, Van, Türkiye*
[2] *Van Yüzüncü Yıl University, Faculty of Veterinary Medicine, Department of Pathology, 65040, Van, Türkiye*

Received: 08.07.2025 Accepted: 10.12.2025

ABSTRACT Diabetes mellitus is a major public health concern. Bee bread (Perga), rich in bioactive compounds, has gained attention in apitherapy for its potential therapeutic properties. This study aimed to investigate the antidiabetic potential of bee bread in streptozotocin (STZ)-induced diabetic rats through histopathological, immunohistochemical, and biochemical analyses. A total of 40 male Wistar albino rats were randomly divided into five groups: Control, perga (0.5 g/kg), diabetes (STZ, 55 mg/kg), diabetes+perga (STZ, 55 mg/kg+perga, 0.5 g/kg), and diabetes+acarbose (STZ, 55 mg/kg+acarbose, 20 mg/kg). Experimental diabetes was induced by a single intraperitoneal STZ injection. Perga and acarbose were administered daily via oral gavage throughout the experiment. Blood glucose levels were monitored periodically from tail vein samples. Pancreatic tissues were examined histopathologically and immunohistochemically. Serum levels of ALT, AST, ALP, LDH, total cholesterol, triglyceride, creatinine, urea, and glucose were analyzed using an automated analyzer with commercial kits. STZ administration resulted in marked pancreatic damage and a significant decrease in insulin expression. Biochemical analyses revealed notable diabetes-related alterations. Perga treatment partially alleviated hyperglycemia, improved pancreatic histopathology, and enhanced insulin immunoexpression. However, adverse alterations in liver enzyme levels were observed in the Perga-treated diabetic group. These findings suggest that bee bread may exert only limited antidiabetic effects in STZ-induced experimental diabetes. Nevertheless, the observed hepatic effects warrant further comprehensive studies to clarify the safety and efficacy of bee bread as an antidiabetic agent.

Keywords: *Bee bread, Diabetes mellitus, Histopathology, Immunohistochemistry, Streptozotocin.*

ÖZ

Diyabetik Sıçanlarda Arı Ekmeğinin (Perga) Antidiyabetik Etkilerinin Araştırılması: Histopatolojik, İmmünohistokimyasal ve Biyokimyasal Bir Çalışma

Diabetes mellitus, önemli bir halk sağlığı sorunu olarak öne çıkmaktadır. Biyoaktif bileşenler açısından zengin olan arı ekmeği (Perga), apiterapide potansiyel tedavi edici etkileri nedeniyle ilgi görmektedir. Bu çalışmada, streptozotosin (STZ) ile oluşturulan deneysel diyabet modelinde arı ekmeğinin antidiyabetik potansiyelinin histopatolojik, immünohistokimyasal ve biyokimyasal olarak değerlendirilmesi amaçlanmıştır. Çalışmada 40 adet erkek Wistar albino sıçanı rastgele beş gruba ayrılmıştır: Kontrol, perga (0.5 g/kg), diyabet (STZ, 55 mg/kg), diyabet+perga (STZ, 55 mg/kg+perga, 0.5 g/kg) ve diyabet+akarboz (STZ, 55 mg/kg+akarboz, 20 mg/kg). Diyabet, tek doz STZ enjeksiyonu ile indüklenmiştir. Perga ve akarboz uygulamaları deney süresi boyunca günlük olarak gastrik gavaj yöntemiyle gerçekleştirilmiştir. Deney süresince belirli aralıklarla kuyruk veninden kan glukoz düzeyleri ölçülmüş; deney sonunda pankreas dokuları histopatolojik ve immünohistokimyasal olarak incelenmiştir. Serumda ALT, AST, ALP, LDH, total kolesterol, trigliserid, kreatinin, üre ve glukoz düzeyleri otoanalizör ve ticari kitler kullanılarak analiz edilmiştir. STZ uygulaması, pankreas dokusunda belirgin histopatolojik lezyonlara ve immunohistokimyasal olarak insülin ekspresyonunda anlamlı azalmaya yol açmıştır. Biyokimyasal analizlerde diyabete bağlı olarak önemli değişiklikler gözlenmiştir. Perga uygulaması, hiperglisemiyi kısmen baskılayarak kan glukoz düzeylerinde azalma sağlamış; pankreatik histopatolojik bulgularda ve insülin immunekspresyonunda iyileştirici etkiler göstermiştir. Ancak, perga ile tedavi grubunda karaciğer enzim düzeylerinde olumsuz değişiklikler saptanmıştır. Elde edilen bulgular, perganın STZ ile oluşturulan deneysel diyabet modelinde yalnızca sınırlı antidiyabetik etkiler gösterebileceğini ortaya koymaktadır. Bununla birlikte, karaciğer üzerine gözlemlenen etkiler dikkate alındığında, perganın antidiyabetik etkinliğinin ve güvenirliliğinin daha ileri çalışmalarla desteklenmesi gerekmektedir.

Anahtar Kelimeler: *Arı ekmeği, Diabetes mellitus, Histopatoloji, İmmünohistokimya, Streptozotosin.*

✉ *Corresponding author: turanyaman@yyu.edu.tr

INTRODUCTION

Diabetes mellitus (DM) is a chronic metabolic disorder characterized by the selective destruction of pancreatic β-cells, leading to insulin deficiency and persistent hyperglycemia. This condition contributes to the development of complications such as cardiovascular diseases, neuropathy, nephropathy, and hepatic dysfunction (Calcutt et al. 2009; Yaman et al. 2017). Hyperglycemia plays a central role in the pathogenesis of DM by triggering oxidative stress, which exacerbates cellular damage and accelerates disease progression (Oguntibeju 2019a).

Oxidative stress, defined as an imbalance between excessive production of reactive oxygen species (ROS) and insufficient antioxidant defense mechanisms, causes significant cellular and tissue injury. It is well established that oxidative stress contributes to diabetic microangiopathy and macroangiopathy by promoting vascular endothelial dysfunction (Dubsky et al. 2023). Streptozotocin (STZ), a nitrosourea derivative commonly used to induce experimental diabetes in laboratory animals, selectively exerts toxic effects on pancreatic β-cells, resulting in hyperglycemia and oxidative stress that mimic the pathophysiology of diabetes (Ohkuwa et al. 1995; Szkudelski 2001).

Current antidiabetic drugs are often associated with adverse effects such as hypoglycemia, lactic acidosis, and gastrointestinal disturbances, limiting their therapeutic application (Oguntibeju 2019a; Oguntibeju 2019b). Consequently, there is a growing demand for effective, safe, and affordable alternative treatment strategies. In this context, traditional medicinal plants and natural products have gained considerable attention as potential therapeutic options (Ijaola et al. 2014).

Perga (bee bread) is a natural product obtained by the fermentation of pollen by bees. It is rich in proteins, vitamins (C, B, K, E, folic acid), polyphenols, and minerals (Markiewicz et al. 2013; Aksoy et al. 2024). Due to its high content of phenolic compounds and α-tocopherol, perga exhibits strong antioxidant properties, which have been reported to mitigate oxidative stress-induced tissue damage (Borycka et al. 2015; Sobral et al. 2017). Additionally, perga has been reported to support detoxification processes and exerts protective and restorative effects, particularly in hepatic tissues (Nagai et al. 2005; Kieliszek et al. 2018).

The aim of this study is to evaluate the tissue-protective effects of perga in a streptozotocin-induced experimental diabetes model using histopathological, immunohistochemical, and biochemical methods.

MATERIAL AND METHODS

The local ethics committee of Van Yuzuncu Yil University Animal Experiments approved the study (24/04/2025, 2025/04-21).

Experimental Animals

In this study, male Wistar albino rats weighing between 170-200 grams were used. The animals were obtained from the Experimental Medicine Application and Research Center of Van Yuzuncu Yil University. Rats were housed in standard plastic cages under controlled environmental conditions (22±2 °C temperature, 60% humidity, 12-hour light/dark cycle) with ad-libitum access to tap water and standard pellet rat chow. At the beginning of the study, all rats were weighed and randomly divided into groups to ensure homogeneous weight distribution. Animals with body weights significantly below or above the group average were excluded. Body weights were recorded periodically on days 0, 14, and 28 of the experimental periods.

Bee Bread (Perga)

Fresh bee bread was dried at 35 °C for 4 hours, ground into a fine powder using a blender, and stored at -20 °C until use (Zakaria et al. 2021). During the 4-week experimental period, perga was administered daily by oral gavage at a dose of 0.5 g/kg body weight (Zakaria et al. 2021; Kosedag and Gulaboglu 2023).

Acarbose

Acarbose tablets, an antidiabetic agent, were administered to the designated group of Wistar albino rats at a dose of 20 mg/kg by dissolving in water and delivering via oral gavage (Doğan and Celik 2016).

Induction of Diabetes with Streptozotocin

Characteristics of Streptozotocin

Streptozotocin (STZ) is a nitrosourea derivative with a molecular weight of 265.2 Da and the chemical formula $C_8H_{15}N_3O7$. It appears as a pale-yellow powder, is mutagenic, toxic, and carcinogenic, and begins to degrade at 115 °C. STZ is soluble in alcohols, ketones, and water but is unstable in solution; therefore, it is freshly prepared immediately before use. Following administration, STZ selectively destroys pancreatic β-cells and exerts toxic effects on the liver and kidneys. In experimental studies, it is commonly administered via intraperitoneal (i.p.) or intravenous (i.v.) injection to induce diabetes.

Induction Protocol

A single dose of STZ (55 mg/kg body weight) was prepared in 0.1 M sodium citrate buffer (pH 4.5) and administered intraperitoneally to rats after overnight fasting (Banerjee et al., 2013). Blood glucose levels were measured 72 hours post-injection using tail vein blood samples. Rats with fasting blood glucose levels exceeding 200 mg/dL were considered diabetic.

Experimental Groups

A total of 40 rats were randomly divided into five groups (n=8 per group) as follows, and the experiment was continued for 4 weeks:

Control: Received only standard pellet feed and water.

Perga: Received perga (0.5 g/kg body weight/day) via oral gavage in 1 mL distilled water, along with standard pellet feed and water.

STZ: Received a single dose of STZ (55 mg/kg ip) and standard pellet feed.

STZ+perga: Three days after STZ administration (upon confirmation of hyperglycemia ≥200 mg/dL), perga (0.5 g/kg/day) was administered daily by oral gavage. Rats were fed standard pellet feed.

STZ+acarbose: Three days after STZ administration (hyperglycemia ≥200 mg/dL), acarbose (20 mg/kg/day) was administered daily via oral gavage. Rats received standard pellet feed.

Sample Collection and Biochemical Analyses

At the end of the experimental period, rats were anesthetized with ketamine, and blood samples were collected from the heart using syringes. Blood samples were used for biochemical analyses including ALT, AST, ALP, LDH, total cholesterol, triglycerides, creatinine, urea, and glucose levels. Biochemical analyses were studied on

an ARCHITECT c1616200 autoanalyzer using an Abbott brand commercial kit.

Histopathological Examination

Pancreatic tissue samples were fixed in 10% buffered formalin, embedded in paraffin blocks, and sectioned at 4 µm thickness using a microtome. Sections were stained with hematoxylin-eosin (H&E) and examined under a light microscope to evaluate morphological alterations in the Langerhans islets, including degeneration, necrosis, and other pathological findings. Samples from other organs were also fixed in formalin for future analyses.

Immunohistochemical Examination

For immunohistochemical evaluation, pancreatic sections were subjected to insulin immunostaining using the avidin-biotin complex (ABC) method (Yaman et al. 2017). The density of insulin-positive cells was assessed semi-quantitatively.

Statistical Analysis

Biochemical data were expressed as mean±standard deviation (X±SD) and analyzed using Minitab for Windows software. One-way analysis of variance (ANOVA) followed by Tukey post-hoc test was used to compare means between groups. Differences in pathological findings were assessed using the chi-square (χ^2) test. A p-value of <0.05 was considered statistically significant.

RESULTS

Comparison of Body Weights of the Groups

Changes in body weights at the beginning, middle, and end of the study are presented in Table 1. No significant difference was observed between the initial and final weights in the STZ and STZ+acarbose groups. However, a decrease in body weight was detected in the STZ+perga group. Only the perga group showed a significant increase in body weight (p<0.05).

Table 1: Comparison of Body Weight Changes Between Groups Throughout the Study.

	Control	Perga	STZ	STZ+ perga	STZ+ acarbose
First Weighting	189.57 ±13.9$^{a, b}$	190.43 ±11.5$^{a, b}$	183.37 ±17.2$^{a, b}$	193.00 ±4.65^{a}	176.85 ±13.20^{b}
Second Weighting	209.42 ±27.0^{a}	216.86 ±15.0$^{a, \&}$	173.38 ±15.6^{b}	166.50 ±14.7$^{b, \&}$	159.71 ±13.37^{b}
Third Weighting	243.00 ±15.89$^{a, \&, \$}$	253.71 ±15.4$^{a, \&, \$}$	182.29 ±34.3^{b}	163.57 ±13.1$^{b, \&, \$}$	176.40 ±39.07^{b}

Different letters in the same line indicate statistical significance (p<0.05). &; compared with the first weighing, $; compared with the second weighing (p<0.05).

Histopathological Findings

In H&E-stained pancreatic sections of the control and perga groups, the tissue preserved its normal histological structure. Langerhans islets contained an adequate number of cells, had clear and regular boundaries, and cells appeared morphologically normal.

In contrast, the STZ group exhibited marked histopathological changes in pancreatic tissue. Islet structures were reduced in size, cell numbers decreased, and boundaries became indistinct. Widespread vacuolization in cells and scattered, pyknotic nuclei were noted. Additionally, degenerative changes in the exocrine pancreas and inflammatory cell infiltration around the parenchyma and blood vessels were observed.

Pancreatic sections of the STZ+perga group showed similar features to the STZ group, although a relative increase in cell numbers within the Langerhans islets was noted. Histopathological findings in the STZ+acarbose group resembled those of the STZ+perga group (Figure 1).

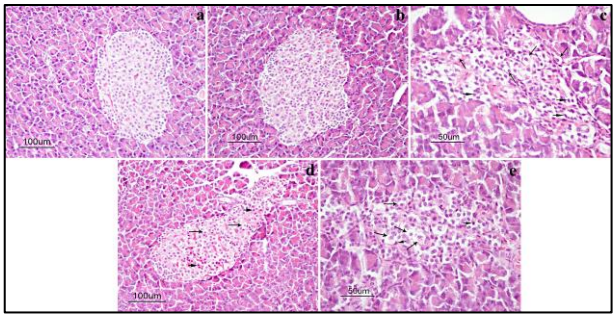

Figure 1: Effects of perga on STZ-induced histopathological changes in the pancreas sections (H&E).

A=Control group and B=Perga group: The islets of Langerhans exhibit a normal histological structure. C=STZ group: Marked atrophy and shrinkage of the islets of Langerhans are evident, accompanied by cells exhibiting vacuolated cytoplasm (long arrows) and dispersed pyknotic nuclei (short arrows). D=STZ+perga group: In the partially preserved islet architecture, cells with vacuolated cytoplasm (long arrows) and necrotic cells (short arrows) are observed. E=STZ+acarbose group: The islets of Langerhans contain cells with vacuolated cytoplasm (long arrows) and pyknotic nuclei (short arrows).

Immunohistochemical Findings

In the control and perga groups, prominent insulin immunopositive reactivity was detected in β-cells of Langerhans islets, indicating preserved insulin synthesis and secretion capacity in both groups. Conversely, insulin immunoreactivity markedly decreased in the STZ group compared to control, reflecting the toxic effect of STZ on β-cells leading to a marked reduction in insulin production. Relative increases in insulin immunoreactivity were observed in the STZ+perga and STZ+acarbose groups compared to the STZ group (Figure 2).

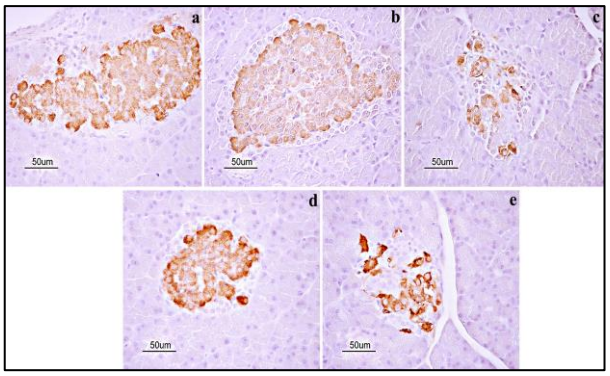

Figure 2: Immunohistochemical Evaluation of Insulin Expression in Pancreatic Sections (ABC Method, Hematoxylin Counterstaining).

A=Control group: Strong insulin immunopositivity is observed in β cells. B=Perga group: Intense insulin immunopositivity is also evident in β cells. C=STZ group: A marked reduction in the number of insulin-immunopositive β cells is observed. D=STZ+perga group: Compared to the STZ group, an increase in insulin immunoreactivity is detected in β cells. E=STZ+acarbose group: A partial increase in insulin immunoreactivity is observed in β cells relative to the STZ group.

Biochemical Results

Comparison of Blood Glucose Levels

Blood glucose levels are summarized in Table 2. At the beginning of the study, fasting blood glucose levels were similar across all groups without significant differences (p>0.05).

On day 3 after STZ administration, glucose levels in the STZ-treated groups were significantly higher than those in control and perga groups ($p<0.05$).

On day 14, the STZ group showed significantly higher glucose levels compared to control, perga, and STZ+acarbose groups ($p<0.05$). The STZ+perga group had lower glucose levels than the STZ group, but this difference was not statistically significant ($p>0.05$). No significant difference was observed between STZ+perga and STZ+acarbose groups ($p>0.05$), although both had significantly higher glucose levels than control and perga groups ($p<0.05$).

At the end of the study (day 28), the highest fasting glucose level was measured in the STZ group, significantly elevated compared to control, perga, and STZ+perga groups ($p<0.05$). The difference between the STZ and STZ+acarbose groups was not significant ($p>0.05$). The STZ+perga group showed lower glucose levels than STZ+acarbose, but the difference was not statistically significant ($p>0.05$).

Fasting glucose levels in control and perga groups remained similar throughout the study without significant differences ($p>0.05$).

Table 2: Comparison of blood glucose levels between groups.

	Control	Perga	STZ	STZ+ perga	STZ+ acarbose
Day 0	116.17 ±11.00^{a*}	111.57 ±4.28^{a}	115.60 ±5.81^{a}	112.50 ±9.79^{a}	106.67 ±13.28^{a}
Day 3	114.00 ±12.24^{c}	110.66 ±12.24^{c}	430.88 ±35.73$^{a, x}$	374.00 ±49.47$^{b, x}$	372.00 ±37.56^{b,x}
Day 14	112.85 ±12.48^{c}	94.42 ±6.45$^{c, x}$	502.71 ±91.26$^{a, x}$	451.57 ±53.02$^{a, b, x, y}$	383.60 ±98.22$^{b, x}$
Day 28	109.14 ±8.61^{c}	101.28 ±6.92$^{c, x, y}$	538.33 ±81.10 $^{a, x, y}$	475.00 ±35.88 $^{b, x, y}$	506.80 ±69.32$^{a, b,x,y,z}$

*; different letters in the same line indicate statistical significance. x; compared with the first day ($p<0.05$), y; compared with the second weighing ($p<0.05$), z: compared with the third day ($p<0.05$).

Comparison of Serum Biochemical Parameters

As shown in Table 3, ALP activity was highest in the STZ+perga group and lowest in the control group ($p<0.05$). The STZ+acarbose group also exhibited significantly higher ALP levels compared to control and some other groups. Serum ALT levels were highest in the STZ+acarbose group, with significant increases observed in the STZ and STZ+perga groups compared to control and perga groups ($p<0.05$). Serum AST levels were similar between the control and perga groups ($p>0.05$). No significant differences were observed among the STZ-treated groups ($p>0.05$). However, AST levels in the STZ+perga and STZ+acarbose groups were significantly higher compared to the control and perga groups ($p<0.05$), but not significantly different from the STZ group ($p>0.05$)

Serum cholesterol levels were significantly higher in the perga group compared to the control, STZ, and STZ+perga groups ($p<0.05$). However, no significant differences were found among the control, STZ, STZ+perga, and STZ+acarbose groups ($p>0.05$).

Serum glucose levels showed no significant difference between the control and perga groups ($p>0.05$). The highest glucose level was observed in the STZ group, which was significantly higher than those in the control, STZ+perga, and perga groups ($p<0.05$). The STZ+perga group had significantly lower glucose levels compared to the STZ and STZ+acarbose groups, but significantly higher than the control and perga groups ($p<0.05$).

Serum LDH activity was significantly elevated in the STZ+perga group compared to the perga and STZ+acarbose groups ($p<0.05$), while no significant differences were found among the control, STZ, perga, and STZ+acarbose groups ($p>0.05$).

Triglyceride levels were significantly higher in the STZ+acarbose group compared to the control, STZ+perga, and perga groups ($p<0.05$), but did not differ significantly from the STZ group ($p>0.05$).

Finally, serum urea levels were significantly elevated in all STZ-treated groups compared to the control and perga groups ($p<0.05$).

Table 3: Serum biochemical parameters in the study groups.

	Control	STZ	STZ+ perga	Perga	STZ+ acarbose
ALP	148.25 ±17,79^{d}	562.60 ±195.61^{c}	995.50 ±93.68^{a}	161.14 ±23.98^{d}	830.20 ±137.56^{b}
ALT	34.15 ±2.90^{c}	262.80 ±70.32^{b}	378.10 ±94.63^{b}	33.32 ±3.06^{c}	689.52 ±286.02^{a}
AST	80.60 ±9.11^{b}	463.00 ±112.27^{a,b}	677.17 ±183.21^{a}	79.54 ±5.72^{b}	742.36 ±492.22^{a}
Cholesterol (mg/dl)	60.78 ±5.56^{b}	55.52 ±7.46^{b}	59.25 ±7.60^{b}	70.94 ±5.63^{a}	63.26 ±11.08^{a,b}
Creatinine	0.31 ±0.02^{c}	0.41 ±0.04^{a,b}	0.42 ±0.92^{a}	0.33 ±0.02^{c}	0.38 ±0.01^{b}
Glucose	175.76± 20.52^{c}	812.80 ±75.87^{a}	582.10 ±31.14^{b}	173.52 ±27.62^{c}	768.44 ±85.48^{a}
LDH	618.43 ±190.2^{a,b}	584.60 ±230.05^{a,b}	837.00 ±242.09^{a}	511.14 ±123.57^{b}	515.40 ±230.31^{b}
Triglyceride (mg/dl)	47.21 ±10.16^{c}	85.94 ±37.74^{a,b}	46.32 ±10.24^{c}	59.62 ±27.32^{b,c}	100.70 ±30.95^{a}
Urea	48.85 ±5.56^{b}	115.40 ±11.63^{a}	110.65 ±12.85^{a}	54.87 ±5.97^{b}	110.50 ±22.20^{a}

*: Different letters in the same line indicate statistical significance ($p<0.05$).

DISCUSSION AND CONCLUSION

In recent years, the potential of traditional medicinal plants as complementary or alternative therapeutic agents for various chronic diseases, including diabetes mellitus (DM), has been increasingly investigated. In this context, it has been reported that herbal products may provide therapeutic benefits without causing toxic effects, thanks to their antioxidant content (Jin et al. 2008). In particular, phenolic compounds and flavonoids may support β-cell regeneration by suppressing reactive oxygen species (ROS) and may play a protective role against pancreatic damage induced by streptozotocin (STZ) (Alvarez et al. 2004). In the present study, the effects of perga, which is rich in antioxidants, on glycemic control, histopathological changes, and organ functions were evaluated in an STZ-induced diabetic rat model.

In the present study, our findings revealed that STZ administration caused significant increases in fasting and serum glucose levels, and these elevations persisted throughout the experimental period, reflecting the cytotoxic effect of STZ on pancreatic β-cells. The fasting and serum glucose levels in the STZ group were significantly higher than those in the control and perga groups, indicating the toxic effect of STZ on β-cells (Lenzen 2008). It was observed that perga, when administered in combination with STZ, partially reduced both fasting and serum glucose levels. The glucose levels in the STZ+perga group were significantly lower compared to the STZ and STZ+acarbose groups. This result suggests that perga may exert a partial ameliorative effect on hyperglycemia by alleviating pancreatic β-cell damage through its bioactive components (Viuda-Martos et al. 2008; Aboulghazi et al.

2024). However, glucose levels did not reach those of the control group, indicating that the effect provided by perga was partial and limited.

Histopathological evaluation revealed that STZ caused marked vacuolar degeneration and necrosis in the islets of Langerhans. These findings are consistent with previous studies related to the selective β-cell toxicity of STZ (Szkudelski 2001; Lenzen 2008; Yaman and Doğan 2016; Yaman et al. 2017). In contrast, less pronounced histological damage and relatively preserved β-cell integrity were observed in the STZ+perga group. This observation suggests that perga may alleviate oxidative stress-induced cellular damage due to its bioactive components (Komosinska-Vassev et al. 2015).

In our study, a marked decrease in insulin immunopositivity was detected in the pancreatic islets of Langerhans in the STZ group. These findings are consistent with previous studies reporting the cytotoxic effects of STZ on β-cells (Szkudelski 2001; Lenzen 2008). The antidiabetic effects of antioxidant compounds have been associated with their potential to support insulin production by remaining β-cells or to promote the recovery of damaged cells (Ahrens 2011). In the present study, an increase in immunopositive insulin reactivity was observed in the STZ+perga group. This finding suggests that the antioxidant phenolic compounds present in perga may partially preserve insulin expression by supporting the functions of the remaining β-cells (Komosinska-Vassev et al. 2015).

Previous studies on STZ-induced diabetic models have reported histopathological changes such as hepatic degeneration, glycogen accumulation, and acidophilic cytoplasm, along with significant increases in serum enzyme levels including ALT, AST, and ALP (Zhuo et al. 2008; Yazdi 2019). Similarly, in the present study, STZ administration led to significant elevations in the activities of these enzymes. Notably, perga treatment further accentuated this increase. This finding suggests that certain components of perga may exhibit a synergistic interaction with STZ, potentially enhancing hepatotoxic effects. The absence of such effects in healthy rats treated with perga implies that this toxicity emerges within the diabetic pathophysiological context. This indicates that perga may adversely affect liver function in diabetic individuals and should therefore be carefully evaluated prior to clinical use (Poretsky 2010).

The effects of STZ on renal function are also significant. Elevated levels of urea and creatinine are key indicators of diabetes-related renal dysfunction (Almdal and Vilstrup 1988). In our study, marked increases in these parameters were observed in STZ-induced diabetic rats, consistent with previous findings (Yaman and Kömüroğlu 2018; Ceriello et al. 2000). However, perga administration did not produce a significant ameliorative effect on these parameters. This suggests that the renoprotective potential of perga may be limited or that its efficacy may be insufficient at certain doses and durations.

Regarding lipid metabolism, a significant increase in serum cholesterol levels was observed in the perga group. Although the effects of pollen and bee bread on lipid profiles have been previously reported (Fatrcová-Šramková et al. 2013), in this study, perga did not exhibit the expected protective effect against STZ-induced hyperlipidemia. This outcome may be related to insufficient dosage and duration of administration or to factors within the model that limit the pharmacodynamic response to perga.

Although Perga is known for its antioxidant content, the absence of direct measurements of oxidative stress markers (e.g., MDA, SOD, CAT, GSH) represents a methodological limitation. The study therefore cannot conclusively link the observed pancreatic improvements to antioxidant activity. Additionally, only a single dose of Perga was administered; the lack of dose–response data limits conclusions regarding both efficacy and potential toxicity. Including multiple doses in future studies would provide a clearer understanding of Perga's therapeutic window and organ-specific effects. In this study, the findings demonstrated that perga exerted a partial ameliorative effect against hyperglycemia and may support insulin expression by mitigating pancreatic β-cell damage. Histopathological analysis revealed that the islet damage induced by STZ was alleviated when perga was co-administered, with relatively preserved β-cell integrity. However, the increase in hepatic enzyme levels following perga administration and the lack of significant improvement in renal function parameters and lipid profile suggest that perga does not provide uniform protection across all systems. In particular, the potential hepatotoxic effects of perga highlight the need for careful consideration of its use in diabetic individuals. Moreover, the absence of measured antioxidant parameters and the use of a single-dose design limit the interpretability of the observed antioxidant-related claims and prevent a clearer understanding of Perga's dose-dependent efficacy and safety. In conclusion, while perga appears to be a promising natural agent for glycemic control and pancreatic protection in STZ-induced diabetic models, its organ-specific effects warrant further comprehensive toxicological and pharmacodynamic investigations.

CONFLICTS OF INTEREST

The authors report no conflicts of interest.

ACKNOWLEDGMENT

This study is summarized from the master's thesis of the author Mehmet ÇUBUKÇU.

AUTHOR CONTRIBUTIONS

Idea/Concept: TY, ÇM
Supervision/Consultancy: TY, ÇM
Data Collection and/or Processing: TY, ÇM
Analysis and/or Interpretation: TY, ÇM
Writing the Article: TY, ÇM
Critical Review: TY, ÇM

REFERENCES

Aboulghazi A, Fadil M, Touzani S, et al (2024). Phenolic screening and mixture design optimization for in vitro assessment of antioxidant and antimicrobial activities of honey, propolis, and bee pollen. *J Food Biochem*, 2024(1), 8246224.

Ahrens B (2011). Antibodies in metabolic diseases. *New biotechnology*, 28(5), 530-537.

Aksoy A, Altunatmaz SS, Aksu F et al. (2024). Bee bread as a functional product: phenolic compounds, amino acid, sugar, and organic acid profiles. *Foods*, 13(5), 795.

Almdal TP, Vilstrup H (1988). Strict insulin therapy normalises organ nitrogen contents and the capacity of urea nitrogen synthesis in experimental diabetes in rats. *Diabetologia*, 31, 114-118.

Alvarez JF, Barbera A, Nadal B, et al (2004). Stable and functional regeneration of pancreatic beta-cell population in n-STZ rats treated with tungstate. *Diabetologia*, 47, 470-477.

Borycka K, Grabek-Lejko D, Kasprzyk I (2015). Antioxidant and antibacterial properties of commercial bee pollen products. *J Apic Res,* 54, 1-12.

Calcutt N, Cooper M, Kern T, Schmidt AM (2009). Therapies for hyperglycaemia- induced diabetic complications: from animal models to clinical trials. *Nat Rev Dru Discov*, 8(5), 417-429.

Ceriello A, Morocutti A, Franceschina M, et al (2000). Defective intracellular Antioxidant Enzyme Production in Type 1 Diabetic Patients with Nephropathy. *Am Diabetes Assoc*. 49(12), 2170-2177.

Doğan A, Çelik İ (2016). Healing effects of sumac (Rhus coriaria) in streptozotocin-induced diabetic rats. *Pharm biol*, 54(10), 2092-2102.

Dubsky M, Veleba J, Sojakova D, et al (2023). Endothelial dysfunction in diabetes mellitus: new insights. *Int J Mol Sci,* 24(13), 10705.

Fatrcová-Šramková K, Nôžková J, Kačániová M, et al (2013). Antioxidant and antimicrobial properties of monofloral bee pollen. *J Environ Sci Health B*, 48(2), 133-138.

Ijaola TO, Osunkiyesi AA, Taiwo AA, et al (2014). Antidiabetic effect of Ipomoea batatas in normal and alloxan-induced diabetic rats. *IOSR-JAC,* 7(5), 16-25.

Jin L, Xue HY, Jin LJ, Li SY, Xu YP (2008). Antioxidant and pancreas-protective effect of aucubin on rats with streptozotocin-induced diabetes. *Eur J Pharmacol*, 582(1-3), 162-167.

Kieliszek M, Piwowarek K, Kot AM et al (2018). Pollen and bee bread as new health-oriented products: A review. *Trends Food Sci Technol*, 71, 170-180.

Komosinska-Vassev K, Olczyk P, Kaźmierczak J, Mencner L, Olczyk K (2015). Bee pollen: chemical composition and therapeutic application. *Evid Based Complement Alternat Med*, 2015(1), 297425.

Kosedag M, Gulaboglu M (2023). Pollen and bee bread expressed highest anti-inflammatory activities among bee products in chronic inflammation: an experimental study with cotton pellet granuloma in rats. *Inflammopharmacology*, 31, 1967-1975.

Lenzen S (2008). The mechanisms of alloxan-and streptozotocin-induced diabetes. *Diabetologia*, 51(2), 216-226.

Markiewicz-Zukowska R, Naliwajko SK, Bartosiuk E et al (2013). Chemical composition and antioxidant activity of beebread, and its influence on the glioblastoma cell line (U87MG). *J Apic Sci*, 57(2), 147.

Nagai T, Nagashima T, Suzuki N, Inoue, R (2005). Antioxidant activity and angiotensin I–converting enzyme inhibition by enzymatic hydrolysates from bee bread. *Zeitschrift für Naturforschung C*, 60(1-2), 133–138.

Oguntibeju OO (2019a). Hypoglycaemic and anti-diabetic activity of selected African medicinal plants. *Int J Physiol Pathophysiol Pharmacol*, 11(6), 224-237.

Oguntibeju OO (2019b). Type 2 diabetes mellitus, oxidative strees and inflammation: examining the links. *Int J Physiol Pathophysiol Pharmacol*, 11(3), 45–63.

Ohkuwa T, Sato Y, Naoi M (1995). Hydroxyl radical formation in diabetic ratöinduced by streptozotocin. *Life Sci*, 56, 1789-1798.

Poretsky L (2010). Principles of Diabetes Mellitus. 2nd ed., Springer, Boston, MA, USA.

Sobral F, Calhelha RC, Barros L et al (2017). Flavonoid Composition and Antitumor Activity of Bee Bread Collected in Northeast Portugal. *Molecules*, 22, 248.

Szkudelski T (2001). The mechanism of alloxan and streptozotocin action in B cells of the rat pancreas. *Physiol Res,* 50(6), 537-546.

Viuda-Martos M, Ruiz-Navajas Y, Fernández-López J et al (2008). Functional properties of honey, propolis, and royal jelly. *J Food Sci*, 73(9), R117-R124.

Yaman T, Doğan A (2016). Streptozotosin ile diyabet oluşturulan sıçanlarda meşe palamudu (Quercus branti Lindl.) ekstraktların karaciğer ve pankreası koruyucu etkileri. *Dicle Üniv Vet Fak Der*, 1(2), 7-15.

Yaman T, Kömüroğlu, AU (2018). Effects of Juniperus communis L. Oil on Nephropathy in Experimental Diabetic Rats. *Harran Üniv Vet Fak Derg*, 7(2), 192-199.

Yaman T, Uyar A, Celik I et al (2017). Histopathological and immunohistochemical study of antidiabetic effects of Heracleum persicum extract in experimentally diabetic rats. *IJPER*, 51(3), 450-457.

Yazdi H (2019). Liver dysfunction and oxidative stress in streptozotocin-induced diabetic rats: protective role of Artemisia turanica. *J Pharmacopuncture*, 22(2), 109.

Zakaria Z, Othman ZA, Suleiman JB (2021). Hepatoprotective effect of bee bread in metabolic dysfunction-associated fatty liver disease (MAFLD) rats: Impact on oxidative stress and inflammation. *Antioxidants*, 10(12), 2031.

Van Veterinary Journal

https://dergipark.org.tr/tr/pub/vanvetj

Cite this article as: **Deniz B, Sona Karakuş A, Denizhan V (2026).** Investigation on Ear Mites (*Otodectes cynotis*) in Cats Brought to Veterinary Clinics for Treatment in İstanbul Province. *Van Vet J*, 37(1), 7-10. DOI: https://doi.org/10.36483/vanvetj.1748420

ISSN: 2149-3359 **Original Article** e-ISSN: 2149-8644

Investigation on Ear Mites (*Otodectes cynotis*) in Cats Brought to Veterinary Clinics for Treatment in İstanbul Province

Bilal DENİZ[1] Ayşe SONA KARAKUŞ[2,*] Vural DENİZHAN[2]

[1] *Gaziosmanpaşa Education and Research Hospital, 34255, İstanbul, Türkiye*
[2] *Van Yüzüncü Yıl University, Faculty of Veterinary Medicine, Department of Parasitology, 65080, Van, Türkiye*

Received: 23.07.2025 Accepted: 11.03.2026

ABSTRACT *Otodectes cynotis* infestation is one of the most common parasitic causes of otitis externa in cats and represents a significant health concern in small animal practice. This study aimed to evaluate the prevalence of *O. cynotis* infestation in client-owned cats presented to private veterinary clinics in Istanbul between September 2023 and September 2024. The study population consisted of 319 cats that were brought to the clinics for various medical reasons, including routine examinations and non-otological complaints. No pre-selection was made based on the presence of clinical signs of ear mange, and all cats were included consecutively during the study period. Each cat underwent clinical, otoscopic, and microscopic examination. Clinical signs observed in infested cats included head shaking, pruritus, dark ceruminous discharge, erythema, and erosions in the external ear canal. Infestation was confirmed in 83 cats (26.01%). Breed-based analysis revealed the highest positivity rate in Tabby cats (30.9%), followed by Scottish Fold and British Shorthair cats (12.8%), while no infestation was detected in Persian or Russian Blue cats. A statistically significant association was found between breed and infestation (p=0.001). No significant difference was observed between males (26.8%) and females (25.3%) (p=0.76). Although infestation rates decreased with age (0-6 months: 34.2%, 6–12 months: 26.1%, ≥12 months: 21.6%), this trend was not statistically significant (p=0.121). These findings indicate that breed may influence susceptibility to *O. cynotis*, whereas age and sex do not appear to be significant risk factors. Early diagnosis and routine parasitological screening are essential for effective control of feline otoacariasis.

Keywords: *Cat, Ear mite, İstanbul, Otodectes cynotis, Prevalence, Veterinary clinics.*

ÖZ

İstanbul İlinde Tedavi Amaçlı Veteriner Kliniklerine Getirilen Kedilerde Kulak Uyuzu (*Otodectes cynotis*) Üzerine Araştırma

Otodectes cynotis infestasyonu, kedilerde otitis externa'nın en yaygın paraziter nedenlerinden biri olup, küçük hayvan hekimliğinde önemli bir sağlık sorunu olarak kabul edilmektedir. Bu çalışmanın amacı, Eylül 2023 ile Eylül 2024 tarihleri arasında İstanbul'daki özel veteriner kliniklerine getirilen sahipli kedilerde *O. cynotis* enfestasyonunun prevalansını değerlendirmektir. Çalışma popülasyonu, rutin muayeneler ve kulakla ilişkili olmayan şikâyetler de dâhil olmak üzere çeşitli tıbbi nedenlerle kliniğe getirilen 319 kediden oluşmuştur. Kulak uyuzu belirtilerinin varlığına göre herhangi bir ön seçim yapılmamış ve çalışma süresince başvuran tüm kediler ardışık olarak dâhil edilmiştir. Her bir kedi klinik, otoskopik ve mikroskobik muayeneden geçirilmiştir. Enfeste kedilerde gözlenen klinik bulgular arasında baş sallama, pruritus, koyu renkli serumenöz akıntı, eritem ve dış kulak kanalında erozyonlar yer almıştır. Toplam 83 kedide (%26.01) enfestasyon doğrulanmıştır. Irka göre yapılan analizde en yüksek pozitiflik oranı Tekir kedilerde (%30.9) saptanmış, bunu Scottish Fold ve British Shorthair kediler izlemiş (%12,8); Persian ve Russian Blue kedilerde ise infestasyona rastlanmamıştır. Irk ile enfestasyon arasında istatistiksel olarak anlamlı bir ilişki bulunmuştur (p=0.001). Erkek (%26.8) ve dişi (%25.3) kediler arasında anlamlı bir fark saptanmamıştır (p=0.76). Yaş arttıkça enfestasyon oranlarında azalma gözlenmiş (0-6 ay: %34.2; 6–12 ay: %26.1; ≥12 ay: %21.6), ancak bu eğilim istatistiksel olarak anlamlı bulunmamıştır (p=0.121). Bu bulgular, ırkın *O. cynotis* enfestasyonuna duyarlılığı etkileyebileceğini, ancak yaş ve cinsiyetin anlamlı risk faktörleri olmadığını göstermektedir. Kedi otoakarozisinin etkin kontrolü için erken tanı ve rutin parazitolojik taramalar büyük önem taşımaktadır.

Anahtar Kelimeler: *Kedi, Kulak akarı, İstanbul, Otodectes cynotis, Prevalans, Veteriner klinikleri.*

✉ *Corresponding author: aysesona@yyu.edu.tr

INTRODUCTION

Otocariasis is a globally prevalent parasitic infestation caused by *Otodectes cynotis* (Acari: Psoroptidae). This non-burrowing obligate ectoparasite inhabits the vertical and horizontal portions of the external ear canal and plays a significant etiological role in feline ear diseases (Wall and Shearer 2001). Transmission primarily occurs through direct contact between animals, and infestation is particularly common in young cats, although dogs, foxes, ferrets, and occasionally humans may also be affected (Medleau and Hnilica 2006; Chen et al. 2008; Russell et al. 2013). While most clinical cases are diagnosed in kittens (Lefkaditis et al. 2009), infestations have also been reported in dogs, foxes, and ferrets (Scott et al. 2001; Beugnet et al. 2014), and occasionally in humans (Chen et al. 2008; Xhaxhiu et al. 2009; Maazi et al. 2010). Although *O. cynotis* primarily localizes within the ear canal, mites may also be detected on the head, neck, scapular region, limbs, and tail (Scott and Horn 1987; Curtis 2004).

Epidemiological investigations have demonstrated variable prevalence rates of *O. cynotis* infestation in cats. Perego et al. (2013) identified *O. cynotis* as the primary cause of otitis externa in 53.3% of 187 stray cats. However, infestation does not invariably result in overt clinical disease. Host-related factors, particularly age and immune status, may influence both susceptibility and clinical expression. In this context, young animals appear to be more susceptible, and subclinical infestations may occur without evident clinical signs. Supporting this observation, Lefkaditis et al. (2009) reported that 14% of urban kittens aged six months or younger in Greece tested positive for ear mites despite the absence of clinical symptoms. Furthermore, the relationship between clinical severity and mite burden is not always proportional; severe otic lesions and dense dark debris have been observed in animals harboring only a few mites, whereas clinically normal ears may contain 50 to 100 mites (Bowman 2014). A multicenter study conducted by Beugnet et al. (2014) across seven Southern and Central European countries detected ear mites in 17.4% of 1.519 pet cats presented for non-parasitic conditions. Similarly, a prevalence rate of 25.5% was reported in pet cats in Greece (Sotiraki et al. 2001).

Otitis externa, defined as inflammation of the external auditory canal, is one of the most frequently encountered ear disorders in small animal veterinary practice. The condition develops following colonization by bacteria, fungi, or parasites, resulting in local tissue damage and inflammatory responses. In cats, *O. cynotis* is considered a primary etiological agent of otitis externa and one of the most important ectoparasitic agents affecting the species (Griffin 1993; Wall and Shearer 2001). Clinically, the disease may lead to excessive ceruminous discharge, pruritus, erythema, and progressive tissue damage within the ear canal. If left untreated, inflammation may extend to the middle ear (otitis media) and further into the inner ear (otitis interna), potentially resulting in irreversible hearing loss and vestibular dysfunction (Jacobson 2002).

The aim of the present study was to determine the prevalence of *O. cynotis* infestation in cats presented to private veterinary clinics in Istanbul and to evaluate its association with individual risk factors, including age, sex, and breed. Additionally, the relationship between clinical findings and infestation status was assessed. By providing updated regional data obtained from clinical cases in Istanbul, this study contributes to the epidemiological understanding of feline *O. cynotis* infestation.

MATERIAL AND METHODS

Ethical Approval

This study was approved by the Van Yüzüncü Yıl University Local Animal Experiments Ethics Committee (File No: E-27552122-604.01.02-425226; Decision No: 2023/11-03) dated 28 September 2023.

Study Area and Period

This study was conducted between September 2023 and September 2024 in Istanbul, Türkiye. Private veterinary clinics located in various districts of the city participated in the study and contributed to sample collection.

Study Population

A total of 319 client-owned cats presented to participating private veterinary clinics during the study period were included consecutively. Among these, 85 cats were presented with ear-related complaints such as pruritus, head shaking, or ear discharge, whereas the remaining cats were brought for routine examinations or medical conditions unrelated to ear disease. No pre-selection was made based on suspected otoacariasis, and all cats were examined systematically regardless of presenting complaint.

Clinical and Otoscopic Examination

Each cat underwent a detailed physical examination with particular emphasis on the external ear canals. Otoscopic examination was performed using a standard veterinary otoscope under gentle manual restraint. Both ears were systematically evaluated for erythema, ceruminous discharge, crust formation, erosions, ulcerations, canal stenosis, and visible mites. Clinical signs were recorded descriptively. No standardized clinical severity scoring system was applied.

Sample Collection and Laboratory Analysis

Ear swabs and scrapings were collected from both ears using sterile cotton swabs and curettes. Samples were preserved in 70% ethanol until laboratory examination. Microscopic analysis was performed to detect the presence of *O. cynotis*. Samples containing dense or dried cerumen were treated with liquid paraffin, immersion oil, or 10% potassium hydroxide (KOH) solution to enhance visualization and facilitate dispersion on glass slides. Prepared slides were examined under a light microscope (Olympus CX23, Olympus Corporation, Japan) at 10x and 40x magnifications, and the presence of adult, nymphal, and larval stages of *O. cynotis* was recorded.

Data Recording and Statistical Analysis

Data regarding age, sex, breed, and infestation status were recorded for each animal. Cats were categorized into age groups (0–6 months, 6–12 months, and ≥12 months) and breed groups (Tabby, Scottish Fold, British Shorthair, Persian, Russian Blue, and others). Statistical analyses were performed using SPSS software (version X). Associations between infestation status and categorical variables (breed, age group, and sex) were evaluated using the chi-square test. Statistical significance was set at $p<0.05$.

RESULTS

Between September 2023 and September 2024, 319 cats presented to private veterinary clinics in Istanbul were examined for *O. cynotis* infestation. Clinically infested cats exhibited restlessness, head shaking, ear scratching, dark brown to black ceruminous discharge, crusting, localized erythema, and erosions in the external ear canal. Otoscopic

examination revealed grayish-white structures within the ear canal, and microscopic evaluation confirmed the presence of adult *O. cynotis* mites (Figure 1).

Of the 319 examined cats, 83 were positive for infestation, corresponding to an overall prevalence of 26.01%. Among the 83 positive cases, 72 were Tabby (22.57% of total cats), 9 Scottish Fold (2.82%), and 2 British Shorthair (0.62%). No infestation was detected in Persian or Russian Blue cats. When positivity rates were calculated within breed groups, Tabby cats showed a significantly higher positivity rate compared to other breeds (30.9% vs. 12.8%; p=0.001). Of the 319 examined cats, 153 were male and 166 were female. Infestation was detected in 41/153 males (26.8%) and 42/166 females (25.3%). No statistically significant association was found between sex and infestation status (p=0.76). Positivity rates according to age groups were 34.2% (0–6 months), 26.1% (6–12 months), and 21.6% (≥12 months). Although a decreasing trend with increasing age was observed, the difference was not statistically significant (p=0.121) (Table 1). Overall, breed was significantly associated with infestation risk, whereas sex and age were not statistically significant factors.

Figure 1: Otodectes cynotis observed under a microscope at 10x magnification

Table 1: Statistical evaluation of the association between *Otodectes cynotis* infestation and demographic variables (breed, sex, and age group) in examined cats.

Variable	Category	Positive (n)	Negative (n)	Total (n)	Positive (%)	Negative (%)	p value
Breed	Tabby	72	161	233	30.9	69.1	**0.001***
	Other	11	75	86	12.8	87.2	
Sex	Female	42	124	166	25.3	74.7	0.76
	Male	41	112	153	26.8	73.2	
Age Group	0–6 months	27	52	79	34.2	65.8	0.121
	6–12 months	24	68	92	26.1	73.9	
	≥12 months	32	116	148	21.6	78.4	
Total		83	236	319	26.01	74.0	

DISCUSSION AND CONCLUSION

Otodectes cynotis infestation is globally recognized as a major cause of external ear disease, reportedly accounting for 50–80% of otitis externa cases (Wall and Shearer 2001; Nuttall 2015). Studies conducted in Türkiye have demonstrated marked regional variability in infestation rates, including 6% in Ankara (Mimimoğlu 1954) and 8.3% in Elazığ (Dinçer et al. 1980). In Van Province, no prevalence rate was reported, as the study focused on the treatment of naturally infested cats (Özkan et al. 2013). In Alanya (Antalya), the prevalence of *O. cynotis* infestation was reported as 27.7% (28/105), with lifestyle identified as a significant risk factor (Acar and Altınok Yipel 2016). In contrast, a prevalence of 1.7% was reported in Konya (Ceylan et al. 2025). Within this epidemiological context, the prevalence of *O. cynotis* infestation in the present study was 26.01%, which is comparable to the rate reported in Alanya but considerably higher than those documented in Konya and other regions. These differences may reflect variations in geographical and climatic conditions, environmental exposure, preventive antiparasitic practices, and the demographic and clinical characteristics of the sampled populations. Furthermore, differences in sampling strategies and the proportion of cats presented with ear-related complaints may have influenced the reported prevalence rates.

Breed-related differences emerged as statistically significant in the current study, with Tabby cats exhibiting a markedly higher positivity rate compared to other breeds. Similar observations have been reported by Acar and Altınok Yipel (2016), who emphasized the influence of environmental exposure and breed-related factors on infestation rates. In the present study, the positivity rate in Tabby cats reached 30.9%, exceeding that observed in Scottish Fold, British Shorthair, and Persian cats. These findings suggest that genetic background, lifestyle characteristics, grooming behavior, or increased environmental contact may contribute to higher susceptibility. Consistent with this interpretation, El Dakhly et al. (2024) reported elevated infestation rates in certain regional cat populations, indicating that breed-associated susceptibility may be multifactorial and influenced by both intrinsic and extrinsic determinants.

Sex was not identified as a significant risk factor in the present study. Infestation rates were comparable between males (26.8%) and females (25.3%), with no statistically significant difference (p=0.76). These findings are in agreement with previous reports demonstrating no association between sex and *O. cynotis* infestation (Gram et al. 1994; Lefkaditis et al. 2009; Vickers et al. 2015). This

consistency across studies supports the notion that transmission dynamics are primarily driven by direct contact and environmental exposure rather than sex-related biological factors.

Age-related patterns indicated higher positivity among younger cats, particularly those aged 0-6 months (34.2%), followed by 6–12 months (26.1%) and ≥12 months (21.6%). Although a decreasing trend with advancing age was observed, the difference did not reach statistical significance (p=0.121). Previous studies have frequently reported increased infestation rates in kittens, especially between 3 and 6 months of age (Gram et al. 1994; Kavitha et al. 2013; Yang and Huang 2016), possibly due to immature immune responses and close contact within litters. Conversely, other investigations have not identified a significant association between age and infestation (Lopez 1993; Perego et al. 2014). Variability among studies may reflect differences in study design, population structure, environmental conditions, and preventive health measures.

Overall, the findings indicate that breed may represent a significant predisposing factor for *O. cynotis* infestation, whereas sex and age alone do not appear to be decisive determinants of susceptibility. The relatively high prevalence observed in this urban population underscores the ongoing epidemiological relevance of this parasite and highlights the importance of routine screening and preventive management strategies in companion animal practice.

CONFLICTS OF INTEREST

The authors report no conflicts of interest.

ACKNOWLEDGMENT

This manuscript is derived from the master's thesis of Bilal Deniz.

AUTHOR CONTRIBUTIONS

Idea/Concept: BD, ASK, VD
Supervision/Consultancy: BD, ASK
Data Collection and/or Processing: BD, ASK
Analysis and/or Interpretation: BD, ASK, VD
Writing the Article: ASK, VD
Critical Review: ASK, VD

REFERENCES

Acar A, Altınok Yipel F (2016). Factor related to the frequency of cat ear mites (*Otodectes cynotis*). *Kafkas Univ Vet Fak Derg*, 22(1), 75-78.

Al-Hosary A AT, Mostafa W (2022). Epidemiological study on feline otoacariasis with special reference for therapeutic trials. *Pak J Zool*, 54(2), 755–761.

Beugnet F, Bourdeau P, Chalvet-Monfray K et al. (2014). Parasites of domestic owned cats in Europe: co-infestations and risk factors. *Parasit Vectors*, 7, 291.

Bowman A (2014). Otodectes cynotis. Obtenido de American Association of Veterinary Parasitologists: https://www. aavp. org/wiki/arthropods/arachnids/astigmata/otodectes-cynotis.

Ceylan C, İder M, Evci A et al. (2025). Internal and external parasites prevalence of domestic cats in Konya province. *J Adv VetBio Sci Tech, 10*(1), 1–6.

Chen CL, Wang YM, Liu CF, Wang JY (2008). The effect of water-soluble chitosan on macrophage activation and the attenuation of mite allergen-induced airway inflammation. *Biomater,* 29, 2173–2182.

Curtis CF (2004). Current trends in the treatment of sarcoptes, cheyletiella and otodectes mite infestations in dogs and cats. *Vet Dermatol*, 15, 108–114.

Dinçer Ş, Cantoray R, Taşan E (1980). Elazığ sokak kedilerinde görülen iç ve dış parazitler ile bunların yayılış oranları üzerine araştırmalar. *Fırat Üniv Vet Fak Derg*, 5(1), 7–15.

El Dakhly KM, Bakry MA, Abdel Rahim MM, Arafa WM, Mohamed HI (2025). Insights into the prevalence and diagnosis of feline otoacariasis in Egypt. *J Parasit Dis*, 49(1), 193-206.

Gram D, Payton AJ, Gerig TM, Bevier DE (1994). Treating ear mites in cats: a comparison of subcutaneous and topical ivermectin. *Veterinary Medicine*, 89(12), 1122-1125.

Griffin CE (1993). Otitis externa and otitis media. In C. E. Griffin, K. W. Kwochka, & J. M. MacDonald (Eds.), *Current Veterinary Dermatology: The Science and Art of Therapy* (pp. 245–262). Mosby Year Book.

Jacobson LS (2002). Diagnosis and medical treatment of otitis externa in the dog and cat. *J S Afr Vet Assoc*, 73(4), 162–170.

Kavitha S, Venkatesan M, Nagarajan B, Thirunavukkarasu PS, Nambi AP (2013). Clinical management of feline otodectosis–a study of 11 patients. *Intas Polivet*, 14(2), 331–332.

Lefkaditis MA, Koukeri SE, Mihalca AD (2009). Prevalence and intensity of *Otodectes cynotis* in kittens from Thessaloniki area, Greece. *Vet Parasitol*, 163, 374–375.

Lopez RA (1993). Of mites and man. *J Am Vet Med Assoc*, 203(5), 606–607.

Maazi N, Jamshidi S, Hadadzadeh H (2010). Ear mite infestation in four imported dogs from Thailand.

Medleau L, Hnilica K (2006). Parasitic skin diseases. In *Small Animal Dermatology* (2nd ed., pp. 99–138). Saunders Elsevier.

Mimimoğlu M (1954). Ankara ilinde kedi parazitleri üzerine yapılan bir araştırma. *Ankara Üniv Vet Fak Derg*, 1(1), 1–10.

Nuttall T (2015). Otitis Externa: An Essential Guide to Diagnosis and Treatment. By Richard G. Harvey and Sue Paterson, CRC Press, London, 2014, pp. 162

Özkan C, Karaca M, Özdal N (2013). Van kedilerinde *Otodectes cynotis*'in tedavisinde selamectin kullanımının etkinliği. *Turkiye Parazitol Derg*, 37(4), 269–272.

Perego R, Proverbio D, Bagnagatti De Giorgi G et al. (2013). Prevalence of otitis externa in stray cats in northern Italy. *J Feline Med Surg*, 16, 483–490.

Russell R, Otranto D, Wall R (2013). Mites. In *Encyclopedia of Medical and Veterinary Entomology* (pp. 209–242). CABI.

Scott DW, Horn Jr RT (1987). Zoonotic dermatoses of dogs and cats. *Vet Clin North Am Small Anim Pract*, 17, 117–144.

Scott DW, Miller W, Griffin C (2001). Parasitic skin diseases. In *Muller & Kirk's Small Animal Dermatology* (6th ed., pp. 476–484). W. B. Saunders Company.

Sotiraki ST, Koutinas AF, Leontides LS, Adamama-Moraitou KK, Himonasa CA (2001). Factors affecting the frequency of ear canal and face infestation by *Otodectes cynotis* in the cat. *Vet Parasitol*, 96, 309–315.

Vickers TW, Clifford DL, Garcelon DK et al. (2015). Pathology and epidemiology of ceruminous gland tumors among endangered Santa Catalina Island foxes (*Urocyon littoralis catalinae*) in the Channel Islands, USA. *PLoS One*, 10(11), e0143211.

Wall R, Shearer D (2001). *Veterinary ectoparasites: biology, pathology and control* (2nd ed.). Wiley-Blackwell, USA.

Xhaxhiu D, Kusi I, Rapti D et al. (2009). Ectoparasites of dogs and cats in Albania. *Parasitol Res*, 105, 1577–1587.

Yang C, Huang HP (2016). Evidence-based veterinary dermatology: a review of published studies of treatments for *Otodectes cynotis* (ear mite) infestation in cats. *Vet Dermatol*, 27(4), 221.e1–e56.

Van Veterinary Journal

https://dergipark.org.tr/tr/pub/vanvetj

Cite this article as: **Öner S, Metli M (2026).** The Effects of Different Essential Oil Treatments on the Microbiological Quality Changes of Cold Strored Green Tiger Shrimp (*Penaeus semisulcatus*, De Hann 1844). *Van Vet J*, 37(1), 11-17. DOI: https://doi.org/10.36483/vanvetj.1768102

ISSN: 2149-3359 **Araştırma Makalesi** e-ISSN: 2149-8644

Soğukta Depolanan Yeşil Kaplan Karidesinin (*Penaeus semisulcatus*, De Hann 1844) Mikrobiyolojik Kalite Değişiklikleri Üzerinde Farklı Esansiyel Yağ Uygulamalarının Etkileri

Süleyman ÖNER[1] Murat METLİ[2,*]

[1] *Muğla Sıtkı Koçman Üniversitesi, Milas Meslek Yüksekokulu, Otel Lokanta ve İkram Hizmetleri Bölümü, 48200, Muğla, Türkiye*
[2] *Muğla Sıtkı Koçman Üniversitesi, Veteriner Fakültesi, Gıda Hijyeni ve Teknolojisi Anabilim Dalı, 48200, Muğla, Türkiye*

Geliş Tarihi: 19.08.2025 Kabul Tarihi: 27.01.2026

ÖZ

Kolay bozulabilme özelliğine sahip karideslerin raf ömrünü arttırabilmek amacıyla farklı esansiyel yağların (timol, karvakrol ve eugenol) vakum paketlenmiş ve soğukta depolanmış yeşil kaplan karidesleri (*Penaeus semisulcatus*, De Hann 1844) üzerinde mikrobiyolojik etkileri araştırılmıştır. %1 oranındaki timol, karvakrol, eugenolün daldırma yöntemiyle muamele edilen deney grupları ile kontrol grubu vakum paketlenerek soğukta (4±1 °C) depolanmıştır. Başlangıçta mikrobiyolojik (toplam mezofilik aerobik bakteri sayımı - TMAB, toplam mezofilik anerobik bakteri sayımı - TMANB, toplam koliform bakteri sayımı, toplam maya sayımı, toplam küf sayımı) ve besin değerleri (Ham protein, lipit tayini, kuru madde, kül tayini) analizleri yapılmıştır. Depolama sürecinde periyodik olarak 4., 8., 12., 16., 20. ve 24. günlerde mikrobiyolojik analizler yapılmıştır. Eugenolün TMAB, TMANB, toplam koliform, maya ve küf bakterilerine karşı en etkili esansiyel yağ asidi olduğu gözlenmiş, bunu timol, karvakrol takip etmiştir. Tüm sonuçlar göz önüne alındığında, hem kontrol grubu hem de deney gruplarının kendi aralarında ve depolama günleri arasında anlamlı istatistiksel fark tespit edilmiştir ($p<0.01$). Çalışma süresince mikrobiyolojik parametrelerin değişimine bakıldığında raf ömrü açısından en iyi mikrobiyal baskılamanın eugenol uygulanan grupta olduğu, sonra sırasıyla timol ve karvakrol uygulanan grupların geldiği gözlenmiştir. Su ürünlerinde bozulmanın yavaşlatılması amacıyla esansiyel yağ olarak başta eugenol olmak üzere timol ve karvakrol uygulamaları tavsiye edilmektedir.

Anahtar Kelimeler: *Esansiyel yağ asidi, Eugenol, Karides, Karvakrol, Mikrobiyolojik kalite, Timol.*

ABSTRACT

The Effects of Different Essential Oil Treatments on the Microbiological Quality Changes of Cold Stored Green Tiger Shrimp (*Penaeus semisulcatus*, De Hann 1844)

In order to extend the freshness and improve the shelf life of perishable shrimp samples, different essential oil treatments were applied to vacuum-packaged and refrigerated green tiger shrimp (*Penaeus semisulcatus*, De Hann 1844) samples. Experimental groups were treated with 1% thymol, carvacrol, and eugenol via immersion, and both treatment and control groups were placed in vacuum packs after day 0 samples were collected and stored at refrigerated temperatures (4±1 °C) for 24 days. During the storage period microbiological changes occurred in shrimp samples were examined Initial, microbiological (total mesophilic aerobic bacteria count - TMAB, total mesophilic anaerobic bacteria count - TMANB, total coliform bacteria count, total yeast count, total mold count) and nutritional aspects (crude protein, lipid determination, dry matter, ash determination) of shrimp samples were analyzed on the day 0 then microbiological analyses were performed on the 4th, 8th, 12th, 16th, 20th and 24th days of storage. Eugenol was observed to be the most effective essential fatty acid against TMAB, TMANB, total coliform, yeast and mold bacteria, followed by thymol and carvacrol. Considering all the results, a significant statistical difference was found between both the control and experimental groups and between storage days ($p<0.01$). When the changes in microbiological parameters were examined during the study period, it was observed that the best microbial suppression in terms of shelf life was in the group treated with eugenol, followed by the groups treated with thymol and carvacrol, respectively. To slow down spoilage in seafood, the application of essential oils, primarily eugenol, but also thymol and carvacrol, is recommended.

Keywords: *Carvacrol, Essential fatty acid, Eugenol, Microbiological quality Shrimp, Thymol.*

✉ *Corresponding author: muratmetli@gmail.com

GİRİŞ

Her gelişmiş canlı gibi insanların da sağlıklı bir yaşam sürdürebilmeleri için çeşitli gıda gruplarının içinde bulunduğu bir diyetle yeterli ve dengeli beslenmeleri gerekmektedir. Hayvansal kaynaklı gıdalar, dengeli beslenmenin en önemli ögelerindendir. Hayvansal gıdalar içinde de su ürünleri; düşük bağ doku oranı, kolay sindirilebilirlik, esansiyel aminoasit zenginliği, kalp ve damar sağlığı için önemi son yıllarda daha iyi anlaşılan çoklu doymamış yağ asitlerini önemli miktarda içermesiyle öne çıkmaktadır (Govzman ve ark. 2021).

Su ürünleri insan beslenmesinde geniş bir yelpazeye sahiptir ve balıklar su ürünleri içinde en çok tüketilen grubu oluşturmaktadır. Ancak karides gibi balık dışı su ürünleri de insan beslenmesinde önemli bir yer tutmaktadır. Tüm dünyada olduğu gibi Türkiye'de de karides çeşitleri, su ürünleri içinde lüks ürün olarak sınıflandırılır ve bu sayede ticari olarak su ürünlerinin önemli bir bileşenidir (Hınıslıoğlu ve ark. 2024). Türkiye İstatistik Kurumu'nun (TÜİK) derlediği verilere göre Türkiye'de 2024 yılında avcılık yoluyla 4467.3 ton, yetiştiricilik yoluyla da 20 ton karides üretilmiştir. Avlanan toplam karidesin 724 tonunu yeşil kaplan karidesi (Jumbo karides) oluşturmuştur.

Karidesin yenilebilir kısımları esansiyel aminoasit içeriği zengin, besleyici bir hayvansal gıdadır. Bağdoku oranının az ve besin unsurlarının basit yapıda olması karidesin sindirilebilirliğini arttırmasına rağmen, bozulabilirliğinin daha kolay olmasına da neden olmaktadır. Karides etinin basit yapıda olması ve serbest aminoasit miktarının kırmızı ete göre daha fazla olması bozulma yapıcı bakterilerin kolaylıkla faaliyet göstermesine olanak sağlayarak, avlanma sonrası gerekli hijyenik tedbirlerin alınmaması durumunda, depolama süresine ve depolama sıcaklığına da bağlı olarak hızlı bir bozulmaya neden olabilmektedir. Bu durumda hem mikrobiyolojik hem de yapısal enzimatik faaliyetlerin etkisiyle başta duyusal olmak üzere fiziksel, kimyasal değişimler ortaya çıkmakta, ürünün tüketilebilirliği azalmaktadır (Chakraborty 2025).

Karideslerin bozulmalarını önlemek ve raf ömrünü arttırabilmek amacıyla sentetik antimikrobiyaller kullanılması bir seçenek olarak düşünülebilir. Ancak sentetik antimikrobiyaller insan organizmasında istenmeyen sağlık sorunlarına neden olabilmesi nedeniyle, tüketiciler tarafından çok fazla tercih edilmemektedir. Bu nedenle gıda muhafazasında, raf ömrünü arttırmada ve gıda kaynaklı biyolojik tehlikelerin önlenmesinde, geleneksel olarak gıdaların duyusal özelliklerini iyileştirmede yardımcı madde olarak kullanılagelen baharatlar ve doğal aromatik bitkilerin kullanımı gittikçe yaygınlaşmaktadır. Gıdaların bozulmadan muhafaza edilebilmesinde doğal katkı maddelerinin kullanımı, bunların arasında da esansiyel yağların tercih edilmesi her geçen gün artmaktadır (Saeed ve ark. 2022).

Hayvansal gıdaların raf ömrünü arttırmak amacıyla kullanılabilen esansiyel yağlar arasında timol, karvakrol ve eugenol dikkati çekmektedir (Maurya ve ark. 2021). Timol, dünya mutfağında olduğu gibi Türk mutfağında da oldukça yaygın olarak kullanılan kekikten (*Thymus vulgaris*) ekstrakte edilen, bakteri, maya ve küfler üzerinde oluşturduğu antimikrobiyal etkiyle kullanım alanı gittikçe artan önemli bir esansiyel yağdır. Mikroorganizmaları inhibe etme etkisini, mikroorganizma hücre membranlarında yapısal ve işlevsel zarar oluşturarak göstermektedir (Escobar ve ark. 2020).

Karvakrol de kekikten elde edilen bir esansiyel yağ asididir. Karvakrol antibakteriyel ve antihelmintik özellikleri ile kullanım alanı bulmaktadır. Bunun yanı sıra ilaçların bileşiminde kullanılarak birçok hastalığın tedavisinde yararlanılmaktadır. Karvakrol genel olarak güvenli kabul edilen - Generally Recognized As Safe (GRAS) olarak sınıflandırılmıştır. Karvakrol toksin üretimini engelleyici etkisiyle gıda teknolojisinde önem kazanmıştır. Karvakrol bakteriyel membrana hasar vererek biyosidal özellik gösteren bir bileşiktir. Karvakrol, *Staphylococcus epidermis*, *Staphylococcus aureus*, *Klebsiella pneumonia*, *Escherichia coli*, *Streptococcus pneumonia*, *Proteus mirabilis*, *Serratia* spp., *Enterobacter* spp.'ye karşı iyi bir antibakteriyel etkiye sahip olmasının yanında *Aspergillus niger*, *Aspergillus flavus*, *Candida* spp., *Alternaria alternata*, *Trichoderma viride*, *Penicillium rubrum* ve dermatofitler dahil olmak üzere farklı mantarlar üzerinde antifungal etkileri vardır. Karvakrol timol ile birlikte kullanıldığında sinerjik etkiyle, gıda kaynaklı patojenlere karşı daha yüksek antibakteriyel kapasiteye ulaşabilmektedir (Imran ve ark. 2022).

Gıda muhafazasında kullanılması tavsiye edilen bir diğer doğal bileşik olan eugenol, birçok bitki türünde çeşitli konsantrasyonlarda bulunmasına rağmen, en fazla bulunduğu bitki, karakteristik aromasından da sorumlu olduğu karanfil ağacı (*Syzygium aromaticum)*'dır. Eugenol, çok çeşitli Gram pozitif ve Gram negatif bakteri ve mantarlar ile *Giardia lamblia*, *Fasciola gigantica* ve *Haemonchus contortus* gibi bir dizi parazit de dahil olmak üzere birçok insan patojenine karşı antimikrobiyel etkiler göstermiştir. Dahası, eugenol karbon tetraklorür (CCl_4) kaynaklı hepatotoksisiteye karşı da koruma sağlamaktadır. Eugenol, kendine has bir kokuya sahip olması, öteden beri gıdalarda baharat şeklinde kullanılması yanında önemli bir antioksidan etkiye de sahiptir. FDA tarafından da GRAS olarak sınıflandırılmıştır (Ulanowska ve Olas 2021).

Bu çalışmada, vakum paketlenerek soğukta depolanan karideslere, farklı esansiyel yağlar uygulanmasının mikrobiyolojik etkilerinin araştırılması amaçlanmıştır.

MATERYAL VE METOT

Bu çalışma, Hayvan Deneyleri Etik Kurullarının Çalışma Usul ve Esasları Hakkında Yönetmeliğin 8. Maddesinin (8). Fıkrasının k) bendinin 2. alt bendi uyarınca HADYEK'in iznine tabi değildir. Bu çalışmada elde edilen veri, bilgi ve belgeler akademik ve etik kurallar çerçevesinde elde edilmiştir.

Çalışmada; İskenderun Körfezi'nde avlanma usulü olarak trol ağlarıyla avlandığı bilgisine ulaşılan karidesler (*Penaeus semisulcatus*), İskenderun Balıkçı Barınağı'ndan satın alındıktan sonra içinde buz bulunan strafor kutularla laboratuvara transfer edilmiştir. Mustafa Kemal Üniversitesi Veteriner Fakültesi Besin Hijyeni ve Teknolojisi Anabilim Dalı Uygulama ve Araştırma Laboratuvarı'nda hijyenik şartlarda kabuklarından ayrılarak temizlenmiş, distile suyla yıkandıktan sonra her bir grup 3.75 kg olacak şekilde 4 gruba ayrılmıştır. Çalışmada kullanılan esansiyel yağların çözdürülmesi için %10 etil alkol dilüsyonu (1:9 oranında alkol /distile su) kullanılmıştır. Kontrol grubu esansiyel yağ içermeyen %10 etil alkol dilüsyonu ile muamele edilmiştir.

Çalışma tasarımında karidesler; kekik kaynaklı karvakrol ve timol ile karanfil kaynaklı eugenol esansiyel yağlarının %1 oranındaki çözeltileri ile daldırma şeklinde 5 dk muamele edilmişlerdir. Bu amaçla karidesler %1 timol uygulanan grup (I. Grup), %1 karvakrol uygulanan grup

(II. Grup), %1 eugenol uygulanan grup (III. Grup) olarak deney gruplarına ve IV. Grup olarak ise kontrol grubuna ayrılmışlardır. Timol için Sigma Aldrich T0501, karvakrol için Sigma Aldrich 282197 ve eugenol için Sigma Aldrich E51791 ticari esansiyel yağlarının %1 oranındaki çözeltileri kullanılmıştır. Hem deney grupları hem de kontrol grubu için kullanılan karides örnekleri, 100'er g' lık polyamid yapıda vakum poşetlere yerleştirilmiş ve Laica SPA Viale del Lavaro, 1036020 Barbarano - Vicenza Italy marka - model vakum makinesi kullanılarak vakum paketleme yapılmıştır. Üç tekerrürlü analiz yapılacak sayıda hazırlanan örnekler +4 °C'ye sahip buzdolabı ortamında depolanmış ve mikrobiyolojik analizler 0., 4., 8., 12., 16., 20., 24. günlerde her tekrar iki paralleli olacak şekilde yapılmış, raf ömürleri incelenmiştir.

Besinsel özelliklerin belirlendiği biyokimyasal analizlerden ham protein analizi Association of Official Analytical Chemists (AOAC, 1984)'de belirtilen metoda göre, ham yağ analizi Hanson ve Olley (1963) tarafından modifiye edilen, Bligh ve Dyer metoduyla (1959), kuru madde ve ham kül analizi Mattissek ve ark. (1988)'nın bildirdiği yönteme göre, nem içeriği Ludorff ve Meyer (1973)'de belirtilen metoda göre yapılmıştır.

Mikrobiyolojik analiz olarak, TMAB, TMANB, toplam koliform bakteri sayımı ile maya-küf sayımı yapılmıştır. Koloni oluşturma birimleri log10 kob/g olarak hesaplanmıştır. Mikrobiyolojik analizlerde TMAB sayımı için Plate Count Agar (PCA), TMANB sayımı için Anaerobik Agar (AA), toplam koliform bakteri sayımı için Violed Red Bile Agar (VRB), maya ve küf sayımı için Potato Dextrose Agar (PDA) kullanılmıştır (ICMSF, 1986; ISO 4832, 2006).

Korelasyon ve standart sapma hesaplamalarında, her bir depolama günü ve deney gruplarının üç tekerrüre uygun olarak karşılaştırmaları yapılmıştır. Kimyasal analizlerin verileri SPSS 16 istatistik programında Duncan çoklu karşılaştırma testi ile işlenmiştir.

BULGULAR

Çalışma materyali olarak kullanılan *Penaus semisulcatus*'un besin değerleri Tablo 1'de verilmiştir. Protein, ham yağ, kuru madde, ham kül ve nem oranları sırasıyla %20.13, %1.13, %23.67, %2.06, %76.39 olarak bulunmuştur.

Çalışmanın ilk günü olan 0. günde tüm gruplar için TMAB değerleri 3.84-3.85 log kob/g aralığında saptanmıştır (Tablo 2). Depolama süresince tespit edilen TMAB sayılarının tüm gruplarda arttığı belirlenmiştir. En yüksek değere kontrol grubunda 24. günde 8.28 log kob/g değeri ile ulaşılmış, bunu sırasıyla karvakrol 7.73 log kob/g, timol 7.41 log10kob/g ve eugenol 7.17 log kob/g grupları takip etmiştir. Özellikle deney gruplarının depolama günleri arasında istatistiksel olarak farklılıklar ($p<0.01$) olduğu gibi hem deneysel grupların kendi arasında hem de kontrol grubu arasında istatistiksel farklılıklar gözlenmiştir ($p<0.01$).

Tablo 1: Taze karides etinin besin kompozisyonu.

Table 1: Nutritional composition of fresh shrimp meat.

Besin değerleri	(%) Ortalama ± Standart sapma
Protein	20.13 ± 0.41
Lipid	1.13 ± 0.11
Kuru madde	23.67 ± 0.57
Kül	2.06 ± 0.24
Nem	76.39 ± 1.42

Elde edilen TMANB sayılarında en yüksek değere kontrol grubunun 24. gününde 7.24 log kob/g ile ulaşılmış; timol, karvakrol ve eugenol gruplarında da yine 24. günde sırasıyla 6.34 log kob/g, 6.59 log kob/g ve 6.09 log kob/g sonuçları elde edilmiştir (Tablo 3). Hem kontrol hem de deney gruplarında depolamanın ilerleyen günlerinde TMANB sayısında artış gözlenmiştir.

Toplam koliform bakteri sayımında en küçük değere <2. log10 kob/g değeri ile 0. günde ulaşılmıştır (Tablo 4). 0. gün haricinde depolamanın en düşük koliform değerine de eugenol grubunda rastlanmıştır. Depolama süresince de tüm gruplarda artış gözlenmiştir. En yüksek toplam koliform değerine kontrol grubunda erişilmiş, kontrol grubunu da karvakrol, timol grupları izlemiştir. Tüm uygulama grupları ve günleri arasında istatistiksel olarak farklılıklar belirlenmiştir ($p<0.01$). Bu sonuçlara göre, eugenol ve timolün antibakteriyel özelliklerinin öne çıktığı kanısına varılmıştır.

Depolama süresince hem kontrol hem de uygulama gruplarında maya ve küf değerlerinde artış tespit edilmiştir (Tablo 5 ve 6). Maya küf artışına karşı en etkili uygulamanın Eugenol olduğu gözlemlenmiş, bunu da timol, karvakrol etkinliği takip etmiştir. Uygulama grupları ve günleri arasında istatistiksel olarak farklılıklar bulunmuştur ($p<0.01$).

Tablo 2: Depolama süresince karides etinde TMAB sayımı (ortalama±standart sapma log kob/g).

Table 2: TMAB count in shrimp meat during storage (mean±standard deviation log cfu/g).

Gün	GRUPLAR			
	Kontrol	**Timol**	**Karvakrol**	**Eugenol**
0	3.84±0.03^{ay}	3.85±0.07 ^{av}	3.84±0.07 ^{av}	3.85±0.05 ^{av}
4	5.69±0.14 ^{av}	4.28±0.08 ^{cu}	4.78±0.12^{bu}	4.20±0.10 ^{cu}
8	6.23±0.15 ^{au}	5.29±0.14 ^{bt}	5.42±0.11 ^{bt}	5.10±0.08 ^{ct}
12	6.45±0.20 ^{at}	5.34±0.09 $^{b\ ct}$	5.51±0.15 ^{bt}	5.17±0.10 ^{ct}
16	6.77±0.13 ^{as}	5.58±0.13 ^{cs}	5.86±0.11 ^{bs}	5.33±0.14^{ds}
20	7.29±0.17 ^{ar}	5.87±0.09 ^{cr}	6.29±0.12 ^{br}	5.84±0.11 ^{cr}
24	8.28±0.18 ^{ap}	7.41±0.09 ^{cp}	7.73±0.18 ^{bp}	7.17±0.13 ^{dp}

Aynı sütunda farklı harflerle belirtilen (a-d) ortalamalar arasında önemli fark ($p<0.01$) vardır. Satırlar arasında belirtilen farklı harfler (p,r,s,t,u,v,y) her bir grubun depolama süresince farklılıklarını göstermektedir ($p<0.01$).

Tablo 3: Depolama süresince karides etinde TMANB sayımı (ortalama±standart sapma log kob/g).
Table 3: TMANB count in shrimp meat during storage (mean±standard deviation log cfu/g).

Gün	GRUPLAR			
	Kontrol	Timol	Karvakrol	Eugenol
0	3.33±0.02^{av}	3.35±0.03 ^{ay}	3.31±0.06 ^{av}	3.34±0.06 ^{ay}
4	5.59±0.17 ^{au}	3.89±0.09^{cv}	4.28±0.13 ^{bu}	3.7±0.08^{dv}
8	5.85±0.10 ^{at}	4.72±0.08 ^{cu}	4.96±0.13 ^{bt}	4.64±0.09 ^{cu}
12	6.24±0.15 ^{as}	5.04±0.14 ^{ct}	5.50±0.10 ^{bs}	5.13±0.15 ^{ct}
16	6.36±0.17 ^{as}	5.41±0.15 ^{cbs}	5.55±0.12 ^{cbs}	5.32±0.07 ^{cs}
20	6.68±0.22 ^{ar}	5.82±0.09 $^{c\ r}$	6.33±0.20 ^{br}	5.74±0.16 ^{cr}
24	7.24±0.20 ^{ap}	6.34±0.12 ^{cp}	6.59±0.27 ^{bp}	6.09±0.14 ^{dp}

Aynı sütunda farklı harflerle belirtilen (a-d) ortalamalar arasında önemli fark (p<0.01) vardır. Satırlar arasında belirtilen farklı harfler (p,r,s,t,u,v,y) her bir grubun depolama süresince farklılıklarını göstermektedir (p<0.01).

Tablo 4: Depolama süresince karides etinde toplam koliform bakteri sayımı (ortalama±standart sapma log kob/g).
Table 4: Total coliform bacteria count in shrimp meat during storage (mean±standard deviation log cfu/g).

GÜNLER	GRUPLAR			
	Kontrol	Timol	Karvakrol	Eugenol
0	< 2.0^{ay}	< 2.0^{ay}	< 2.0^{ay}	< 2.0^{ay}
4	3.22±0.14^{av}	2.14±0.10^{cu}	2.62±0.15^{bv}	< 2.0^{av}
8	3.57±0.11^{au}	2.52±0.10^{ct}	2.90±0.15 ^{bu}	2.58±0.10^{cu}
12	4.20±0.16 ^{at}	3.30±0.14^{cs}	3.56±0.11 ^{bt}	3.12±0.12^{dt}
16	4.41±0.22^{as}	3.60±0.10^{cr}	4.18±0.14 ^{bs}	3.52±0.12^{cs}
20	4.66±0.17^{ar}	4.42±0.14^{bp}	4.37±0.25 ^{br}	4.13±0.10^{cr}
24	4.96±0.27^{ap}	4.34±0.14^{cbp}	4.65±0.15 ^{cbp}	4.43±0.17^{cp}

Aynı sütunda farklı harflerle belirtilen (a-d) ortalamalar arasında önemli fark (p<0.01) vardır. Satırlar arasında belirtilen farklı harfler (p,r,s,t,u,v,y) her bir grubun depolama süresince farklılıklarını göstermektedir (p<0.01).

Tablo 5: Depolama süresince karides etinde toplam maya sayımı (ortalama±standart sapma log kob/g).
Table 5: Total yeast count in shrimp meat during storage (mean±standard deviation log cfu/g).

GÜNLER	GRUPLAR			
	Kontrol	Timol	Karvakrol	Eugenol
0	3.36±0.02^{au}	3.35±0.03 ^{av}	3.36±0.02 ^{av}	3.37±0.02 ^{av}
4	4.51±0.15 ^{at}	3.82±0.08 ^{cu}	4.03±0.05^{bu}	3.74±0.06^{cu}
8	5.33±0.22 ^{as}	4.58±0.13 ^{bt}	4.56±0.17 ^{bt}	4.23±0.15 ^{ct}
12	5.69±0.20 ^{ar}	5.12±0.11 ^{bs}	5.14±0.16 ^{bs}	4.79±0.14 ^{cs}
16	6.28±0.25 ^{ap}	5.36±0.09 ^{cbr}	5.50±0.17 $^{b\ cr}$	5.21±0.14 ^{cr}
20	6.42±0.32^{ap}	5.69±0.16 ^{bp}	5.64±0.18 ^{br}	5.37±0.19 ^{cr}
24	6.70±0.24 ^{ap}	5.82±0.23 ^{cp}	6.10±0.23 ^{bp}	5.56±0.12^{dp}

Aynı sütunda farklı harflerle belirtilen (a-d) ortalamalar arasında önemli fark (p<0.01) vardır. Satırlar arasında belirtilen farklı harfler (p,r,s,t,u,v,y) her bir grubun depolama süresince farklılıklarını göstermektedir (p<0.01).

Tablo 6: Depolama süresince karides etinde toplam küf sayımı (ortalama±standart sapma log kob/g).
Table 6: Total mold count in shrimp meat during storage (mean±standard deviation log cfu/g).

GÜNLER	GRUPLAR			
	Kontrol	Timol	Karvakrol	Eugenol
0	3.46±0.03^{au}	3.44±0.02 ^{av}	3.45±0.03 ^{ay}	3.45±0.03 ^{av}
4	4.46±0.24 ^{at}	3.75±0.12^{cu}	4.21±0.18^{bv}	3.83±0.10 ^{cu}
8	5.32±0.27 ^{as}	4.55±0.17 ^{ct}	4.80±0.13 ^{bu}	4.30±0.14^{dt}
12	5.75±0.18 ^{ar}	5.06±0.11 ^{cs}	5.28±0.15 ^{bt}	4.90±0.17 ^{cs}
16	5.91±0.18 ^{ap}	5.37±0.20 ^{cbr}	5.55±0.19 ^{bcs}	5.18±0.10 ^{cr}
20	6.35±0.23 ^{ap}	5.48±0.25 ^{cbr}	5.76±0.13 ^{bcr}	5.55±0.18 ^{cp}
24	6.58±0.27 ^{ap}	5.95±0.15 ^{cp}	6.35±0.16 ^{bp}	5.69±0.19 ^{dp}

Aynı sütunda farklı harflerle belirtilen (a-d) ortalamalar arasında önemli fark (p<0.01) vardır. Satırlar arasında belirtilen farklı harfler (p,r,s,t,u,v,y) her bir grubun depolama süresince farklılıklarını göstermektedir (p<0.01).

TARTIŞMA VE SONUÇ

Uzun süreli depolama ömrüne sahip, albenisi yüksek taze karides üretmek için tuzlama, soğutma, dondurma, kurutma, tütsüleme, konserveleme, güneşte kurutma, fermente etme, kızartma ve ızgara gibi çeşitli kombinasyonlarda düşük-orta ve yüksek sıcaklıkta işleme yöntemleri kullanılır. Farklı teknikler kullanan ve farklı uygulamalara sahip olan tüm bu işleme yöntemleri, dondurma, ısıtma, oksidasyon ve yüksek tuz konsantrasyonlarına maruz bırakma nedeniyle fiziksel ve kimyasal değişikliklere neden olduğundan, balığın organoleptik, fiziksel, kimyasal ve besinsel özellikleri üzerinde önemli bir etkiye sahiptir (AlFaris ve ark. 2022).

Çalışmamızda yeşil kaplan karidesleri raf ömürlerini uzatmak amacıyla %1 konsantrasyonunda timol, karvakrol ve eugenol ile muamele edilmiş ve 24. güne kadar vakum pakette soğuk ortamda (+4 ℃) depolanmıştır. Besinsel değerlerini tespit etmek amacıyla 0. günde yapılan kimyasal analizlerde karideslerin protein değeri %20.13 olarak bulunmuştur. AlFaris ve ark. (2022) taze yeşil kaplan karidesinin (*Penaeus semisulcatus*) protein içeriğini %18.39 bulmuşlardır. Değişik rasyonlarla karides beslemesi yapan Xie ve ark. (2023) çalışma sonunda *Litopenaeus vannamei* türü karideslerde protein içeriğinin %14.59 ile 15.88 arasında olduğunu tespit etmişlerdir. Li ve ark. (2021) *Litopenaeus vannamei* türü karideslerin alt türlerinin besin bileşimlerini karşılaştırdıkları araştırmalarında protein miktarını % 21.1 ile %22.3 arasında bulmuşlardır. Talukdar ve ark. (2020) 6 çeşit rasyon reçetesi uyguladıkları *Litopenaeus vannamei* türü karides yavrularında protein oranlarını % 14.42 ile %15.82 arasında bulmuşlardır.

Burada rapor edilen çalışmada karideslerin ham yağ değeri %1.13 bulunmuştur. Talukdar ve ark. (2020) besleme performansını merak ettikleri *Litopenaeus vannamei* türü karides yavrularında ham yağ oranının %1.99 ile %2.32 arasında bulmuşlardır. Li ve ark. (2021) akuakültüre aldıkları *Litopenaeus vannamei* türü karideslerin 4 alt türünün besin bileşimlerini karşılaştırdıkları araştırmalarında ham yağ miktarını %0.8 ile %1.1 arasında bulmuşlardır. AlFaris ve ark. (2022) taze yeşil kaplan karidesinin (*Penaeus semisulcatus*) gaz kromatografi yöntemiyle yaptıkları analizle yağ içeriğini %3.75 bulmuşlardır. Değişik rasyon reçeteleri uygulayarak karides beslemesi yapan Xie ve ark. (2023) çalışma sonunda *Litopenaeus vannamei* türü karideslerde yağ içeriğini %2.38 ile 2.49 arasında tespit etmişlerdir.

Çalışmamızın 3. besin değeri olan karideslerin ham kül değeri %2.06 olarak tespit edilmiştir. Hindistan'dan Talukdar ve ark. (2020) besleme performansını araştırdıkları *Litopenaeus vannamei* türü karides yavrularına uyguladıkları 60 günlük rasyon programı sonunda ham kül oranının test ettikleri gruplar arasında %4.42 ile %5.11 arasında değiştiğini gözlemişlerdir. Çinli araştırmacılardan Li ve ark. (2021) akuakültüre uygunluklarını inceledikleri *Litopenaeus vannamei* türü karideslerin 4 alt türünün besin bileşimlerini karşılaştırdıkları araştırmalarında ham kül miktarını %1.6 ile %1.7 arasında bulmuşlardır. AlFaris ve ark. (2022) burada rapor edilen çalışmanın da konusu olan taze yeşil kaplan karidesinin (*Penaeus semisulcatus*) ham kül içeriğini %2.81 bulmuşlardır. Yine Çin'den, uyguladıkları protein içeriği farklı rasyon reçeteleri ile karides beslemesi yapan Xie ve ark. (2023) çalışma sonunda *Litopenaeus vannamei* türü karideslerde ham kül miktarını %3.27 ile 3.36 arasında tespit etmişlerdir.

Burada sonuçları tartışılan çalışmada incelenen karideslerin nem ve kuru madde içerikleri sırasıyla %76.39 ve %23.67 olarak tespit edilmiştir. Talukdar ve ark. (2020) besleme performansını inceledikleri *Litopenaeus vannamei* türü karides yavrularında nem oranını %75.46 ile %75.81 ve kuru madde oranını %24.19 ile %24.54 arasında bulmuşlardır. Li ve ark. (2021) akuakültüre aldıkları *Litopenaeus vannamei* türü karideslerin 4 alt türünün besin bileşimlerini karşılaştırdıkları araştırmalarında nem oranını %74.6 ile % 76.5 ve kuru madde oranını %23.5 ile %25.4 arasında bulmuşlardır AlFaris ve ark. (2022) taze yeşil kaplan karidesinin (*Penaeus semisulcatus*) nem ve kuru madde içeriğini sırasıyla %73.77 ve %26.23 arasında bulmuşlardır. Değişik rasyon reçeteleri uygulayarak karides beslemesi yapan Xie ve ark. (2023) çalışma sonunda *Litopenaeus vannamei* türü karideslerde nem oranını %77.77 ile %78.53 ve kuru madde oranını %21.47 ile %22.23 arasında tespit etmişlerdir.

Diğer araştırıcıların yapmış oldukları çalışmalar ve burada sunulan çalışmanın besin bileşimiyle ilgili sonuçları genel olarak karşılaştırıldığında birbirlerine çok yakın veriler olduğu gibi farklı verilerin de elde edildiği dikkati çekmektedir. Aynı türler incelenmiş olsa da besin değerindeki bu farklılıkların, karideslerin avcılık veya akuakültür yoluyla elde edilmesi, sezonsal değişiklikler, karideslerin göç, beslenme durumu, büyüklükleri ve farklı analiz metodlarının kullanılması gibi çok çeşitli faktörler tarafından oluşturabileceği düşünülmektedir.

Araştırmanın sonucunda elde edilen mikrobiyolojik sonuçlar irdelendiğinde tüm mikroorganizma gruplarında başlangıç yükünün normal hatta iyi hijyenik sınırlarda olmasına rağmen depolamanın ilerleyen günlerinde gruplara göre değişen artışlar gözlenmiştir. Çalışmanın hipotezine yönelik beklentiye uygun olarak deneysel gruplarda özellikle de eugenol ve timol uygulamasının yapıldığı gruplarda belirgin bir antibakteriyel etki gözlenmiştir. Su ürünlerinde mikrobiyal bozulmaya, canlının yaşam alanı dâhil, avlanma, ürün işleme süreçlerinde bulaşan mikroorganizmaların aktiviteleri sebep olmaktadır. Ancak bozulma yapıcı mikroorganizmaların asıl kaynağı su ürününün avlandığı ya da yetiştirildiği sudur. Su hayvanı canlılığını devam ettirirken, deri, solungaç gibi dış yüzeyi ve bağırsaklarındaki bakterilerin, su ürününün tüketilebilir kısımlarına geçmesi söz konusu değildir. Ancak post mortem dönemde canlı savunma sisteminin ortadan kalkması ve ortam koşullarının etkisiyle bozulma başlar (Erdem ve ark. 2022)

Çalışmamızın mikrobiyolojik parametre sonuçlarının tartışmasını yapabilmek için literatürde yeteri kadar benzer çalışmaya rastlanmamıştır. Bu nedenle aynı mikrobiyolojik parametreler ve test edilen muhafaza yöntemleri olmasa da benzer tarafları dikkate alınarak tartışılmaya çalışılmıştır.

He ve ark. (2022) dezenfektan etkili hafif asidik elektrolize su (SAEW) kullanarak elde ettikleri buz içinde sakladıkları *Penaeus vannamei* türü karideslerin 7 günlük depolama sürecinde TMAB sayısını analiz etmişler ve başlangıçta 4.8 log kob/g olan mikrobiyal yükün 7. günde 3 log kob/g'ın altına düştüğünü göstermişlerdir. Mousavi ve ark. (2022) *Litopenaeus vannamei* türü karideslerin raf ömrünü ve muhafaza süresini arttırmak amacıyla kayan ark deşarj cihazı ile termal olmayan plazma üreterek karidese uygulamışlar, tekniğin uygulanması esnasında kullanılan argon gazı oranı %100 olduğunda TMAB sayısını 1.2 log kob/g, %50 olduğunda ise 5.41 log kob/g olarak tespit

etmişlerdir. Babaei ve ark. (2024) çinko oksit nanopartiküllü jelatin/aljinat kompozit kaplamalar kullanarak *Litopenaeus vannamei* türü karideslerin buzdolabı sıcaklığındaki raf ömrünü uzatma amacıyla yaptıkları deneysel çalışmada TMAB değerini, 0. günde 3.3 log kob/g, bozulma belirtilerinin başladığı 7. günde de 7 log kob/g'ın üzerinde bulmuşlardır. Osanloo ve ark. (2023) *Litopenaeus vannamei* türü karideslerin buzdolabı sıcaklığında bozulmasını önlemek ve raf ömrünü uzatmak amacıyla *Zataria multiflora* ve *Cuminum cyminum* baharatlarından elde edilen esansiyel yağları (EO) içeren aljinat sodyum nanopartikülleri ile kaplayarak 15 günlük süreyle depolamışlar ve başlangıçta 2 log kob/g olan TMAB değerinin, depolama sonunda kontrol grubunda 4 log kob/g'a çıktığını, deney grubunda ise 3 log kob/g olduğunu rapor etmişlerdir.

Gram ve ark. (1987) MAP ile paketledikleri ürünlerde mikrobiyal çoğalmanın durduğunu ve mikrobiyal yükte azalma olduğunu tespit etmişlerdir. Kabuksuz karideslerin soğukta ve su sıcaklığında depolanması sırasında, bozulmada en güçlü etken olarak H_2S inhibe edici anaerobik bakteri türlerinin olduğu düşünülmüştür. Balığın bozulma sınırı, 6 log10 kob/g miktardaki H_2S indirgeyen anaerobik bakteri sayısı olarak belirlenmiştir. Kostaki ve ark. (2009), levrek filetosunu modifiye atmosfer paketleyerek ve kekik yağı ilave ederek +4 °C'de 21 gün süreyle depolamışlar ve raf ömrü üzerine çalışmalarda bulunmuşlardır. H_2S indirgeyen *S.putrefaciens* gibi anaerobik bakteriler çalışmanın başında 10^2 kob/g değeri ile kritik limitin altında tespit edilmiştir. Sonrasında ise 7. günde kontrol grubu değeri 6 log kob/g'a yükselmiştir. Can ve ark. (2007) ise eugenolün farklı konsantrasyonlarıyla muamele ettikleri vakum paketlenmiş aynalı sazan filetolarını buzdolabı ortamında depolayarak bu kombine uygulamanın raf ömrü üzerine antimikrobiyal etkisini incelemişlerdir. %1 eugenol uygulamasının 7. gününde TMANB sayısını 6.71 log kob/g ve 14. gündeki 7.25 log kob/g olarak tespit etmişlerdir.

Sultana ve ark (2021) Bangladeş'te geleneksel ve gelişmiş olarak sınıfladıkları karides çiftliklerinden aldıkları su örneklerinde fekal koliform sayısını ortalamalarını en düşük 2.69 log kob/g, en yüksek 4.05 log kob/g olarak tespit etmişlerdir. Elbashir ve ark. (2023) ABD Maryland Eyaletinde 4 ayrı satış noktasından aldıkları, karides örneklerinden ithal olanların %63.3'ünde yerli olanların da %8,2'sinde toplam koliform pozitif olarak tespit etmişlerdir. Nakamura ve ark. (2022) Bangkok'ta bir halk pazarından aldıkları 19 adet ve bir süpermarketten aldıkları 8 adet bir tür geleneksel Tayland fermente karides ezmesi olan kapide fekal koliform varlığını araştırmışlar; halk pazarı örneklerinin 6'sında süpermarket örneklerinin 1'inde pozitif sonuca ulaşmışlardır. Das ve ark. (2020) Hindistan'da inceledikleri 17 karides örneğinin hepsinde fekal koliforma rastlamışlardır.

Brezilya'dan Freitas ve ark (2020) kuru tuzlu karides örneklerinde yaptıkları maya-küf analizinde en düşük 2.00 log kob/g en yüksek 6,01 log kob/g toplam maya-küf sayısını tespit etmişlerdir. Nasser ve Amin (2025), mikro dalga kullanarak kuruttukları ve kraker haline getirdikleri karides örneklerinin hiçbirinde maya–küf tespit edememişlerdir. Marasinghe (2022) ve ark. *Penaeus monodon* türü karideslerin raf ömrünü uzatmak amacıyla 1, 2, 3, 5 ve 10 kGy dozlarda ışınlama yapmışlar, kontrol grubunda ve 1 kGy dozunda ışınlama yapılan grupta sırasıyla 4.97 log kob/g ve 2.87 log kob/g maya–küf tespit ettikleri halde diğer gruplarda hiç maya–küf üremesi gözlemleyememişlerdir.

Çalışmamızda test edilen timol, karvakrol ve eugenol esansiyel yağ asitlerinin karideslerin bozulmasında ve hijyenik kalitesinde önemli rol oynayan mikrobiyolojik parametreler üzerindeki etkileriyle dünyada yapılan benzer çalışmaların sonuçları karşılaştırıldığında yakın sonuçların olduğu gibi çok farklı sonuçların da olduğu gözlemlenmektedir. Bunun nedeninin karideslerin çok çeşitli yollarla istihsali (avcılık, akuakültür), karides materyalinin taze veya ürüne dönüştürülmüş olmaları, karides türlerinin farklı olması, test edilen muhafaza usullerinin çok farklı yöntemler olması (ışınlama, mikrodalga uygulaması, MAP, farklı esansiyel yağ asitlerinin kullanımı, plazma uygulaması, çeşitli ürün kaplama yöntemlerinin kullanılması vb.) satış noktalarının hijyenik kalitesinin ve manüplasyonların çok farklı olması olabilir.

Çalışma süresince mikrobiyolojik parametrelerin değişimine bakıldığında raf ömrü açısından en iyi mikrobiyal baskılamanın eugenol uygulanan grupta olduğu, sonra sırasıyla timol ve karvakrol uygulanan grupların geldiği gözlenmiştir. Su ürünlerinde bozulmanın yavaşlatılması amacıyla esansiyel yağ olarak başta eugenol olmak üzere timol ve karvakrol uygulamaları tercih edilebilir. Bundan sonra yapılacak çalışmalarda farklı gaz oranlarını içeren modifiye gaz paketleme ile kombine, farklı dozların uygulandığı ve her yörenin kendi damak tadına yakın olan esansiyel yağlar kullanılarak, daha düşük sıcaklık derecesinde daha uzun süreli depolama denemeleri yapılabilir.

ÇIKAR ÇATIŞMASI

Yazarlar bu çalışma için herhangi bir çıkar çatışması olmadığını beyan ederler.

TEŞEKKÜR VE BİLGİLENDİRME

Bu araştırma, Hatay Mustafa Kemal Üniversitesi Bilimsel Araştırma Projeleri Koordinatörlüğü tarafından "1004 D 0103" numaralı proje kapsamında finanse edilmiştir.

Bu çalışma, yazar Süleyman ÖNER'in doktora tezinin kamuoyuna açık olarak savunulmuş halidir.

Araştırmanın tamamlanmasında verdiği danışmanlık için Prof. Dr. Yasemin BİRCAN YILDIRIM'a teşekkür ederiz.

YAZAR KATKILARI

Fikir/Kavram: SÖ
Denetleme/Danışmanlık: MM
Veri Toplama ve/veya İşleme: SÖ
Analiz ve/veya Yorum: SÖ, MM
Makalenin Yazımı: MM
Eleştirel İnceleme: SÖ, MM

KAYNAKLAR

AlFaris NA, Alshammari GM, AlTamimi JZ et al. (2022). Evaluating the effects of different processing methods on the nutritional composition of shrimp and the antioxidant activity of shrimp powder. *Saudi J Biol Sci*, 29(1), 640–649.

AOAC (1984). Official Methods of Analysis. 14th edn. Association of Analytical Chemists, Washington DC, USA.

Babaei S, Mojarrad M, Zamir TR et al. (2024). Enhancing the shelf life of white leg shrimp (*Litopenaeus vannamei*) coated with alginate/gelatin incorporated with zinc oxide nanoparticles during refrigerator storage. *J Food Meas Charact*, 18, 6829–6842.

Bligh GE, Dyer FW. (1959). A rapid method of total lipid extraction and purification. *Can J Biochem Physiol*, 37, 911-917.

Can ÖP, Arslan A, Özdemir P. (2007). Eugenolün çiğ balık filetolarının muhafaza süresi üzerine etkisi. *Fırat Üniversitesi Doğu Araştırmaları Dergisi*, 5(2), 125-128.

Chakraborty, K. (2025). Recent Advances in Shrimp Nutrition and the Nutritional Significance of Shrimp to Human Health. Singh, P., Singh, A., Tyagi, A., Benjakul, S. (Eds) Shrimp Culture Technology (pp. 313-339). Springer, Singapore.

Das O, Lekshmi M, Kumar S, Nayak BB. (2020). Incidence of norovirus in tropical seafood harbouring fecal indicator bacteria. *Mar Pollut Bull*, 150, 110777.

Elbashir S, Jahncke M, DePaola A. et al. (2023). Prevalence and abundance of bacterial pathogens of concern in shrimp, catfish and tilapia obtained at retail stores in Maryland, USA. *Pathogens*, 12(2), 187.

Erdem ME, Tunçtaş N, Köstekli B, Keskin İ. (2022). Su ürünlerinde kullanılan paketleme yöntemleri: Vakum paketleme, MAP, biosensörler, oksijen emici etiketler. *J Anatol Env Anim Sci*, 7(2), 128-137

Escobar A, Perez M, Romanelli G, Blustein G. (2020). Thymol bioactivity: A review focusing on practical applications. *Arab J Chem,* 13, 9243–9269.

Freitas J, Pereira Neto LM, Silva TIB et al. (2020). Counting and identification of molds and yeasts in dry salted shrimp commercialized in Rio Branco, Acre, Brazil. *Food Sci Technol Campinas*, 41(Suppl. 1), 284-289.

Govzman S, Looby S, Wang X, Butler F, Gibney ER (2021). A systematic review of the determinants of seafood consumption. *Br J Nutr*, 126(1), 66–80.

Gram L, Trolle G, Huss HH (1987). Detection of specific spoilage bacteriafrom fish stored at low 0°C and high 20°C temperatures. *Int J Food Microbiol,* 4, 65–72

Hanson SWF ve Olley J. (1963). Application of the Bligh and Dyer method of lipid extraction to tissue homogenates. *Biochem J*, 89, 101-102.

He Y, He Z, Xu Y, Zhao X, Zhao L, Yang H (2022). Preservative effect of slightly acid electrolysed water ice generated by the developed sanitising unit on shrimp (*Penaeus vannamei*). *Food Control*, 136, 108876

Hınıslıoğlu KN, Aslanyavrusu G, Başkan S, Kocatepe D (2024). Su ürünleri tüketimi, diyet listelerindeki yeri ve önemi. *EBSHealth*, 3(3), 106-118.

ICMSF 1986. International commission on microbiological spesifictions for foods, sampling plans for fish and shellfish. In: ICMSF, Microorganisms in Foods. Sampling for Microbiological Analysis: Principles and Sciencetific Applications, 2: 2, University of Toronto Press, Toronto.

Imran M, Aslam M, Alsagaby SA et al. (2022). Therapeutic application of carvacrol: A comprehensive review. *Food Sci Nutr,* 10, 3544–3561.

Kostaki M, Giatrakou V, Savvaidis IN, Kontominas M G (2009). Combined effect of MAP and thyme essential oil on the microbiological, chemical and sensory attributes of organically aquacultured sea bass (*Dicentrarchus labrax*) fillets. *Food Microbiol*, 26(5), 475-482.

Li X, Wang Y, Li H et al. (2021). Chemical and quality evaluation of Pacific white shrimp *Litopenaeus vannamei*: Influence of strains on flesh nutrition. *Food Sci Nutr,* 9, 5352–5360.

Ludorff W ve Meyer V (1973). Fishe und Fisherzeuge. Z. Auflage. Verlag Paul Parey in Berlin und Hamburg, 209-210.

Marasinghe BNA, Rathnayake RMNP, Ranasinghe RDR, Madurakanthi AAG, Senevirathne WSM (2022). Effect of gamma irradiation on microbial, physical and chemical parameters of postharvest Penaeus monodon F. *Radiat Phys Chem Oxf Engl*, 192, 109883.

Matissek R, Schnepel FM ve Steiner G (1988). Lebensmittel- Analytick. (pp. 440). Springer Verlag Berlin, Tokyo.

Maurya A, Prasad J, Das S, Dwivedy AK (2021). Essential oils and their application in food safety. *Front Sustain Food Syst*, 5, 1-25.

Mousavi M, Hosseini SM, Hosseini H et al. (2022). Gliding arc plasma discharge conditions on microbial, physicochemical, and sensory properties of shrimp (Litopenaeus vannamei): In vivo and ın vitro studies. *Food Bioproc Tech*, 15, 2327–2343.

Nakamura A, Kondo A, Takahashi H et al. (2022). Microbiological safety and microbiota of Kapi, Thai traditional fermented shrimp paste, from different sources. *LWT - Food Sci Technol*, 154, 112763.

Nasser AH, Amin HF (2025). Impact of microwave-drying on the quality of innovative shrimp and clams snacks. *Egypt J Aquat Biol Fish*, 29(1), 2779–2793.

Osanloo M, Eskandari Z, Zarenezhad E, Qasemi H, Nematollahi A (2023). Studying the microbial, chemical, and sensory characteristics of shrimp coated with alginate sodium nanoparticles containing *Zataria multiflora* and *Cuminum cyminum* essential oils. *Food Sci Nutr,* 11, 2823–2837.

Ozogul F, Çetinkaya A, Abed NEL et al. (2024). The effect of carvacrol, thymol, eugenol and α-terpineol in combination with vacuum packaging on quality indicators of anchovy fillets. *Food Biosci,* 59, 104008

Saeed K, Pasha I, Chughtai MFJ, Zaryab A, Bukhari H, Zuhair M (2022). Application of essential oils in food industry: challenges and innovation. *J Essent Oil Res*, 34(2), 97–110.

Sultana S, Sayeduzzaman, Shams FI, Hossain SJ, Sarower G (2021). Quantification of the coliform bacteria and detection of enterovirulent *Escherichia coli* strains using strain specific genes in shrimp farms. *J Aqua Tech Deve*, 4(006).

Talukdar A, Deo AD, Sahu NP et al. (2020). Effects of different levels of dietary protein on the growth performance, nutrient utilization, digestive enzymes and physiological status of white shrimp, Litopenaeus vannamei juveniles reared in inland saline water. *Aquac Nutr,* 27, 77–90.

TÜİK (2025) Veritabanları (MEDAS). Erişim tarihi: 7 Ağustos 2025. Erişim adresi: https://biruni.tuik.gov.tr/medas/?locale=tr

Ulanowska M, Olas B (2021). Biological properties and prospects for the application of eugenol - a review. *Int J Mol Sci*, 22(7), 3671-3684.

Xie S, Wei D, Fang W et al. (2023). Survival and protein synthesis of post-larval White Shrimp, *Litopenaeus vannamei* were affected by dietary protein level. *Anim Feed Sci Technol*, 263, 114462

Van Veterinary Journal

https://dergipark.org.tr/tr/pub/vanvetj

Cite this article as: **Belhan S, Kömüroğlu AU (2026).** The Effect of Orally Administered Collagen on Testosterone Hormone and Sperm Count in Streptozotocin-Applied Rats. *Van Vet J*, 37(1), 18-21. DOI: https://doi.org/10.36483/vanvetj.1781364

ISSN: 2149-3359 **Original Article** e-ISSN: 2149-8644

The Effect of Orally Administered Collagen on Testosterone Hormone and Sperm Count in Streptozotocin-Applied Rats

Saadet BELHAN[1,*] Ahmet Ufuk KÖMÜROĞLU[2]

[1] *Van Yuzuncu Yil University, Faculty of Veterinary Medicine, Department of Reproduction and Artificial Insemination, 65080, Van, Türkiye*
[2] *Van Yuzuncu Yil University, Vocational School of Health Services, 65080, Van, Türkiye*

Received: 11.09.2025 Accepted: 09.12.2025

ABSTRACT Diabetes mellitus is a common metabolic disorder characterized by chronic hyperglycemia resulting from impaired insulin secretion or action. Collagen, the most abundant structural protein in the body, plays a critical role in tissues such as skin, bone, cartilage, blood vessels, and testis. This study aimed to investigate the effects of oral collagen supplementation on serum testosterone levels and sperm count in diabetic rats. A total of 32 male Wistar albino rats were randomly assigned into four groups: Control, Diabetes mellitus, Diabetes mellitus+Collagen, and Collagen. Diabetes mellitus was induced via a single intraperitoneal injection of streptozotocin (55 mg/kg), while collagen peptide was administered daily by gastric gavage at a dose of 600 mg/kg for 28 days. Serum testosterone levels were measured using Enzyme-Linked Immunosorbent Assay (ELISA). The results demonstrated a significant decrease in testosterone ($p<0.05$) and sperm count ($p<0.001$) in the Diabetes mellitus group, whereas the Diabetes mellitus+Collagen group exhibited partial improvement in both parameters. In the Collagen-only group, testosterone levels and sperm count were comparable to the Control group, indicating a limited effect of collagen under normal physiological conditions. These findings suggest that collagen may partially mitigate diabetes-induced testicular dysfunction by supporting the structural integrity of testicular tissue and promoting spermatogenesis. Overall, the results indicate that collagen supplementation could support testicular function under diabetic conditions, but further studies with larger sample sizes and longer durations are warranted to better elucidate its therapeutic potential.

Keywords: *Collagen, Diabetes mellitus, Rat, Sperm, Testosterone.*

ÖZ

Streptozotosin Uygulanan Ratlarda Oral Yolla Verilen Kolajenin Testosteron Hormonu ve Sperm Sayısı Üzerindeki Etkisi

Diyabetes mellitus, insülin salgısının veya etkisinin bozulmasından kaynaklanan kronik hiperglisemi ile karakterize yaygın bir metabolik bozukluktur. Vücutta en bol bulunan yapısal protein olan kolajen, deri, kemik, kıkırdak, kan damarları ve testis gibi dokularda kritik bir rol oynar. Bu çalışma, oral kolajen takviyesinin diyabetik sıçanlarda serum testosteron düzeyleri ve sperm sayısı üzerindeki etkilerini araştırmayı amaçlamıştır. Toplam 32 erkek Wistar albino sıçan, rastgele dört gruba ayrılmıştır: Kontrol, Diyabetes mellitus, Diyabetes mellitus+Kolajen ve Kolajen. Diyabetes mellitus, tek bir intraperitoneal streptozotosin enjeksiyonu (55 mg/kg) ile indüklenmiş, kolajen peptidi ise 28 gün boyunca günlük olarak gastrik gavaj yoluyla 600 mg/kg dozunda uygulanmıştır. Serum testosteron düzeyleri ELISA yöntemi ile ölçülmüştür. Sonuçlar, Diyabetes mellitus grubunda testosteron ($p<0.05$) ve sperm sayısında ($p<0.001$) anlamlı bir azalma olduğunu göstermiştir; buna karşın Diyabetes mellitus+Kolajen grubunda her iki parametrede kısmi bir iyileşme gözlenmiştir. Sadece Kolajen verilen grupta, testosteron düzeyleri ve sperm sayısı Kontrol grubu ile karşılaştırılabilir düzeyde bulunmuş ve normal fizyolojik koşullar altında kolajenin sınırlı bir etkisi olduğu görülmüştür. Bu bulgular, kolajenin testis dokusunun yapısal bütünlüğünü destekleyerek ve spermatogenezi teşvik ederek diyabete bağlı testiküler disfonksiyonu kısmen azaltabileceğini göstermektedir. Genel olarak, sonuçlar kolajen takviyesinin diyabetik koşullar altında testis fonksiyonunu destekleyebileceğini göstermektedir; ancak terapötik potansiyelini daha iyi anlamak için daha büyük örneklem büyüklükleri ve daha uzun süreli çalışmalar gerekmektedir.

Anahtar Kelimeler: *Kolajen, Rat, Sperm, Şeker hastalığı, Testosteron.*

✉ *Corresponding author: saadetbelhan@yyu.edu.tr

INTRODUCTION

Diabetes mellitus represents a significant metabolic disorder that affects multiple organ systems and exerts considerable negative impacts on male reproductive health (Jena et al. 2024; Jin et al. 2025). Its global prevalence continues to rise, with type 2 diabetes comprising the majority of diagnosed cases (Lovic et al. 2020; Lotti and Maggi 2023). Both clinical observations and experimental studies have indicated that this metabolic condition induces extensive and multifactorial damage within the male reproductive system (Huang et al. 2024; Chen et al. 2025). While the precise mechanisms underlying diabetes-related male reproductive dysfunction remain incompletely understood, current research identifies testicular impairment, disruptions in spermatogenesis, and structural changes in the testicular microenvironment as central pathological features (Faheem et al. 2025).

Diabetes disrupts the structure of the basement membrane through advanced glycation end-products and oxidative stress, leading to membrane thickening at the microvascular level and impairing ECM stability (Tsilibary 2003). In the testis, this process has been associated with increased expression of type IV collagen and laminin α5, with ECM accumulation weakening basement membrane integrity and adversely affecting spermatogenesis (Khordad et al. 2020). Furthermore, the observed elevation of type I collagen levels in diabetes has been linked to impaired seminiferous tubule morphology, germ cell loss, and reduced spermatogenesis, supporting the critical role of ECM balance in maintaining testicular function (Bondarenko et al. 2012).

Diabetes has been reported to diminish testicular antioxidant defenses and trigger germ cell apoptosis, resulting in decreased testosterone production. Reduced testosterone levels subsequently impair epididymal function and overall reproductive competence (Kiani et al. 2025). Experimental studies in diabetic rat models further demonstrate significant alterations in sexual behavior, accompanied by lowered serum concentrations of testosterone, Follicle Stimulating Hormone (FSH), and Luteinizing Hormone (LH) (Abdel-Wahab et al. 2024).

Collagen is the most plentiful structural protein in the body and is essential for the integrity of various tissues, such as skin, bones, cartilage, blood vessels, and testes (Shoulders and Raines 2009). It is particularly abundant in the basal membrane of seminiferous tubules and the interstitial regions, where it helps maintain the microenvironment required for spermatogenesis, ensures the stability of the blood–testis barrier, and supports germ cell differentiation (Cheng et al. 2010). In diabetic conditions, disruptions in collagen balance within the basal membrane, along with excessive connective tissue accumulation, have been linked to reduced sperm production (Xu et al. 2025).

This study aims to evaluate the effects of oral collagen supplementation on testosterone levels and sperm count in rats modeled with streptozotocin-induced diabetes. The limited number of studies examining the effects of collagen on male reproductive function in diabetic patients constitutes the unique value of this study. In this context, the study aims to demonstrate the potential role of collagen in reducing diabetes-related fertility disorders through a holistic approach.

MATERIAL AND METHODS

The experimental animals utilized in this study were sourced from the Experimental Research Application and Research Center of Van Yuzuncu Yil University. A total of 32 adult male Wistar albino rats, aged 8–12 weeks and with comparable average body weights, were included in the study. Throughout the experimental period, animals were kept under standard laboratory conditions including 23±1 °C temperature, 50-60% relative humidity, and a 12-h light/12-h dark cycle. Sterile drinking water and standard pellet chow were provided ad libitum. Rats were housed individually in polycarbonate cages with wood shavings as bedding, and cages were cleaned twice weekly. All animal experiments were carried out following prior approval from the Local Ethics Committee on Animal Experiments at Van Yuzuncu Yil University (Date: 28.08.2025 Approval No: 2025/09-02) and adhered to all applicable ethical standards and guidelines.

Induction of the Diabetes Model

The experimental diabetes model was created using streptozotocin (STZ). Diabetes was induced by a single intraperitoneal injection of STZ at 55 mg/kg, after it was dissolved in 0.1 M citrate buffer (pH 4.5). Seventy-two hours after the injection, blood samples were obtained from the tail vein, and glucose levels were measured using a glucometer. Rats exhibiting blood glucose concentrations above 200 mg/dL were considered diabetic (Kumar et al. 2016; Maranduca and Serban 2022).

Formation of Experimental Groups

A total of 32 male Wistar albino rats were randomly allocated into four experimental groups as follows:

Control group: Rats in this group did not receive any treatment.

Diabetes mellitus group: Rats in which diabetes was induced via streptozotocin but received no subsequent intervention (Kumar et al. 2016; Maranduca and Serban 2022).

Diabetes mellitus+Collagen group: Diabetic rats received oral administration of collagen peptides at 600 mg/kg via gastric gavage for 28 consecutive days (Kumar et al. 2016; Maranduca and Serban, 2022; Vijayan et al. 2022). Collagen group: Healthy rats administered collagen peptides at 600 mg/kg orally via gastric gavage for 28 days (Vijayan et al. 2022).

Measurement of Testosterone Levels

Serum testosterone concentrations were measured using a commercial ELISA kit (Cat. No: ELK10883). The kit has a sensitivity of 0.64 ng/mL and a measurement range of 1.56–100 ng/mL.

Collection of Sperm from the Cauda Epididymis and Assessment of Sperm Count

Twenty-four hours after the completion of the experimental period, one testis from each rat was surgically excised under anesthesia. Sperm samples were obtained from the cauda epididymis according to the procedure of a previous study (Sönmez et al. 2005). In brief, the epididymides were finely minced with anatomical scissors in 2 mL of physiological saline within a Petri dish and incubated at room temperature for 15 minutes to allow complete sperm release.

Sperm concentration was measured using a slightly adapted version of the method described by Sönmez et al. (2005), in which an Eppendorf tube was used instead of the conventional hemocytometer. Ten microliters of the

epididymal suspension in physiological saline were added to 990 µL of eosin solution in an Eppendorf tube and vortexed for 15 seconds. About 10 µL of the diluted sample was placed into the counting chambers of a Thoma slide and allowed to settle for 5 minutes. Sperm cells were later analyzed and counted using a phase-contrast microscope at 400× magnification.

Statistical Analysis

Statistical analyses related to testosterone were performed using SPSS version 20.0 (SPSS Inc., Chicago, IL, USA). Data are presented as mean±standard deviation. Differences among groups were evaluated using one-way ANOVA, followed by Duncan's multiple range test for post hoc comparisons. A p-value≤0.05 was considered statistically significant. Differences between groups regarding sperm parameters were evaluated using one-way analysis of variance (ANOVA), and Tukey's HSD post hoc test was employed to determine significant differences.

RESULTS

Serum testosterone concentrations in the diabetes mellitus group were significantly reduced compared to the control and diabetes mellitus+collagen groups ($p<0.05$). Rats in the diabetes mellitus+collagen group displayed markedly higher serum testosterone levels than those in all other groups ($p<0.05$). No significant difference was observed between the collagen group and the diabetes mellitus group regarding serum testosterone levels ($p>0.05$).

Similarly, sperm density in the diabetes mellitus group was significantly lower than that in the control and diabetes mellitus+collagen groups ($p<0.001$). In contrast, sperm density in the diabetes mellitus+collagen group was significantly higher than in all other groups ($p<0.001$), whereas no significant difference was detected between the collagen and diabetes mellitus groups ($p>0.001$).

Table 1: The effect of collagen on testosterone hormone and sperm concentration in streptozotocin-administered rats.

	Control (n=8)	Diabetes mellitus (n=8)	Diabetes mellitus+Collagen (n=8)	Collagen (n=8)	p value
Testosterone (pg/ml)	39.25±3.22^{b}	33.40±1.97^{c}	48.33±2.19^{a}	35.40±1.97^{c}	(p<0.05)
Sperm Density (× 10^6)	70.37±1.59^{b}	52.62±1.06^{c}	79.37±1.40^{a}	54.25±1.03^{c}	(p<0.001)

a, b, c: Statistical differences between groups indicated with different letters in the same row are significant.

DISCUSSION AND CONCLUSION

This research examined the impact of orally administered collagen on testosterone levels and sperm count in rats with streptozotocin-induced diabetes. The findings indicate that diabetes adversely affects the male reproductive system, mainly evidenced by reduced testosterone and impaired sperm production.

In the current study, no statistically significant difference was detected between the testosterone levels of the diabetes group and those of the group receiving collagen supplementation alone. Although this result may seem unexpected at first glance, it is consistent with previous findings. In healthy individuals, testicular tissue architecture, Leydig cell function, and vascular integrity are maintained under normal physiological conditions (França et al. 2005; Skinner 2005). Consequently, exogenous collagen is not expected to substantially enhance testosterone synthesis. Collagen, as a principal component of the extracellular matrix, provides structural support to the seminiferous tubules (Hadley and Dym 1987). Furthermore, collagen within the extracellular matrix of spermatogonial stem cells contributes to a three-dimensional scaffold that preserves tubular morphology and mechanical stability (Kahsai et al. 1997). Collagen has also been reported to participate in the formation of intercellular tight junctions, in addition to its structural role (Siu et al. 2003). Therefore, the finding that testosterone levels in the collagen-only group remained comparable to the control group and did not differ significantly from the diabetes group is consistent with these established roles.

The present study demonstrated significant reductions in both sperm count and serum testosterone levels in the diabetic group, consistent with previous literature reports (AlTamimi et al. 2021; Imani et al. 2021; Khalil et al. 2021;

Andlib et al. 2023; Hasan et al. 2023). It is widely recognized that diabetes mellitus, particularly type 2 diabetes, impairs sperm production through multiple interconnected mechanisms. The hormonal imbalances negatively affect critical stages of spermatogenesis, particularly the primary meiotic division, thereby compromising Sertoli and Leydig cell function. In addition, reductions in Sertoli cell numbers and insufficient lactate production limit the energy supply essential for germ cell survival, ultimately promoting increased germ cell apoptosis (Andlib et al. 2023; Gregorič et al. 2025).

In the present study, reductions in both sperm count and testosterone levels were observed solely in the group receiving collagen supplementation when compared to the control group, a result that aligns with previous findings (Hasan et al. 2023).

The observed increase in sperm count in the diabetes+collagen group compared with the diabetes group is a significant finding. This suggests that collagen may help maintain the integrity of the basal membrane in the testes, thereby mitigating structural disruptions within the seminiferous tubules. The extracellular matrix is known to play a regulatory role in spermatogenesis (Siu and Cheng 2008). Nevertheless, the inability of collagen supplementation to fully restore sperm count in diabetic rats is not unexpected, as pathological processes induced by diabetes, including oxidative stress and vascular damage, cannot be entirely reversed through extracellular matrix support alone. Recent evidence indicates that diabetes-associated testicular injury is multifactorial and is accompanied by substantial impairment of antioxidant defense systems. These findings underscore the importance of therapeutic strategies that simultaneously

target multiple mechanisms rather than relying on single-target interventions (Xu et al. 2023; Soetan et al. 2024; Kiani et al. 2025).The relatively small number of animals per group, inter-individual biological variability, and the inherent fluctuations in hormonal parameters and the spermatogenesis process may have limited the detection of statistically significant differences. In this context, the lack of a difference in testosterone levels between the diabetes group and the collagen-only group represents a physiologically normal finding, which can be attributed both to the limited effect of collagen on hormone production in healthy rats and to methodological constraints.

Study findings suggest that collagen may act primarily by maintaining testicular tissue integrity and supporting spermatogenesis, rather than directly increasing hormone production. In conclusion, this study provides novel findings that contribute to the existing knowledge gap regarding the effects of oral collagen administration on testosterone levels and sperm count in streptozotocin-induced diabetic rats and suggests that collagen may serve as a potential adjunctive agent in the treatment of diabetes-associated reproductive dysfunction. The lack of histopathological evaluation, lack of oxidative stress marker measurements, and inability to assess collagen bioavailability represent significant methodological limitations. Therefore, future studies investigating tissue-level changes through histological analysis, assessing oxidative stress parameters, and incorporating comparative dose-response designs are recommended.

CONFLICTS OF INTEREST

The authors report no conflicts of interest.

AUTHOR CONTRIBUTIONS

Idea/Concept: SB, AUK
Supervision/Consultancy: SB
Data Collection and/or Processing: SB
Analysis and/or Interpretation: SB, AUK
Writing the Article: SB
Critical Review: SB,AUK

REFERENCES

Abdel-Wahab BA, El-Shoura EAM, Habeeb MS et al. (2025). Piperazine ferulate impact on diabetes-induced testicular dysfunction: Unveiling genetic insights, MAPK/ERK/JNK pathways, and TGF-β signaling. *Naunyn Schmiedebergs Arch Pharmacol*, 398(6), 6719–6737.

AlTamimi JZ, AlFaris NA, Aljabryn DH et al. (2021). Ellagic acid improved diabetes mellitus-induced testicular damage and sperm abnormalities by activation of Nrf2. *Saudi J Biol Sci*, 28(8), 4300–4310.

Andlib N, Sajad M, Kumar R, Thakur SC (2023). Abnormalities in sex hormones and sexual dysfunction in males with diabetes mellitus: A mechanistic insight. *Acta Histochem*, 125, 151974.

Bondarenko LB, Shayakhmetova GM, Matvienko AV, Kovalenko VM (2012). Diabetes-mediated changes in rat type I collagen and spermatogenesis indices. *Rom J Diabetes Nutr Metab Dis,* 19(3), 245-254.

Chen ZF, Shen YF, Gao DW et al. (2025). Metabolic pathways and male fertility: Exploring the role of Sertoli cells in energy homeostasis and spermatogenesis. *Am J Physiol Endocrinol Metab*, 329(2), E160–E178.

Cheng CY, Wong EWP, Yan HHN, Mruk DD (2010). Regulation of spermatogenesis in the microenvironment of the seminiferous epithelium: New insights and advances. *Mol Cell Endocrinol*, 315(1–2), 49–56.

Faheem H, Alawadhi R, Basha EH et al. (2025). Ameliorating immune-dependent inflammation and apoptosis by targeting TLR4/MYD88/NF-κB pathway by celastrol mitigates the diabetic reproductive dysfunction. *Physiol Genomics*, 57(3), 103–114.

França LR, Avelar GF, Almeida FFL (2005). Spermatogenesis and sperm transit through the epididymis in mammals with emphasis on pigs. *Theriogenology*, 63(2), 300–318.

Gregorič N, Šikonja J, Janež A et al. (2025). Semaglutide improved sperm morphology in obese men with type 2 diabetes mellitus and functional hypogonadism. *Diabetes Obes Metab*, 27, 519–528.

Hadley MA, Dym M (1987). Immunocytochemistry of extracellular matrix in the lamina propria of the rat testis: Electron microscopic localization. *Biol Reprod*, 37(5), 1283–1289.

Hasan BF, Hilal JA, Alwan NA (2023). Effect of oral administration of Collagen-α® on reproductive activity and growth efficiency of mature male rabbit. *Iran J Ichthyol*, Special Issue, 85–89.

Huang R, Chen J, Guo B et al. (2024). Diabetes-induced male infertility: Potential mechanisms and treatment options. *Mol Med*, 30, 11.

Imani M, Talebi AR, Fesahat F et al. (2021). Sperm parameters, DNA integrity, and protamine expression in patients with type II diabetes mellitus. *J Obstet Gynaecol*, 41(3), 439–446.

Jena L, Kaur P, Singh T et al. (2024). Gene expression analysis in T2DM and its associated microvascular diabetic complications: Focus on risk factor and RAAS pathway. *Mol Neurobiol*, 61, 8656–8667.

Jin T, Li F, Wei W et al. (2025). SDF2L1 downregulation mediates high glucose-caused Schwann cell dysfunction by inhibiting nuclear import of TFEB and CREB via KPNA3. *Exp Neurol*, 390, 115273.

Kahsai TZ, Enders GC, Gunwar S et al. (1997). Seminiferous tubule basement membrane: Composition and organization of type IV collagen chains, and the linkage of alpha3(IV) and alpha5(IV) chains. *J Biol Chem*, 272(27), 17023–17032.

Khalil ASM, Giribabu N, Yelumalai S et al. (2021). Myristic acid defends against testicular oxidative stress, inflammation, apoptosis: Restoration of spermatogenesis, steroidogenesis in diabetic rats. *Life Sci*, 278, 119605.

Khordad E, Nikravesh MR, Jalali M, Fazel AR, Sankian M (2020). Diabetes up-regulated collagen IV and laminin α5 genes in mRNA and protein levels in seminiferous tubules of C57BL/6 adult mice. *Cell Mol Biol (Noisy-le-Grand),* 66(5), 162–168.

Kiani M, Mehranjani MS, Shariatzadeh MA (2025). Myoinositol improves sperm parameters in diabetic rats by reducing oxidative stress and regulating apoptosis-related genes. *J Mol Histol*, 56, 165.

Kumar V, Jain P, Rathore K, Ahmed Z (2016). Biological evaluation of *Pupalia lappacea* for antidiabetic, antiadipogenic, and hypolipidemic activity both in vitro and in vivo. *Scientifica*, 2016, 1–10.

Lotti F, Maggi M (2023). Effects of diabetes mellitus on sperm quality and fertility outcomes: Clinical evidence. *Andrology*, 11(3), 399–416.

Lovic D, Piperidou A, Zografou I et al. (2020). The growing epidemic of diabetes mellitus. *Curr Vasc Pharmacol*, 18(2), 104–109.

Maranduca I, Serban G (2022). Effective dose of streptozotocin to induce diabetes mellitus in albino Wistar rats. *Farmacia*, 70(4), 448–455.

Shoulders MD, Raines RT (2009). Collagen structure and stability. *Annu Rev Biochem*, 78, 929–958.

Siu MKY, Cheng CY (2008). Extracellular matrix and its role in spermatogenesis. In: Cheng CY (ed) *Molecular mechanisms in spermatogenesis* (pp 74–91). Springer.

Siu MK, Lee WM, Cheng CY (2003). The interplay of collagen IV, tumor necrosis factor-alpha, gelatinase B (matrix metalloprotease-9), and tissue inhibitor of metalloproteases-1 in the basal lamina regulates Sertoli cell-tight junction dynamics in the rat testis. *Endocrinology*, 144(1), 371–387.

Skinner MK (2005). Regulation of primordial follicle assembly and development. *Hum Reprod Update*, 11(5), 461–471.

Soetan OA, Ajao FO, Ajayi AF (2024). Erythritol attenuates testicular dysfunction in diabetic rat via suppression of oxidative stress, inflammation and apoptosis. *Biochem Biophys Res Commun*, 690, 149254.

Sonmez M, Turk G, Yüce A (2005). The effect of ascorbic acid supplementation on sperm quality, lipid peroxidation and testosterone levels of male Wistar rats. *Theriogenoly*, 63(6), 2063–2072.

Tsilibary EC (2003). Microvascular basement membranes in diabetes mellitus. *J Pathol,* 200(4), 537–546.

Xu R, Wang F, Zhang Z et al. (2023). Diabetes-induced autophagy dysregulation engenders testicular impairment via oxidative stress. *Oxid Med Cell Longev*, 2023, 4365895.

Xu Y, Hu P, Chen W et al. (2025). Testicular fibrosis pathology, diagnosis, pathogenesis, and treatment: A perspective on related diseases. *Andrology*, 13(6), 1322–1332.

Vijayan DK, Raman SP, Dara PK et al. (2022). In vivo anti-lipidemic and antioxidant potential of collagen peptides obtained from great hammerhead shark skin waste. *J Food Sci Technol*, 59(3), 1140–115.

Van Veterinary Journal

https://dergipark.org.tr/tr/pub/vanvetj

Cite this article as: **Aktaş Şenocak E, İleritürk M (2026).** Effect of Borage Seed Oil Against Lead Acetate Neurotoxicity in Rats. *Van Vet J*, 37(1), 22-27. DOI: https://doi.org/10.36483/vanvetj.1789129

ISSN: 2149-3359 **Original Article** e-ISSN: 2149-8644

Effect of Borage Seed Oil Against Lead Acetate Neurotoxicity in Rats

Esra AKTAŞ ŞENOCAK[1,*] Mustafa İLERİTÜRK[1]

[1] *Atatürk University, Horasan Vocational School of Higher Education, Department of Animal Science, 25800, Erzurum, Türkiye*

Received: 22.09.2025 Accepted: 04.02.2026

ABSTRACT Lead (Pb) is a highly toxic heavy metal that has long been widely used in industry, agriculture, and the cosmetics sector. It also poses serious public health risks due to its tendency to accumulate in the body and to induce pronounced neurotoxicity, particularly by damaging the central nervous system via oxidative stress–mediated mechanisms. In the present study, the biochemical effects of lead acetate-induced neurotoxicity and the potential protective role of borage seed oil (Borago oil, BSO), known for its high medicinal and nutritional value, were evaluated in the brain tissue of rats by assessing oxidative stress parameters. A total of 30 Sprague Dawley rats were randomly divided into five groups. Neurotoxicity was induced by intraperitoneal administration of lead acetate at a dose of 20 mg/kg for 7 consecutive days. Borage oil was administered orally at doses of 50 and 100 mg/kg for 14 days. Malondialdehyde (MDA) levels in the rat brain tissue were measured using manual biochemical method, while the expression levels of superoxide dismutase (SOD), catalase (CAT), and glutathione peroxidase (GPx) were determined by RT-PCR. Collectively, these findings indicate that borage seed oil partially alleviated Pb- associated oxidative stress alterationsin brain tissue, as evidenced by reduced lipid peroxidation (decreased MDA; $p<0.001$) and upregulated mRNA expression of antioxidant enzymes (SOD, CAT, and GPx) compared with the Pb group (overall ANOVA $p<0.001$; Tukey's post hoc test). Moreover, the 100 mg/kg dose tended to produce greater improvements in oxidative stress–related parameters than the 50 mg/kg dose.

Keywords: *Lead acetate, Neurotoxicity, Oxidative stress, Rat.*

ÖZ

Sıçanlarda Kurşun Asetat Nörotoksisitesine Karşı Hodan Tohum Yağının Etkisi

Kurşun (Pb), uzun süredir endüstri, tarım ve kozmetik sektörlerinde yaygın olarak kullanılan oldukça toksik bir ağır metaldir. Ayrıca vücutta birikme ve özellikle oksidatif stres aracılığıyla merkezi sinir sistemine zarar vererek belirgin nörotoksisiteye yol açma eğilimiyle ciddi halk sağlığı riskleri oluşturmaktadır. Bu çalışmada, yüksek tıbbi ve besinsel değeri ile bilinen hodan tohum yağının (Hodan yağı, BSO) potansiyel koruyucu rolü ve kurşun asetat kaynaklı nörotoksisitenin biyokimyasal etkileri, sıçanların beyin dokusunda oksidatif stres parametrelerinin değerlendirilmesi yoluyla araştırılmıştır. Toplam 30 Sprague Dawley sıçanı rastgele beş gruba ayrılmıştır. Nörotoksisite, 7 gün boyunca 20 mg/kg dozunda intraperitoneal kurşun asetat uygulamasıyla oluşturulmuştur. Hodan yağı 14 gün boyunca 50 ve 100 mg/kg dozlarında oral yoldan uygulanmıştır. Sıçan beyin dokusunda malondialdehit (MDA) düzeyleri manuel biyokimyasal metod kullanılarak ölçülürken, süperoksit dismutaz (SOD), katalaz (CAT) ve glutatyon peroksidaz (GPx) ekspresyon düzeyleri RT-PCR ile belirlenmiştir. Toplu olarak, bu bulgular, hodan tohumu yağının, kurşunla ilişkili oksidatif stres değişikliklerini beyin dokusunda kısmen hafiflettiğini göstermektedir; bu durum, kurşun grubuna kıyasla lipid peroksidasyonunda azalma (MDA'da azalma; $p<0.001$) ve antioksidan enzimlerin (SOD, CAT ve GPx) mRNA ekspresyonunda artış (genel ANOVA $p<0.001$; Tukey'in post hoc testi) ile kanıtlanmıştır. Dahası, 100 mg/kg dozu, 50 mg/kg dozuna kıyasla oksidatif stresle ilgili parametrelerde daha büyük iyileşmeler sağlama eğilimindeydi.

Anahtar Kelimeler: *Kurşun asetat, Nörotoksisite, Oksidatif stres, Sıçan.*

INTRODUCTION

Heavy metals adversely affect tissues and lead to dysfunctions in various physiological systems (Famurewa et al. 2022; Yipel and Tekeli 2022). Lead (Pb), a highly toxic heavy metal, has been extensively used for centuries in numerous fields such as industry, agriculture, and cosmetics, despite being an environmental pollutant. Its applications have included the production of ammunition, batteries, metal alloys, gasoline, paints, toys, pesticides,

✉ *Corresponding author: esenocak@atauni.edu.tr

and cosmetic products. However, due to its toxic effects, its use has been increasingly restricted in recent years. Although dermal absorption is limited, lead primarily enters the body through the respiratory and gastrointestinal systems. Once absorbed, it disrupts oxidative balance and induces inflammation in various tissues, causing detrimental effects on the nervous system, immune system, respiratory organs, kidneys, cardiovascular system, skeletal structure, blood cells, reproductive functions, and embryonic development (Song et al. 2017; Niu et al. 2023). The long-term accumulation of Pb in soft tissues, bones, and other organs complicates its elimination from the body (Mesalam et al. 2023; Jomova et al. 2024). The central nervous system is identified as one of the most affected systems of lead exposure. Children, in particular, represent the most vulnerable group for Pb toxicity, which can result in irreversible outcomes such as neurodevelopmental impairments, cognitive deficits, and behavioral disorders (Neal and Guilarte 2010; Ali et al. 2024). Although the precise mechanisms underlying lead-induced neurotoxicity have not yet been fully elucidated, existing studies suggest that oxidative stress, neuroinflammation, apoptosis, and disruptions in cellular signaling pathways may contribute to its development. Research has highlighted the significant role of oxidative stress in Pb toxicity (Paduraru et al. 2021; Ramírez Ortega et al. 2021). Following lead exposure, increased levels of reactive oxygen species (ROS) are known to interact with critical cellular macromolecules such as lipids, proteins, and nucleic acids, thereby causing tissue damage (Saber et al. 2022). Recently, the use of plant-derived antioxidants has garnered significant interest as a method to avoid or alleviate the detrimental effects caused by heavy metals.

Borage (*Borago officinalis* L.), a member of the Boraginaceae family, is also known by various names such as star flower, ıspıt, and kaldirik. It is a herbaceous and hairy plant, typically reaching a height of 70 to 100 cm, with predominantly blue flowers, although white or pink variants are occasionally observed. Borage blooms from June to July and is commonly found in the Mediterranean region, as well as in parts of Europe, South America, and Asia (Farhadi et al. 2012; Asadi Samani et al. 2014). The plant materials from which borage oil is obtained include the aerial parts and the seeds of the plant. Due to its high gamma-linolenic acid (GLA) content, the oil is considered a valuable raw material for both food and pharmaceutical applications (Michalak et al. 2023). Phytochemical investigations have shown that borage is abundant in bioactive constituents, including carbohydrates, essential fatty acids, and phytosteroids. It also contains a broad range of polyphenols such as quercetin, isorhamnetin, kaempferol, rosmarinic acid, chlorogenic acid, caffeic acid, sinapic acid, p-coumaric acid, gentisic acid, vanillic acid, and p-hydroxybenzoic acid. Moreover, borage includes tannins, saponins, mucilaginous compounds, tocopherols, allantoin, mineral salts, vitamins, and various organic acids like citric, malic, acetic, lactic, and ascorbic acids, as well as volatile oils. (Mhamdi et al. 2009; Asadi-Samani et al. 2014). Due to its active compound content, B. officinalis plant extract can be used in topical skin formulations with anti-inflammatory, anti-aging, UV-protective, soothing, or emollient effects (Seo et al. 2018; Michalak et al. 2023). Other studies suggest that borage may serve as a supportive treatment for diabetic neuropathy, as well as respiratory, urinary, and dermatological disorders, in addition to cardiovascular and inflammatory diseases (Kast 2001; Gilani et al. 2007; Asadi-Samani et al. 2014). Experimental studies have demonstrated that borage herb exhibits antioxidant properties by reducing oxidative stress levels (Bandonien and Murkovic 2002; Conforti et al. 2008). GLA, known for its beneficial effects on brain aging, is found in higher concentrations in borage seed oil compared to other plants (Wainwright et al. 2003; Tanwar et al. 2021). In one study, the effects of borage extract on amyloid β-induced memory impairment were investigated, and it was observed that it may ameliorate cognitive dysfunction and oxidative damage in hippocampal tissue (Ghahremanitamadon et al. 2014).

The present study was designed to investigate, from a biochemical perspective, the effects of cold-pressed borage seed oil, known for its anti-inflammatory and antioxidant properties, on brain tissue in a rat model of experimentally induced lead acetate neurotoxicity.

MATERIAL AND METHODS

Laboratory Animals

Thirty male Sprague-Dawley rats, each weighing between 200 and 250 grams, were employed in this investigation. The animals were acquired from the Atatürk University Medical Experimental Research and Application Center. They were housed under standard laboratory conditions at a temperature of 21 °C (±1 °C), with a 12-hour light/dark cycle. In order to guarantee acclimatization, the rodents were permitted a seven-day adaptation period prior to the experimental procedures, during which they were granted unrestricted access to food and water. To reduce stress-related confounding, animals were handled habituatively, procedures were performed by the same trained personnel in a quiet room, and the control animals underwent the same handling and administration schedule (oral and i.p. physiological saline) as the experimental groups. Ethical approval for the study was obtained in accordance with the established protocols of the Atatürk University Local Ethics Committee for Animal Experiments (Decision No. 66, dated 26.03.2025).

Chemicals

Sigma-Aldrich (St. Louis, MO, USA) supplied all of the chemicals, including lead acetate (CAS No: 6080-56-4). To induce toxicity, lead acetate was dissolved in physiological saline and administered intraperitoneally (i.p.) at a dose of 20 mg/kg for 7 consecutive days (Abdel Moneim et al. 2011; Yousef et al. 2019).

Plant Material

Cold-pressed borage oil (GLA, 20%), extracted from the seeds of the borage plant, was commercially obtained from a supplier (Hly Aromaterapi–Art de Huile, Istanbul, Türkiye). It was administered orally to rats via gastric gavage at doses of 50 and 100 mg/kg for 14 days (Ghahremanitamadon et al. 2014; Komaki et al. 2015).

Experimental Design

The investigation involved 30 male Sprague-Dawley rats. Each of the five groups of rats consisted of six animals chosen at random. Animals were followed for a total of 14 days. BSO was administered orally once daily for 14 days (days 1–14). Lead acetate (20 mg/kg, ip) was administered once daily for 7 days (days 1–7). The experimental groups were designed as follows: Group 1 (Control): Rats received both oral (days 14) and intraperitoneal (days 7) administration of physiological saline. Group 2 (BSO 100): Rats were orally administered borage seed oil at a dose of 100 mg/kg for 14 consecutive days. Group 3 (Pb): Rats received lead acetate dissolved in physiological saline at a dose of 20 mg/kg via ip injection for 7 consecutive days.

Group 4 (Pb+BSO 50): Rats were first administered lead acetate (20 mg/kg, ip) for 7 days, followed 30 minutes later by oral administration of borage seed oil at a dose of 50 mg/kg. Group 5 (Pb+BSO 100): Rats were first administered lead acetate (20 mg/kg, ip) for 7 days, followed 30 minutes later by oral administration of borage seed oil at a dose of 100 mg/kg.

Intraperitoneal injections were performed using standard technique in the lower abdominal quadrant with sterile disposable syringes/needles, and all injections were administered at a constant volume (0.5 mL/kg). Oral administrations were delivered by gastric gavage at a constant volume (0.5 mL/kg). All treatments were administered once daily within the same time window (09:00–11:00) to minimize circadian variability.

Sample Collection

Twenty-four hours after the final administration of lead acetate, the rats were euthanized by decapitation under light sevoflurane anesthesia, and brain tissues were rapidly excised. During transfer, tissues were briefly exposed to room temperature (≤2–5 min) and otherwise kept on ice. Samples were divided for biochemical and gene expression analyses; tissues allocated for gene expression were handled using RNase-free tools, snap-frozen in liquid nitrogen, and stored at −80 °C until RNA extraction (RNAlater was not used), and then kept under deep-freeze conditions until subsequent biochemical and molecular assessments. Samples were labeled with coded identifiers, and investigators performing biochemical assays and gene expression analyses, as well as statistical analyses, were blinded to group allocation. Treatment administration could not be blinded due to practical constraints.

MDA Measurement in Brain Tissue

Lipid peroxidation was evaluated by determining malondialdehyde (MDA) levels in brain tissue samples. The tissues were homogenized in 1.15% KCl solution under cold conditions, followed by centrifugation at 3,500 rpm for 15 minutes. MDA levels were determined using the thiobarbituric acid reactive substances (TBARS) assay as described by Placer et al. Tissue homogenates were reacted with thiobarbituric acid (TBA) reagent and heated at 100 °C for 60 min**.** After cooling, an extraction step was performed using n-butanol: pyridine (15:1, v/v)**.** The mixture was centrifuged to obtain the supernatant, and absorbance was measured spectrophotometrically at 532 nm (BioTek, USA). Results were expressed as nmol/g tissue (Placer et al. 1966).

Primer Design and RNA Isolation

Primers for the SOD, CAT, and GPx genes were designed using the Primer-BLAST tool available on NCBI (Table 1). Brain tissue samples (60 mg) were homogenized in 1 mL of QIAzol® Lysis Reagent (Qiagen Cat. No. 79306). Afterward, 200 µL of chloroform was introduced to the samples, which were then centrifuged at 12,000 ×g for 20 minutes at 4 °C. Next, 500 µL of isopropanol was added to the aqueous phase, and the mixture was centrifuged at 12,000 ×g for 10 minutes. The pellet that was obtained was rinsed with ethanol that was 75%, and then it was centrifuged at a speed of 7.500×g for a duration of 5 minutes. After dissolving the RNA in water that had been treated with DEPC and did not contain RNase, the concentration of the RNA was analyzed by measuring its wavelength at 260/280 nm. RNA samples were treated with DNase I (Thermo Scientific) to remove any residual genomic DNA. Complementary DNA (cDNA) synthesis was performed using the miScript Reverse Transcription Kit (Applied Biosystems), following the manufacturer's protocol. The quality and concentration of the cDNA were measured at 260/280 nm and standardized prior to storage at −20 °C. β-Actin was used as the reference gene. The reaction mixture contained SYBR® Green qPCR Mastermix (Qiagen, Cat. No. 330500), gene-specific primers, cDNA templates, and nuclease-free water. All studies were conducted in triplicate, and relative gene expression was assessed using the $2^{-\Delta\Delta CT}$ technique, as described. (Livak and Schmittgen, 2001).

Table 1: Primer sequences used for real-time PCR.

Gene	Sequences (5'-3')	Accession No
SOD	F: AATGTGGCTGCTGGAAAGGA R: GCTTCCAGCATTTCCAGTCT	NM_017050.1
GPx	F: CAAGGTGCTGCTCATTGAGA R: ATGTCCGAACTGATTGCACG	NM_030826.4
CAT	F: CTGAGAGAGTGGTACATGCA R: AATCGGACGGCAATAGGAGT	NM_012520.2
β-Actin	F: CAGCCTTCCTTCTTGGGTATG R: AGCTCAGTAACAGTCCGCCT	NM_031144.3

Statistical Analysis

Data were evaluated using SPSS version 22.0. Group differences were reviewed using one-way ANOVA, followed by multiple comparisons conducted using Tukey's post hoc test. All data points are presented as mean±standard error of the mean (SEM), with statistical significance defined at $p<0.05$.

RESULTS

It was observed that Pb administration significantly increased MDA levels in brain tissue by enhancing lipid peroxidation. In contrast, borage seed oil treatment markedly reduced lipid peroxidation, as evidenced by a significant decrease in MDA levels ($p<0.001$). The results related to MDA levels in brain tissue are presented in Figure 1.

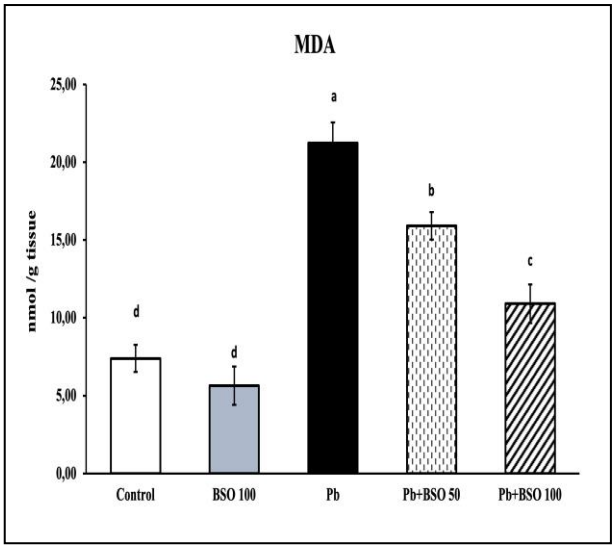

Figure 1: MDA levels in the brains of rats.

a, b, c, d: Different letters indicate a significant difference between groups ($p<0.05$). Data are presented as mean±standard error (n=6).

The effect of Pb-induced brain toxicity on SOD was evaluated by analyzing gene expression levels, as shown in Figure 2. A significant decrease was observed in the Pb group compared to the other groups ($p<0.001$). In contrast, a significant increase in SOD expression levels was observed in the treatment groups (Pb+BSO 50 and Pb+BSO 100) compared to Pb group ($p<0.001$).

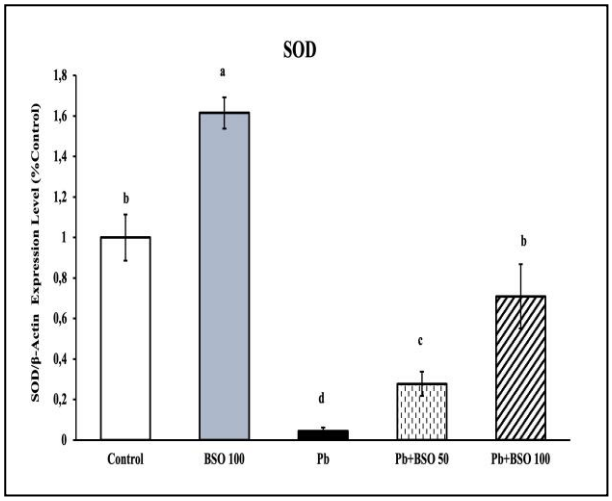

Figure 2: The mRNA transcript level of SOD in the brain of rats.

a, b, c, d: Different letters indicate a significant difference between groups ($p<0.05$). Data are presented as mean±standard error (n=6).

The effects of Pb exposure and BSO treatments on CAT gene expression in brain tissue were evaluated. One-way ANOVA revealed a significant overall group effect ($p<0.001$). CAT expression was significantly downregulated in the Pb group, whereas BSO co-administration (Pb+BSO 50 and Pb+BSO 100) increased CAT expression compared with Pb, partially restoring it toward control levels. In contrast, BSO 100 alone did not differ significantly from the control group, as indicated by Tukey's letter-based multiple comparison results.

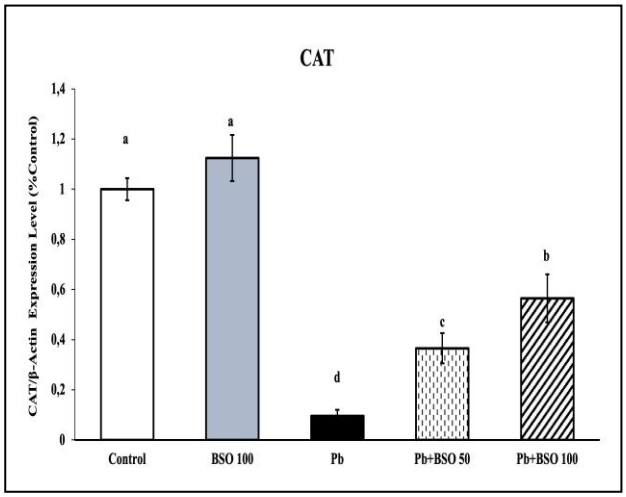

Figure 3: The mRNA transcript level of CAT in the brain of rats.

a, b, c, d: Different letters indicate a significant difference between groups ($p<0.05$). Data are presented as mean±standard error (n=6).

As shown in Figure 4, Pb administration resulted in a significant decrease in GPx gene expression levels compared to the control group. In contrast, the treatment groups restored the reduced expression levels.

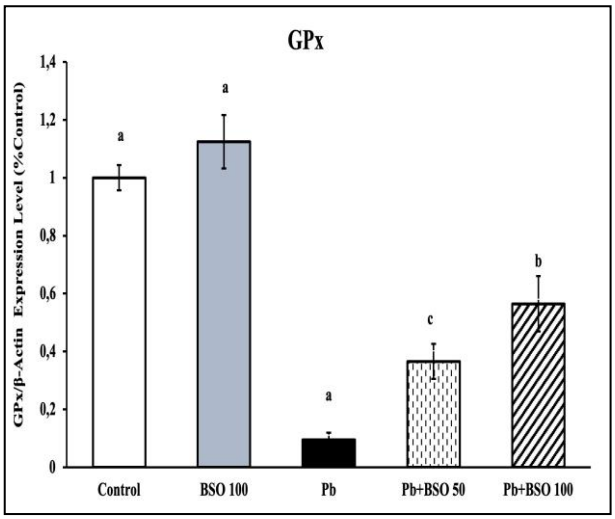

Figure 4: The mRNA transcript level of GPx in the brain of rats.

a, b, c, d: Different letters indicate a significant difference between groups ($p<0.05$). Data are presented as mean±standard error (n=6).

The findings indicate that Pb exposure increased MDA levels while decreasing the mRNA expression of SOD, CAT, and GPx. Based on these results, borage seed oil treatment partially alleviated Pb-associated oxidative stress alterations by reducing lipid peroxidation and upregulating the mRNA expression of antioxidant enzymes (SOD, CAT, and GPx).

DISCUSSION AND CONCLUSION

Lead is a widespread environmental toxic metal that can exert serious neurological effects on human health. Even low-level exposure has been reported to cause permanent structural and functional impairments in the central nervous system. Epidemiological data have shown that individuals with continuous exposure to lead exhibit a higher incidence of various neurological disorders, including cognitive decline, behavioral changes, and motor coordination impairments, as well as reproductive and cardiovascular dysfunctions (Ben-Azu et al. 2022). These effects of lead are associated with multifaceted pathophysiological processes such as disruption of the blood-brain barrier, impairment of glial cell integrity, induction of oxidative stress mechanisms, and interference with synaptic transmission (Yallapragada and Velaga 2015). Therefore, understanding the molecular mechanisms underlying lead-induced neurotoxicity is of critical importance for the prevention and treatment of neurological diseases.

Lead exposure elevates the generation of reactive oxygen species (ROS) while inhibiting the action of antioxidants. During this process, peroxidative damage to cell membranes intensifies, rendering neuronal cells more susceptible to oxidative injury (Velaga et al. 2014; Alqahtani and Albasher 2021). Studies have shown that lead neurotoxicity is associated with glutathione depletion in brain tissue and a reduction in antioxidant enzymes such as CAT and SOD (Singh et al. 2016; Yao et al. 2020). In a study investigating brain damage induced by lead (20 mg/kg) administered for five days in rats, increased lead concentrations were reported in both blood and brain tissues. Furthermore, decreases in GSH, CAT, SOD, and GPx activities were observed, accompanied by an increase in MDA levels (Abdel Moneim et al. 2011). In another study involving rats exposed to lead acetate-induced neurotoxicity, an increase in cortical lipid peroxidation

was observed, along with a significant reduction in the levels and activities of glutathione, superoxide dismutase, catalase, and glutathione peroxidase (Yousef et al. 2019). In this study, we investigated the effects of borage seed oil on Pb-associated oxidative stress alterations in brain tissue**,** focusing on lipid peroxidation and antioxidant defense–related gene expression.

Borage seed oil, which contains a higher concentration of gamma-linolenic acid (GLA) compared to other plants, is converted in the body to dihomo-γ-linolenic acid (DGLA), which promotes the production of the anti-inflammatory prostaglandin E1 (PGE1). The suppression of chronic inflammation, in turn, reduces oxidative stress by inhibiting ROS production (Das 2006). Moreover, the memory-protective effects of borage are attributed to its high γ-linolenic acid (GLA) content, which has a strong free radical scavenging capacity (Komaki et al. 2015). Although studies on the effects of borage seed oil on brain tissue are limited, several studies have reported its beneficial effects (Komaki et al. 2015; Barati et al. 2016). Borage extract has been shown to exert protective effects against amyloid β-induced memory impairment (Ghahremanitamadon et al. 2014). Another study reported that an extract obtained from *Borago officinalis* L. flowers regulated CAT and SOD activities in Neuro-2a cells exposed to H_2O_2-induced oxidative stress (Moliner et al. 2022). Additionally, research suggests that the GLA-rich content of borage may reduce MDA levels in damaged tissues while increasing SOD, CAT, and GSH levels, thereby exhibiting a potential neuroimmunomodulatory effect (Rahimi et al. 2024).

The findings of the present study, in line with the existing literature, demonstrated that lead exposure significantly increased MDA levels in brain tissue while decreasing the mRNA expression levels of SOD, CAT, and GPx. MDA is a well-known biomarker of lipid peroxidation, and its elevated levels indicate compromised membrane integrity. In the groups treated with borage seed oil, a significant reduction in MDA levels was observed, together with an upregulation of SOD, CAT, and GPx mRNA expression. Collectively, our findings indicate that borage seed oil may protect neuronal membranes by suppressing lipid peroxidation and enhancing the antioxidant defense system by reducing ROS generation. However, due to the limited number of studies in the literature on this subject, further research is warranted. These findings suggest that borage seed oil may contribute to the modulation of oxidative stress–related pathways under Pb exposure; however, the present data should be interpreted as preliminary evidence limited to oxidative stress markers and transcriptional changes. Notably, this study assessed MDA and antioxidant enzyme mRNA expression and did not include measurements of enzyme activity/protein levels, histopathological evaluation, neuroinflammatory markers, neuronal injury indicators, or behavioral outcomes. Therefore, no definitive conclusions can be drawn regarding direct neuroprotection or functional recovery. Future studies incorporating these endpoints are warranted to confirm whether the observed transcriptional modulation translates into functional and structural neuroprotective effects.

CONFLICTS OF INTEREST

The authors report no conflicts of interest.

AUTHOR CONTRIBUTIONS

Idea/Concept: EAS, Mİ
Supervision/Consultancy: EAS
Data Collection and/or Processing: EAS, Mİ
Analysis and/or Interpretation: EAS, Mİ
Writing the Article: EAS
Critical Review: Mİ

REFERENCES

Abdel Moneim AE, Dkhil MA, Al-Quraishy S (2011). Effects of flaxseed oil on lead acetate-induced neurotoxicity in rats. *Biol Trace Elem Res*, 144(1), 904–913.

Ali S, Naseer S, Rehman M, Wei Z (2024). Recent trends and sources of lead toxicity: A review of state-of-the-art nano-remediation strategies. *J Nanopart Res*, 26(7), 168.

Alqahtani WS, Albasher G (2021). *Moringa oleifera* Lam. extract rescues lead-induced oxidative stress, inflammation, and apoptosis in the rat cerebral cortex. *J Food Biochem*, 45(1), e13579.

Asadi-Samani M, Bahmani M, Rafieian-Kopaei M (2014). The chemical composition, botanical characteristic and biological activities of *Borago officinalis*: a review. *Asian Pac J Trop Med*, 7, 22–28.

Bandonien D, Murkovic M (2002). The detection of radical scavenging compounds in crude extract of borage (*Borago officinalis* L.) by using an on-line HPLC-DPPH method. *J Biochem Biophys Methods*, 53, 45–49.

Barati E, Asl SS, Pourbakhsh SA, Jamshidian M, Shahidi S (2016). Effect of borage on hippocampal TNF-α protein and gene in the amyloid β-peptide (25–35)-induced Alzheimer model in rat. *Biosci Biotechnol Res Asia*, 13(1), 37–42.

Ben-Azu B, Adebayo OG, Wopara I et al. (2022). Lead acetate induces hippocampal pyramidal neuron degeneration in mice via up-regulation of executioner caspase-3, oxido-inflammatory stress expression and decreased BDNF and cholinergic activity: Reversal effects of *Gingko biloba* supplement. *J Trace Elem Med Biol*, 71, 126919.

Conforti F, Sosa S, Marrelli M et al. (2008). In vivo anti-inflammatory and in vitro antioxidant activities of Mediterranean dietary plants. *J Ethnopharmacol*, 116, 144–151.

Das UN (2006). Essential fatty acids: Biochemistry, physiology and pathology. *Biotechnol J*, 1, 420–439.

Famurewa AC, Renu K, Eladl MA et al. (2022). Hesperidin and hesperetin against heavy metal toxicity: Insight on the molecular mechanism of mitigation. *Biomed Pharmacother*, 149, 112914.

Farhadi R, Balashahri M, Tilebeni H, Sadeghi M (2012). Pharmacology of borage (*Borago officinalis* L.) medicinal plant. *Int J Agron Plant Prod*, 3(2), 73–77.

Ghahremanitamadon F, Shahidi S, Zargooshnia S et al. (2014). Protective effects of *Borago officinalis* extract on amyloid β-peptide (25–35)-induced memory impairment in male rats: A behavioral study. *Biomed Res Int*, 798535.

Gilani AH, Bashir S, Khan AU (2007). Pharmacological basis for the use of *Borago officinalis* in gastrointestinal, respiratory and cardiovascular disorders. *J Ethnopharmacol*, 114(3), 393–399.

Kast RE (2001). Borage oil reduction of rheumatoid arthritis activity may be mediated by increased cAMP that suppresses tumor necrosis factor-alpha. *Int Immunopharmacol*, 1, 2197–2199.

Komaki A, Rasouli B, Shahidi S (2015). Anxiolytic effect of *Borago officinalis* (Boraginaceae) extract in male rats. *Avicenna J Neuro Psycho*, 2, 34–38.

Livak KJ, Schmittgen TD (2001). Analysis of relative gene expression data using real-time quantitative PCR and the 2−ΔΔCT method. *Methods*, 25, 402–408.

Mhamdi B, Wannes WA, Bourgou S, Marzouk B (2009). Biochemical characterization of borage (*Borago officinalis* L.) seeds. *J Food Biochem*, 33, 331–341.

Michalak M, Zagórska-Dziok M, Klimek-Szczykutowicz M, Szopa A (2023). Phenolic profile and comparison of the antioxidant, anti-ageing, anti-inflammatory, and protective activities of *Borago officinalis* extracts on skin cells. *Molecules*, 28(2), 868.

Moliner C, Cásedas G, Barros L et al. (2022). Neuroprotective profile of edible flowers of borage (*Borago officinalis* L.) in two different models: *Caenorhabditis elegans* and Neuro-2a cells. *Antioxidants*, 11(7), 1244.

Neal AP, Guilarte TR (2010). Molecular neurobiology of lead (Pb2+): Effects on synaptic function. *Mol Neurobiol*, 42(3), 151–160.

Niu C, Dong M, Niu Y (2023). Lead toxicity and potential therapeutic effect of plant-derived polyphenols. *Phytomedicine*, 114, 154789.

Paduraru E, Flocea EI, Lazado CC et al. (2021). Vitamin C mitigates oxidative stress and behavioral impairments induced by deltamethrin and lead toxicity in zebrafish. *Int J Mol Sci*, 22, 12714.

Placer ZA, Cushman LL, Johnson BC (1966). Estimation of product of lipid peroxidation (malonyl dialdehyde) in biochemical systems. *Anal Biochem*, 16, 359–364.

Rahimi K, Nourishirazi A, Delaviz H, Ghotbeddin Z (2024). Antinociceptive effects of gamma-linolenic acid in the formalin test in the rats. *Ann Med Surg*, 86, 2677–2683.

Ramírez Ortega D, González Esquivel DF, Blanco Ayala T et al. (2021). Cognitive impairment induced by lead exposure during lifespan: Mechanisms of lead neurotoxicity. *Toxics*, 9, 23.

Saber TM, Abo-Elmaaty AMA, Said EN et al. (2022). *Alhagi maurorum* ethanolic extract rescues hepato-neurotoxicity and neurobehavioral alterations induced by lead in rats via abrogating oxidative stress and the caspase-3-dependent apoptotic pathway. *Antioxidants*, 11, 1992.

Seo SA, Park B, Hwang E, Park SY, Yi TH (2018). *Borago officinalis* L. attenuates UVB-induced skin photodamage via regulation of AP-1 and Nrf2/ARE pathway in normal human dermal fibroblasts and promotion of collagen synthesis in hairless mice. *Exp Gerontol*, 107, 178–186.

Singh PK, Nath R, Ahmad MK et al. (2016). Attenuation of lead neurotoxicity by supplementation of polyunsaturated fatty acid in Wistar rats. *Nutr Neurosci*, 19, 396–405.

Song XB, Liu G, Liu F et al. (2017). Autophagy blockade and lysosomal membrane permeabilization contribute to lead-induced nephrotoxicity in primary rat proximal tubular cells. *Cell Death Dis*, 8(6), 2863.

Tanwar B, Goyal A, Kumar V, Rasane P, Sihag MK (2021). Borage (*Borago officinalis*) seed. In: *Oilseeds: Health Attributes and Food Applications*, 351–371.

Velaga MK, Basuri CK, Robinson Taylor KS et al. (2014). Ameliorative effects of *Bacopa monniera* on lead-induced oxidative stress in different regions of rat brain. *Drug Chem Toxicol*, 37, 357–364.

Wainwright PE, Huang YS, DeMichele SJ et al. (2003). Effects of high-γ-linolenic acid canola oil compared with borage oil on reproduction, growth, and brain and behavioral development in mice. *Lipids*, 38, 171–178.

Yallapragada PR, Velaga MK (2015). Effect of *Ginkgo biloba* extract on lead-induced oxidative stress in different regions of rat brain. *J Environ Pathol Toxicol Oncol*, 34, 161–173.

Yao J, Qiao H, Jin Z et al. (2020). *Ginkgo biloba* and its constituent 6-hydroxykynurenic acid as well as its proanthocyanidins exert neurorestorative effects against cerebral ischemia. *Planta Med*, 86, 696–707.

Yipel M, Tekeli İO (2022). Essential and non-essential metal concentrations in shrimps from Iskenderun Bay, Türkiye. *Harran Univ Vet Fak Derg*, 11, 257–262.

Yousef AOS, Fahad AA, Moneim AEA et al. (2019). The neuroprotective role of coenzyme Q10 against lead acetate-induced neurotoxicity is mediated by antioxidant, anti-inflammatory and anti-apoptotic activities. *Int J Environ Res Public Health*, 16, 2895.

Van Veterinary Journal

https://dergipark.org.tr/tr/pub/vanvetj

Cite this article as: **Aydoğdu YE, Sağun E (2026).** Presence of Escherichia coli O157:H7 in Minced Meat and Determination of Antibiotic Resistance. *Van Vet J*, 37(1), 28-35. DOI: https://doi.org/10.36483/vanvetj.1790854

ISSN: 2149-3359 **Araştırma Makalesi** e-ISSN: 2149-8644

Kıymalarda *Escherichia coli* O157:H7 Varlığı ve Antibiyotik Dirençliliklerinin Belirlenmesi

Yunus Emre AYDOĞDU[1,*] Emrullah SAĞUN[2]

[1] *Van Yüzüncü Yıl Üniversitesi, Sağlık Bilimleri Enstitüsü, 65080, Van, Türkiye*
[2] *Van Yüzüncü Yıl Üniversitesi, Veteriner Fakültesi, Besin Hijyeni ve Teknolojisi Anabilim Dalı, 65080, Van, Türkiye*

Geliş Tarihi: 25.09.2026 Kabul Tarihi: 06.01.2026

ÖZ

Bu araştırma, Van ilinde 2022 yılı Ocak-Mayıs aylarında satışa sunulan 50 adet koyun kıyması ve 50 adet sığır kıyması olmak üzere toplam 100 kıyma örneğinde *Escherichia coli* O157:H7 kontaminasyonu ve elde edilen izolatların antibiyotik dirençliliklerini belirlemek amacıyla yapılmıştır. Toplanan kıyma örneklerinde *E. coli* O157:H7'nin varlığının belirlenmesi için novobiocin katkılı modifiye Tripton Soy Broth (m-TSB) ile ön zenginleştirme yapıldıktan sonra cefixime tellurite katkılı Sorbitol MacConkey Agar (CT-SMAC) ve LEVINE Eosin-Methylene Blue (EMB) Agar'a ekim yapıldı. Biyokimyasal testler sonucunda *E. coli* O157:H7 şüpheli kolonilere polivalan *E. coli* O157 antiserumu ile aglütinasyon testi yapıldı ve aglütinasyon gösteren kolonilere de *E. coli* O157:H7 varlığını tespit etmek amacıyla H7 antiserumu ile tüp aglütinasyon testi yapıldı. Aglütinasyon gösteren koloniler *E. coli* O157:H7 pozitif olarak değerlendirildi ve bu koloniler Polimeraz Zincir Reaksiyonu (PCR) yöntemi ile de doğrulandı. Koyun kıyma örneklerinin 7'sinde (%14) ve sığır kıyma örneklerinin 17'sinde (%34) olmak üzere toplam 24 örnekte *E. coli* O157:H7 pozitif olarak tespit edildi. Pozitif olarak değerlendirilen örneklerden 51 adet *E. coli* O157:H7 izolatı elde edildi. İzolatların tamamının (%100) sefalatine, 26'sının (%50.98) ampisiline, 25'nin (%49.01) amoksisilin/klavulanik asite, 23'ünün (%45.09) eritromisine, 18'inin (%35.30) amikasine, 10'unun (%19.60) gentamisine, 9'unun (%17.64) norfloksasine, 7'sinin (%13.72) kloramfenikole, 5'inin (%9.80) polimiksin B ve kanamisine, 4'ünün (%7.85) ertapeneme ve 2'sinin (%3.93) sefotaksime karşı dirençli olduğu belirlendi. Sonuç olarak; Van piyasasında satışa sunulan kıymaların hijyenik kalitesinin iyi olmadığı ve üretimin herhangi bir aşamasında *E. coli* O157:H7 ile kontamine olduğu belirlenmiştir. Aynı zamanda bu izolatların antimikrobiyal dirençliliğinin yüksek olmasının da halk sağlığı açısından potansiyel bir tehlike oluşturabileceği kanaatine varılmıştır. Kıyma ve kıyma türevi olan ürünler ambalajsız olarak ve hiçbir önlem alınmadan açıkta satış yapan işletmelerden alınmamalı, gıda güvenliği için hijyen ve denetim standartlarını karşılayan işletmelerdeki ambalajlı ürünler tercih edilmelidir.

Anahtar Kelimeler: *Antibiyotik dirençliliği, Escherichia coli O157:H7, Kıyma, PCR.*

ABSTRACT

Presence of *Escherichia coli* O157:H7 in Minced Meat and Determination of Antibiotic Resistance

This study was conducted to determine the contamination of 100 minced meat samples (50 lamb and 50 beef) sold in Van province between January and May 2022 with *Escherichia coli* O157:H7 and the antibiotic resistance of the obtained isolates. To determine the presence of *E. coli* O157:H7 in the collected minced meat samples, pre-enrichment with novobiocin-added modified Tryptone Soy Broth (m-TSB) was performed, followed by plating on cefixime tellurite-added Sorbitol MacConkey Agar (CT-SMAC) and LEVINE Eosin-Methylene Blue (EMB) Agar. Biochemical tests revealed suspected *E. coli* O157:H7 isolates were subjected to agglutination tests with polyvalent *E. coli* O157 antiserum, and colonies showing agglutination were further tested for the presence of *E. coli* O157:H7 using tube agglutination tests with H7 antiserum. Colonies showing agglutination were evaluated as positive for *E. coli* O157:H7. Colonies that tested positive for *E. coli* O157:H7 were also confirmed by Polymerase Chain Reaction (PCR). *E. coli* O157:H7 was detected as positive in a total of 24 samples, 7 (14%) of lamb mince samples and 17 (34%) of beef mince samples, which were also confirmed by PCR method. From 24 minced meat samples that tested positive for *E. coli* O157:H7, 51 *E. coli* O157:H7 isolates were obtained. All isolates (100%) were found to be resistant to cephalathine, 26 (50.98%) to ampicillin, 25 (49.01%) to amoxicillin/clavulanic acid, 23 (45.09%) to erythromycin, 18 (35.30%) to amikacin, 10 (19.60%) to gentamicin, 9 (17.64%) to norfloxacin, 7 (13.72%) to chloramphenicol, 5 (9.80%) to polymyxin B and kanamycin, 4 (7.85%) to ertapenem, and 2 (3.93%) to cefotaxime. In conclusion, it was determined that the hygienic quality of minced meat offered for consumption in the Van market is poor and that it is contaminated with *E. coli* O157:H7 at some stage of production. It was also concluded that the high level of antimicrobial resistance of these isolates could pose a potential threat to public health. Minced meat and minced meat products should not be purchased from businesses selling them unpackaged and openly; for food safety, only packaged products that meet hygiene and inspection standards should be preferred.

Keywords: *Antibiotic resistance, Escherichia coli O157:H7, Minced meat, PCR.*

✉ *Corresponding author: yunusemreayd@windowslive.com

GİRİŞ

Beslenme, insanların hayatını devam ettirebilmesi için temel ihtiyaçlarından birisidir (Aydogdu ve Küçük 2018). Vücudun ihtiyaç duyduğu gıdaların yeterli düzeyde alınması, yeterli ve dengeli bir beslenme ile mümkündür (Tinta ve ark. 2020). Et ve et ürünleri protein, demir, çinko, B_{12} ve esansiyel amino asitler içermeleri nedeniyle beslenmede önemli bir yere sahiptir. Gıdaların uygun olmayan şartlarda üretilmesi, muhafaza ve depolama şartlarının uygun olmaması, tekrar ısıtma ve çapraz bulaşma gibi çeşitli faktörler gıdalardan kaynaklanan enfeksiyonlara sebep olmaktadır (Velusamy ve ark. 2012; Aytaç ve Taban 2014).

Gıdalarda, özellikle et ve et ürünlerinde gelişebilen bazı mikroorganizmalar gıdaların bozulmasına sebep olurken, bazı mikroorganizmalar da gıdalarda herhangi bir bozulma oluşturmadan, bu gıdaları tüketen insanlarda çeşitli enfeksiyonlara ve gıda zehirlenmelerine sebep olabilmektedir. Patojen mikroorganizmalar gıdalarda düşük sayılarda bulunsalar bile insanlarda gıda kaynaklı enfeksiyonlara neden olabilmektedirler. Gıda kaynaklı enfeksiyonlara hatta ölümlere neden olabilen ve en yaygın olarak görülen mikroorganizmalar *Campylobacter jejuni*, *Escherichia coli, Listeria monocytogenes*, *Salmonella* spp. dir. İkinci derecede görülme sıklığına göre ise *Staphylococcus aureus*, *Bacillus cereus*, *Shigella* spp. ve *Clostridial* enfeksiyonlar gelmektedir (Balpetek ve Gürbüz 2010; Sağlam ve Şeker 2016).

E. coli insanların ve birçok sıcakkanlı hayvanın sindirim sisteminde ve bağırsak florasında bulunur, bağışıklık azaldığında dokular ve kana geçerek enfeksiyon oluşmasına neden olur. Gıdalarda fekal bulaşmanın belirlenmesinde temel indikatör mikroorganizması olarak kabul edilen *Escherichia coli*'nin önemli patojen serotiplerinden biri olan *E. coli* O157:H7 ilk kez 1975 yılında Kaliforniya'da kanlı diyare semptomları gösteren bir kadın hastadan izole edilmiştir. Bu serotipin gıda kaynaklı bir patojen olarak önemi ise, 1982 yılında Amerika Birleşik Devletleri ve Kanada'da faaliyet gösteren fast food işletmelerinde yeterli ısıl işlem uygulanmadan tüketilen hamburgerlerin neden olduğu iki ayrı ishal salgını sonrasında anlaşılmıştır (Park ve ark. 1999).

E. coli O157:H7 serotipi 157 adet somatik (O) ve 7 adet de flagellar (H) antijenine sahip olması sebebiyle bu şekilde adlandırılmıştır (Karmali ve ark. 1983). β glukoronidaz enzim aktivitesine sahip olmaması, sorbitolü 48 saatte fermente edememesi, 44.5 °C'nin üzerinde üreyememesi, enterohemolizin üretmesi ve "eae" genine sahip olması ile diğer *E. coli* serotiplerinden ayrılmaktadır (Nataro ve Kaper 1998).

E. coli O157:H7'nin virulensi adezin, hemolizin, intimin, O157 lipopolisakkaritleri, shiga toksin ve tip III sekresyon sistemi gibi birçok faktöre bağlıdır. *E. coli* O157:H7'nin *S. dysenteriae* tip 1'in ürettiği toksine benzer özellikte "shiga benzeri toksin 1 (stx 1)" ve "shiga benzeri toksin 2 (stx 2)" olarak isimlendirilen farklı iki toksin de üretmektedir. *E. coli* O157:H7'nin patojenitesi ürettiği toksinlerin Vero ve HeLa doku kültür hücrelerine yapmış olduğu toksik etkilerden kaynaklanmaktadır. Bu toksik etkileri nedeniyle verotoksin 1 ve verotoksin 2 olarak da isimlendirilmektedir. Verotoksin üreten *E. coli* O157:H7 en tehlikeli gıda patojenleri arasında değerlendirilmektedir. H7 antijen dışındaki farklı H antijenleri de tanımlanmış, ancak bunların verotoksijenik olmadığı belirtilmiştir (Park ve ark. 1999).

E. coli O157:H7 serotipi, soğuk koşullarda depolanan ya da dondurulan gıdalar ile asidik özellik gösteren ve su aktivitesi düşük olan ürünlerde uzun süre canlı kalabilmekte, ayrıca elverişsiz çevresel koşullara uyum sağlayarak direnç geliştirebilmektedir (Leenanon ve Drake 2001).

E. coli O157:H7'nin infeksiyöz dozu 1-100 kob/g'dır. Düşük dozlarda enfeksiyon yapabilmeleri, mide asidine dirençli olmasındandır. *E. coli* O157:H7, pH'sı düşük ortamlarda asite tolerans geliştirerek böylelikle canlılığını korur (Park ve ark. 1999). İnsanlardaki *E. coli* O157:H7 infeksiyonlarının önemli kaynağı infekte sığırlardır. *E. coli* O157:H7'nin toprakta 130 gün ve dışkıda 50 gün canlı kalabildiği ve enfeksiyon yapma özelliğini koruduğu bildirilmiştir (Karmali ve ark. 1983).

E. coli O157:H7 serotipi, insanlarda başlıca Hemorajik Kolitis (HC), Hemolitik Üremik Sendrom (HUS) ve Trombotik Trombositopenik Purpura (TTP) hastalıklarına yol açabilmektedir (Coia 1998).

E. coli O157:H7 enfeksiyonlarından korunmada en etkili yöntem termal inaktivasyondur. *E. coli* O157:H7'nin optimum pH değeri 7.2 olup pH 5.7-7.5 aralığında iyi ürerken pH değeri 3.6 olan ve buzdolabında muhafaza edilen gıdalarda canlılığını koruyabilmekte, pH değeri 4.0 olan sıvı ortamlarda ise üreyebilmektedir. *E. coli* O157:H7'nin asidik koşullara dirençli olması onu diğer patojenlerden ayıran en önemli özelliklerinden birisidir (Erol 2007).

Bu araştırma, Van piyasasında satışa sunulan kıymalarda *E. coli* O157:H7'nin varlığını ve yaygınlığını tespit etmek ve elde edilen izolatların antimikrobiyal dirençliliklerini belirlemek amacıyla yapılmıştır.

MATERYAL VE METOT

Bu araştırmanın onayı Van Yüzüncü Yıl Üniversitesi Hayvan Deneyleri Yerel Etik Kurulu'nun 25.03.2021 tarihli 2021/03-04 sayılı kararıyla alınmıştır.

Çalışma materyali olarak Ocak-Mayıs 2022'de Van ilinden market, kasap, şarküteri gibi et ve et ürünleri satışı yapılan yerlerden en az 250 g olacak şekilde toplam 100 adet kıyma örneği (50 adet koyun kıyması, 50 adet sığır kıyması) toplandı. Örnekler steril cam kavanozlara aseptik koşullarda alındı ve +4 °C'de soğuk zinciri sağlayabilen kaplarda laboratuvara getirilerek en kısa sürede analizleri yapıldı.

E. coli O157:H7 İzolasyonu ve İdentifikasyonu

Her bir kıyma örneğinden steril stomacher torbalara 25'er g tartıldı ve üzerine 225 ml m-TSB ilave edilip stomacherde 2 dakika süreyle homojenize edildi. Homojenizat ön zenginlestirme amacıyla 37 °C'de 18-24 saat inkübe edildi. İnkübasyon işlemi sonrası, bir öze dolusu kültür Cefixime Tellurite katkılı (Oxoid, SR0172) Sorbitol MacConkey (SMAC) (LabM, Lab 161) Agar ve LEVINE Eosin-Methylene Blue (EMB) (LabM, Lab 061) Agar'a çizme yöntemi ile ekildi ve 37 °C'de 18-24 saat inkübe edildi. Üreyen şüpheli kolonilerden (kırmızı renkli ve metalik parlak mor renkli) Gram boyama yapıldı. Gram negatif olan bakteriler Nutrient Agar (DIFCO, 0001-17)'a saf kültür kontrolleri için ekildi. Nutrient Agar'da üretilen bakterilere oksidaz ve bazı biyokimyasal testler (üreaz, sülfid indol motilite (SIM), mannitol, lizin dekarboksilaz, methyl red, voges proskauer, citrate) yapıldı (TS 2003; TS 2017). Biyokimyasal testlerden sonra şüpheli olarak belirlenen kolonilere M44 ticari kiti ile firmanın test uygulama prosedürüne göre *E. coli* O157 Latex aglütinasyon testi (Microgen, *E. coli* O157 Latex M44)

uygulandı (March ve Ratnam 1989). Test sonucunda aglütinasyon gösteren koloniler *E. coli* O157 pozitif olarak değerlendirildi. *E. coli* O157 olarak belirlenen kolonilere *E. coli* O157:H7 varlığını tespit etmek için H7 antiserumu (Denka Seıken-295354) ile firmanın test uygulama prosedürüne göre tüp aglütinasyon testi uygulandı (Sakazaki 1992). Test sonucunda aglütinasyon gösteren koloniler *E. coli* O157:H7 pozitif olarak değerlendirildi ve Polimeraz Zincir Reaksiyonu (PCR) yöntemi kullanılarak doğrulandı.

Kıyma örneklerinden izole edilen *E. coli* O157:H7 kolonilerinden DNA ekstraksiyonu ve PCR amplifikasyonu için kaynatma yöntemi kullanıldı (Pehlivanoğlu ve ark. 2016).

E. coli O157:H7 şüpheli izolatlarının PCR ile konfirmasyonunda, Sharma ve Dean-Nystrom'un (2003) geliştirdiği primer çifti (5'-GACTGCAAAGACGTATGTAGATTCG-3'; 5'-ATCTATCCCTCTGACATCAACTGC-3', 150bp) kullanıldı. PCR işlemi Lee ve ark. (2012)'nın belirttiği yönteme göre yapıldı.

Antibiyotik Dirençliliğinin Belirlenmesi

Elde edilen *E. coli* O157:H7 izolatlarının antibiyotik dirençlilikleri, Avrupa Antimikrobiyal Duyarlılık Testi Komitesi (European Committee on Antimicrobial Susceptibility Testing, EUCAST) ile Klinik ve Laboratuvar Standartları Enstitüsü (Clinical & Laboratory Standards Institute, CLSI) klavuzlarına göre Kirby-Bauer disk difüzyon metodu esas alınarak belirlenmiştir (CLSI 2010; EUCAST 2021). Araştırmada kullanılan antibiyotik diskleri ve değerlendirme ölçüleri Tablo 1'de sunulmuştur.

Referans Suşlar

Bu araştırmada, Van Yüzüncü Yıl Üniversitesi Veteriner Fakültesi Besin Hijyeni ve Teknolojisi Anabilim Dalı kültür koleksiyonundan temin edilen *E. coli* O157:H7 (ATCC®43895) referans suşu kullanıldı.

Tablo 1: Çalışmada kullanılan antibiyotik diskleri ve değerlendirme ölçüleri.

Table 1: Antibiotic disks and evaluation dimensions used in the study.

		Değerlendirme (mm)		
Antibiyotik disk	**Dozu (µg)**	**S**	**I**	**R**
Amikacin (A)*	30	≥18	***	<18
Amoksisilin/Klavulanik asit (AUG)*	20-10	≥19	***	<19
Ampisilin (AMP) *	10	≥14	***	<14
Eritromisin (E) **	15	≥12	9-11	≤8
Gentamisin (GEN)*	10	≥17	***	<17
Kloramfenikol (C)*	30	≥17	***	<17
Sefotaksim (CTX)*	30	≥20	***	≤17
Sefalatin (KF) *	30	≥20	***	≤19
Norfloksasin (NOR)*	10	≥22	***	<22
Kanamisin (K)**	30	≥18	14-17	≤13
Polimiksin B (PB)*	300 IU	≥19	***	13
Trimethoprim-Sulfamethoxazole (SXT)*	1.25-23.75	≥14	***	≤11
Ertapenem (ETP)*	10	≥25	***	<25

*EUCAST, 2021' e göre değerlendirildi. **CLSI, 2010 (M100S)'a göre değerlendirildi. ***EUCAST, 2021'ye göre orta düzey yoktur. S: Duyarlı; I: Orta düzey; R: Dirençli.

BULGULAR

2022 yılı Ocak ve Mayıs ayları arasında Van ilinde market, kasap ve şarküterilerden alınarak analizi yapılan 50 adedi sığır ve 50 adedi de koyun kıyması olmak üzere toplam 100 adet kıyma örneğinin 24'ünde (%24) *E. coli* O157:H7 izole edilmiştir. Örneklerin 17'sinin (%34) sığır kıyması, 7'sinin (%14) ise koyun kıyması olduğu tespit edilmiştir.

E. coli O157:H7 pozitif tespit edilen örneklerin aylara göre dağılımı Tablo 2'de sunulmuştur.

E. coli O157:H7 yönünden pozitif bulunan 24 kıyma örneğinin analiz edilmesi sonucunda toplam 51 adet *E. coli* O157:H7 izolatı elde edilmiş olup, PCR yöntemiyle doğrulanan amplikonlara ait agaroz jel elektroforez görüntüsü Şekil 1'de sunulmuştur.

Tablo 2: *E. coli* O157:H7 pozitif örneklerin aylara göre dağılımı.

Table 2: Distribution of *E. coli* O157:H7 positive samples by month.

Aylar	Sığır kıyması (n)	Pozitif (n)	Koyun kıyması (n)	Pozitif (n)	Toplam (n)	Toplam Pozitif (n)
Ocak	10	0	11	3	21	3
Şubat	10	0	10	0	20	0
Mart	12	5	12	2	24	7
Nisan	9	4	9	1	18	5
Mayıs	9	8	8	1	17	9
Toplam	**50**	**17**	**50**	**7**	**100**	**24**

n: Örnek sayısı

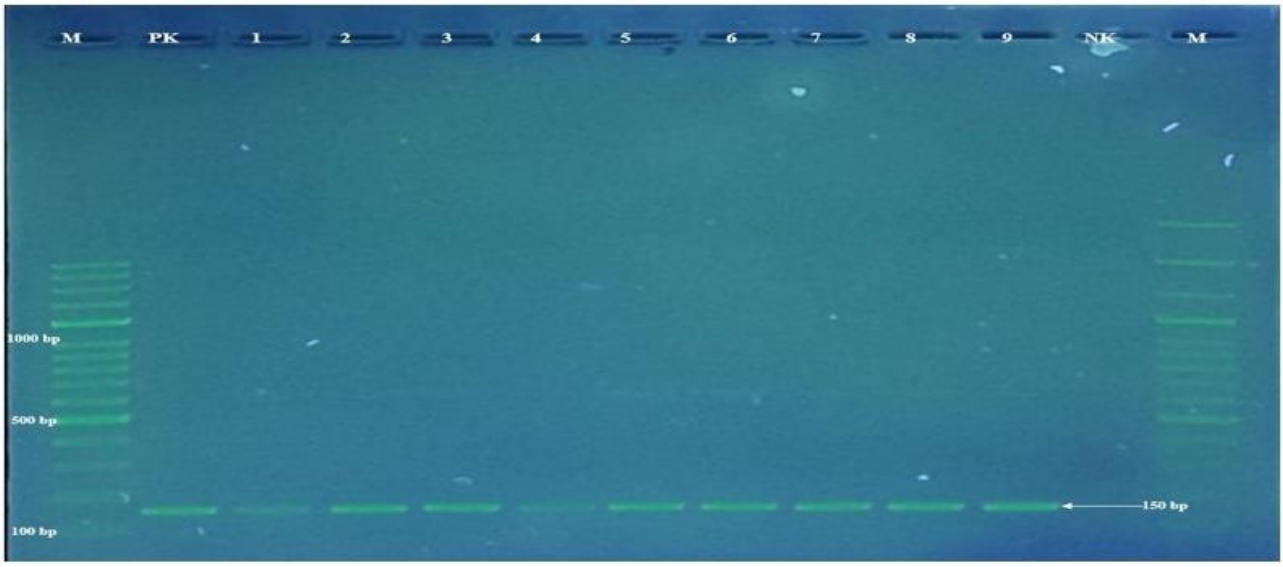

Şekil 1: M: Marker(100 bp); PK: Pozitif Kontrol *E. coli* O157: H7ATCC® 43895; 1-9: *E. coli* O157 H:7 izolatları 150 bp); NK: Negatif kontrol.

Figure 1: M: Marker (100 bp); PK: Positive Control *E. coli* O157: H7ATCC® 43895; 1-9: *E. coli* O157 H:7 isolates (150 bp); NK: Negative control.

Araştırmada 24 kıyma örneğinden elde edilen toplam 51 adet *E. coli* O157:H7 izolatının tamamının (%100) sefalatine, 26'sının (%50.98) ampisiline, 25'nin (%49.01) amoksisilin/klavulanik asite, 23'ünün (%45.09) eritromisine, 18'inin (%35.30) amikasine, 10'unun (%19.60) gentamisine, 9'unun (%17.64) norfloksasine, 7'sinin (%13.72) kloramfenikole, 5'inin (%9.80) polimiksin B ve kanamisine, 4'ünün (%7.85) ertapeneme, ve 2'sinin (%3.93) sefotaksime karşı dirençli olduğu belirlendi. İzolatların 49'unun (%96.07) sefotaksime, 47'sinin (%92.15) ertapeneme, 46'sının (%90.20) polimiksin B'ye, 41'inin (%80.40) gentamisine, 40'ının (%78.43) trimetoprim-sülfametoksazole, 38'inin (%74.50) norfloksasine, 33'ünün (%64.70) amikasine, 31'inin (%60.78) kloramfenikole, 26'sının (%50.99) amoksisilin/klavulanik asite ve 14'ünün (%27.45) kanamisine duyarlı olduğu belirlendi (Tablo 3).

Bu araştırmada Kirby–Bauer disk difüzyon yöntemi kullanılarak gerçekleştirilen antibiyogram analizleri sonucunda, kıyma örneklerinden izole edilen toplam 51 adet *E. coli* O157:H7 izolatına ait antibiyotik direnç profilleri Tablo 4'te verilmiştir.

Tablo 3: Kıyma örneklerinden elde edilen *E. coli* O157:H7 izolatlarının antibiyotiklere karşı dirençlilik ve duyarlılık düzeyleri.
Table 3: Antibiotic resistance and susceptibility levels of *E. coli* O157: H7 isolates obtained from minced meat samples.

Antibiyotikler	Dirençli n (%)	Orta Duyarlı n (%)	Duyarlı n (%)
Sefalatin	51 (%100)	-	-
Ampisilin	26 (%50.98)	-	-
Amoksisilin/Klavulanik asit	25 (%49.01)	-	26 (%50.99)
Eritromisin	23 (%45.09)	-	-
Amikasin	18 (%35.30)	-	33 (%64.70)
Gentamisin	10 (%19.60)	-	41 (%80.40)
Norfloksasin	9 (%17.64)	-	38 (%74.50)
Kloramfenikol	7 (%13.72)	-	31 (%60.78)
Kanamisin	5 (%9.80)	32 (%62.75)	14 (%27.45)
Polimiksin	5 (%9.80)	-	46 (%90.20)
Ertapenem	4 (%7.85)	-	47 (%92.15)
Sefotaksim	2 (%3.93)	-	49 (%96.07)
Trimetoprim-sülfametoksazol	-	-	40 (%78.43)

n: Pozitif izolat sayısı

Tablo 4: Kıyma örneklerinden elde edilen *E. coli* O157:H7 izolatlarının antibiyotik direnci.
Table 4: Antibiotic resistance of *E. coli* O157:H7 isolates obtained from minced meat samples.

İzolatlar	AK	AUG	AMP	E	ETP	CN	C	CTX	KF	NOR	K	PB	SXT
İzolat 1	S	R	R	R	S	S	S	S	R	R	R	S	S
İzolat 2	S	R	R	R	S	R	S	S	R	S	I	S	S
İzolat 3	S	S	-	-	S	S	-	S	R	-	I	S	-
İzolat 4	R	S	-	-	S	S	R	S	R	S	S	S	-
İzolat 5	S	R	R	R	S	S	S	S	R	S	I	S	S
İzolat 6	R	S	R	R	S	S	R	S	R	R	I	S	S
İzolat 7	R	S	-	-	S	S	S	R	R	R	S	S	-
İzolat 8	S	S	-	-	S	R	-	S	R	R	I	S	-
İzolat 9	S	S	-	-	S	S	-	S	R	R	I	S	-
İzolat 10	S	R	R	R	S	R	-	S	R	S	R	S	-
İzolat 11	R	R	R	R	S	S	S	S	R	S	I	S	S
İzolat 12	R	S	-	R	S	S	-	S	R	R	I	S	-
İzolat 13	S	R	R	R	S	S	S	S	R	S	S	S	S
İzolat 14	S	R	R	R	S	S	S	S	R	S	S	S	S
İzolat 15	S	S	-	R	S	R	R	S	R	S	R	S	S
İzolat 16	S	S	-	-	S	R	S	S	R	S	I	R	S
İzolat 17	R	S	R	-	S	S	S	S	R	S	I	S	S
İzolat 18	R	R	R	-	S	S	S	S	R	S	I	S	S
İzolat 19	S	R	R	-	R	S	S	S	R	S	I	S	S
İzolat 20	R	R	R	-	S	S	S	S	R	S	I	S	S
İzolat 21	S	R	R	R	S	S	S	S	R	S	I	S	S
İzolat 22	S	S	-	-	S	S	-	S	R	S	S	S	S
İzolat 23	S	S	-	R	S	S	R	S	R	S	I	S	S
İzolat 24	S	S	-	-	S	S	-	S	R	-	I	S	S
İzolat 25	R	S	-	-	S	S	-	S	R	-	S	S	S
İzolat 26	R	R	-	R	R	S	S	R	R	R	S	S	S
İzolat 27	S	S	R	-	S	S	S	S	R	S	I	R	S
İzolat 28	R	R	-	R	S	S	S	S	R	S	I	S	S
İzolat 29	R	R	-	-	S	S	-	S	R	R	I	S	S
İzolat 30	R	R	R	R	S	S	S	S	R	S	I	S	S
İzolat 31	S	S	-	R	S	S	S	S	R	S	I	S	-
İzolat 32	S	R	R	-	S	R	S	S	R	S	I	S	S
İzolat 33	R	S	-	-	S	S	-	S	R	S	S	S	S
İzolat 34	S	S	-	R	S	R	-	S	R	S	I	R	S
İzolat 35	S	R	R	-	S	S	S	S	R	S	S	S	S
İzolat 36	S	R	R	-	S	S	S	S	R	S	I	S	S
İzolat 37	S	R	R	-	R	S	S	S	R	S	S	S	S
İzolat 38	R	S	-	-	S	S	S	S	R	S	S	R	-
İzolat 39	S	R	R	R	S	S	S	S	R	S	I	S	S
İzolat 40	S	R	R	-	S	S	S	S	R	S	S	S	S
İzolat 41	R	S	-	-	S	S	R	S	R	S	S	S	-
İzolat 42	S	R	R	R	S	S	S	S	R	S	I	S	S
İzolat 43	S	R	R	-	R	S	S	S	R	S	I	S	S
İzolat 44	S	S	-	R	S	R	R	S	R	S	R	S	S
İzolat 45	S	R	R	R	S	S	S	S	R	S	S	S	S
İzolat 46	S	S	-	R	S	R	R	S	R	S	R	S	S

R: Dirençli, I: Orta Duyarlı, S: Duyarlı.

AK: Amikasin, AUG: Amoksisilin/Klavulanik asit, AMP: Ampisilin, E: Eritromisin, ETP: Ertapenem, CN: Gentamisin, C: Kloramfenikol, CTX: Sefotaksim, KF: Sefalatin, NOR: Norfloksasin, K: Kanamisin, PB: Polimiksin B, SXT: Trimetoprim-sülfametoksazol.

Tablo 4 (Devamı): Kıyma örneklerinden elde edilen *E. coli* O157:H7 izolatlarının antibiyotik direnci.
Table 4 (Continued): Antibiotic resistance of *E. coli* O157:H7 isolates obtained from minced meat samples.

İzolatlar	AK	AUG	AMP	E	ETP	CN	C	CTX	KF	NOR	K	PB	SXT
İzolat 47	S	S	-	-	S	R	S	S	R	S	I	R	S
İzolat 48	R	S	R	-	S	S	S	S	R	S	I	S	S
İzolat 49	S	S	-	-	S	S	-	S	R	-	I	S	S
İzolat 50	R	R	R	R	S	S	S	S	R	S	I	S	S
İzolat 51	S	S	-	-	S	S	-	S	R	R	I	S	-

R: Dirençli, I: Orta Duyarlı, S: Duyarlı.

AK: Amikasin, AUG: Amoksisilin/Klavulanik asit, AMP: Ampisilin, E: Eritromisin, ETP: Ertapenem, CN: Gentamisin, C: Kloramfenikol, CTX: Sefotaksim, KF: Sefalatin, NOR: Norfloksasin, K: Kanamisin, PB: Polimiksin B, SXT: Trimetoprim-sülfametoksazol.

TARTIŞMA VE SONUÇ

E. coli O157:H7, gıdalar aracılığıyla bulaşan hastalık etkenleri arasında önemli bir patojen olarak kabul edilmektedir. Hayvansal kaynaklı gıdalardan özellikle et ve et ürünleri ile süt ürünleri, kontamine olmuş sular ve hayvan dışkısıyla temas eden meyve ve sebzelerin tüketilmesiyle hastalık etkenleri salgınların oluşmasına yol açabilmektedir (WHO 2014). Avrupa'da Shigatoksin üreten *E. coli* vakalarının 2021 yılında *Campylobacter* spp, *Salmonella* spp. ve *Yersinia* spp.'den sonra insanlarda en yaygın görülen dördüncü zoonoz olduğu bildirilmiştir (EFSA ve ECDC 2022).

Ülkemizde kırmızı et tüketimi en çok kıyma şeklinde tercih edilmektedir (Tatlıyer Tunaz ve ark. 2022). Etlerin kıyma haline getirilmesi sırasında mikroorganizmaların etin her tarafına dağılması, kas dokusundaki doğal bariyerlerin ortadan kalkması ve hücre sıvısının kıyma kitlesine karışması bakterilerin üremesi için uygun bir ortam oluşturmaktadır. Bu durumda, ortamda bulunan mikroorganizmalar uygun şartlar oluştuğunda çoğalarak etin bozulmasına sebep olabileceği gibi halk sağlığını da önemli ölçüde tehdit edebilmektedirler (Başkaya ve ark. 2004).

E. coli O157:H7 enfeksiyonlarının çok önemli bir kısmının başta iyi pişirilmemiş et ve pastörize edilmemiş meyve suları olmak üzere sığır etinden üretilen et ürünleri, çiğ sütten üretilen peynirler, iyi yıkanmamış sebze, meyve ve salata malzemelerinden kaynaklandığı bildirilmiştir (Venter 2000; CDC 2021). *E. coli* O157:H7'nin sebep olduğu birçok enfeksiyonun, özellikle de sığır kaynaklı kontamine gıdaların tüketilmesi sonucu meydana geldiği bildirilmiştir (Nataro ve Kaper 1998).

Bu araştırmada toplam 100 adet kıyma örneğinin 24'ünde (%24) (sığır kıymalarının 17'sinde (%34) koyun kıymalarının da 7'sinde (%14)) *E. coli* O157:H7 identifiye edilmiştir. Konuyla ilgili yapılan çalışmalarda, kıymalarda farklı oranlarda *E. coli* O157:H7 tespit edildiği bildirilmiştir. Bu araştırmada elde edilen bulgular, bu konuda benzer çalışmalar yapan araştırmacıların Abong'o ve Momba (2009), Sarımehmetoglu ve ark. (2009), Balpetek ve Gürbüz (2010), Çadırcı ve ark. (2010), Direkel ve ark. (2010), Ertaş ve ark. (2013), Aydemir Atasever ve Atasever (2015) ve Bekar ve Vatansever'in (2019) elde ettiği bulgulardan yüksek bulunmuştur. Bulgular arasındaki farklılıkların kıymaların üretildiği etin mikrobiyal kalitesi, kıyma çekilmesi esnasında ve sonrasında meydana gelen kontaminasyonlar, kullanılan ekipmanın hijyenik durumu, muhafaza şartları, mevsimsel farklılıklar ve analiz metotlarının farklılıklarından kaynaklanabileceği düşünülmektedir.

Bu araştırmada *E. coli* O157:H7 oranı sığır kıymalarında koyun kıymalarına oranla daha yüksek bulunmuştur. Bu durum *E. coli* O157:H7'nin en önemli kaynağının sığırlar olmasından kaynaklanmış olabilir. Nitekim Alişarlı ve Akman (2004) ile Aksu ve ark. (1999)'da *E. coli* O157:H7'yi sığır kıymalarında koyun kıymalarından daha yüksek oranda tespit etmişlerdir.

Koyun kıyması örneklerinden izole edilen *E. coli* O157:H7 izolatları koyun kaynaklı olabileceği gibi etlerin hazırlanması ve kıyma çekilmesi sırasında çapraz kontaminasyonla sığır etlerinden de bulaşmış olabilir.

Yapılan bazı çalışmalarda kıyma örneklerinde *E. coli* O157:H7'nin yaygınlığının mevsimsel olarak farklılık gösterdiği ve bakterinin mezofilik karakterde olması nedeniyle ilkbahar ve yaz mevsimlerinde kış mevsimine göre daha yüksek oranda tespit edildiği bildirilmektedir (Chapman ve ark. 2001). Bu araştırmada da alınan örneklerde *E. coli* O157:H7'nin tespit edilme oranının ilkbahar ve yaz aylarında, kış aylarına göre çok yüksek olduğu görülmektedir (Tablo 2). Bu araştırmanın sonuçlarına benzer şekilde Can ve Elmalı (2017) da inceledikleri örneklerde *E. coli* O157'yi en fazla ilkbaharda izole ettiklerini bildirmişlerdir. Cagney ve ark. (2004) en fazla *E. coli* O157:H7 izolasyonunu Mart ayında aldıkları örneklerden elde ettiklerini belirtmişlerdir.

Antimikrobiyaller, enfeksiyona sebep olan mikroorganizmaların metabolizmalarını bozarak tedavi sağlayan preparatlardır. Bunların insan ve hayvan sağlığında aşırı ve kontrolsüz kullanımı antimikrobiyal direnç oluşmasına neden olabilmektedir (EFSA ve ECDC 2015; WHO 2020).

Araştırmada, kıyma örneklerinden elde edilen *E. coli* O157:H7 izolatlarının %100'ü sefalatine karşı dirençli bulunmuştur. Bunu sırasıyla ampisilin (%50.98), amoksisilin-klavulanik asit (%49.01), eritromisin (%45.09), amikasin (%35.30), gentamisin (%19.60), norfloksasin (%17.64), kloramfenikol (%13.72), kanamisin ile polimiksin B (%9.80), ertapenem (%7.85) ve sefotaksim (%3.93) izlemiş olup trimetoprim-sülfametoksazola karşı ise dirençlilik oluşmamıştır.

Bu araştırmada kıyma örneklerinden elde edilen *E. coli* O157:H7 izolatlarının farklı farklı antibiyotiklere karşı direnç profilleri ayrıntılı biçimde değerlendirilmiş ve elde edilen bulgular literatürdeki sonuçlarla karşılaştırılmıştır. Çalışmanın en dikkat çekici bulgusu, izolatların tamamının (%100) sefalatine dirençli olmasıdır. Bu oran, birçok çalışmada bildirilen oranlardan yüksek olmakla birlikte (Srinivasan ve ark. 2007; Bekele ve ark. 2014; Elabbasy ve ark. 2021) bazı araştırmacıların ise hiç direnç tespit etmediği bulgularla çelişmektedir (Zhao ve ark. 2001). Bu durum araştırma yaptığımız bölgede sefalatin etkinliğinin belirgin şekilde azalmış olabileceğini ve bu antibiyotiğin

tedavi veya koruyucu amaçlı kullanımının direnç gelişimini hızlandırmış olabileceğini düşündürmektedir.

Araştırmada ampisilin (%50.98) ve amoksisilin-klavulanik asit (%49.01) için saptanan direnç oranları da dikkat çekici düzeydedir. Yapılan araştırmalar ile karşılaştırıldığında bu değerlerin bazı çalışmalarda bildirilen oranlardan yüksek, bazılarından düşük olduğu görülmektedir (Srinivasan ve ark. 2007; Bekele ve ark. 2014; Atabey ve ark. 2021; Haile ve ark. 2022). Bu değişkenlik, antibiyotiklerin hayvansal üretimde kullanımı, bölgesel uygulama pratikleri ve çevresel kontaminasyonun direnç gelişiminde önemli bir rol oynadığını göstermektedir. Eritromisin, amikasin, gentamisin ve norfloksasin gibi farklı etki mekanizmalarına sahip antibiyotiklerde de benzer bir durum gözlenmiş ve direnç oranlarının ülkeden ülkeye ve çalışmadan çalışmaya farklılıklar gösterdiği görülmüştür (Abreham ve ark. 2019; Elabbasy ve ark. 2021; Fayemi ve ark. 2021; Gugsa ve ark. 2022). Bu durum, *E. coli* O157:H7 gibi zoonotik potansiyele sahip bakterilerin bulunduğu ekosistemlerde antimikrobiyal kullanım yoğunluğu ve çeşitliliğinin direnç profilini güçlü şekilde etkilediğini göstermektedir.

Kloramfenikol, kanamisin, polimiksin B, ertapenem ve sefotaksim gibi daha sınırlı kullanılan antibiyotiklerde direnç oranlarının nispeten düşük olması dikkat çekicidir. Bu durum, söz konusu antibiyotiklerin çalışma yaptığımız bölgede daha sınırlı kullanılmasıyla ilişkili olabilir (Sirinivasan ve ark. 2007; Adzitey ve ark. 2020; Joseph ve Kalyanikutty 2022). Bununla birlikte bazı çalışmalarda bu antibiyotiklere karşı hiç direnç bildirilmemiş olması (Bekele ve ark. 2014; Atabey ve ark. 2021; Tadese ve ark. 2021; Al-Imam ve Flayyih 2022; Haile ve ark. 2022) bu araştırmada elde edilen düşük düzeyli direnç oranlarının bölgesel veya çevresel faktörlerden etkilenebileceğini düşündürmektedir. Trimetoprim-sülfametoksazol için hiç direnç tespit edilmemiş olması ise bu antibiyotiğin hâlâ etkinliğini büyük ölçüde koruduğunu göstermektedir. Ancak diğer çalışmalarda farklı direnç oranlarının bildirilmiş olması (Zhao ve ark. 2001; Adzitey ve ark. 2020; Elabbasy ve ark. 2021), bu ilacın gelecekte direnç gelişimi açısından risk taşıdığını ortaya koymaktadır.

Genel olarak değerlendirildiğinde, çalışmada elde edilen bulgular *E. coli* O157:H7 izolatlarının geniş bir antibiyotik yelpazesinde değişken direnç profilleri sergilediğini ve özellikle sık kullanılan antibiyotiklerde direnç oranlarının kaygı verici düzeylere ulaşmış olabileceğini göstermektedir. Bu durum, antimikrobiyal dirençle mücadelede izleme çalışmalarının ve rasyonel antibiyotik kullanım politikalarının önemini bir kez daha ortaya koymaktadır.

E. coli O157:H7 1-100 kob/g kadar düşük miktarlarda bile enfeksiyon oluşturabileceğinden (Bell 2002), yemek hazırlanırken pişirilmeden önce veya pişirildikten sonraki aşamalarda çapraz kontaminasyon oluşmamasına dikkat edilmesi önem arz etmektedir. *E. coli* O157: H7'nin insanlara bulaşması kontamine suların (akarsu, göl, gölet vs.) kullanılması ile de olabilmektedir (Hilborn ve ark. 1999). Bu nedenle sığırlar başta olmak üzere diğer sıcakkanlı hayvanların ulaşabildiği suların *E. coli* O157:H7 ile kontamine olabileceği ihtimali göz ardı edilmemelidir. Üretiminde hayvan gübreleri kullanılan ve kontamine sularla sulanarak yetiştirilen meyve ve sebzeler etkeni taşıyabilir, bunların iyi yıkanmaması ve çiğ olarak tüketilmesi durumunda da etken çapraz kontaminasyonla ısı işlemi görmüş gıdalara bulaşarak halk sağlığı riski oluşturabilir.

Sonuç olarak; Van piyasasında satışa sunulan kıymaların hijyenik kalitesinin iyi olmadığı ve üretimin herhangi bir aşamasında *E. coli* O157:H7 ile kontamine olduğu görülmüştür. Başta *E. coli* O157:H7 olmak üzere gıda kaynaklı enfeksiyonlardan korunmak için kesim ve sonrası et ürünlerinin hazırlandığı her aşamada personel ve ekipman hijyenine dikkat edilmeli, etler her türlü kontaminasyondan korunmalı ve düşük sıcaklıklarda muhafaza edilmeli, kıymaların kullanılmasından sonra eller iyice yıkanmalı, çapraz kontaminasyonların önlenmesi için kıyma pişmiş gıdalarla temas etmemeli, üretim ve satış noktalarında çalışan personeller ile tüketiciler hijyen ve enfeksiyonlar konusunda bilinçlendirilmelidir. Ayrıca, tedavi amacıyla kullanılan antibiyotiklerin et ve süt gibi hayvansal ürünlerde kalıntı oluşturup oluşturmadığı sürekli olarak kontrol edilmelidir. Bu patojenin halk sağlığı açısından potansiyel bir tehlike olduğu unutulmamalıdır.

ÇIKAR ÇATIŞMASI

Yazarlar bu çalışma için herhangi bir çıkar çatışması olmadığını beyan ederler.

TEŞEKKÜR VE BİLGİLENDİRME

Bu araştırma Van Yüzüncü Yıl Üniversitesi Bilimsel Araştırma Projeleri Koordinatörlüğü tarafından "TYL-2021-9655" nolu proje olarak desteklenmiştir.

Bu çalışma "Kıymalarda Escherichia coli O157:H7 Varlığı ve Antibiyotik Dirençliliklerinin Belirlenmesi" isimli Yüksek Lisans Tezinden özetlenmiştir.

YAZAR KATKILARI

Fikir/Kavram: ES, YEA
Denetleme/Danışmanlık: ES
Veri Toplama ve/veya İşleme: ES, YEA
Analiz ve/veya Yorum: ES, YEA
Makalenin Yazımı: ES, YEA
Eleştirel İnceleme: ES

KAYNAKLAR

Abong'o BO, Momba MN (2009). Prevalence and characterization of *Escherichia coli* O157: H7 isolates from meat and meat products sold in Amathole District, Eastern Cape Province of South Africa. *Food Microbiol*, 26(2), 173-176.

Abreham S, Teklu A, Cox E, Sisay Tessema T (2019). *Escherichia coli* O157:H7: distribution, molecular characterization, antimicrobial resistance patterns and source of contamination of sheep and goat carcasses at an export abattoir, Mojdo, Ethiopia. *BMC Microbiol*, 19(1), 215.

Adzitey F (2020). Incidence and antimicrobial susceptibility of *Escherichia coli* isolated from beef (meat muscle, liver and kidney) samples in Wa Abattoir, Ghana. *Cogent Food Agric*, 6(1), 1718269.

Aksu H, Arun ÖÖ, Aydın A, Uğur M (1999). *Escherichia coli* 0157:H7'nin hayvansal kökenli çeşitli gıda maddelerinde varlığı, *Pendik Vet Mikrobiyol Derg*, 30(2), 77- 81.

Al-Imam MJ, Flayyih MT (2022). Molecular characterization of some virulence factors in multidrug resistance *Escherichia coli* O157:H7 isolates in Iraqi hospitals. *BNIHS*, 140(1), 1631-1637.

Alişarlı M, Akman HN (2004). Perakende satılan kıymaların *Escherichia coli* O157 yönünden incelenmesi. *Van Vet J,* 15(1-2) 65-69.

Atabey C, Kahraman T, Koluman A (2021). Prevalence and Antibiotic Resistance of *Salmonella* spp., *E. coli* O157, and *L. Monocytogenes* in Meat and Dairy Products. *Animal Health Prod and Hyg*, 10(1), 17-22.

Aydemir Atasever M, Atasever M (2015). Kıymalarda bazı patojenlerin izolasyon ve identifikasyonu. *İstanbul Üniv Vet Fak Derg*, 41(1), 60-68.

Aydogdu MH, Küçük N (2018). Türkiye'de kırmızı et tüketimindeki son değişikliklerin genel analizi. *IOSRJEF*, 9(6), 1-8.

Aytaç SA, Taban BM (2014). Food-borne microbial diseases and control: Food-borne infections and intoxications. New York. Food Processing: Strategies for Quality Assessment. Springer.

Balpetek D, Gürbüz Ü (2010). Investigations on the presence of *E. coli* O157: H7 in some meat products. *Eurasian J Vet Sci*, 26(1), 25-31.

Başkaya R, Karaca T, Sevinç İ ve ark. (2004). İstanbul'da Satışa Sunulan Hazır Kıymaların Histolojik, Mikrobiyolojik ve Serolojik Kalitesi. *Van Vet J,* 15(1), 41-46.

Bekar E (2019). Etlerde *Escherichia coli* O157:H7 varlığının araştırılması Yüksek lisans tezi Kafkas Üniversitesi, Sağlık Bilimleri Enstitüsü, Kars, Türkiye.

Bekele T, Zewde G, Tefera G, Feleke A, Zerom K (2014). *Escherichia coli* O157:H7 in Raw Meat in Addis Ababa, Ethiopia: Prevalence at an Abattoir and Retailers and Antimicrobial Susceptibility. *Int J Food Contamination*, 1(4), 1-8.

Bell C (2002). Approach to the control of entero-haemorrhagic *Escherichia coli* (EHEC). *Int J Food Microbiol*, 78(3), 197-216.

Cagney C, Crowley H, Duffy G et al. (2004). Prevalence and numbers of *Escherichia coli* O157:H7 in minced beef and beef burgers from butcher shops and supermarkets in the Republic of Ireland. *Food Microbiol*, 21, 203-212.

Can HY, Elmalı M (2017). Seasonal distribution and virulence properties of *Escherichia coli* O157, *Escherichia coli* O157: H7 isolated from minced meat and traditional cheese samples. *Kocatepe Vet J*, 10(4), 256-263.

CDC (2021). *E. coli* Outbreak Linked to Baby Spinach and *E. coli* Outbreak Linked to Packaget Salads. Erişim Tarihi: 16 Aralık 2022. Erişim Adresi: https://www.cdc.gov/ecoli/2021-outbreaks.html.

Chapman PA (2001). Ellin M, Ashton R, Shafique W. Comparison of culture, PCR and immunoassays for detecting *Escherichia coli* O157 following enrichment culture and immunomagnetic separation performed on naturally contaminated raw meat products. *Int J Food Microbiol*, 68(1-2), 11-20.

CLSI (2010). Performance Standards for Antimicrobial Susceptibility Testing, M100S, 26th Edition, USA.

Coia JE (1998). Clinical, microbiological and epidemiological aspects of *Escherichia coli* O157 infection. *FEMS Immunol Med Microbiol*, 20(1), 1-9.

Çadırcı Ö, Sırıken B, İnat G, Kevenk TO (2010). The prevalence of *Escherichia coli* O157 and O157: H7 in ground beef and raw meatball by immunomagnetic separation and the detection of virulence genes using multiplex PCR. *Meat Sci*, 84(3), 553-556.

Direkel Ş, Yıldız Ç, Aydın FE, Emekdaş G (2010). Mersin İli Yenişehir İlçesi'nde Satışa Sunulan Çiğ Kıymaların Mikrobiyolojik Kalitesinin Değerlendirilmesi. *Mersin Üniv Sağ Bil Derg*, 3(2), 8-14.

Elabbasy MT, Hussein MA, Algahtani FD et al. (2021). MALDI-TOF MS Based typing for rapid screening of multiple antibiotic resistance *E. coli* and virulent non-o157 shiga toxin-producing *E. coli* ısolated from the slaughterhouse settings and beef carcasses. *Food*, 10(4), 820.

Erol İ (2007). Gıda Hijyeni ve Mikrobiyolojisi. 1. Baskı. Pozitif Matbaacılık, Ankara.

Ertaş N, Gonülalan Z, Yildirim Y ve ark. (2013). Detection of *Escherichia coli* O157:H7 using immunomagnetic separation and mPCR in Turkish foods of animal origin. *Letters in Applied Microbiol*, 57 (4), 373-379.

EUCAST (2021). European Committee on Antimicrobial Susceptibility Testing (EUCAST) Breakpoint tables for interpretation of MICs and zone diameters Version 11.0 Acces Data 01 Ocak 2021. Erişim Adresi: https://www.eucast.org/fileadmin/src/media/PDFs/EUCAST_files/Breakpoint_tables/v_11.0_Breakpoint_Tables.pdf.

EFSA and ECDC (2015). European Food Safety Authority and European Centre for Disease Prevention and Control (EFSA and ECDC). EU summary report on antimicrobial resistance in zoonotic and indicator bacteria from humans, animals and food in 2013. *EFSA J*, 13(2), 4036.

EFSA and ECDC (2022). European Food Safety Authority and European Centre for Disease Prevention and Control (EFSA and ECDC). The European Union one health 2021 zoonoses report. *EFSA J*, 20(12), 7666.

Fayemi OE, Akanni GB, Elegbeleye JA, Aboaba OO, Njage PM (2021). Prevalence, characterization and antibiotic resistance of Shiga toxigenic *Escherichia coli* serogroups isolated from fresh beef and locally processed ready-to-eat meat products in Lagos, Nigeria. *Int J Food Microbiol*, 347, 109191.

Gugsa G, Weldeselassie M, Tsegaye Y et al. (2022). Isolation, characterization, and antimicrobial susceptibility pattern of *Escherichia coli* O157:H7 from foods of bovine origin in Mekelle, Tigray, Ethiopia. *Front Vet Sci*, 9, 924736.

Haile AF, Alonso S, Berhe N (2022). Prevalence, Antibiogram, and Multidrug-Resistant Profile of *E. coli* O157: H7 in Retail Raw Beef in Addis Ababa, Ethiopia. *Front Vet Sci*, 24(9), 734896.

Hilborn ED, Mermin JH, Mshar PA et al. (1999). A multistate outbreak of *Escherichia coli* O157:H7 infections associated with consumption of mesclun lettuce. *Arch Intern Med,* 159, 1758-1764.

Joseph J, Kalyanikutty S (2022). Occurrence of multiple drug-resistant Shiga toxigenic *Escherichia coli* in raw milk samples collected from retail outlets in South India. *J Food Sci Technol*, 59(6), 2150-2159.

Karmali M, Petric M, Steele B, Lim C (1983). Sporadic cases of haemolytic-uraemic syndrome associated with faecal cytotoxin and cytotoxin-producing *Escherichia coli* in stools. *The Lancet*, 321(8325), 619-620.

Leenanon B, Drake MA (2001). Acid Stress, Starvation and Cold Stress Affect Post stress Behavior of *Escherichia coli* O157:H7 and Non-pathogenic *Escherichia coli*. *J Food Prot*, 64(7), 970-974.

Lee PY, Costumbrado J, Hsu CY, Kim YH (2012). Agarose Gel Electrophoresis for the Separation of DNA Fragments. *JOVE*, 62, e3923.

March SB, Ratnam SJ (1989). Latex agglutination test for detection of Escherichia coli serotype O157. *J Clinic Microbiol*, 27(7), 1675–1677.

Nataro JP, Kaper JB (1998). Diarrheagenic *Escherichia coli*. *Clin Microbiol Rev*, 11(1), 142-201.

Park S, Worobo RW, Durst RA (1999). *Escherichia coli* O157: H7 as an emerging foodborne pathogen: a literature review. Critical Rev Food Sci, 39(6), 481-502.

Pehlivanoğlu F, Turutoglu H, Ozturk D (2016). CTX-M-15-type extended spectrum betalactamase-producing Escherichia coli as causative agent of bovine mastitis. *Foodborne Pathogen Dis*, 13(9), 477-82.

Sağlam D, Şeker E (2016). Gıda kaynaklı bakteriyel patojenler. *Kocatepe Vet J*, 9(2), 105-113.

Sakazaki R (1992). Serotyping of diarrheagenic *E. coli*. *Media Circle,* 34, 117.

Sarımehmetoglu B, Aksoy MH, Ayaz ND et al. (2009). Detection of *Escherichia coli* O157:H7 in ground beef using immunomagnetic separation and multiplex PCR. *Food Control*, 20, 357-361.

Sharma VK, Dean-Nystrom EA (2003). Detection of enterohemorrhagic *Escherichia coli* O157: H7 by using a multiplex real-time PCR assay for genes encoding intimin and Shiga toxins. *Vet Microbiol,* 93(3), 247-260.

Srinivasan V, Nguyen LT, Headrick SI, Murinda SE, Oliver SP (2007). Antimicrobial resistance patterns of Shiga toxin-producing *Escherichia coli* O157:H7 and O157:H7- from different origins. *Microbiol Drug Res*, 13(1), 44-51.

Tadese ND, Gebremedhi EZ, Moges F et al. (2021). Occurrence and Antibiogram of *Escherichia coli* O157: H7 in Raw Beef and Hygienic Practices in Abattoir and Retailer Shops in Ambo Town, Ethiopia. *Vet Med Int*, 8846592.

Tatlıyer Tunaz A, Kaygısız A, Arslan O (2022). Tüketicilerin Kırmızı Et Tüketimi ve Hayvan Refahı Konusundaki Bilinç Düzeylerinin Araştırılması. *Atatürk Üniv Ziraat Fak Derg*, 3(1), 24-30.

Tinta Y, Polopadang V, Sudirmman, Vidyaningrum G (2020). Comparative Analysis of Knowledge, Attitudes and Balanced Nutrition Practices in Urban and Rural High School Students in Pinrang Regency, 2(1), 18-23.

TS (2003). Türk Standartları. Gıda ve Hayvan Yemlerinin Mikrobiyolojisi-*Escherichia coli* O157'nin Tespiti için Yatay Yöntem. TS EN ISO 16654. Türk Standartları Enstitüsü, Ankara.

TS (2017). Türk Standartları. Gıda ve Hayvan Yemlerinin Mikrobiyolojisi-*Eschericha coli* 0157'nin Tespiti için Yatay Yöntem (ISO 16654:2001/Amd 1:2017) TS EN ISO 16654/A1. Türk Standartları Enstitüsü, Ankara.

Van de Venter T (2000). Emerging food-borne diseases: a global responsibility. *Food Nut Agric,* 26, 4-13.

Velusamy V, Arshak K, Korostynka O, Vaseashta A, Adley C (2012). Real Time Detection of Foodborne Pathogens- For Food Quality Monitoring & Biosecurity. (Technological Innovations in Sensing and Detection of Chemical, Biological, Radiological, Nuclear Threats and Ecological Terrorism, Springer Publishers, USA: Ed. Vaseashta AT, Braman E, Susmann P.), 149- 158.

WHO (2014). World Health Organization. Antimicrobial resistance: global report on surveillance, France.

WHO (2020). World Health Organization. Food safety. Erişim Adresi: https://www.who.int/news-room/fact-sheets/detail/food-safety

Zhao S, White DG, Ge B (2001). Identification and characterization of integron-mediated antibiotic resistance among Shiga toxin-producing *Escherichia coli* isolates. *Appl Environ Microbiol*, 67(4), 1558-64.

Van Veterinary Journal

https://dergipark.org.tr/tr/pub/vanvetj

Cite this article as: **Koyun H, Koncagül S, Özkan C et al. (2026).** Detection of Microsatellite Polymorphisms in Van Cats on Some Phenotype Characteristics. *Van Vet J*, 37(1), 36-43. DOI: https://doi.org/10.36483/vanvetj.1791025

ISSN: 2149-3359 **Original Article** e-ISSN: 2149-8644

Detection of Microsatellite Polymorphisms in Van Cats on Some Phenotype Characteristics

Hasan KOYUN[1,*] Seyrani KONCAGÜL[2] Cumali ÖZKAN[3] Mürsel KÜÇÜK[4] Hasan ÇELİKYÜREK[1] Muhammed Furkan ÜSTÜN[1] Selahaddin KİRAZ[5] Ayhan YILMAZ[6] Abdullah YEŞİLOVA[1] Kadir KARAKUŞ[7] Turgut AYGÜN[8] Abdullah KAYA[3]

[1] *Van Yüzüncü Yıl University, Faculty of Agricultural, Department of Animal Sciences, 65080, Van, Türkiye*
[2] *Ankara University, Faculty of Agricultural, Department of Animal Sciences, 06140, Ankara, Türkiye*
[3] *Van Yüzüncü Yıl University, Faculty of Veterinary Medicine, Department of Internal Diseases, 65080, Van, Türkiye*
[4] *Gazi University, Department of Medical Services and Techniques, Health Services Vocational School, 06560, Ankara, Türkiye*
[5] *Harran University, Faculty of Agricultural, Department of Animal Sciences, 63300, Şanlıurfa, Türkiye*
[6] *Bitlis Eren University, Faculty of Agriculture, Department of Animal Sciences, 56100, Bitlis, Türkiye*
[7] *Malatya Turgut Özal University, Faculty of Agricultural, Department of Animal Sciences, 44210, Malatya, Türkiye*
[8] *Bingöl University, Faculty of Veterinary Science, Department of Animal Sciences and Animal Nutrition, 12000, Bingöl, Türkiye*

Received: 25.09.2025 Accepted: 09.01.2026

ABSTRACT Using molecular genetic markers, it is possible to determine the desired genotypes while preserving the genetics of endangered species, thereby increasing or decreasing genetic diversity in populations. The Van cat is one of the endangered species living in the Lake Van region. Microsatellite markers are commonly used to estimate genetic diversity and genetic differentiation in a population. The aim of this study was to characterize the genetic structure and determine the genetic differentiation of the protected Van cat population based on the phenotypes of eye color, coat length and three points on the head. For this purpose, 25 male and 41 female cats were selected and four microsatellite loci (FCA 176, 478, 547, 688) were selected from the whole genome of the domestic cat. Based on the results of the statistical analysis, it was found that the influence of the 4 microsatellites on gender was not significant ($p \geq 0.05$). In addition, loci FCA176, 478, 547 and 688 had no effect on eye color and distribution. Although coat length and locus FCA176 were not statistically significant, it had a value of $p=0.0534$, which is very close to the p-value of 0.05. An important result was that the association between the three-point birthmark on the head and the FCA478 marker was highly significant ($p \leq 0.05$).

Keywords: *Genetic polymorphisms, Genetic resources, Microsatellite markers, Van cats.*

ÖZ

Van Kedilerinde Mikrosatellit Polimorizmlerinin Bazı Fenotip Karakteristiklerinde Saptanması

Moleküler genetik belirteçler kullanılarak, nesli tükenme tehlikesi altında olan türlerin genetik yapısı korunurken istenilen genotiplerin belirlenmesi ve böylece popülasyonlarda genetik çeşitliliğin artırılması veya azaltılması mümkün olmaktadır. Van kedisi, Van Gölü havzasında yaşayan ve koruma altındaki türlerden biridir. Mikrosatellit belirteçler, bir popülasyondaki genetik çeşitliliği ve genetik farklılaşmayı tahmin etmek amacıyla yaygın olarak kullanılmaktadır. Bu çalışmanın amacı, Van kedisi koruma popülasyonunun genetik yapısını karakterize etmek ve göz rengi, tüy uzunluğu ve baş üzerinde bulunan üçlü benek fenotiplerine dayalı olarak genetik farklılaşmayı belirlemektir. Bu amaçla, 25 erkek ve 41 dişi kedi seçilmiş olup evcil kedinin tüm genomunda yer alan dört mikrosatellit lokusu (FCA176, 478, 547, 688) incelenmiştir. İstatistiksel analiz sonuçlarına göre, dört mikrosatellitin cinsiyet üzerine etkisi önemsiz bulunmuştur ($p \geq 0.05$). Ayrıca FCA176, 478, 547 ve 688 lokuslarının göz rengi ve dağılımı üzerinde herhangi bir etkisinin olmadığı belirlenmiştir. Tüy uzunluğu ile FCA176 lokusu arasındaki ilişki istatistiksel olarak anlamlı bulunmamış olmakla birlikte $p=0.0534$ değeri, 0.05 anlamlılık düzeyine oldukça yakın çıkmıştır. Çalışmanın önemli bir sonucu ise baş üzerinde bulunan üçlü benek ile FCA478 belirteci arasındaki ilişkinin yüksek derecede anlamlı olarak bulunmuştur ($p \leq 0.05$).

Anahtar Kelimeler: *Genetik kaynaklar, Genetik polimorfizm, Mikrosatellit belirteçler, Van kedileri.*

✉ *Corresponding author: hkoyun@yyu.edu.tr

INTRODUCTION

Due to its geographical location, the Lake Van basin is home to some region-specific animal species such as the Pearl Mullet, the Karakaş, and the Norduz sheep and goats. Like other animals native to the Lake Van region in eastern Türkiye, the Van cats, which belong to the Felidae family, are among the characteristic breeds found in the Lake Van region at an altitude of 1726 meters with the coordinates 38.6140° N, 42.9182° E (Vigliotti et al. 2014).

In addition, the name of this appealing breed of cat comes from Van, the city in eastern Türkiye, and Lake Van, the largest soda lake in the world, which surrounds it. Van cats are also well adapted and have evolved naturally in certain regions of southwest Asia, such as the western parts of Armenia, Azerbaijan, Georgia and Iran. Furthermore, the characteristic phenotypes of Van cats include a heterochromatic eye color, a silky white coat color and a birthmark on the head between the two ears, which is characterized by three black dots (a three-point birthmark). This birthmark on the head often disappears in the first 6–8 months after birth. Besides, several positive behaviors are not observed in other cat breeds, including a strong emotional bond with humans, a dog-like loyalty to people, and a preference for swimming and playing with water (Odabaşıoğlu and Ateş 2000).

As already mentioned, the most remarkable phenotypic characteristic of Van cats is their different eye color, known as heterochromia. Heterochromia is a change in the color and structure of the iris that can be congenital. The color change can affect one eye alone or both eyes and can be partial, segmental, or complete. Heterochromia is caused by the absence of melanin in the whole eye or in part of the eye (Olson et al. 1989; Cargill et al. 2003; Bergastrom et al. 2014; Guha et Matiy 2014; Deane-Coe et al. 2018; Moscatelli et al. 2020).

Although the heterochromatic eyes in Van cats have three different phenotypic structures; both blue, both amber, or one eye blue and the other amber, the blue-amber colors are not constant in the right-left direction.

Various molecular genetic methods and gene markers are used in the study of living organisms at the genome level, in molecular identification and in the detection of genetic variation. The development of DNA-based genetic markers has revolutionized genome research for more than three decades. In addition, different gene markers have been used together with the polymerase chain reaction (PCR), particularly in the mapping of plant, animal and human genes and in molecular genetic studies. These include RFLP (Restriction Fragment Length Polymorphism), RAPD (Random Amplified Polymorphic DNA), AFLP (Amplified Fragment Length Polymorphism), SSLP (Single-Strand Length Polymorphism), Simple Sequence Repeats (SSRs) or microsatellites and SNP (Single Nucleotide Polymorphisms) (Weber and May 1989; Koyun et al. 2021).

Microsatellites are present in both prokaryotic and eukaryotic genomes. These are commonly referred to as simple sequence repeats (SSRs), short tandem repeats (STRs) and simple sequence length polymorphisms (SSLPs). There are approximately 100 microsatellites per locus, each of which has a length of 1–6 bp. Microsatellite repeat elements are usually present in the form of double, triple, and quaternary nucleotide sequences. In the mammalian (especially human) genome, microsatellite sequences CA and TG are the most abundant Moreover, microsatellite loci are very widely distributed and abundant in the in the genomes of living organisms (Vaiman et al. 1994; Velmala et al. 1994). Furthermore, microsatellite polymorphism is defined as repeated base sequence motifs that differ in number from one living genome to another. Polymorphism information coefficients (PIC) are high, averaging 60% (Koncagül et al 2024). They are very useful for the study of genetic differences within a population and between populations because they are highly variable, have a high mutation rate, occur in large numbers and are distributed throughout the genome, are passed on co-dominantly, and are not affected by selection. They also allow easy and inexpensive genotyping of individuals studied in the laboratory using the PCR technique. Therefore, microsatellites are widely recognized as highly informative genetic markers for the analysis of phylogenetic trees, population structures, genomic variation, evolutionary processes and fingerprints (Eizirik et al. 2003).

Microsatellite gene markers are also widely used in the genome of domestic cats (*Felis catus*) worldwide, for genetic variation, genetic distance, parental identification, and determination of disease QTLs (İmes et al. 2006; Haeringen et al. 2007; Lipinski et al. 2007; Ur Rehman 2008).

The number and density of melanin pigments in the anterior part of the iris determine eye color in mammals. If there is too much melanin, brown eyes develop. There is a difference in color between the two irides, called heterochromia or heterochromia iridum. The entire iris may be affected, or only part of the iris may be affected (sectoral heterochromia). The condition of heterochromia, which refers to a cat with two different colored eyes, is usually inherited. In most cases, heterochromia is harmless to the cat and does not affect its vision. Furthermore, one eye of an odd-eyed cat is blue, while the other eye is either green, yellow, amber or brown. Cats also are prone to having complete heterochromia, which occurs in some other animals, including humans. Sectoral (partial) heterochromia occurs when two different colors coexist in the same iris. White cats are most likely to be affected by this condition, but so are cats of any other color. (Geigy et al. 2007; Hartwell 2017; Chomdej 2018; Nganyongpanit 2018; Lui and Stokkermans 2023).

Cats with odd-eyed coloration have either the dominant white gene, which masks all other color genes, or the recessive white gene. The white-spotted gene not only causes a bicolored coat but also prevents the production of melanin. The result is a cat with one blue eye and one green, yellow, amber or brown eye. About 15 to 40% of solid white cats have one or two blue eyes (Geigy et al 2007). Moreover, interestingly, a three-point birthmark on the head, which appears after birth and gradually disappears later in life, has been identified as a phenotypic trait in Van cats (Odabaşıoğlu and Ateş 2000).

For almost 20 years, Van cats have been protected and cared for at the Van Cat Shelter of Van Yuzuncu Yil University, taking into account management, nutrition, reproduction, health and welfare. The Van cat has long been threatened with extinction because its genotype has deteriorated or been lost due to uncontrolled breeding by its owners and animal smuggling. Although it has no great economic value, the survival of these animals is very important for the preservation of native genetic resources. However, for the continuation of the Van cat lineage, it is very important to establish pedigrees to determine the associations between (or among) genetic markers and phenotypic characteristics of the Van cat breed, such as

eye color, coat color, and a three-point birthmark on the head along with their behavioral characteristics.

The purpose of this study is to initially determine microsatellite polymorphisms in Van cats and whether there is a genetic relationship between microsatellite markers and some phenotypic traits of eye color, coat texture, and a three-point birthmark on the head.

MATERIAL AND METHODS

This study was conducted with the approval document of the Local Ethics Committee for Animal Experiments of Van Yuzuncu Yil University (YÜHADYEK) dated 09.02.2009 with the number B.30.2.YYÜ.0.0506.00/300-0053. Thus, no invasive procedures were performed on the animals and no animal experiments were performed according to the legal definitions in Europe (Subject 5f of Article 1, Chapter I of Directive 2010/63/eu of the European Parliament and of the Council). Furthermore, we declare that animal welfare and safety were priorities in this study and that the Helsinki principles and protocol were carefully followed.

Animal Supply and Phenotype Records and Measurement

66 experimental animals were selected from the Van Yuzuncu Yil University cat house by selecting and recording the mother and kittens (25 males and 41 females) of different ages for the study. The quantitative data set was created based on phenotypic data of cats according to their eye color structure and coat appearance. The phenotypic characteristics in the dataset were sex, age, eye color right-left, coat length (long-short), and a three-dot birthmark on the head (present-absent).

DNA Isolation, and Oligo-Selection

Feline genomic DNA was extracted from individual samples by buccal cell collection using the Buccal Amp DNA Extraction Kit (http://www.epibio.com/docs/default-source/protocols/buccalamp-dna-extraction-kit-quickextract). Oral epithelial cells were collected with a brush from the cheeks and tongues of cats. The collected brushes were soaked in a special solution of the kit, vortexed for 10 sec and incubated at 65°C for 1 min. The samples were incubated at 98°C for 2 min after vortexing for 15 sec. Finally, the purified genomic DNA was stored at -20°C after vortexing for 15 sec.

Considering oligos, microsatellite loci with high PIC coefficients from 4 different cat chromosomes were identified by accessing the cat GenBank (access: http://www.ncbi.nlm.nih.gov/genome/guide/feliscatus/index.html) and based on (Monetti-Raymond et al. 1999) Table 1 and 2).

Table 1: Information on cat microsatellites and PCR conditions.

Micro sattellites	Chromosomes	Forward Primer	Reverse Primer	TM F/R
FCA547	C2	TGGTCATACAGGTGACAAAACA	CTGACAGTATGGAGCCTGCA	58.9/60.0
FCA176	A1	GGAAACTTGGAAAGCAAAACC	TCCACAGTTGGAGTTCTTAAGG	60.0/58.4
FCA478	X	TATATGTATGTGCGCGTGTACC	GATCGTGGTTTTTTGACACTTG	58.5/59.5
FCA688	A3	GTCAGGCTTTGTGCTGACAA	TACAGATCTGCACAAGAATCCC	60.0/59.2

Table 2: Four different microsatellite loci chosen from the genome of the domestic cat (Felis catus), along with the heterozygosity coefficient and PCR yields.

Microsatellites	Locus	Heterozygosity (%)	PCR yield (base pair; bp)
FCA176	A1	0.97	215-251 bp
FCA478	X	0.85	194-218 bp
FCA547	C2	0.81	237-251 bp
FCA688	A3	0.85	288-320 bp

PCR Conditions and Visualization of PCR Products

The best PCR conditions were found for each locus, focusing on the amount of $MgCl_2$ and the hybridization temperature. The following PCR mixing solutions and concentrations were used, as shown in Table 3.

1X TBE, a buffer solution containing Tris base, boric acid, and EDTA, was used for electrophoresis of PCR products. Agarose gels prepared at different concentrations were treated with ethidium bromide (EtBr) to visualize the PCR bands under UV light (Sambrook et al. 1989).

Allele Counting and Heterozygosity (*H*) and Polymorphism Information Coefficient (PIC) Calculation

Allelic variants of the microsatellites were determined and counted on agarose gels of different concentrations, and heterozygosity (H) and polymorphism information coefficient (PIC) were calculated using the formulas shown below (Ott 1992).

Table 3: PCR master mix and concentrations.

PCR master mix	µl
dH_2O	15.18
10X buffer	2.5
$MgCl_2$	1.5
DMSO	0.32
dNTPs	0.5
Primer F	1.5
Primer R	1.5
Taq Polimerase	0.14
DNA	2.0
Total	**25**

For heterozygosity (H);

H= 1- (Σ p_i^2) (1)

p_i: frequency of an allele of the gene

For the polymorphism information coefficient (PIC);

PIC= 1- (Σ p_i^2)- Σ $p_i^2 p_j^2$ (2)

p_i: the frequency of an allele of a gene

p_j: other allele frequencies of the gene

Statistical Analysis

Statistical relationships between genetic markers and phenotypic traits were determined with the Proc Glimmix procedure in SAS software using the statistical software package (SAS 2023).

$$Y_{ijkl} = Sex_i + \sum_{j=1}^{4}\sum_{k=1}^{3} marker_{jk} + e_{ijkl}$$

where,

Y_{ijkl} =eye color, head birthmark or coat structure

Sex_i =effect of ith sex (male or female)

$\sum_{j=1}^{4}\sum_{k=1}^{3} marker_{jk}$ =effect of kth genotype of jth locus (FCA176, FCA478, FCA547, FCA688)

e_{ijkl} = random residual

RESULTS

The distribution and frequency of eye color observed in cats are shown in Figure 1. Accordingly, the frequencies of cats with eye color BB and cats with eye color BA were the highest and equal (0.30). The frequency of cats with eye color AA was 0.23, while cats with eye color AB had the lowest frequency (0.17).

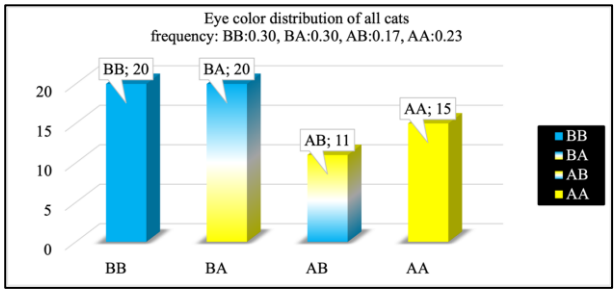

Figure 1: Distribution and frequency of all cats according to eye color and position. (AA; both eyes in amber color, BB; both eyes in blue color, AB; right amber-left blue, BA; right blue-left amber).

In Figure 3, male cats with BA eye color and position had the highest frequency (0.32), while male cats with AB and BB eye color and position had the lowest frequency (0.20).

The highest frequency of female cats with BB eye color and position was 0.37, while the lowest frequency was 0.15, as shown in Figure 4.

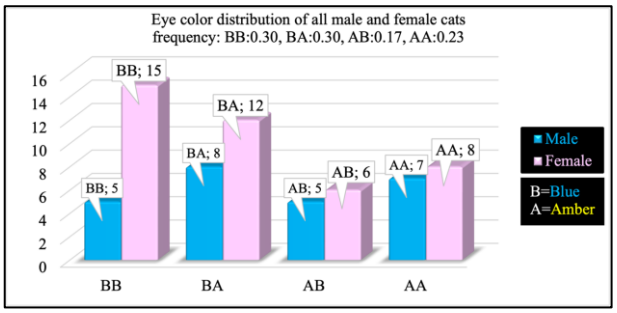

Figure 2: Distribution and frequency of all male and female cats according to eye color and position. (AA; both eyes in amber color, BB; both eyes in blue color, AB; right amber-left blue, BA; right blue-left amber).

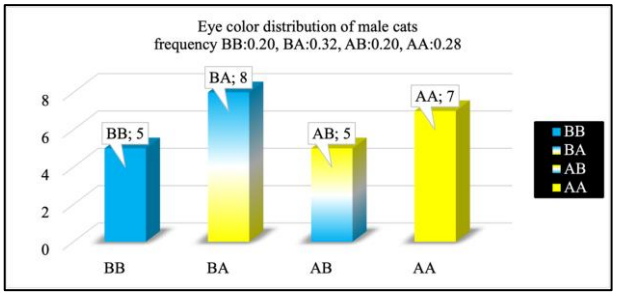

Figure 3: Distribution and frequencies of male cats according to eye color and location. (AA; both eyes in amber color, BB; both eyes in blue color, AB; right amber-left blue, BA; right blue-left amber).

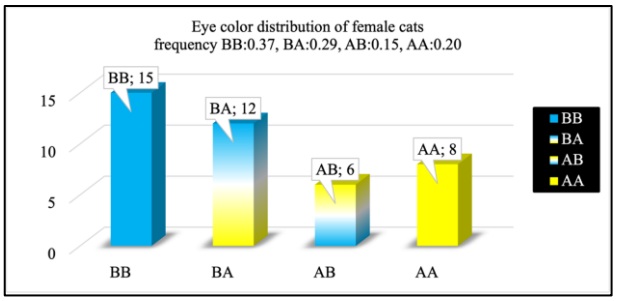

Figure 4: Distribution and frequencies of female cats according to eye color and location. (AA; both eyes in amber color, BB; both eyes in blue color, AB; right amber-left blue, BA; right blue-left amber).

PCR Results

The four cat microsatellite loci for which PCR conditions were set as a gradient (Tables 1 and 2) were observed at 56-59 °C, and the microsatellite loci of interest were amplified by PCR (at 57 °C) (Figures 5-8). Each observed individual was genotyped for four loci, and the genotype data were determined. In Table 4, the genotypic data observed for each locus were analyzed categorically (binomially). They were coded as 0(1/1), 1(1/2), 2(2/2), and their frequencies were calculated.

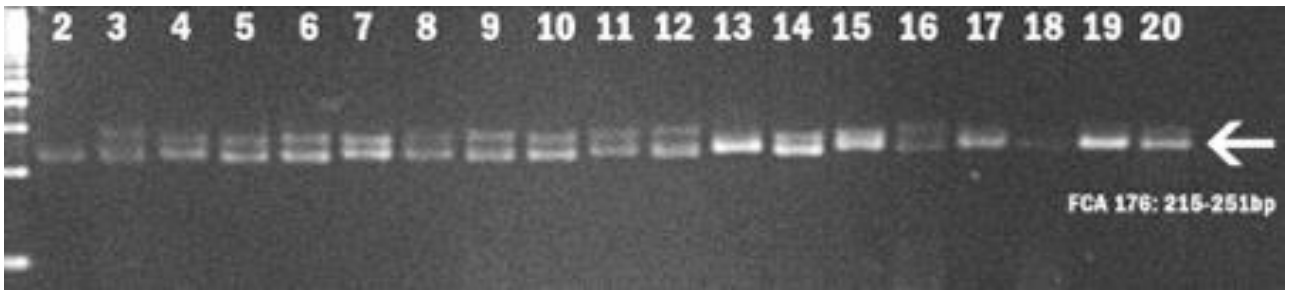

Figure 5: The PCR results for the FCA176 locus. A 4% agarose gel with a 100-bp DNA ladder (lane 1) and the elongation temperature was set to 57 °C.

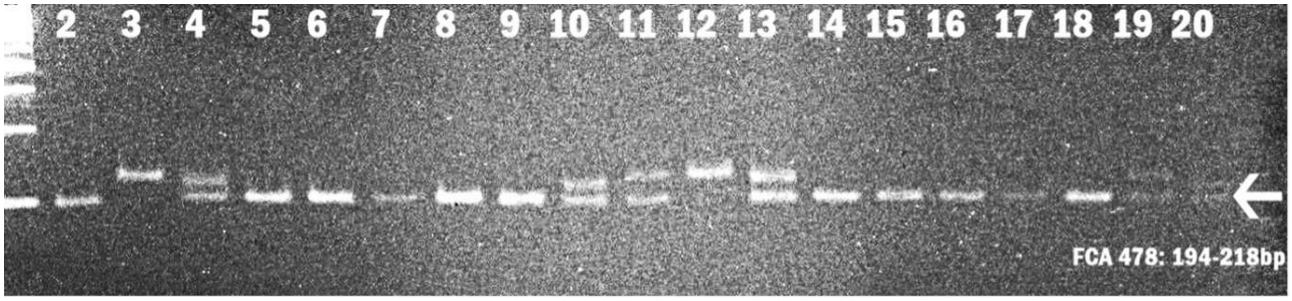

Figure 6: The PCR results for the FCA478 locus. A 4% agarose gel with a 100-bp DNA ladder (lane 1) and the elongation temperature was set to 57 °C.

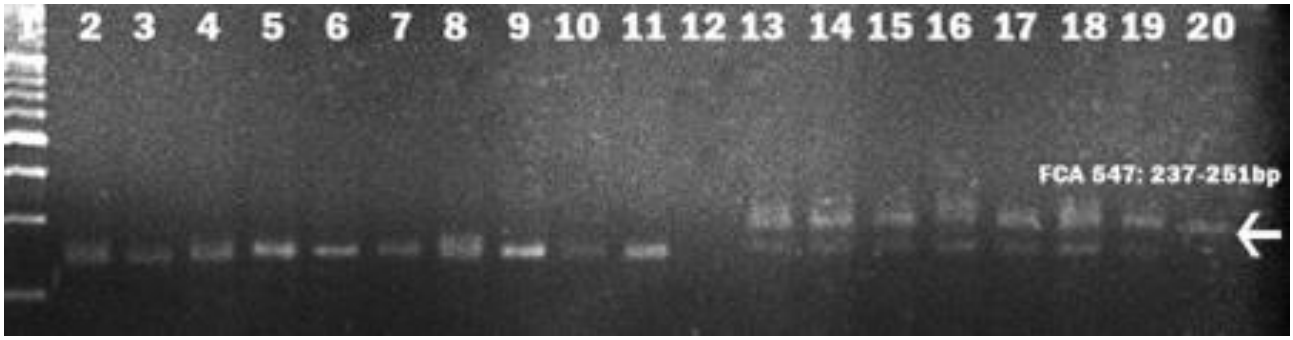

Figure 7: The PCR results for the FCA547 locus. A 4% agarose gel with a 100-bp DNA ladder (lane 1) and the elongation temperature was set to 57 °C.

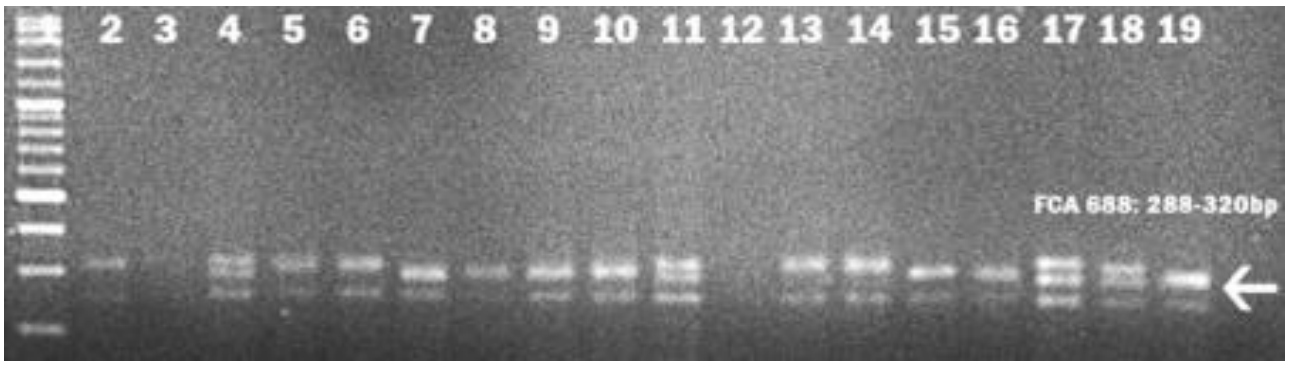

Figure 8: The PCR results for the FCA688 locus. A 4% agarose gel with a 100-bp DNA ladder (lane 1) and the elongation temperature was set to 57 °C.

Table 4: Observed alleles of genotyped microsatellite loci and their estimated size.

Microsatellites	Allele number	Frequency	PCR yield (bp)
FCA176	2 (0, 1)	0.51; 0.49	215-251
FCA478	3 (0, 1, 2)	0.47; 0.24; 029	194-218
FCA547	2 (0, 1)	0.76; 0.24	237-251
FCA688	3 (0, 1, 2)	0.13; 0.47; 0.30	288-320

According to the results of the statistical analysis, the influence of 4 microsatellites on gender was found to be insignificant (p≥0.05, Table 6-8). In addition, loci FCA176, 478, 547 and 688 had no effect on eye color and distribution. Although coat length and locus FCA176 were not statistically significant, it had a value of p=0.0534, which is very close to the p value of 0.05 (Table 6). An important result was that the association between the three-point birthmark on the head and the marker FCA478 was highly significant (p≤0.05, Table 8).

Table 5: Association analysis between eye color and microsatellite markers.

Effect	DF	F Value	Pr>F
Gender	1	0.46	0.5030
FCA176	1	0.17	0.6820
FCA478	2	0.32	0.7271
FCA547	1	0.68	0.4124
FCA688	2	1.20	0.3113

Table 6: Association analysis between coat length and microsatellite markers.

Effect	DF	F Value	Pr>F
Gender	1	3.03	0.0888
FCA176	1	3.93	0.0534
FCA478	2	1.17	0.3189
FCA547	1	1.87	0.1786
FCA688	2	1.57	0.2183

Table 7: Association analysis between a three-point birthmark on the head and microsatellite markers.

Effect	DF	F Value	Pr>F
Gender	1	0.26	0.6118
FCA176	1	0.98	0.3275
FCA478	2	3.38	0.0427
FCA547	1	0.01	0.9074
FCA688	2	0.08	0.9259

Table 8: Heterozygosity (H), Polymorphism Information Coefficient (PIC) of the microsatellites.

Microsatellites	*H* (%)	PIC (%)
FCA176	0.452	0.353
FCA478	0.431	0.341
FCA547	0.210	0.189
FCA688	0.501	0.378

Among the cats used in this study, the marker FCA547 had the lowest value (0.21) in terms of heterozygosity (%), while the microsatellite marker FCA688 had the highest value (0.501). When looking at the polymorphism information content (PIC), the marker FCA547 also showed the lowest value (0.189), while the microsatellite marker FCA688 had the highest PIC value (0.378) (Table 8).

DISCUSSION AND CONCLUSION

The research studies conducted to date on Van cats are brief; first, Şenler (1986) observed that there was no difference between the sexes in Van cats in terms of eye color, but deafness due to white coat color was noted even in small numbers. The researcher reported that the live weight of adult Van cats was 2824 g and 3568 g for females and males, respectively. Also, İnal (1992) examined the morphological characteristics of 150 Van cats. He reported that 41.35% of the Van cats were shorthair cats and 58.65% were longhair cats. The researcher reported the distribution of eye color in Van cats in terms of both eyes blue (23.99%), both eyes amber (12.68%), and one eye blue, the other amber (63.33%). Moreover, in a study (Ateş, 2000) investigating the reproductive characteristics of Van cats, the percentage of estrus, birth rate, number of kittens per gestation and gestation length were reported as 88%, 55.12%, 3.21±0.20% and 62.93±0.30, respectively. In this study, measurements of the live weight and body measurements of the Van cats were also taken at various times. Besides, in a study on the content of trace elements in the serum of Van cats, Altunok et al. (2007) reported that the content of trace elements in blood serum is determined by eye color and sex.

In recent years, various studies have been carried out in Türkiye, albeit at a limited level, to identify and conserve the indigenous genetic resources of livestock and pet or companion animals, and local genotypes are being identified using molecular methods. In this context, the first genetic study on Van cats was conducted by (Ateş 2000). In this study, the polymorphism of blood proteins was examined using 7 enzyme loci in Van cats and other cats and the phylogenetic relationships were examined. In their study, neither the individual Van cats nor the specimens of other cat species showed variations in the enzyme loci CA1, SOD, GPI and GOT. However, all cats showed genetic variation in the PGD, ME and ESD loci. Thus, three of the seven gene-enzyme systems (43%) were polymorphic with two alleles, contributing to an estimated heterozygosity of between 0.33 and 0.49 in Van cats. When three polymorphic loci were examined, PGD provided the greatest discrimination. Based on the phylogenetic tree, the Van, Persian, Turkish Angora and Turkish Tekir cats are distinct from the Persian cat.

It was mainly molecular genetic studies using microsatellite markers that investigated the genetic distance and relationship of wild cats such as cheetahs, pumas and lions, as well as population divergence in domestic cats (Hille et al 2000; Driscoll et al. 2002; Altunok et al. 2007; Altunok et al. 2011).

In this study, genetic associations between 4 different microsatellite markers for domestic cats and the phenotypic traits of eye color and position, coat length and three-point birthmark on the head of Van cats were preliminarily investigated. When analyzing the association between the microsatellite loci FCA176, 478, 547 and 688, no statistical association was found between sex and any of the microsatellite markers (Tables 5-7). Similarly, no associations were observed between eye color and position with any of the microsatellite markers (Table 5). On the other hand, a statistically moderate but almost significant association was found between coat length and the microsatellite marker FCA 176 (Table 6). Remarkably, the association between a three-point birthmark on the head and the microsatellite marker FCA478 was statistically significant (Table 7). When Table 8 is

compared with (Lui and Stokkermans 2023), it can be said that both *H* and PIC values determined in this study are quite low. (Lui and Stokkermans 2023), used 253 microsatellite markers to capture more genomic regions and create their first-generation genetic map for the domestic cat. In addition, the number of cat samples in their study was quite high (108) and came from multiple generations.

As for the studies on heterochromia in cats, conducted a preliminary investigation to determine the association between variations in the gene and heterochromia iridis on three exons of the endothelin receptor type B gene (*EDNRB*) in Thai odd-eyed cats. Using DNA sequencing, variations near the three exons of EDNRB were not statistically associated with feline heterochromia iridis in this study.

Recent reports have described a new coat and eye pattern in cats. The trait, called dominant blue eyes (DBE), has been confirmed as autosomal dominant in various feline breeding lines. The condition is known as dominant blue eyes (DBE) and involves one or more blue eyes or color particles with minimal white spots. Several breeding lines have been developed for DBE in cats, and deafness has been identified as an associated trait in some of these lines (Abitbol et al. 2025).

In their previous study, Abitbol et al. (2024) used single nucleotide polymorphisms (SNPs) to identify two variants in the PAX3 (paired box 3) gene associated with DBE in Maine Coon and Celestial cats. However, there was no evidence of an underlying variant in other DBE breeding lines. On the other hand, in a genome-wide association study of British cats, they identified a single region on chromosome C1 associated with DBE. Using samples from 14 lineages of DBE cats, they genotyped the three PAX3 variants and found these variants were absent in four lineages. Furthermore, in a similar study, Abitbol et al. (2025) updated the segregation of the variant with the dominant inheritance pattern observed in this DBE line, referred to by breeders as the Agostino line.

Türkiye is one of the few countries in the world with a great diversity of animal species, and Van cats contribute to this biodiversity in Türkiye as well as other farm animals.

The use of molecular genetic techniques can be applied to improve animal breeding by determining genetic relationships in animal populations, identifying traits and genes and implementing these relationships into breeding methods. Based on the results of this study, FCA 176, which is moderately associated with coat length, and FCA 478, which is significantly associated with a three-point birthmark on this trait, could be used as potential informative markers in future genetic studies with Van cats or other domestic cats.

There is no doubt that in future studies of this type one could definitely increase the number of detected markers and achieve a much greater genomic coverage with a much larger number of cats with pedigree records. In addition, SNP markers and chip technologies should be used as much as possible to find important associations other than microsatellite markers.

CONFLICTS OF INTEREST

All contributing authors of this research have declared that there is no conflict of interest regarding this study.

ACKNOWLEDGMENT

We would like to thank the Van Yüzüncü Yıl University Scientific Research Projects Department (YYÜ-BAP) for their contributions to this research project, which was financially supported by the Van Yüzüncü Yıl University Scientific Research Projects Directorate under project number 2008-ZF-069.

This study was orally presented at the European Biotechnology Congress held in Dubrovnik, Croatia, between May 25 and 27, 2017.

AUTHOR CONTRIBUTIONS

Idea/Concept: HK, SK, CÖ, MK, HÇ, MFÜ, SK, AY, AY, KK, TA, AK
Supervision/Consultancy: HK
Data Collection and/or Processing: CÖ, MK, HÇ, AY, KK, TA, AK
Analysis and/or Interpretation: HK, SK, HÇ., MFÜ
Writing the Article: HK, SK, MFÜ
Critical Review: HK, SK, CÖ, MK, HÇ, MFÜ, SK, AY, AY, KK, TA, AK

REFERENCES

Abitbol M, Cloquell A, Kaczmarska A et al. (2025). Dominant blue eyes in Maine Coon cats: New PAX3 variant and updated phenotypic data. *Anim Genet*, 56, e70020.

Abitbol M, Dufaure de Citres C, Rudd Garces G, et al. (2024). Different founding effects underlie dominant blue eyes (DBE) in the domestic cat. *Animals,* 14, 1845.

Alhaddad H, Khan R, Grahn RA, Gandolfi B et al. (2013). Extent of linkage disequilibrium in the domestic cat, felis silvestris catus, and ıts breeds. *Plos One,* 8, e53537.

Altunok V, Yazar E, Yüksek N (2007). Selected blood serum element in Van (Turkey) cats. *Acta Vet Brno*, 76, 171-177.

Altunok N, Yuksek N, Berkman CC, Agaoglu ZT, Togan I (2011). Genetic structure and variation of Van cats. *Biochem Genet,* 49, 511–522.

Ateş CT (2000). Van Kedilerinde morfolojik ve fizyolojik özellikler ile tek gözlülüğün dağılımının araştırılması. YYÜ Sağlık Bilimleri Enstitüsü (Doktora tezi), Van.

Bergstrom BE, Labelle AL, Pryde ME, Hamor RE, Myrna KE (2014) Prevalence of ophthalmic disease in blue-eyed horses. *Equine Vet Edu,* 26, 438–440.

Cargill EJ, Famula TR, Strain GM, Murphy KE (2003). Heritability and segregation analysis of deafness in U: S. Dalmations. *Genet,* 166, 1385-1393.

Chomdej S, Leelawattanakul P, Buddhachat K et al. (2018). Preliminary study on association of EDNRB gene with heterochromia iridis in cats (Felis catus). *Kafkas Univ Vet Fak Derg,* 24, 853-858.

Deane-Coe PE, Chu ET, Slavney A, Boyko AR, Sams AJ (2018). Direct-to-consumer DNA testing of 6,000 dogs reveals 98.6-kb duplication associated with blue eyes and heterochromia in Siberian Huskies. *PLoS Genet,* 14, e1007648.

Driscoll CA, Menotti-Raymond M, Nelson G, Goldstein D, O'Brien SJ (2002). Genomic microsatellites as evolutionary chronometers: a test in wild cats. *Genome Res,* 12, 414-423.

Eizirik E, Yuhki N, Johnson WE et al. (2003). Molecular genetics and evolution of melanism in the cat family. *Current Bio,* 13, 448–453.

Geigy CA, Heid S, Steffen F, Danielson K, Jaggy A, Gaillard C (2007). Does a pleiotropic gene explain deafness and blue irises in white cats? *Vet J,* 173, 548-553.

Guha M and Maity D (2014) Heterochromia Iridis- A Case Study. *Exploratory Anim and Med Res,* 4, 240-245.

Haeringen H, Van Haeringen W, Lyons LA (2007). An international parentage and identification panel for the domestic cat (Felis catus). *Anim Genet,* 38, 371–377.

Hartwell S (2017). White cats eye colours and deafness. DOI http://messybeast.com/whitecat.htm.

Hille A, Pelz O, Trinzen M, Schlegel M, Peters G (2000). Using microsatellite markers for genetic individualization of European wildcats (Felis silvestris) and domestic cats. *Bonn Zool Beitr,* 49, 165-176.

Imes DL, Geary LA, Grahn RA, Lyons LA (2006). Albinism in the domestic cat (Felis catus) is associated with a tyrosinase (TYR) mutation. *Anim Genet*, 37, 175–178.

İnal MS (1992). Van kedisinde göz pigmentlerinin biyolojik dağılımı. YYÜ Fen Bilimleri Enstitüsü (Yüksek Lisans tezi), Van, Türkiye.

Koncagül S, Kiraz S, Koyun H (2024). Detection of putative loci affecting milk yield in Turkish Awassi sheep using microsatellite markers. *Trop Anim Health Prod,* 56, 322.

Koyun H, Kiraz S, Karaca S et al. (2021). Single nucleotide polymorphisms of GDF9 gene/exon 2 region and their associations with milk yield and milk content traits in Karakaş and Norduz sheep breeds. *Turkish J Vet Anim Sci* 45, 881–889.

Lecis R, Pierpaoli M, Birò ZS et al. (2006). Bayesian analyses of admixture in wild and domestic cats (Felis silvestris) using linked microsatellite loci. *Mol Ecol* 15, 119-131.

Lipinski MJ, Amigues Y, Blasi M et al. (2007). An international parentage and identification panel for the domestic cat (Felis catus). *Anim Genet,* 38, 371–377.

Lui F, and Stokkermans TJ (2023). Heterochromia. StatPearls Publishing LLC. https://www.ncbi.nlm.nih.gov/books/NBK574499/.

Mahmoodi S, Rajeoni AH, Zeinolabedini M, Javanmard A, Banabazi MH (2024). Elucidating genetic variability between randomly bred domestic cats and Persian domestic cats from different geographical locations using microsatellite markers. *Vet Med and Sci,* 10, e70004.

Menotti-Raymond M, David VA, Lyons LA et al. (1999). A genetic linkage map of microsatellites in the domestic cat (felis catus), *Genomicsn*, 1, 9-23.

Moscatelli G, Bovo S, Schiavo G et al. (2020). Genome-wide association studies for iris pigmentation and heterochromia patterns in Large White pigs. *Anim Genet,* 51, 409–419.

Odabaşıoğlu F, Ateş CT (**2000**) Van kedisi (Van cat). (pp.1-6). Selçuk University Press, Konya, Türkiye.

Olson M, Hood L, Cantor C, Botstein D (1989). A common language for physical mapping of the human genome. *Sci,* 245, 1434-1435.

Ott J (1992). Analysis of Genetic Linkage. (pp. 23-36). The John Hopkins University press, Revised Second (Ed), New Jersey, USA.

SAS (SAS Institute, Inc.) (2023). SAS/STAT® 9.4: User's Guide

Sambrook J, Fritsch EF, Maniatis T. (1989). Molecular cloning: A laboratory manual. (2nd ed.), 3 vol. Cold-412 Spring Harbor, New York.

Şenler N (1986). Van kedisi, biyolojisi ve davranış özellikleri. YYÜ Fen Bilimleri Enstitüsü (Yüksek Lisans tezi), Van, Turkiye.

Ur Rehman H (2008). Heterochromia. *CMAJ,* 179, 447-448.

Vaiman D, Mercier D, Moazami-Goudarzi K et al (1994). Set of 99 cattle microsatellites: characterization, synteny mapping, and polymorphism. *Mamm Genome,* 5, 288–297.

Vigliotti L, Channell JET, Stockhecke M (**2014).** Paleomagnetism of Lake Van sediments: chronology and paleoenvironment since 350 ka. *Quat Sci Rev,* 104, 18-29.

Weber JL, May PE (1989). Abundunt class of human DNA polymorphism which can be typed using the polymerase chain reaction. *Am J of Hum Genet,* 44, 388-396.

Van Veterinary Journal

https://dergipark.org.tr/tr/pub/vanvetj

Cite this article as: **Yunus HA, Bakıcı C, Batur B et al. (2026).** A Retrospective Study on the Effects of Face-to-Face and Online Teaching Methods on Student Performance in Veterinary Anatomy Education. *Van Vet J*, 37(1), 44-53. DOI: https://doi.org/10.36483/vanvetj.1795049

ISSN: 2149-3359 **Original Article** e-ISSN: 2149-8644

A Retrospective Study on the Effects of Face-to-Face and Online Teaching Methods on Student Performance in Veterinary Anatomy Education

Hasen Awel YUNUS[1] Caner BAKICI[1,*] Barış BATUR[1,2] Ali Alparslan SAYIM[2,3] Aytaç AKÇAY[3] Çağdaş OTO[1]

[1] *Ankara University, Faculty of Veterinary Medicine, Department of Anatomy, 06070, Ankara, Türkiye*
[2] *Ankara University, Graduate School of Health Sciences, 06070, Ankara, Türkiye*
[3] *Ankara University, Faculty of Veterinary Medicine, Department of Biostatistics, 06070, Ankara, Türkiye*

Received: 02.10.2025 Accepted: 24.12.2025

ABSTRACT The Coronavirus Disease 2019 (COVID-19) pandemic triggered a rapid shift from face-to-face to online learning, significantly impacting anatomy education, which relies heavily on practical training. This retrospective study evaluated the effects of face-to-face, online, and hybrid teaching on student performance in Anatomy-I and Anatomy-II courses in Turkish and English veterinary programs at Ankara University from 2017 to 2021. A total of 1.496 students (Turkish: 1.253; English: 243) were included, with academic years categorized as pre-pandemic, acute pandemic, and prolonged pandemic. Performance was analyzed using Chi-square, t-tests, Kappa agreement, and odds ratios. Results showed higher success rates in online Anatomy-II courses, especially in 2020–2021. Anatomy-I outcomes varied, and female students consistently outperformed male students. The hybrid model produced mixed results. Online education, when well-structured, was as effective as traditional methods. Future anatomy education should adopt hybrid models that combine digital flexibility with essential in-person practice.

Keywords: *COVID-19 pandemic, Hybrid teaching, Student performance, Veterinary anatomy education.*

ÖZ

Veteriner Anatomi Eğitiminde Yüz Yüze ve Çevrimiçi Öğretim Yöntemlerinin Öğrenci Performansına Etkilerinin Retrospektif Bir Çalışması

Koronavirüs hastalığı (COVID-19) salgını, yüz yüze eğitimden çevrimiçi eğitime hızlı bir geçişe neden olmuş ve uygulama eğitimine büyük ölçüde dayanan anatomi eğitimini önemli ölçüde etkilemiştir. Bu retrospektif çalışma, 2017-2021 yılları arasında Ankara Üniversitesi'ndeki Türkçe ve İngilizce veteriner hekimliği programlarında Anatomi-I ve Anatomi-II derslerinde yüz yüze, çevrimiçi ve karma öğretimin öğrenci performansına etkilerini değerlendirmiştir. Toplam 1.496 öğrenci (Türkçe: 1.253; İngilizce: 243) çalışmaya dahil edildi ve akademik yıllar pandemi öncesi, akut pandemi ve uzayan pandemi dönemi olarak kategorize edildi. Performans, Ki-kare, t-testleri, Kappa uyumu ve olasılık oranları kullanılarak analiz edildi. Sonuçlar, özellikle 2020-2021'de çevrimiçi Anatomi-II derslerinde daha yüksek başarı oranları gösterdi. Anatomi-I sonuçları değişiklik gösterdi ve kız öğrenciler erkek öğrencilerden sürekli olarak daha iyi performans gösterdi. Hibrit model karışık sonuçlar verdi. İyi yapılandırılmış çevrimiçi eğitim, geleneksel yöntemler kadar etkiliydi. Gelecekteki anatomi eğitimi, dijital esnekliği temel yüz yüze uygulamalarla birleştiren hibrit modelleri benimsemelidir.

Anahtar Kelimeler: *Covid-19 salgını, Hibrit öğretim, Öğrenci performansı, Veteriner anatomi eğitimi.*

INTRODUCTION

The Coronavirus Disease 2019 (COVID-19) pandemic has profoundly impacted nations globally, disrupting daily life and challenging established systems across various sectors (Mishrif 2024). One of the most affected fields is education, including medical anatomy education, which has had to adapt rapidly to unprecedented circumstances. Universities and other educational institutions were compelled to transform their traditional education models, shifting from in-person instruction to distance learning (Longhurst et al. 2020; Darici et al. 2021). This sudden transition exposed significant shortcomings in the preparedness and infrastructure necessary for effective distance education. Traditionally reliant on hands-on, face-to-face instruction, anatomy education was rapidly transitioned to online methods to continue the academic process during these extraordinary circumstances (Bauler et al. 2022).

✉ *Corresponding author: vetcanerbakici@gmail.com

This shift introduced various new methodologies aimed at supporting and enhancing online learning for students. Anatomy education during the pandemic primarily utilized two forms of distance education: asynchronous and synchronous (Yoo et al. 2021; Chaker et al. 2025). Asynchronous distance education allows students to access learning materials at their own pace through podcasts, recorded lectures, and videos. In contrast, synchronous distance education involves real-time interaction through virtual classrooms and live video conferences (Lu et al. 2011; Sakaue et al. 2024; Jones et al. 2025).

Currently, many medical schools have adopted a blended approach, often referred to as the "flipped classroom" model. In this scenario, students benefit from the advantages of both asynchronous and synchronous learning. They can review materials independently at their convenience and participate in live sessions to deepen their understanding and clarify doubts (Mok 2014; Shi et al. 2018; Veeramani et al. 2015).

In Türkiye, following the government's COVID-19 guidelines, in-person classes were suspended, and education shifted to virtual learning in 2020 to ensure public health safety. The education in Ankara University Faculty of Veterinary Medicine comprises five academic years. Each academic year has two semesters that last 14 weeks. The gross anatomy program integrates theoretical instruction with hands-on practical training and consists of systematic anatomy 1 and systematic anatomy 2 with 3 hours of lecture and 4 hours of practical sessions per week for each lesson in each semester. Systematic Anatomy 1 and 2 are offered in the first and second semesters, respectively. Before COVID-19, theoretical sessions were given face-to-face, and practical sessions were held in the dissection hall in small groups of students under the supervision of a group of anatomy academicians. The final assessment is conducted as an oral examination at the end of each semester and is taken in an oral exam. During the lockdown period, theoretical sessions were conducted online using the electronic learning platform with PowerPoint presentations, and practical lessons were conducted through online videos prepared by academic staff and cadavers and other supplementary educational materials were sent to students via WhatsApp groups. In this period, different online final assessment strategies are used at the end of each semester. One of them was taken in writing for the theoretical part and as a spotter test for the practical part on a university platform. The other one was an online oral assessment same as a face-to-face assessment.

Research during the pandemic has revealed several critical issues, including technological disparities among students and institutions, insufficient training for educators in online teaching methods, and a lack of robust digital platforms for large-scale remote learning (Khaled et al. 2022). The sudden shift from face-to-face education to predominantly online systems posed numerous challenges, such as technical difficulties, limited access to digital resources, and the absence of direct interaction with teachers and peers (Davarpanah et al. 2023; Csorba et al. 2024). This abrupt transition has created significant uncertainty regarding veterinary students' academic outcomes. While some immediate effects are clear, such as technological access disparities and varying levels of engagement, the long-term issues are equally concerning (Goncalves and Capucha 2020; Muca et al. 2022). These include potential declines in academic performance, increased educational inequalities, and adverse impacts on veterinary students' mental health and motivation. Addressing these concerns is essential to ensure veterinary students receive a quality education and are adequately prepared for future academic and professional endeavors. Understanding and mitigating the challenges of distance learning is imperative to achieve this goal (Bonacini and Murat 2023).

The technique of assessment remains a vital and challenging issue, as highlighted by numerous studies. The sudden transition from face-to-face to online teaching imposed an additional responsibility on educators to evaluate students and ensure they meet specified standards (Devi and Chand 2024). This shift necessitated a reevaluation of assessment methods to maintain the integrity and effectiveness of evaluations, particularly for objective structured practical examinations (OSPE) in anatomy classes (Bhagat et al. 2014; Dissabandara et al. 2023; Sil et al. 2024). Despite the innovative approaches to online and blended learning, there is a significant gap in understanding the effectiveness of these three modalities in assessing student performance in bilingual veterinary anatomy programs (Dooley et al. 2018; Kelly et al. 2021).

We hypothesize that student performance in anatomy courses varies significantly depending on the mode of education, with potential advantages in hybrid or face-to-face models. Therefore, this retrospective study aims to compare student success across online, face-to-face, and hybrid teaching methods by analyzing performance data from anatomy courses in Turkish and English programs. By addressing these critical questions, this study seeks to contribute to the development of robust assessment strategies that uphold academic standards and ensure meaningful evaluations of student competencies.

MATERIAL AND METHODS

Ethics Statement

The required approvals for survey analyses were also obtained from the Ethics Committee of Ankara University of Health Sciences (Approval Number: 2025-07-110).

Study Design

A retrospective study was conducted to evaluate undergraduate students' performance with face-to-face, online and hybrid teaching and assessment methods in Turkish program and English programs during the COVID - 19 pre-pandemic (Academic Year (AY) 2017-2018 and AY 2018-2019), the COVID-19 acute pandemic (AY 2019-2020) and the COVID-19 prolonged pandemic (AY 2020-2021) periods in Türkiye. Since Ankara University Faculty of Veterinary Medicine is the only university in Türkiye authorized to offer an English program, only students studying at this university were included in the study (Table 1).

Participants

This study included undergraduate students in Turkish program (n=1253) and English program (n=243) who attended anatomy lessons at the Ankara University Faculty of Veterinary Medicine. Anatomy 1 was given in the first semester of the year and Anatomy 2 was given in the second semester in Ankara University. In consecutive four years (2017-2020), students were exposed to three different teaching and assessment methods. Throughout these years, the same lecturers delivered instruction for Anatomy 1 and Anatomy 2. In the AY 2017-2018 and 2018-2019, students attended lessons face-to-face for the theoretical and practical parts and exams face-to-face oral exam for midterm and final exams. In the AY 2019-2020,

during the first half of the year, students attended lessons face-to-face for the theoretical and practical parts and exams face-to-face oral exam for midterm and final exams, while in the second half of the year, teaching and exams were conducted using the online teaching and assessment method. This AY students faced a hybrid education method. In the AY 2020-2021, all teaching and assessment were conducted through the online method. In this year, students in the English program were assessed via an online oral exam, mirroring the structure of face-to-face assessments. The AY 2019-2020 experienced all periods of anatomy teaching and assessment methods. This class is uniquely placed to compare all style educations and the study took advantage of this opportunity by seeking students' qualitative views on the assessment formats.

Setting

Anatomy is taught during the first year of the five-year program at Ankara University Faculty of Veterinary Medicine. Anatomy 1 covers the locomotor system (bones, joints, and muscles), digestive system, and respiratory system in the first semester, while Anatomy 2 includes the urogenital system, cardiovascular system, endocrine system, nervous system, and sense organs in the second semester. The total anatomy education time is 196 hours (first semester: 42 theoretical, 56 practical; second semester: 42 theoretical, 56 practical). There are no traditional didactic lectures in the practical lessons. Team-based learning in terms of six-seven students study together.

In the AY 2017-2018 and 2018-2019, students attended lessons face-to-face for the theoretical and practical lessons and exams face-to-face oral exam for all exams. In the second year of the AY 2019-2020 and the whole AY 2020-2021 education strategy changed to online education and assessment. The theoretical sessions were conducted online using the electronic learning platform with PowerPoint presentations, and practical lessons were conducted online videos prepared by academic staff of protection cadavers and other supplementary educational materials were sent to students via WhatsApp groups. In this period, different online final assessment strategies are used at the end of each semester for two different programs. In Turkish and English programs, AY 2019-2020 was taken in writing for the theoretical part was taken in answering questions with choosing best answer and open ended questions on traditional atlas pictures on a university platform. Exam questions were negotiated among three anatomy specialists prior to student administration to ensure that memory and application levels were covered in the assessment (Boulos 2022). Anatomy examination consisted of 40 single best answers questions and online assessment time was one hour. There was no negative marking for choosing a wrong answer. Students were permitted to revise and change their answers within the allocated time and before submitting the examination.

Control Variables

Teaching staff consistency: The same lecturers taught both Anatomy 1 and Anatomy 2 throughout the study period (AY 2017–2021), ensuring no confounding variation in instructor expertise or delivery.

Curriculum and Resources

The course content, hours, and team-based learning structure remained unchanged across all years; only the delivery mode (face-to-face vs. online) and assessment methods differed.

Table 1: Education and assessment methods of undergraduate veterinary students studying in Turkish and English programs.

Academic Year	Teaching Methods	Assessment Methods
2017-2018	Face-to-face	Face-to-face
2018-2019	Face-to-face	Face-to-face
2019-2020	Face-to-face (First semester)	Face-to-face (First semester)
	Online (Second semester)	Online (Second semester)
2020-2021	Online	Online *

Assessment Design and Standardization

Face-to-face exams (AY 2017–2019): Oral exams were conducted uniformly by anatomy faculty, with questions drawn from a pre-approved pool to ensure consistency in difficulty and scope. Online exams (AY 2019–2021): Written exams (Turkish/English program, 2019–2020): Questions (40 single-best-answer and open-ended) were validated by three anatomy specialists to cover memory and application levels (Boulos 2022). The 1-hour time limit and lack of negative scoring were standardized. Online oral exams (English program, 2020–2021): Mirrored face-to-face oral assessments in structure and grading rubrics, with faculty trained to administer them virtually under timed conditions

Statistical Analysis

Student performance was compared across pre-pandemic (AY 2017–2019), acute pandemic (AY 2019–2020), and prolonged pandemic (AY 2020–2021) periods, controlling for program language (Turkish/English) and anatomy course (1 vs. 2). These data were used to estimate the impact of face-to-face teaching and assessment, hybrid teaching and assessment, and online teaching and online assessment for two different education programs and student performance according to Anatomy 1 and Anatomy 2 lessons passing grades. Data was analyzed using SPSS version 27.0. Descriptive statistics for the data were calculated and presented as "percentage (n%)" or "mean±standard deviation", based on the distribution of the data. Comparisons of percentages for final, make-up, and passing grades in anatomy courses based on educational models and gender were conducted using Chi-square analysis. The mean passing grades of the courses were compared using the Student's t-test. The agreement between online and F2F (face to face) education for Anatomy-I and Anatomy-II courses was assessed using Kappa analysis. The probability of passing Anatomy-I compared to students who failed Anatomy-II was assessed by calculating the odds ratio (OR). The level of significance was set at $p<0.05$.

RESULTS

In the Turkish program, Anatomy-I had the highest passing rate in 2020, followed by 2018, with 2017 being the lowest. For Anatomy-II, 2019 had the highest rate, followed by 2020, while 2017 remained the lowest (Figure 1).

In the English program, Anatomy-I had the highest passing rate in 2019, then 2018, with 2017 being the lowest. For Anatomy-II, 2019 also ranked highest, followed by 2020, while 2018 was the lowest (Figure 2).

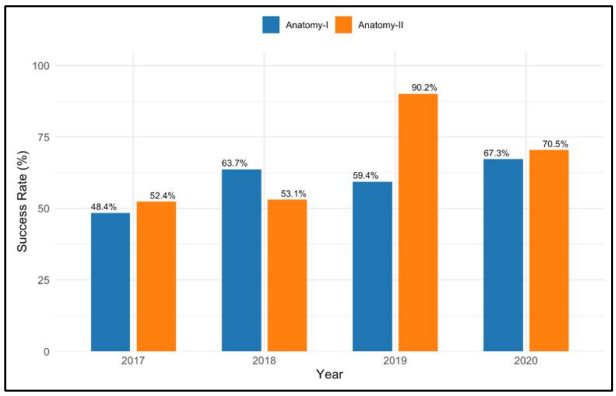

Figure 1: Success percentages by year (Turkish program).

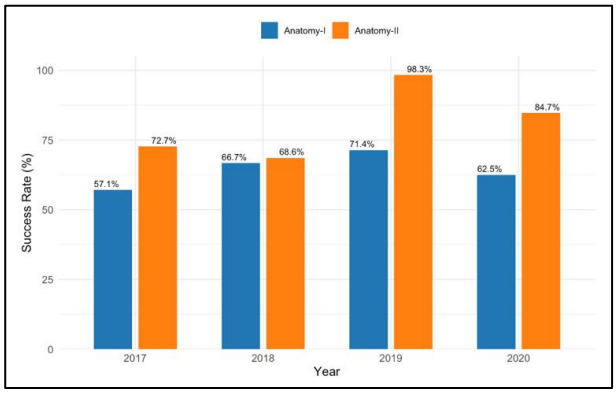

Figure 2: Success percentages by year (English program).

Anatomy-I Turkish Course Success Rates Comparison

Comparison of Anatomy-I Course Success Rates

For the Turkish Program's Anatomy-I course, no significant difference existed between online and face-to-face models in make-up exams ($p>0.05$), but online final exam and passing rates were significantly higher ($p<0.05$; Table 2). Gender analysis revealed: (1) No gender differences in make-up exams ($p>0.05$), but females outperformed males in final exams and passing rates ($p<0.05$; Table 2); (2) This pattern held for both online (Table 3) and face-to-face courses, where females also scored higher in all assessments ($p<0.05$; Table 4 and Table 5).

Table 2: Comparison of Anatomy-I Course General Education Model Course Passing Status Rates (Turkish program for 2017-2018, 2018-2019, 2019-2020 and 2020-2021 academic years).

General	Education model	Course Passing Status		p
		Failed (n%)	Passed (n%)	
Final	Online	123 (43.8%)	158 (56.2%)	<0.001
	Face to face	544 (55.9%)	429 (44.1%)	
Make-up exam	Online	92 (74.8%)	31 (25.2%)	0.606
	Face to face	418 (77.0%)	125 (23.0%)	
All	Online	92 (32.7%)	189 (67.3%)	0.002
	Face to face	418 (43.0%)	555 (57.0%)	

Table 3: Anatomy-I General Comparison of Course Passing Rates by Gender (Turkish program for 2017-2018, 2018-2019, 2019-2020 and 2020-2021 academic years).

Anatomy-I General	Gender	Course Passing Status		p
		Failed (n%)	Passed (n%)	
Final	Male	412 (58.4%)	294 (41.6%)	<0.001
	Female	255 (46.5%)	293 (53.5%)	
Make-up exam	Male	328 (79.8%)	83 (20.2%)	0.012
	Female	182 (71.4%)	73 (28.6%)	
All	Male	328 (46.5%)	378 (53.5%)	<0.001
	Female	182 (33.2%)	366 (66.8%)	

Table 4: Comparison of Course Passing Rates by Gender in Anatomy-I Online Course (Turkish program from 2019-2020 and 2020-2021 academic year).

Anatomy-I Online	Gender	Course Passing Status		p
		Failed (n%)	Passed (n%)	
Final	Male	82 (53.6%)	71 (46.4%)	<0.001
	Female	41 (32.0%)	87 (68.0%)	
Make-up exam	Male	61 (74.4%)	21 (25.6%)	1.000
	Female	31 (75.6%)	10 (24.4%)	
All	Male	61 (39.9%)	92 (60.1%)	0.005
	Female	31 (24.2%)	97 (75.8%)	

Table 5: Comparison of Course Passing Rates of Anatomy-I Face-to-Face Course by Gender (Turkish program from 2017-2018 and 2018-2019 academic year).

Anatomy-I Face to Face	Gender	Course Passing Status		p
		Failed (n%)	Passed (n%)	
Final	Male	330 (59.7%)	223 (40.3%)	0.007
	Female	214 (51.0%)	206 (49.0%)	
Make-up exam	Male	267 (81.2%)	62 (18.8%)	0.004
	Female	151 (70.6%)	63 (29.4%)	
All	Male	267 (48.3%)	286 (51.7%)	<0.001
	Female	151 (36.0%)	269 (64.0%)	

Anatomy-I English Course Success Rates Comparison

There was no statistically significant difference between online and face-to-face education in the Anatomy-I English program course ($p>0.05$) (Table 6). Similarly, no statistically significant difference was found between females and males in the Anatomy-I English program course ($p>0.05$) (Table 7) or the Anatomy-I English online course ($p>0.05$) (Table 8). Likewise, no significant difference was observed between females and males in the Anatomy-I English face-to-face course ($p>0.05$) (Table 9).

Table 6: Comparison of Anatomy-I English Course General Education Model Course Success Rates (English program for 2017-2018, 2018-2019, 2019-2020 and 2020-2021 academic years).

Anatomy-I General (English program)	Education model	Course Passing Status		p
		Failed (n%)	Passed (n%)	
Final	Online	47 (53.4%)	41 (46.6%)	0.512
	Face to face	76 (49.0%)	79 (51.0%)	
Make-up exam	Online	33 (70.2%)	14 (29.8%)	0.993
	Face to face	52 (68.4%)	24 (31.6%)	
All	Online	33 (37.5%)	55 (62.5%)	0.535
	Face to face	52 (33.5%)	103 (66.5%)	

Table 7: Comparison of Course Success Rates of Anatomy-I English Course According to Gender (English program for 2017-2018, 2018-2019, 2019-2020 and 2020-2021 academic years).

Anatomy-I General (English program)	Gender	Course Passing Status		p
		Failed (n%)	Passed (n%)	
Final	Male	64 (54.2%)	54 (45.8%)	0.273
	Female	59 (47.2%)	66 (52.8%)	
Make-up exam	Male	47 (73.4%)	17 (26.6%)	0.375
	Female	38 (64.4%)	21 (35.6%)	
All	Male	47 (39.8%)	71 (60.2%)	0.123
	Female	38 (30.4%)	87 (69.6%)	

Table 8: Comparison of Course Success Rates by Gender in Anatomy-I English Online Course (English program from 2019-2020 and 2020-2021 academic year).

Anatomy-I Online (English program)	Gender	Course Passing Status		p
		Failed (n%)	Passed (n%)	
Final	Male	23(54.8%)	19(45.2%)	0.977
	Female	24(52.2%)	22(47.8%)	
Make-up exam	Male	17(73.9%)	6(26.1%)	0.823
	Female	16(66.7%)	8(33.3%)	
All	Male	17(40.5%)	25(59.5%)	0.741
	Female	16(34.8%)	30(65.2%)	

Anatomy-II Turkish Course Success Rates Comparison

For Anatomy-II, no difference existed between online and face-to-face models in make-up exams (p>0.05), but online students scored higher in final exams and passing rates (p<0.05; Table 9 and Table 10). Females consistently outperformed males in online courses (p<0.05) (Table 11 and Table 12) and overall course performance (Table 10). However, in face-to-face courses, no gender difference existed in final exams (p>0.05), though females scored higher in make-up exams and overall passing (p<0.05; Table 13).

Table 9: Comparison of Course Success Rates by Gender in Anatomy-I English Online Course (English program from 2017-2018 and 2018-2019 academic year).

Anatomy-I Face to face (English program)	Gender	Course Passing Status		p
		Failed (n%)	Passed (n%)	
Final	Male	41(53.9%)	35(46.1%)	0.230
	Female	35(44.3%)	44(55.7%)	
Make-up exam	Male	30(73.2%)	11(26.8%)	0.474
	Female	22(62.9%)	13(37.1%)	
All	Male	30(39.5%)	46(60.5%)	0.125
	Female	22(27.8%)	57(72.2%)	

Table 10: Comparison of Anatomy-II Turkish Course General Education Model Course Success Rates (Turkish program for 2017-2018, 2018-2019, 2019-2020 and 2020-2021 academic years).

Anatomy-II General	Education model	Course Passing Status		p
		Failed (n%)	Passed (n%)	
Final	Online	141 (25.3%)	416 (74.7%)	<0.001
	Face to face	445 (60.5%)	291 (39.5%)	
Make-up exam	Online	91 (68.9%)	41 (31.1%)	0.280
	Face to face	348 (78.2%)	97 (21.8%)	
All	Online	102 (18.3%)	455 (81.7%)	<0.001
	Face to face	348 (47.3%)	388 (52.7%)	

Table 11: Anatomy-II General Comparison of Course Success Rates by Gender (Turkish program for 2017-2018, 2018-2019, 2019-2020 and 2020-2021 academic years).

Anatomy-II General	Gender	Course Passing Status		p
		Failed	Passed	
Final	Male	362 (49.7%)	367 (50.3%)	<0.001
	Female	224 (39.7%)	340 (60.3%)	
Make-up exam	Male	286 (81.0%)	67 (19.0%)	<0.001
	Female	153 (68.3%)	71 (31.7%)	
All	Male	296 (40.6%)	433 (59.4%)	<0.001
	Female	154 (27.3%)	410 (72.7%)	

Anatomy-II English Course Success Rates Comparison

Anatomy-II showed no difference between online and face-to-face models for make-up exams (p>0.05), but online students scored higher in final exams and passing rates (p<0.05; Table 14). No gender differences were found in English program courses, whether overall (Table 15), online (Table 16), or face-to-face (Table 17) (all p>0.05).

Table 12: Comparison of Course Success Rates According to Gender in Anatomy-II Online Course (Turkish program from 2019-2020 and 2020-2021 academic year).

Anatomy-II Online	Gender	Course Passing Status		p
		Failed (n%)	Passed (n%)	
Final	Male	97 (32.1%)	205 (67.9%)	<0.001
	Female	44 (17.3%)	211 (82.7%)	
Make-up exam	Male	68 (77.3%)	20 (22.7%)	0.006
	Female	23 (52.3%)	21 (47.7%)	
All	Male	78 (25.8%)	224 (74.2%)	<0.001
	Female	24 (9.4%)	231 (90.6%)	

Table 13: Comparison of Course Success Rates of Anatomy-II Face-to-Face Course by Gender (Turkish program from 2017-2018 and 2018-2019 academic year).

Anatomy-II Face to face	Gender	Course Passing Status		p
		Failed (n%)	Passed (n%)	
Final	Male	265 (62.1%)	162 (37.9%)	0.297
	Female	180 (58.3%)	129 (41.7%)	
Make-up exam	Male	218 (82.3%)	47 (17.7%)	0.012
	Female	130 (72.2%)	50 (27.8%)	
All	Male	218 (51.1%)	209 (48.9%)	0.016
	Female	130 (42.1%)	179 (57.9%)	

Table 14: Comparison of Anatomy-II English Course General Education Model Course Success Rates (English program for 2017-2018, 2018-2019, 2019-2020 and 2020-2021 academic years).

Anatomy-II General (English program)	Education model	Course Passing Status		p
		Failed (n%)	Passed (n%)	
Final	Online	26 (20.0%)	104 (80.0%)	<0.001
	Face to face	48 (50.5%)	47 (49.5%)	
Make-up exam	Online	11 (44.0%)	14 (56.0%)	0.359
	Face to face	28 (58.3%)	20 (41.7%)	
All	Online	12 (9.2%)	118 (90.8%)	<0.001
	Face to face	28 (29.5%)	67 (70.5%)	

The student performance of final, make-up and passing grades in online and face-to-face anatomy courses for both Turkish and English programs (Table 18). The statistical data for final exams, make-up exams, and overall course passing status in Anatomy-I and Anatomy-II. In the Turkish program, face-to-face students performed better in Anatomy-I, while online students had higher scores in Anatomy-II (Figure 3) (Table 18). Significant differences ($p<0.001$) were observed, particularly in Anatomy-II final exams and course passing rates. However, make-up exam performance showed less variation between the two modes of education. In the English program, results were mixed. Face-to-face students performed slightly better in Anatomy-I final and make-up exams, but online students had higher scores in Anatomy-II. The difference in Anatomy-II was statistically significant ($p<0.001$), especially in final exams and course passing status. Overall, online students performed comparably to or slightly better than their face-to-face counterparts in certain cases, suggesting that online education can be effective, particularly in Anatomy-II courses (Table 18).

Table 15: Comparison of Anatomy-II English Course Success Rates by Gender (English program for 2017-2018, 2018-2019, 2019-2020 and 2020-2021 academic years).

Anatomy-II General (English program)	Gender	Course Passing Status		p
		Failed (n%)	Passed (n%)	
Final	Male	35 (33.3%)	70 (66.7%)	0.894
	Female	39 (32.5%)	81 (67.5%)	
Make-up exam	Male	19 (54.3%)	16 (45.7%)	1.000
	Female	20 (52.6%)	18 (47.4%)	
All	Male	19 (18.1%)	86 (81.9%)	1.000
	Female	21 (17.5%)	99 (82.5%)	

Table 16: Comparison of Course Success Rates of Anatomy-II English Online Course by Gender (English program from 2019-2020 and 2020-2021 academic year).

Anatomy-II Online (English program)	Gender	Course Passing Status		p
		Failed (n%)	Passed (n%)	
Final	Male	12 (20.0%)	48 (80.0%)	1.000
	Female	14 (20.0%)	56 (80.0%)	
Make-up exam	Male	4 (33.3%)	8 (66.7%)	0.529
	Female	7 (53.8%)	6 (46.2%)	
All	Male	4 (6.7%)	56 (93.3%)	0.528
	Female	8 (11.4%)	62 (88.6%)	

Table 17: Comparison of Course Success Rates by Gender in Anatomy-I English Online Course (English program from 2017-2018 and 2018-2019 academic year).

Anatomy-II Face to face (English program)	Gender	Course Passing Status		p
		Failed (n%)	Passed (n%)	
Final	Male	23 (51.1%)	22 (48.9%)	1.000
	Female	25 (50.0%)	25 (50.0%)	
Make-up exam	Male	15 (65.2%)	8 (34.8%)	0.526
	Female	13(52.0%)	12 (48.0%)	
All	Male	15 (33.3%)	30 (66.7%)	0.577
	Female	13 (26.0%)	37 (74.0%)	

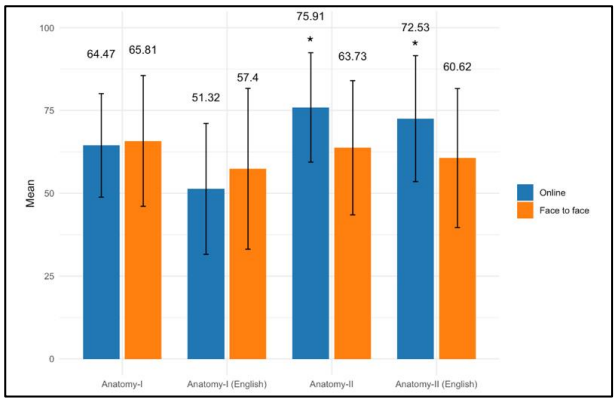

Figure 3: Anatomy Courses Education Model Group Averages Comparison. *: Indicates statistically significant (P<0.05).

Table 18: The student performance in final, make-up and passing grades in online and face-to-face anatomy courses for both Turkish and English programs.

Anatomy	Course Evaluation	Education model	Grade $\bar{x}$ ± SD	p
Anatomy-I (Turkish program)	Final	Online	49.74 ± 19.44	0.001
		Face to face	54.73 ± 22.67	
	Make-up exam	Online	41.57 ± 12.67	0.003
		Face to face	46.69 ± 20.63	
	Course Passing Status	Online	64.47 ± 15.62	0.270
		Face to face	65.81 ± 19.75	
Anatomy-II (Turkish program)	Final	Online	67.18 ± 18.07	<0.001
		Face to face	52.12 ± 22.48	
	Make-up exam	Online	51.46 ± 15.12	0.172
		Face to face	48.35 ± 23.17	
	Course Passing Status	Online	75.91 ± 16.51	<0.001
		Face to face	63.73 ± 20.26	
Anatomy-I General (English program)	Final	Online	51.32 ± 19.77	0.064
		Face to face	56.94 ± 21.39	
	Make-up exam	Online	45.94 ± 13.7	0.089
		Face to face	52.02 ± 17.21	
	Course Passing Status	Online	51.32 ± 19.77	0.069
		Face to face	57.4 ± 24.27	
Anatomy-II General (English program)	Final	Online	68.91 ± 20.98	<0.001
		Face to face	57.4 ± 19.15	
	Make-up exam	Online	58.91 ± 20.17	0.797
		Face to face	57.55 ± 14.71	
	Course Passing Status	Online	72.53 ± 19.02	<0.001
		Face to face	60.62 ± 20.99	

The level of agreement between the Anatomy-I and Anatomy-II courses was assessed using the Kappa test in both face-to-face and online education settings. In face-to-face education, a moderate level of agreement was observed between the two courses (Kappa=0.51). Additionally, students who passed Anatomy-I were 9.63 times more likely to pass Anatomy-II compared to those who did not pass Anatomy-I. In online education, a low level of agreement was found between the Anatomy-I and Anatomy-II courses (Kappa=0.32). Furthermore, students who succeeded Anatomy-I were 6.25 times more likely to success Anatomy-II than those who did not pass Anatomy-I (Table 19).

Table 19: The level of agreement between the Anatomy-I and Anatomy-II courses was assessed using the Kappa test, both in face-to-face and online education settings.

Course	Education model	Course Passing Status	Course Passing Status	
			Passed (n%)	Failed (n%)
Anatomy-II	Face to Face	Passed	184 (74.5%)	63 (25.5%)
		Failed	67 (23.3%)	221 (76.7%)
	Online	Passed	223 (65.6%)	117 (34.4%)
		Failed	25 (23.4%)	82 (76.6%)

DISCUSSION AND CONCLUSION

This retrospective study provides valuable insights into the comparative effectiveness of online and face-to-face education models in veterinary anatomy courses (Anatomy-I and Anatomy-II) across Turkish and English programs. Higher passing rates were observed in the 2019 and 2020 academic years, whereas the lowest in 2017.

The results indicated that students who took the final examination online achieved significantly higher success rates compared to those who took it in a face-to-face setting. This finding aligns with prior research showing that online assessments may sometimes yield higher success rates, potentially due to reduced exam anxiety, flexible timing, or access to supportive learning materials (Daniel 2020; Gupta et al. 2021). However, it contrasts with studies suggesting face-to-face education facilitates better engagement and deeper understanding, leading to higher performance (Pei and Wu 2019). On the other hand, for make-up exams, no significant difference was observed between online and face-to-face modalities, suggesting that at this stage, students' performance may depend more on individual effort and less on the exam format. When examining overall course outcomes, students in online education demonstrated a higher passing rate compared to face-to-face education. This trend supports findings from emergency remote teaching periods during the COVID-19 pandemic, where online formats unexpectedly yielded higher pass rates, potentially due to assessment flexibility (Adedoyin and Soykan 2023). Comparatively, previous studies focusing on Anatomy education have underscored the challenges posed by online formats due to reduced access to cadaveric material and practical demonstrations (Longhurst et al. 2020). Yet the higher pass rates observed in this study during online education might suggest adaptive success in theoretical parts of Anatomy (Franchi 2020) or it may be due to students taking exams remotely may collaborate (e.g., chat groups, video calls), sharing answers in real-time. Research during the pandemic suggests academic misconduct rates increased during online learning periods. For instance, a study by Lancaster and Cotarlan (2021) found a sharp rise in online exam cheating compared to traditional in-person exams.

In this study significant gender differences in passing rates was revealed for Turkish veterinary anatomy education program over four academic years of Anatomy-I course (2017-2021). Female students consistently outperformed

male students in both final and make-up exams. The difference in final exam pass rates between female and male students was statistically significant. This is consistent with earlier studies highlighting that female students often exhibit better academic discipline and engagement in courses (Yaman et al., 2023; Kessels and Van Houtte, 2022). During make-up exams, female students demonstrated a significantly higher pass rate compared to male students, reinforcing the trend of better female performance. Overall, the cumulative course passing rate was also significantly higher for females than males. Similar studies have attributed these gender differences to variations in learning strategies, greater academic commitment, and more effective coping mechanisms among female students (Gwazdauskas et al. 2014).

In comparison of Course Passing Rates of Anatomy-I Face-to-Face Course by Gender in Turkish program during 2017-2018 and 2018-2019 academic year, female students had significantly higher pass rates both in final exams and overall course outcomes. These results are in line with prior studies in medical education that have documented female students' superior performance in preclinical and theoretical courses, often attributed to higher academic engagement and better learning strategies (Al-Angari et al. 2022). In a similar pattern gender Differences in Online Anatomy-I Courses in Turkish program during 2019-2020 and 2020-2021 academic year is a statistically significant difference in final exam pass rates. Female students also had a significantly higher overall passing rate. These findings are consistent with earlier studies suggesting that female students may adapt better to online learning environments, demonstrating higher motivation, better time management, and more effective study strategies (Price, 2006; Coldwell et al., 2007). The make-up exam pass rates did not differ significantly by gender during 2019-2020 and 2020-2021 academic year. Our findings support prior research indicating that female students generally perform better in anatomy courses, whether delivered online or face-to-face. For instance, studies have shown that female students tend to engage more in class and utilize more consistent study habits, which may explain their superior outcomes (Kessels and Van Houtte 2022; Yaman et al. 2023).

The current retrospective study evaluated the effects of face-to-face and online teaching methods on student performance in the Anatomy-I English course within veterinary anatomy education. Our findings demonstrated no statistically significant difference in course success rates between the online and face-to-face education models. Additionally, no gender-based difference in academic performance was observed in either mode of instruction. Our results align with previous research showing equivalent learning outcomes between online and face-to-face education in health-related sciences. Studies comparing online and face-to-face learning in medical education found no significant difference in knowledge gains between the two formats (Pei and Wu 2019; Torda and Shulruf 2021). Similarly, Díez-Pascual et al. (2025) also concluded that blended and fully online learning environments often yield comparable or even better outcomes than face-to-face instruction. Online learning led to significantly higher post-test scores and pre-and post-test score gains compared to offline learning. Additionally, online education was more satisfactory to participants than offline learning (Gao et al. 2022). However, contrary to our findings, some studies have noted superior outcomes in face-to-face settings, especially in courses requiring hands-on practice, such as anatomy. For example, Longhurst et al. (2020) highlighted that students preferred face-to-face anatomy learning, citing better engagement and understanding, particularly for practical components.

The retrospective study examined the effects of online and face-to-face teaching methods on student performance in the Anatomy-II course within the Turkish veterinary anatomy program revealed that students participating in online education achieved significantly higher final exam scores and overall course passing rates compared to those in face-to-face education. No significant difference was found between online and face-to-face students in the make-up exam performance. Moreover, female students outperformed male students in nearly all cases, particularly in the online education setting. Our findings demonstrating better academic outcomes in online anatomy education contrast with some traditional expectations that face-to-face learning, especially for practical courses like anatomy, would yield superior results. The evidence supports that well-structured online learning can be as effective as, or even more effective than, traditional face to face learning in medical education, depending on the instructional design and delivery methods. The transition to online platforms, accelerated by the COVID-19 pandemic, has highlighted the potential for online education to enhance learning outcomes and student satisfaction in medical training (Stevens et al. 2021; Gao et al. 2022).

The retrospective study examined the effects of online and face-to-face teaching methods on student performance in the Anatomy-II course within the English veterinary anatomy program revealed that while there was no statistically significant difference between the online and face-to-face education models for the make-up exam, a significant difference was observed in the final exam and overall course passing rates. Students in the online education model achieved higher final exam scores and course passing rates compared to those in the face-to-face model. This suggests that the online education model may offer certain advantages in terms of student performance, at least in the context of the Anatomy-II course.

The superior performance of students in the online model could be attributed to several factors. Online learning environments often provide greater flexibility, allowing students to learn at their own pace and revisit course materials as needed (Yalcin and Dennen 2024). This flexibility can be particularly beneficial for complex subjects like veterinary anatomy, where students may require additional time to grasp difficult concepts (Stone et al. 2019). Additionally, online platforms often incorporate multimedia resources, interactive tools, and self-assessment modules, which can enhance understanding and retention of anatomical knowledge. These findings align with previous studies that have highlighted the effectiveness of online learning in medical and veterinary education (Pei and Wu 2019; Oliveira et al. 2025). Online learning modules in veterinary education led to improved knowledge retention and student satisfaction compared to traditional lecture-based methods. However, it is important to note that the success of online education may also depend on the specific design and implementation of the course. Not all online courses are created equal, and factors such as the quality of instructional materials, the level of interaction between students and instructors, and the availability of technical support can significantly influence outcomes (Haines et al. 2020; Kelly et al. 2021; Devine et al. 2022). In this study, the online Anatomy-II

course was likely well-structured, with appropriate resources and support systems in place, which may have contributed to the positive results.

In conclusion, this retrospective study demonstrates that online education can be as effective as, and in some cases more effective than, traditional face-to-face methods in veterinary anatomy courses. The higher success rates observed in online learning suggest that when appropriately designed and supported, digital education methods offer a valuable alternative for delivering complex content like anatomy. However, the consistent gender differences, with female students outperforming male students in both formats, highlight the need for further exploration into gender-specific learning strategies. It is important to acknowledge that success in online theoretical assessments may not fully reflect a deep anatomical understanding, particularly regarding the acquisition of hands-on practical skills essential for veterinary practice. While online education shows promise, integrating practical components through blended or hybrid models may help address limitations in hands-on skill acquisition, ensuring comprehensive and equitable anatomy education for veterinary students.

This study has several limitations that should be considered when interpreting the results. The conducted retrospective design introduces potential biases, as we relied on existing academic records rather than controlled experimental data. Variables like student motivation levels, prior knowledge, and pandemic-related stressors could not be standardized or fully accounted for, potentially confounding our results. Also, the result indicated higher pass rates in online courses, which cannot rule out the possibility of academic dishonesty inflating these results. Research shows that online exam cheating increased significantly during pandemic-era remote learning, and our study lacked robust cheating detection methods, like proctoring software or plagiarism checks, that could verify result validity. Lastly, the findings may not generalize beyond Ankara University's specific context, as institutional resources, cultural attitudes toward online learning, and pandemic impacts varied globally. These limitations highlight the need for more systematic, controlled studies to fully understand the comparative effectiveness of different teaching modalities in veterinary anatomy education.

CONFLICTS OF INTEREST

The authors report no conflicts of interest.

ACKNOWLEDGMENT

This study was presented as an oral presentation at the congress named 13th National and 3rd International Veterinary Anatomy Congress and printed as a summary the congress book.

AUTHOR CONTRIBUTIONS

Idea/Concept: HAY, CB, ÇO
Supervision/Consultancy: AA, ÇO
Data Collection and/or Processing: HAY, CB, BB
Analysis and/or Interpretation: AAS, AA
Writing the Article: HAY, CB, BB, AAS
Critical Review: ÇO, AA

REFERENCES

Adedoyin OB, Soykan E (2023). COVID-19 pandemic and online learning: the challenges and opportunities. *Interact Learn Environ*, 31(2), 863-875.

Al-Angari NS, Aldaham AS, Masuadi E, Nadeem M, Alkadi L (2022). The effectiveness of students' performance in preclinical fixed prosthodontics course in predicting subsequent clinical performance. *J Prosthodont*, 31(1), 45-49.

Bauler LD, Lesciotto KM, Lackey-Cornelison W (2022). Factors impacting the rapid transition of anatomy curricula to an online environment in response to Covid-19. *Anat Sci Educ*, 15(2), 221-232.

Bhagat OL, Bhandari B, Mehta B, Sircar S (2014). Objective structured practical examination and conventional practical examination: a comparison of scores. *Med Sci Educ*, 24, 395-399.

Bonacini L, Murat M (2023). Beyond the covid-19 pandemic: remote learning and education inequalities. *Empirica*, 50(1), 207-236.

Boulos AN (2022). Evaluation of the effectiveness of online education in anatomy for medical students during the COVID-19 pandemic. *Ann Anat*, 244, 151973.

Chaker R, Gallot M, Madi A, Collet C, Hoyek N (2025). Teaching human anatomy before during and after covıd-19 pandemic: a longitudinal study on kinesiology students' performance, cognitive load, and congruent embodied learning. *Anat Sci Educ*, 18(1), 48-58.

Coldwell J, Goold A, Craig A, Mustard J (2007). Gender and equity in e-learning. Australas. *J Inf Syst*, 15(1), 9–24.

Csorba LM, Dabija DC (2024). The ımpact of the covıd-19 pandemic on students' future online education behaviour. *Heliyon*, 10(20), e39560.

Daniel SJ (2020). Education and the covıd-19 pandemic. *Prospects*, 49(1), 91-96.

Darici D, Reissner C, Brockhaus J, Missler M (2021). Implementation of a fully digital histology course in the anatomical teaching curriculum during covıd-19 pandemic. *Ann Anat*, *236*, 151718.

Davarpanah SH, Barat Dastjerdi N, Shirzad Z (2023). Student teachers' experiences of online education during the covıd-19 pandemic: challenges and opportunities. *J High Educ Policy Leadersh Stud*, 4(2), 129-135.

Devi R, Chand SP (2024). In-service teachers' perceptions and challenges in online assessments amid covıd-19. *Int J Assess Eval*, 31(2), 45–56.

Devine E, Hunt JA, Anderson SL, Mavromatis MV (2022). Online case-based course in veterinary radiographic interpretation generates better short-and long-term learning outcomes than a virtual lecture-based course. *JVME*, 50(6), 666-676.

Díez-Pascual AM, García-Díaz P, Peña-Capilla R, Jurado-Sanchez B (2025). Face-to-face vs. online learning in science and engineering courses during covıd-19 epoch. *Res Sci Technol Educ*, 43(1), 347-376.

Dissabandara LO, Nawaratna S, Nirthanan S (2023). Fine-tuning the standard setting of objective structured practical examinations in clinical anatomy. *Anat Sci Educ*, 16(3), 486-496.

Dooley LM, Frankland S, Boller E, Tudor E (2018). Implementing the flipped classroom in a veterinary pre-clinical science course: Student engagement, performance, and satisfaction. *JVME*, 45(2), 195-203.

Franchi T (2020). The impact of the covıd-19 pandemic on current anatomy education and future careers: A student's perspective. *Anat Sci Educ*, 13(3), 312–315.

Gao M, Cui Y, Chen H et al. (2022). The efficacy and acceptance of online learning vs. offline learning in medical student education: A systematic review and meta-analysis. *JXYM*, 7 (1).

Goncalves E, Capucha L. (2020). Student-centered and ıct-enabled learning models in veterinarian programs: what changed with covıd-19?. *Educ Sci*, 10(11), 343.

Gupta A, Shrestha RM, Shrestha S, Acharya A, Pandey N (2021). Impact of e-learning during covıd-19 pandemic among medical students in a medical college of nepal: A cross-sectional study. *JNMA*, 59(233), 301-305.

Gwazdauskas, FC, McGilliard ML, Corl BA (2014). Characteristics of student success in an undergraduate physiology and anatomy course. *J Dairy Sci*, 97(10), 6378-6381.

Haines JM, Wardrop KJ, Lindberg CJ et al. (2020). Development and assessment of a formal learning module to educate veterinary students in an intensive care unit about transfusion reactions. *JVECC*, 30(4), 405-410.

Jones K, Miller DJ, Noble P (2025). Did the rapid transition to online learning in response to covıd-19 ımpact students' cognitive load and performance in veterinary anatomy?. *J Vet Med Educ,* 52(1), 70-80.

Kelly RF, Mihm-Carmichael M, Hammond JA (2021). Students' engagement in and perceptions of blended learning in a clinical module in a veterinary degree program. *J Vet Med Educ*, 48(2), 181-195.

Kessels U, Van Houtte, M. (2022). Side effects of academic engagement? How boys' and girls' well-being is related to their engagement and motivational regulation*. Gend. Educ*, 34(6), 627-642.

Khaled A, Hazaymeh WA, Montierre ME (2022). Challenges of online education for teachers and parents in the emirati school system. *Eur J Educ Res*, 11(4), 2345-2355.

Lancaster T, Cotarlan C. (2021) Contract cheating by stem students through a file sharing website: a covıd-19 pandemic perspective. *IJEI*, 17 (1), 1-16.

Longhurst GJ, Stone DM, Dulohery K et al. (2020). Strength, weakness, opportunity, threat (swot) analysis of the adaptations to anatomical education in the United Kingdom and republic of ıreland in response to the covid-19 pandemic. *Anat Sci Educ*, 13(3), 301-311.

Lu D, Wu Z (2011). Internet based chinese language distance education system. *Adv Mater Res*, 143, 457-461.

Mishrif A (2024). covıd-19 effects on the global economy: an overview. *economic effects of the pandemic: ımplications for the economy, Finance and Tourism*, 3-23.

Mok HN (2014). Teaching tip: The flipped classroom. *JISE*, 25 (1), 7 –11.

Muca E, Cavallini D, Odore R et al. (2022). Are veterinary students using technologies and online learning resources for didactic training? A mini-meta analysis. *Educ Sci*, 12(8), 573.

Oliveira D, Soares GSL, Silva Júnior LMD et al. (2025). Preliminary study on online and in-person teaching methods for animal anatomy. *Cienc Rural*, 55, e20240214.

Pei L, Wu H (2019). Does online learning work better than offline learning in undergraduate medical education? A systematic review and meta-analysis. *Med Educ Online*, 24(1), 1666538.

Price L (2006). Gender differences and similarities in online courses: challenging stereotypical views of womenJ. *Comput. Assist. Learn,* 22(5), 349-359.

Sakaue M, Oishi M, Ozawa A et al. (2024). Availability and issues of 3D-printed skull models for veterinary anatomy laboratories from students' perspective before and during the covıd-19 pandemic. *J Vet Med Sci*, 86(10), 1081-1088.

Shi CR, Rana J, Burgin S (2018). Teaching & learning tips 6: the flipped classroom. *Int J Dermatol*, 57(4), 463-466.

Sil A, Das S, Das P, Jayswal D, Das NK (2024). Designing, introducing, and implementing objective structured practical examinations as a formative assessment tool in undergraduate medical pharmacology. *Med Educ Dev*, 17(55), 1-9.

Stevens GJ, Bienz T, Wali N, Condie J, Schismenos S (2021). Online university education is the new normal: but is face-to-face better?. *ITSE*, 18(3), 278-297.

Torda A, Shulruf B (2021). It's what you do, not the way you do it–online versus face-to-face small group teaching in first year medical school. *BMC medical education*, 21, 541.

Veeramani R, Madhugiri VS, Chand P (2015). Perception of MBBS students to "flipped classroom" approach in neuroanatomy module. *Anat Cell Biol*, 48(2), 138-143.

Yalcin Y, Dennen VP (2024). An investigation of the factors that influence online learners' satisfaction with the learning experience. *EAIT*, 29(4), 3807-3836.

Yaman R, Hagen KM, Ghaith S, Luong H, Almader-Douglas D, Langley NR. (2023). Gender bias in medical education: A scoping review. Clin. Teach, 20(4), e13592.

Yoo H, Kim D, Lee YM, Rhyu IJ (2021). Adaptations in anatomy education during covıd-19. *JKMS*, 36(1).

Van Veterinary Journal

https://dergipark.org.tr/tr/pub/vanvetj

Cite this article as: **Çaka Ö, Şahin B, Koçak E et al. (2026).** The Effects of Butylparaben Administration on Oxidative Stress Markers in Rat Brain and Serum. *Van Vet J*, 37(1), 54-60. DOI: https://doi.org/10.36483/vanvetj.1806315

ISSN: 2149-3359 **Original Article** e-ISSN: 2149-8644

The Effects of Butylparaben Administration on Oxidative Stress Markers in Rat Brain and Serum

Özüm ÇAKA[1,*] Büşra ŞAHİN[1] Esra KOÇAK[1] Emine ALTIN[1] Ali ERTEKİN[1] Sena ÇENESİZ[1]

[1] *Ondokuz Mayıs University, Faculty of Veterinary Medicine, Department of Biochemistry, 55270, Samsun, Türkiye*

Received: 18.10.2025 Accepted: 26.02.2026

ABSTRACT Parabens are used for preservative purposes in various fields, especially in pharmaceutical, cosmetic and food products. Recent studies suggest that parabens may affect oxidative stress mechanisms in biological systems and may cause cellular damage. This experiment was created to better understand the possible biological effects of butylparaben (BP) by evaluating the effects of BP administration on oxidative stress parameters in brain tissue, serum and erythrocytes in rats. For this purpose, 28 Wistar Albino rats divided into 4 different groups were administered BP at doses of 0, 100, 200, 400 mg/kg/day by oral gavage. Oxidative stress parameters such as total oxidant status (TOS), total antioxidant status (TAS), oxidative stress index (OSI), glutathione (GSH) and malondialdehyde (MDA) and catalase (CAT) were measured in the brain, serum and erythrocytes of rats. The findings revealed a statistically notable increase in MDA concentrations within the brain tissue of the BP-treated groups evaluated to the control group ($p<0.05$). Nonetheless, the groups did not show any statistically considerable variations in erythrocyte GSH levels, CAT activity, or in serum MDA, TOS, TAS, and OSI parameters ($p>0.05$). These findings provided proof that BP affects oxidative stress by increasing lipid peroxidation but does not produce large changes in the overall oxidative balance, especially since BP was detected in brain regions and the brain is sensitive to lipid peroxidation. This study aims to contribute to further research to understand the effects of BP on oxidative stress in more detail.

Keywords: *Brain, Butylparaben, MDA, Oxidative stress.*

ÖZ

Bütilparaben Uygulamasını Sıçan Beyin ve Serumunda Oksidatif Stres Belirteçleri Üzerine Etkileri

Parabenler, özellikle ilaç, kozmetik ve gıda ürünleri olmak üzere çeşitli alanlarda koruyucu olarak kullanılmaktadır. Son zamanlarda yapılan çalışmalar, parabenlerin biyolojik sistemlerdeki oksidatif stres mekanizmalarını etkileyebileceğini ve hücresel hasara neden olabileceğini göstermektedir. Çalışmamızda, sıçanlarda beyin dokusu, serum ve eritrositlerdeki oksidatif stres parametreleri üzerinde bütilparaben (BP) uygulamasının etkilerini değerlendirerek BP'nin olası biyolojik etkilerini daha iyi anlamayı amaçladık. Bu amaçla, 4 farklı gruba ayrılan 28 Wistar Albino sıçana oral gavaj yoluyla 0, 100, 200, 400 mg/kg/gün dozlarında BP verilmiştir. Sıçanların beyin, serum ve eritrositlerinde katalaz (CAT), glutatyon (GSH), malondialdehit (MDA), total antioksidan kapasite (TAK), total oksidan kapasite (TOK) ve oksidatif stres indeksi (OSİ) gibi oksidatif stres parametreleri ölçülmüştür. Elde edilen sonuçlara göre, BP ile tedavi edilen gruplarda kontrol grubuna kıyasla beyin dokusunda MDA düzeylerinin önemli ölçüde arttığı gözlemlenmiştir ($p<0.05$). Ancak, eritrositlerdeki GSH düzeyleri ve CAT aktivitesi ile serumdaki MDA, TAS, TOS ve OSI düzeyleri açısından gruplar arasında önemli bir fark gözlemlenmemiştir ($p>0.05$). Bu bulgular, BP'nin lipid peroksidasyonunu artırarak oksidatif stresi etkilediğini, ancak genel oksidatif dengede büyük değişiklikler yaratmadığını, özellikle de BP'nin beyin bölgelerinde tespit edildiği ve beynin lipid peroksidasyonuna duyarlı olduğu göz önüne alındığında, kanıtlamıştır. Bu çalışma, BP'nin oksidatif stres üzerindeki etkilerini daha ayrıntılı olarak anlamak için yapılacak daha ileri araştırmalara katkıda bulunmayı amaçlamaktadır.

Anahtar Kelimeler: *Beyin, Bütilparaben, MDA, Oksidatif stres.*

INTRODUCTION

Parabens are a cohorts of synthetic compounds extensively used as conserving agents in the food, cosmetic, and pharmaceutical industries (Błedzka et al. 2014). The widespread use of parabens is largely due to their compositional stability, economic cost, broad-spectrum antimicrobial activity, and reduced potential to cause allergic reactions (Petric et al. 2021; Torfs and

✉ *Corresponding author: ozumcaka1@gmail.com

Brackman, 2021; Wei et al. 2021). Commonly used parabens include ethylparaben (EP), methylparaben (MP), propylparaben (PP), and butylparaben (BP). The use of these parabens is increasing over time (Melo and Queiroz, 2010). BP and PP, the long-chain ester derivatives among parabens, show stronger antimicrobial activity than the shorter-chain parabens. As a result, they are often used together in the formulation of lotions, emulsions, and creams. (Charnock and Finsrud 2007). Studies have shown that parabens and their biotransformation products are widely distributed in the environment, being detected in wastewater, surface waters, sediments, and aquatic organisms such as shellfish. (Liao et al. 2019; Lu et al. 2019). Human encounter to parabens mainly occurs through ingestion or direct contact with products containing these compounds. (Błedzka et al. 2014). Parabens have long been considered safe because they are rapidly metabolized and do not build up in the human body. (Kang et al. 2016). However, subsequent studies have demonstrated that parabens may interfere with the endocrine system and induce oxidative stress. This, in turn, has been suggested to cause deleterious effects in humans and animals (Karwacka et al. 2019). Multiple in vitro investigations utilizing human cell lines have demonstrated that BP can induce inducing cytotoxic and genotoxic effects across several cell types (Yang et al. 2018; Bayulken and Tuylu 2019). Furthermore, BP has been found in multiple parts of the brain, indicating that parabens could potentially pass through the blood-brain barrier (Jeong et al. 2019; Song et al. 2020). BP promotes apoptosis via oxidative stress resulting in endoplasmic reticulum stress (Yang et al. 2018). In a study, parabens were shown to dose-dependently reduce mitochondrial and cytosolic reactive oxygen species (ROS) production (Samarasinghe et al. 2018). Another study indicated that butylparaben may induce oxidative stress in rodents by suppressing antioxidant defence mechanisms (Shah and Verma 2011). ROS generated during oxidative stress may damage proteins, lipids, and nucleic acids through oxidation (Wu et al. 2004). Oxidative stress arises in living organisms when the equilibrium among ROS production and antioxidant defences is disrupted, potentially resulting in lipid peroxidation, membrane instability, protein and deoxyribonucleic acid (DNA) damage degradation within cells (Sakuragui et al. 2013). Accordingly, the analysis of oxidative stress biomarkers is essential for evaluating the impact of prolonged exposure to sublethal concentrations of parabens (Dambal et al. 2017).

The brain exhibits significant vulnerability to oxidative stress, largely attributable to its elevated levels of unsaturated lipids and relatively limited antioxidant defense mechanisms. Oxidative stress, characterized by excessive free radical production and inadequate antioxidant response, plays a crucial role in various neurodegenerative and neuropsychiatric disorders (Cobley et al. 2018; Salim 2017). Nevertheless, the erythrocyte membrane contains a highconcentration of -SH groups, which are integral to preserving cellular oxidative balance (Reglinski et al. 1988). Oxidative stress can cause structural changes in erythrocyte membranes and thus affect enzyme activities that serve as markers for various pathologies (Massaccesi et al. 2020). Building on these findings, the present study aimed to investigate how oral administration of BP by gavage influences oxidative stress levels in the brain, erythrocytes, and serum of rats.

MATERIAL AND METHODS

The study used serum and brain tissue samples obtained from rats belonging to another ethically approved experiment (Ondokuz Mayis University Animal Experiments Local Ethics Committee Date: 28 April 2025, Approval Number: E-68489742-604.02-2500091312).

Animal Material

A total of 28 male Wistar Albino rats (6 weeks old, weighing 200–250 g) were used in the study. The rats were obtained from the Ondokuz Mayis University Experimental Animal Research and Application Center and kept in transparent polycarbonate cages with stainless-steel lids. They were maintained in an air conditioned environment under a 12-hour light and darkness period, at a controlled temperature of 21±3 °C and relative humidity of 50±5%, with conditions monitored by a datalogger. Rats were fed *ad libitum* with pellet feed and tap water during this period.

In the study, 28 rats were allocated into four groups, with every group comprising seven animals. The experimental period was set at 14 days. The administration was performed by oral gavage. The control group administered corn oil at a volume of 0.5 mL only. The other groups were given BP (CAS No: 94-26-8) at doses of 100 mg/kg/day, 200 mg/kg/day, 400 mg/kg/day. BP obtained from Sigma-Aldrich was dissolved in corn oil and given to each group by oral gavage (Aydemir et al. 2019; Ulusu et al. 2020). The experiment was terminated on day 15. Anesthetic induction in rats was achieved via intraperitoneal administration of ketamine (80–130 mg/kg body weight) and xylazine (2–5 mg/kg body weight), in accordance with institutional and American Veterinary Medical Association (AVMA) guidelines to ensure deep anesthesia. Following verification of deep anesthesia, the abdominal cavity was opened, and cardiac puncture was performed to collect blood into ethylenediaminetetraacetic acid (EDTA) containing tubes as a terminal procedure.

Sample Preparation

For the quantification of GSH and MDA, TOS and TAS levels, blood samples were collected from the heart into serum biochemistry tubes containing separator gels. After centrifugation (Nuve, NF-800R) at +4 °C for 10 minutes at 3000 rpm, the obtained serum was aliquoted and kept at −20 °C prior to analysis.

For the assessment of erythrocyte CAT activity, blood specimens were drawn from the heart and collected into EDTA-containing tubes. These specimens were centrifuged at +4 °C for 10 minutes at 3000 rpm to isolate the plasma. The centrifugation procedure was repeated three additional times with the addition of 0.9% NaCl solution at the same ratio. After each centrifugation, the buffy coat was carefully removed. The resulting erythrocytes were then suspended in cold distilled water at a five-fold dilution to prepare the erythrocyte pack. The prepared erythrocyte samples were stored at −20 °C until further analysis.

For the collection of brain tissue, a craniectomy was performed by making incisions in the frontal and parietal regions of the skull. After opening the skull, the spinal cord was severed, and the brain was carefully removed. The brain specimens were then stored at −20 °C until further analysis. At the time of analysis, the brain tissue was diluted 10-fold with commercial buffer solution (BioShop PBS404.100) and homogenized (Bio-Gen PRO200) for 3 minutes for each tissue. The supernatant was then

centrifuged at 3000 rpm at +4 ℃ for 10 minutes and the supernatant was removed.

Biochemical Analyses

Serum and brain tissue supernatant MDA was analysed by the method reported by Yoshioka et al. using Trichloracetic Acid (20%) and Thiobarbutyric Acid (0.67%) solutions (Yoshioka et al. 1979). The optical density of the samples was determined at 535 nm on a UV-Vis spectrophotometer (Thermo Scientific Genesys 10S). A standard graph was generated and concentration values were calculated.

CAT measurement of erythrocyte pack and brain tissue supernatant was performed using prepared phosphate buffer (pH 7.0; 50 mM) and hydrogen peroxide solutions (30 mM) and its principle is based on the monitoring of H_2O and O_2 products formed during the degradation of H_2O_2 by catalase. CAT activity (k/g*Hb, k/g) was calculated (Aebi 1974).

As described by Yuzuak et al, GSH activity in brain tissue supernatant was calculated using a modified Ellman method (Yuzuak et al. 2015). 0.5 mL of supernatant was taken and 2 mL of 0.3 M $Na_2HPO_4.2H_2O$ (CAS No: 10028-24-7) solution was added. After this, 0.2 mL of 5,5'-dithiobis-2-nitrobenzoic acid (DTNB) (0.4 mg/mL 1% sodium citrate) (CAS No: 69-78-3) solution was added to the resulting mixture, allowed to stand at room temperature for 5 min and measured at a wavelength of 412 nm against a blind (distilled water) spectrophotometer. The findings were expressed as µmol/L per gram of tissue.

For determination of blood glutathione level, whole blood collected in EDTA tubes was measured on the day of sacrification. For GSH measurement, DTNB is a chromogenic compound that reacts with sulfhydryl groups to form an intense yellow coloured product. The optical density of the reduced chromogen is determined at 412 nm, exhibiting a direct proportionality to the concentration of GSH (Beutler et al. 1963). A calibrator curve was constructed and GSH concentrations calculated from this curve were divided by haematocrit values to determine GSH levels.

The concentrations of TOS and TAS in both serum and brain tissue supernatants were determined spectrophotometrically using industrial colorimetric assay kits (Rel Assay Diagnostics). The OSI was subsequently computed as the ratio of TOS to TAS values, according to the methods described by Erel (2004, 2005).

Statistical Analysis

SPSS (IBM statistics 27.0; IBM Corp., Armonk, NY, USA) program was used for statistical analysis. Groups were evaluated by Shapiro-Wilk normality test. For the parameters that were found to be normally distributed in the groups, the groups were compared with the parametric test One-Way ANOVA test. Homogeneity of variance was tested with Levene's test. For the parameters that provided homogeneity; Tukey test was used as Post Hoc test in the comparison of the groups. For non-homogeneous parameters, Dunnett's T3 test was used as Post Hoc test for comparison of groups. P values less than 0.05 were considered notable.

RESULTS

In our study, oxidative stress parameters were evaluated in both brain tissues and serum samples in groups applied with different doses of paraben. The MDA concentration in brain tissue was markedly reduced in Group 1 compared with Group 2 ($p<0.001$), Group 3 ($p=0.020$) and Group 4 ($p=0.007$). The GSH levels in Group 2 were significantly higher than those in Group 1 ($p=0.006$), Group 3 ($p<0.001$), and Group 4 ($p=0.008$). There were no statistically notable differences among the groups with respect to CAT, TOS, TAS, and OSI levels ($p>0.05$). Brain tissue MDA, GSH, CAT, TOS, TAS and OSI values are given in Table 1, and their graphs are given in Figure 1.

Our study did not demonstrate any statistically notable differences among the groups regarding serum MDA, TOS, TAS, OSI levels, GSH, and CAT ($p>0.05$). Table 2 presents the data for serum MDA, TOS, TAS, OSI, blood GSH values, and erythrocyte CAT activity. Graphical representations of blood GSH and erythrocyte CAT are shown in Figure 2, while graphs for serum MDA, TOS, TAS, and OSI are provided in Figure 3.

Table 1: Brain tissue MDA, GSH, TAS, TOS, OSI values and CAT activity (X±SD).

Parameters	Group 1	Group 2	Group 3	Group 4
MDA (µmol/g)	53.57±6.34[a]	68.64±6.27[b]	63.59±3.02[b]	64.95±7.19[b]
GSH (µmol/g)	194.34± 40.73[a]	324.88±11.63[b]	166.82±42.98[ac]	197.35±41.75[ac]
CAT (k/g)	0.096±0.06[a]	0.094±0.03[a]	0.027±0.02[a]	0.054±0.05[a]
TAS (mmol Trolox Eq/L)	0.18±0.11[a]	0.23±0.03[a]	0.26±0.09[a]	0.27±0.05[a]
TOS (µmol H_2O_2 Eq/L)	14.84±1.48[a]	14.41±1.95[a]	12.77±1.70[a]	14.20±1.92[a]
OSİ (AU)	91.75±53.06[a]	62.86±14.34[a]	52.92±20.81[a]	52.42±10.97[a]

*abc; Different superscripts are statistically significant ($p<0.05$), same superscripts are not statistically significant ($p>0.05$). Group 1: Control; group 2: 100 mg/kg BP; group 3: 200 mg/kg BP; group 4: 400 mg/kg BP, X: Average value, SD: Standard deviation.

Table 2: Serum MDA, TAS, TOS, OSI; blood GSH and erythrocyte CAT activity (X±SD).

Parameters	Group 1	Group 2	Group 3	Group 4
MDA (µmol/L)	1.43±0.23[a]	2.63±3.29[a]	2.18±1.35[a]	1.49±0.58[a]
GSH (mg/dL)	69.35± 23.27[a]	54.26±10.17[a]	71.05±26.71[a]	85.26±20.76[b]
CAT (k/gHb)	0.00012±0.00006[a]	0.00014±0.00011[a]	0.0001±0.00004[a]	0.0001±0.00003[a]
TAS (mmol Trolox Eq/L)	0.67±0.03[a]	0.70±0.08[a]	0.61±0.05[a]	0.65±0.07[a]
TOS (µmol H_2O_2 Eq/L)	9.32±2.68[a]	7.18±3.67[a]	7.40±1.35[a]	7.87±1.45[a]
OSİ (AU)	13.85±4.24[a]	10.44±5.32[a]	12.26±2.88[a]	11.66±1.88[a]

*ab; Different superscripts are statistically significant ($p<0.05$), same superscripts are not statistically significant ($p>0.05$). Group 1: Control; group 2: 100 mg/kg BP; group 3: 200 mg/kg BP; group 4: 400 mg/kg BP, X: Average value, SD: Standard deviation.

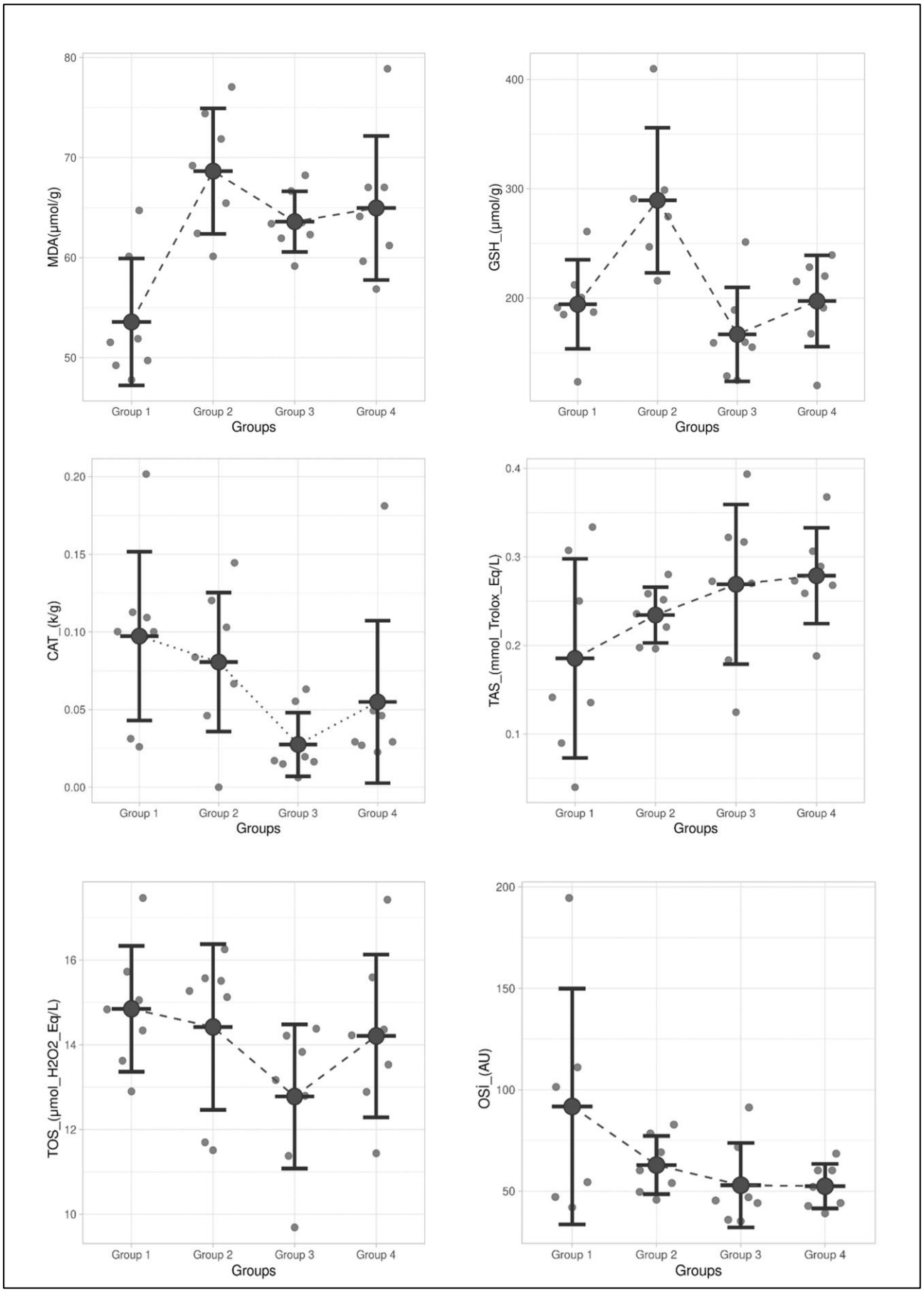

Figure 1: Brain tissue MDA, GSH, TAS, TOS, OSI levels and CAT activity.

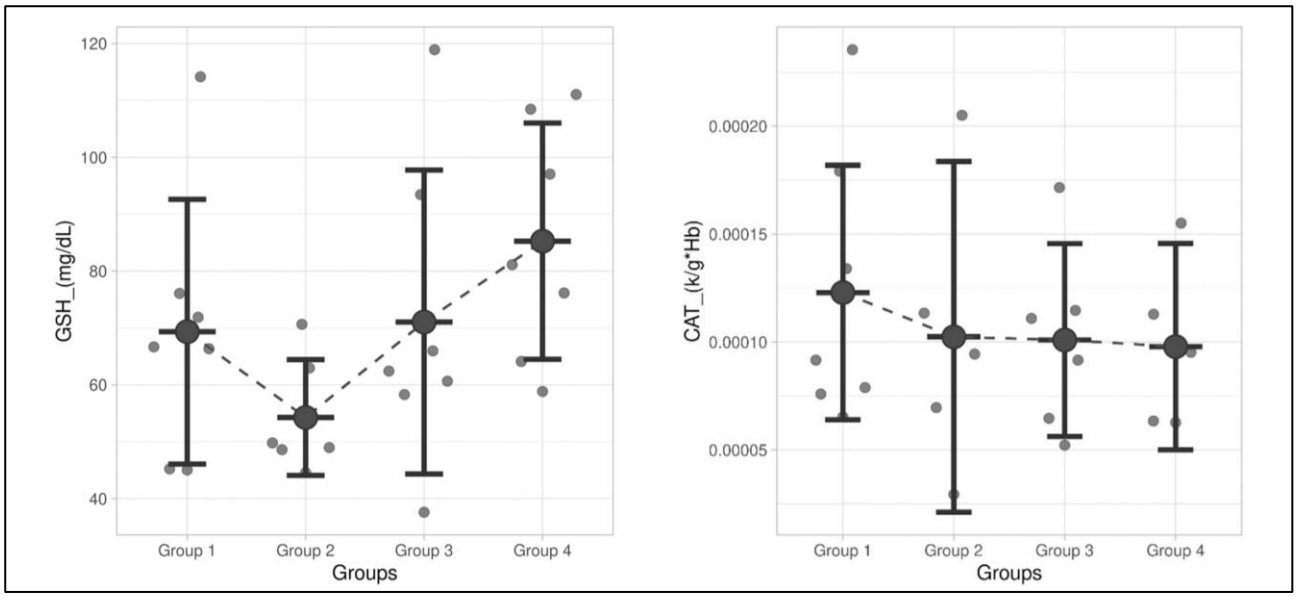

Figure 2: Blood GSH levels and erythrocyte CAT activity.

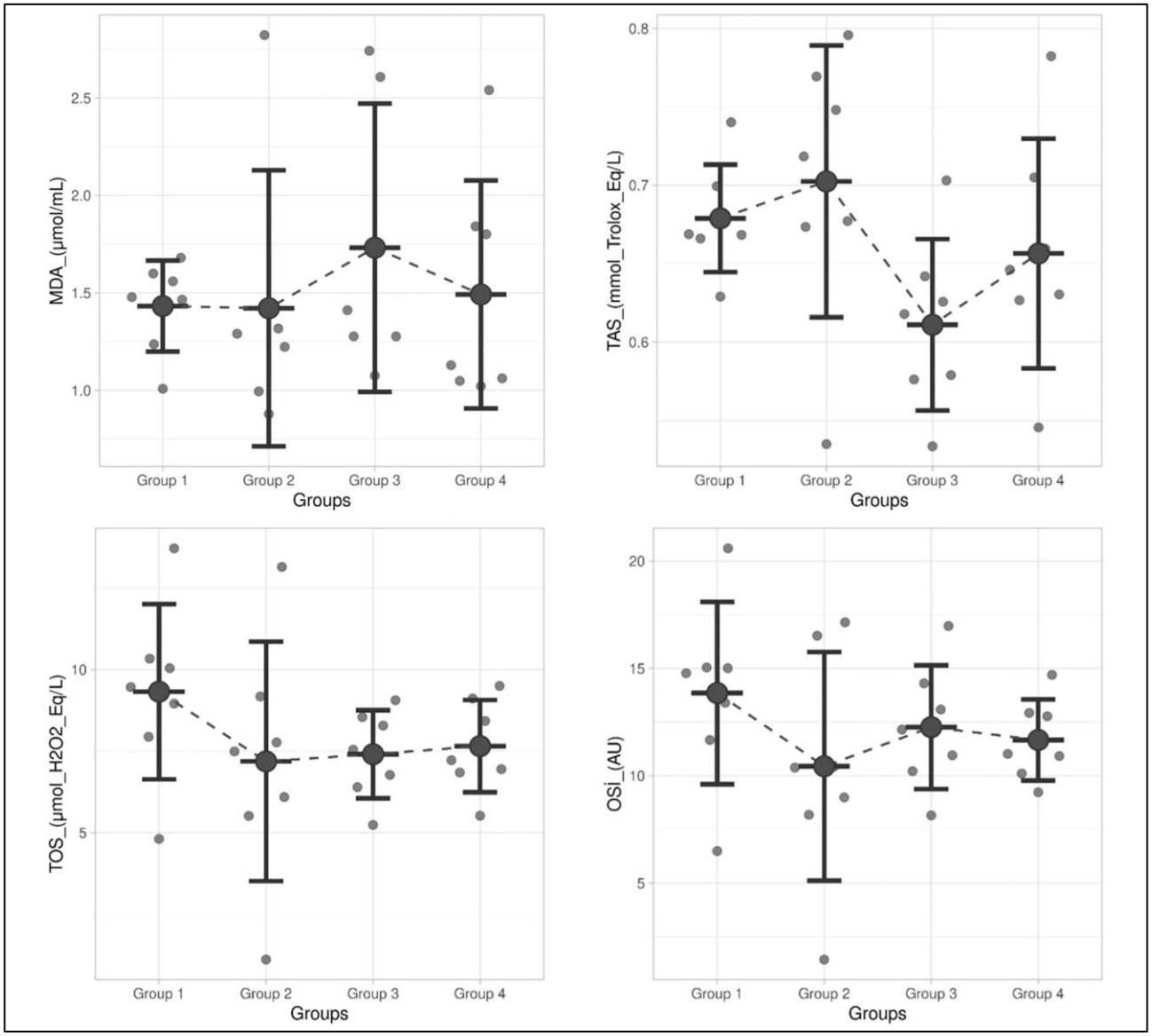

Figure 3: Serum MDA, TAS, TOS and OSI levels.

DISCUSSION AND CONCLUSION

Daily exposure to BP increased by the routine use of commercial goods, particularly cosmetics and pharmaceuticals (Soni et al. 2005). Nevertheless, studies in mammals have connected BP exposure to various reported effects, including toxicity to the reproductive, immune, hepatic (liver), and nervous systems (Kizhedath et al. 2019). Parabens can cause cytotoxicity because of mitochondrial failure due to depletion of cellular ATP by decomposition of oxidative phosphorylation and induction of membrane permeability transition accompanied by mitochondrial depolarization (Soni et al. 2002). Importantly, the finding that BP has been detected across different brain regions suggests that parabens can penetrate the blood-brain barrier (Jeong et al. 2019; Song et al. 2020). Furthermore, parabens can move within cells and alter synaptic activity, which affects their normal function and thus energy production in mitochondria (Suzuki and Okada 2009). In this process, the cell has been reported to produce high amounts of ROS and cause oxidative stress, a behaviour that can lead to cell death (Egea et al. 2012). BP promotes apoptosis via oxidative stress resulting in endoplasmic reticulum stress (Yang et al. 2018). Based on this information, in this study, specifically, we designed this study to comprehensively evaluate how various dosages of BP administration impact the antioxidant protective system and oxidative stress levels within the serum, erythrocytes, and brain tissue of our rat model.

In this study, rats administered different doses of BP exhibited significantly elevated MDA and GSH levels in brain tissue compared to the control group. However, no notable differences were observed among the groups in TAS, TOS, OSI levels, or CAT activity. Similarly, blood GSH levels were notable elevated in Group 4 compared with the control group, while serum TAS, TOS, OSI and CAT, MDA concentrations did not differ significantly among the groups. In a study, it was reported that administration of different doses of BP (200 mg/kg/day, 400 mg/kg/day, 800 mg/kg/day) for 14 days caused an increase in oxidative stress enzymes such as 6-Phosphogluconate Dehydrogenase, Glucose-6-Phosphate Dehydrogenase, Glutathione Reductase, Glutathione S-Transferase, Glutathione Peroxidase in brain tissue and damaged the antioxidant balance (Aydemir et al. 2019). As reported by Ulusu et al. (2020), it was determined that 28 days of BP (100 mg/kg/day, 200 mg/kg/day, 400 mg/kg/day) exposure at different doses increased oxidative stress by disrupting the oxidant-antioxidant balance in liver, testis and spleen tissue in rats (Ulusu et al. 2020). These two studies examined the effects of different BP doses and application times on oxidative stress in various tissues. Ara et al. (2021) found that MDA levels in the testis and ovaries of rats treated with BP and turmeric elevated in the BP-treated group compared to the control group, while GSH, Superoxide Dismutase and CAT activities decreased (Ara et al. 2021). In the study conducted by Shah and Verma on mice, the effect of 30-day BP exposure on liver oxidative stress levels was examined and it was concluded that oral BP administration caused oxidative stress by increasing lipid peroxidation (Shah and Verma 2011). Although previous studies have identified marked differences between groups regarding oxidant-antioxidant balance, our study did not observe any statistically notable differences among the groups. It is hypothesised that the observed differences in results are attributable to variations in BP dose, experiment duration and the studied tissues. Because Aydemir et al. (2019), which we mentioned above, applied a dose higher than our doses for 14 days in their study, while Ulusu et al. (2020) applied the same amount of dose as we applied for 28 days in their study. This situation suggested that the difference between the groups in our study may be due to the short duration of the experiment, especially considering the dose amounts we applied. For this reason, we believe that a longer experimental period may cause significant differences between groups by causing oxidative stress. While MDA level increased significantly in brain tissue, there was no considerable variation in TOS, TAS OSI levels and CAT activity, indicating that BP triggers oxidative stress especially by increasing lipid peroxidation, but the general oxidant-antioxidant balance can be maintained up to certain levels. While MDA increased due to oxidation of lipids in the cell membrane, total oxidant load and oxidative stress index did not change. Lipids account for approximately 50–60% of the dry weight of the brain, and a substantial proportion of lipids in the nervous system is localized in the myelin sheath, a specialized membrane structure that contains the highest lipid content among all biological membranes (Hussain et al. 2019). Especially polyunsaturated fatty acids found in cell membranes can be easily oxidized by free radicals. MDA is a biomarker that occurs because of this oxidation and is an indicator of lipid peroxidation (Blanco-Ayala et al. 2014). In addition, due to the lipophilic properties of BP, it can also accumulate in brain tissue and cause oxidative degradation of lipids in the cell membrane and increase MDA levels (Watanabe et al. 2013). This suggests that BP is effective on specific oxidative mechanisms rather than increasing the overall oxidative load (Ulusu et al. 2020). The fact that CAT activity did not change suggests that the oxidative stress caused by BP proceeds through lipid radicals and peroxidation products rather than species detoxified through catalase such as hydrogen peroxide. Because it has also been reported that parabens cause free radical formation, especially lipid peroxidation and changes in mitochondrial membrane permeability (Nishizawa et al. 2006). In addition, the fact that TAS level remained constant indicates that antioxidant defence systems can resist lipid peroxidation up to a certain level but may not be sufficient if the duration of BP exposure is prolonged. The lack of significant differences in serum oxidative stress parameters suggests that the oxidant–antioxidant balance was maintained, likely due to the buffering capacity of the serum and its effective antioxidant defense system. This indicates that BP exposure did not produce measurable changes at the systemic level. If BP-induced oxidative stress is largely compensated at the cellular level, no significant changes in serum parameters may not be observed.

In conclusion, while BP induces oxidative stress in brain tissue, it appears that this stress specifically targets membrane lipids, and the overall oxidative balance is largely preserved. Because of its high oxygen requirement and lipid rich structure, the brain is particularly sensitive to oxidative stress, though it also maintains robust antioxidant defenses that limit potential damage (Mazlum 2012). For this reason, it is thought that the oxidant-antioxidant balance in brain tissue can be preserved in this study, but changes in the oxidant-antioxidant balance may also occur because of increasing the dose of BP used and the duration of administration in further studies. We believe that this study may serve as an example for future studies.

CONFLICTS OF INTEREST

The authors declare that there is no conflict of interest for this study.

AUTHOR CONTRIBUTIONS

Idea/Concept: ÖÇ
Supervision/Consultancy: AE
Data Collection and/or Processing: BŞ
Analysis and/or Interpretation: EA, EK
Writing the Article: ÖÇ, BŞ
Critical Review: SÇ

REFERENCES

Aebi H (1974). Catalase. Bergmeyer HU (Ed). Methods of Enzymatic Analysis (pp. 673-684). Academic Press Inc., New York.

Ara C, Asmatullah, Butt N et al. (2021). Abnormal steroidogenesis, oxidative stress, and reprotoxicity following prepubertal exposure to butylparaben in mice and protective effect of Curcuma longa. *Environ Sci Pollut,* 28(5), 6111–6121.

Aydemir D, Oztascı B, Barlas N, Ulusu NN (2019). Effects of butylparaben on antioxidant enzyme activities and histopathological changes in rat tissues. *Arh Hig Rada Toksikol,* 70, 315–324.

Guzel Bayulken D, Ayaz Tuylu B, Sinan H, Sivas H (2019). Investigation of genotoxic effects of paraben in cultured human lymphocytes. *Drug Chem Toxicol*, 42(4), 349-356.

Beutler E, Duron O, Kelly BM (1963). Improved method for the determination of blood glutathione. *J Lab Clin Med,* 61, 882–888.

Blanco-Ayala T, Andérica-Romero AC, Pedraza-Chaverri J (2014). New insights into antioxidant strategies against paraquat toxicity. *Free Radic Res,* 48(6), 623–640.

Błedzka D, Gromadzińska J, Wasowicz W (2014). Parabens. From environmental studies to human health. *Environ Int,* 67, 27–42.

Charnock C, Finsrud T (2007). Combining esters of para-hydroxy benzoic acid (parabens) to achieve increased antimicrobial activity. *J Clin Pharm Ther,* 32(6), 567–572.

Cobley JN, Fiorello ML, Bailey DM (2018). 13 reasons why the brain is susceptible to oxidative stress. *Redox Biol,* 15, 490–503.

Dambal VY, Selvan KP, Lite C, Barathi S, Santosh W (2017). Developmental toxicity and induction of vitellogenin in embryo-larval stages of zebrafish (Danio rerio) exposed to methyl Paraben. *Ecotoxicol Environ Saf,* 141, 113–118.

Egea J, Martín-De-Saavedra MD, Parada E et al. (2012). Galantamine elicits neuroprotection by inhibiting iNOS, NADPH oxidase and ROS in hippocampal slices stressed with anoxia/reoxygenation. *Neuropharmacology,* 62(2), 1082–1090.

Erel O (2004). A novel automated method to measure total antioxidant response against potent free radical reactions. *Clin Biochem,* 37(2), 112–119.

Erel O (2005). A new automated colorimetric method for measuring total oxidant status. *Clin Biochem,* 38(12), 1103–1111.

Hussain G, Wang J, Rasul A et al. (2019). Role of cholesterol and sphingolipids in brain development and neurological diseases. *Lipids in health and disease*, *18*(1), 26.

Jeong Y, Xue J, Park KJ, Kannan K, Moon HB (2019). Tissue-Specific Accumulation and Body Burden of Parabens and Their Metabolites in Small Cetaceans. *Environ Sci Technol,* 53(1), 475–481.

Kang HS, Kyung MS, Ko A, et al (2016). Urinary concentrations of parabens and their association with demographic factors: A population-based cross-sectional study. *Environ Res,* 146, 245–251.

Karwacka A, Zamkowska D, Radwan M, Jurewicz J (2019). Exposure to modern, widespread environmental endocrine disrupting chemicals and their effect on the reproductive potential of women: an overview of current epidemiological evidence. *Hum Fertil,* 22(1), 2–25.

Kizhedath A, Wilkinson S, Glassey J (2019). Assessment of hepatotoxicity and dermal toxicity of butyl paraben and methyl paraben using HepG2 and HDFn in vitro models. *Toxicol In Vitro,* 55, 108–115.

Liao C, Shi J, Wang X, Zhu Q, Kannan K (2019). Occurrence and distribution of parabens and bisphenols in sediment from northern Chinese coastal areas. *Environ Pollut,* 253, 759–767.

Lu S, Wang N, Ma S et al. (2019). Parabens and triclosan in shellfish from Shenzhen coastal waters: Bioindication of pollution and human health risks. *Environ Pollut,* 246, 257–263.

Massaccesi L, Galliera E, Corsi Romanelli MM (2020). Erythrocytes as markers of oxidative stress related pathologies. *Mech Ageing Dev,* 191, 111333.

Mazlum B (2012). Antioksidan vitaminler ve psikiyatride kullanımı - antioxidant vitamins and their use in psychiatry. Psikiyatride Güncel Yaklaşımlar- *Curr Approaches Psychiatry*. 4(4), 486–505.

Melo LP, Queiroz MEC (2010). Simultaneous analysis of parabens in cosmetic products by stir bar sorptive extraction and liquid chromatography. *J Sep Sci,* 33(12), 1849–1855.

Nishizawa C, Takeshita K, Ueda JI et al. (2006). Reaction of para-hydroxybenzoic acid esters with singlet oxygen in the presence of glutathione produces glutathione conjugates of hydroquinone, potent inducers of oxidative stress. *Free Radic Res,* 40(3), 233–240.

Petric Z, Ruzić J, Zuntar I (2021). The controversies of parabens - an overview nowadays. *Acta Pharm,* 71(1), 17–32.

Reglinski J, Hoey S, Smith WE, Sturrock RD (1988). Cellular response to oxidative stress at sulfhydryl group receptor sites on the erythrocyte membrane. *J Biol Chem,* 263(25), 12360–12366.

Sakuragui MM, Paulino MG, Pereira CDS et al. (2013). Integrated use of antioxidant enzymes and oxidative damage in two fish species to assess pollution in man-made hydroelectric reservoirs. *Environ Pollut,* 178, 41–51.

Salim S (2017). Oxidative stress and the central nervous system. *J Pharmacol Exp Ther,* 360(1), 201–205.

Samarasinghe SVAC, Krishnan K, Naidu R et al. (2018). Parabens generate reactive oxygen species in human spermatozoa. *Andrology,* 6(4), 532–541.

Shah KH, Verma RJ (2011). Butyl p-hydroxybenzoic acid induces oxidative stress in mice liver - An in vivo study. *Acta Pol Pharm,* 68(6), 875–879.

Song S, He Y, Zhang T et al. (2020). Profiles of parabens and their metabolites in paired maternal-fetal serum, urine and amniotic fluid and their implications for placental transfer. *Ecotoxicol Environ Saf,* 191, 110235.

Soni MG, Carabin IG, Burdock GA (2005). Safety assessment of esters of p-hydroxybenzoic acid (parabens). *Food Chem Toxicol,* 43(7), 985–1015.

Soni MG, Taylor SL, Greenberg NA, Burdock GA (2002). Evaluation of the health aspects of methyl paraben: A review of the published literature. *Food Chem Toxicol,* 40(10), 1335–1373.

Suzuki E, Okada T (2009). TEA-induced long-term potentiation at hippocampal mossy fiber CA3 synapses: Characteristics of its induction and expression. Brain Res, 1247, 21–27.

Torfs E, Brackman G (2021). A perspective on the safety of parabens as preservatives in wound care products. *Int Wound J,* 18(2), 221–232.

Ulusu NN, Aydemir D, Oztasci B, Barlas N (2020). Influence of the butylparaben administration on the oxidative stress metabolism of liver, kidney and spleen. *Turk J Biochem,* 45(6), 689–694.

Watanabe Y, Kojima H, Takeuchi S et al. (2013). Comparative study on transcriptional activity of 17 parabens mediated by estrogen receptor α and β and androgen receptor. *Food Chem Toxicol*, 57, 227–234.

Wei F, Mortimer M, Cheng H, Sang N, Guo L-H (2021). Parabens as chemicals of emerging concern in the environment and humans: A review. *Sci Total Environ,* 778, 146150.

Wu LL, Chiou CC, Chang PY, Wu JT (2004). Urinary 8-OHdG: a marker of oxidative stress to DNA and a risk factor for cancer, atherosclerosis and diabetics. *Clinica Chimica Acta,* 339(1-2), 1–9.

Yang C, Lim W, Bazer FW, Song G (2018). Butyl paraben promotes apoptosis in human trophoblast cells through increased oxidative stress-induced endoplasmic reticulum stress. *Environ Toxicol*, 33(4), 436-445.

Yoshioka T, Kawada K, Shimada T, Mori M (1979). Lipid peroxidation in maternal and cord blood and protective mechanism against activated-oxygen toxicity in the blood. *Am J Obstet Gynecol*, 135(3), 372–376.

Yuzuak H, Akbulut KG, Yuzuak S (2015). The effects of melatonin on the oxidants and antioxidants in the pancreatic tissue during the aging process. *J Clin Exp Investig*, 5(4), 583-588.

Van Veterinary Journal

https://dergipark.org.tr/tr/pub/vanvetj

Cite this article as: **Arslan S, Yenilmez K (2026).** Evaluation of Oxidative Status and Thiol-Disulfide Homeostasis in Cows with Subclinical Hypocalcemia. *Van Vet J*, 37(1), 61-65. DOI: https://doi.org/10.36483/vanvetj.1810978

ISSN: 2149-3359 **Original Article** e-ISSN: 2149-8644

Evaluation of Oxidative Status and Thiol-Disulfide Homeostasis in Cows with Subclinical Hypocalcemia

Sezai ARSLAN[1,*] Kudret YENİLMEZ[2]

[1] *Tekirdağ Namık Kemal University, Faculty of Veterinary Medicine, Department of Internal Diseases, 59030, Tekirdağ, Türkiye*
[2] *Tekirdağ Namık Kemal University, Faculty of Veterinary Medicine, Department of Obstetrics and Gynecology, 59030, Tekirdağ, Türkiye*

Received: 27.09.2025 Accepted: 13.01.2026

ABSTRACT This study aimed to investigate the effects of subclinical hypocalcemia (SCH), identified on the 10th day postpartum in dairy cows, on serum levels of energy metabolites [glucose, triglycerides, and cholesterol], liver enzymes [aspartate aminotransferase (AST) and alanine aminotransferase (ALT)], minerals [calcium (Ca), phosphorus (P), and magnesium (Mg)], and oxidative stress markers [total thiol (TTHIOL), native thiol (NTHIOL), total oxidant status (TOS), and total antioxidant status (TAS)]. The study material consisted of 23 cows with SCH, which were clinically healthy but had serum calcium levels <8.5 mg/dL, and 14 healthy cows with serum calcium levels >8.5 mg/dL. Serum concentrations of AST, ALT, glucose, triglycerides, cholesterol, Mg, P, and Ca were measured using an autoanalyzer, while TAS, TOS, NTHIOL, and TTHIOL levels were determined spectrophotometrically. Serum Ca concentration was found to be significantly ($p<0.001$) lower in the SCH group. No significant differences were detected between the groups in terms of glucose, triglycerides, cholesterol, ALT, AST, Mg, and P levels. TAS and TOS values showed no significant differences; however, NTHIOL and TTHIOL levels were significantly ($p<0.05$) lower in the SCH group. SCH adversely affects not only calcium metabolism but also the antioxidant defense system, leading to an imbalance in thiol-disulfide homeostasis. Therefore, SCH should be considered a metabolic condition that increases oxidative stress burden.

Keywords: *Oxidative stress, Subclinical hypocalcemia, TAS, THIOL, TOS.*

ÖZ

Subklinik Hipokalsemili İneklerde Oksidatif Durum ve Tiyol-Disülfit Homeostazının Değerlendirilmesi

Bu çalışma, doğumdan sonraki 10. günde süt ineklerinde belirlenen subklinik hipokalseminin (SCH), enerji metabolitleri [glikoz, trigliserit ve kolesterol], karaciğer enzimleri [aspartat aminotransferaz (AST) ve alanin aminotransferaz (ALT)], mineraller [kalsiyum (Ca), fosfor (P) ve magnezyum (Mg)] ile oksidatif stres belirteçleri [toplam tiyol (TTHIOL), nativ tiyol (NTHIOL), total oksidan durum (TOS) ve total antioksidan durum (TAS)] üzerindeki etkilerini araştırmayı amaçlamıştır. Çalışma materyalini, klinik olarak sağlıklı ancak serum kalsiyum düzeyleri <8.5 mg/dL olan 23 SCH'li inek ile serum kalsiyum düzeyleri >8.5 mg/dL olan 14 sağlıklı inek oluşturmuştur. Serum AST, ALT, glikoz, trigliserit, kolesterol, Mg, P ve Ca konsantrasyonları otoanalizör kullanılarak ölçülmüş; TAS, TOS, NTHIOL ve TTHIOL düzeyleri ise spektrofotometrik yöntemle belirlenmiştir. SCH grubunda serum Ca konsantrasyonu anlamlı derecede düşük bulunmuştur ($p<0.001$). Glikoz, trigliserit, kolesterol, ALT, AST, Mg ve P düzeyleri açısından gruplar arasında anlamlı bir fark saptanmamıştır. TAS ve TOS değerleri arasında da anlamlı fark gözlenmemiştir; ancak NTHIOL ve TTHIOL düzeyleri SCH grubunda anlamlı derecede düşük bulunmuştur ($p<0.05$). SCH, yalnızca kalsiyum metabolizmasını değil, aynı zamanda antioksidan savunma sistemini de olumsuz etkileyerek tiyol-disülfit homeostazında dengesizliğe yol açmaktadır. Bu nedenle SCH, oksidatif stres yükünü artıran bir metabolik durum olarak değerlendirilmelidir.

Anahtar Kelimeler: *Oksidatif stres, Subklinik hipokalsemi, TAS, THIOL, TOS.*

INTRODUCTION

Hypocalcemia, also referred to as milk fever or parturient paresis, represents one of the most frequently encountered metabolic disorders in dairy cattle. It usually occurs immediately before, during, or after calving, but may also develop in cows during the dry period or mid-lactation (Eddy 2004). In dairy cows, the normal serum calcium concentration ranges between 8.5 and 10 mg/dL

✉ *Corresponding author: sarslan@nku.edu.tr

(Aiello and Moses 2016). Unlike clinical hypocalcemia, subclinical hypocalcemia (SCH) is defined as a decrease in serum Ca levels below 8–8.6 mg/dL in dairy cows without obvious clinical symptoms, leading to metabolic imbalances (Reinhardt et al. 2011; Caixeta et al. 2017). Compared with clinical hypocalcemia, the subclinical form is observed more commonly in dairy cattle populations (Jessica et al. 2018).

Biological free radicals are highly unstable and reactive molecules. They interact with other molecules within the cell and can damage various biological materials such as lipids, proteins, and nucleic acids (Kopáni et al. 2006). Oxidative stress occurs when the production of free radicals exceeds the capacity of the organism's antioxidant systems to counteract or eliminate them (Pizzino et al. 2017; Chaudhary et al. 2023; Tufarelli et al. 2023). Dairy cows frequently undergo oxidative stress during the transition period due to elevated metabolic requirements and exposure to pathogenic stressors (Mirzaei et al. 2025). Evaluating the metabolic status involves measuring the degree of damage caused by free radicals and the organism's corresponding defense response to this stress (Castillo et al. 2005). Rather than evaluating individual antioxidant molecules, measuring the total antioxidant status (TAS) provides biologically more meaningful information for assessing oxidative stress (Castillo et al. 2005).

Thiols are potent antioxidant compounds that possess sulfhydryl (–SH) functional groups. (Eren et al. 2015). Thiols interact with oxidant molecules to generate disulfide bonds (S–S), which can be converted back to thiol groups when required, thereby maintaining a dynamic redox balance (Erel and Neşelioğlu 2014). Thiols eliminate reactive oxygen species (ROS) and free radicals via both enzymatic and non-enzymatic pathways. Therefore, measuring total thiol levels serves as a useful biomarker for evaluating free radical production (Eren et al. 2015). Dynamic thiol–disulfide balance represents a major cellular defense mechanism against the detrimental impacts of oxidative stress. This equilibrium is essential not only for antioxidant protection but also for processes such as detoxification, cellular signaling, apoptosis, and the modulation of enzyme activity (Erel and Neşelioğlu 2014).

Throughout the transition period, dairy cows experience significant physiological adjustments and increased metabolic stress. During this period, oxidative stress contributes substantially to the development of various diseases (Bernabucci et al. 2005). Marked changes in blood biochemical parameters and oxidant–antioxidant balance have been reported during this phase (Balkan et al. 2024). To date, no studies have specifically focused on thiol levels in cows with subclinical hypocalcemia. Therefore, the present study aimed to investigate the effects of subclinical hypocalcemia, a metabolic disorder identified on the 10th day postpartum, on certain biochemical parameters (ALT, AST, glucose, triglycerides, cholesterol, Mg, P, and Ca), oxidative stress indicators (TAS, TOS, TTHIOL and NTHIOL) in dairy cows.

MATERIAL AND METHODS

Ethical Statement

The study was conducted following ethical approval from the Local Ethics Committee for Animal Experiments at Tekirdağ Namık Kemal University (06.03.2025/T2025-), with all methods adhering to the committee's regulations.

Study Material

The study population consisted of multiparous Holstein dairy cows from the same herd and production facility, aged between 3 and 5 years with no history of puerperal diseases and clinically healthy upon examination. Cows with serum total Ca levels <8.5 mg/dL were classified as the SCH group (n=23), while those with serum Ca levels >8.5 mg/dL were classified as the control group (n=14). The cut-off of 8.5 mg/dL (≈2.12 mmol/L) was chosen because it represents the lower bound of the physiological reference range for total serum calcium in adult dairy cows (Aiello and Moses 2016) and is commonly applied as a practical threshold to define postpartum subclinical hypocalcemia (Martinez et al. 2012; Ghasemi et al. 2024). All animals were housed under the same management and feeding conditions and were fed a total mixed ration formulated (Dry matter 55%, crude protein 18%, crude cellulose 12%, crude fat 3.0%, crude ash 8%, starch 25%, sodium 0.25%, 0.7% calcium, 0.37% phosporus, vitamin A 9,000 IU/kg, vitamin D_3 3,000 IU/kg, vitamin E 30 mg/kg, iodine 0.1 mg/kg, cobalt 0.1mg/kg, copper 10 mg/kg, manganese 50 mg/kg, zinc 50 mg/kg, selenium 0.43 mg/kg) specifically for the transition period, twice daily on an ad libitum basis. In addition to the TMR, a mineral–vitamin lick bucket was available in the facility. The lick contained vitamins (A 1000000 IU; D_3 300000 IU; E 250 mg; K_3 15 mg; B_1 500 mg; B_2 150 mg; B_3 1000 mg; B_5 50 mg; B_6 50 mg; biotin 150 mg; folic acid 50 mg) and trace/mineral elements (selenium 25 mg; iodine 125 mg; cobalt 70 mg; manganese 2000 mg; iron 3000 mg; zinc 4500 mg; copper 1500 mg; magnesium 5500 mg, calcium 7.5% and phosphorus 2.6%). Fresh drinking water was provided continuously.

Biochemical Analyses

Blood samples were collected on the 10th day of postpartum. Samples were centrifuged at 3000 rpm for 15 minutes to separate the serum. The obtained serum was stored at –80 °C until analysis. Serum glucose, triglyceride, cholesterol, ALT, AST, Mg, P, and Ca levels were measured by using an autoanalyzer (Randox, UK). Serum TAS, TOS, NTHIOL, and TTHIOL levels were determined colorimetrically using spectrophotometric methods (Epoch, BioTek, Winooski, VT, USA) with commercial kits from Rel Assay Diagnostics (Mega Tıp Sanayi ve Ticaret Ltd. Şti., Türkiye). Oxidative stress index (OSI) was computed as the percentage of TOS relative to TAS [OSI = (TOS / TAS) × 100]. Disulfide concentration was calculated as half the difference between total thiol and native thiol levels [Disulfide = (TTHIOL - NTHIOL) / 2].

Statistical Analyses

Data normality was assessed with the Shapiro-Wilk test. Normally distributed data were analyzed by using the Independent t-test, and non-normal data with the Mann-Whitney U test. Analyses were performed using SPSS (IBM, v24.0). Results are presented as mean±standard error of the mean (X±SEM), and statistical significance set at $p<0.05$.

RESULTS

On the 10th day of postpartum, no clinical signs of hypocalcemia were observed in the cows belonging to the SCH group. All cows were standing, alert, and exhibited normal body temperature, pulse, and respiratory rates. None of the animals showed any signs of clinical metritis, dystocia, retained placenta, abomasal displacement, ketosis, or mastitis.

Serum calcium (Ca) levels were significantly lower in the SCH group compared to the healthy control group ($p<0.001$). No significant differences were found between the groups in terms of phosphorus (P), magnesium (Mg), glucose, lipid profile (total cholesterol and triglycerides), and liver enzymes (AST and ALT) ($p>0.05$) (Table 1).

When antioxidant and oxidant parameters were examined, no statistically differences were found between SCH and healthy cows in terms of serum TAS, TOS, disulfide, disulfide/NTHIOL (%), disulfide/TTHIOL (%), and NTHIOL/TTHIOL (%) levels. However, NTHIOL and TTHIOL concentrations were found to be significantly lower in the SCH group compared to the control group ($p<0.05$) (Table 1).

Table 1: Comparison of selected biochemical, oxidant, and antioxidant parameters between subclinical hypocalcemic and healthy cows.

Parameters	SCH (n:23)	Healthy (Control) (n:14)
ALT (U/L)	58.29±3.30	55.92±3.84
AST (U/L)	111.38±4.91	115.15±2.37
Glucose (mg/dL)	56.92±1.00	57.28±1.60
Cholesterol (mg/dL)	124.79±9.47	137.43±16.15
Triglyceride (mg/dL)	10.74±0.89	11.69±1.36
Ca (mg/dL)	7.98±0.13***	9.88±0.18
P (mg/dL)	6.82±0.19	6.79±0.34
Mg (mg/dL)	2.08±0.06	2.02±0.11
TAS (mmol/L)	1.58±0.20	1.93±0.39
TOS (µmol/L)	6.36±1.62	5.50±1.00
OSI	0.41±0.07	0.54±0.25
NTHIOL (µmol/L)	310.00±38.21*	460.17±54.19
TTHIOL (µmol/L)	349.22±42.46*	510.94±55.49
Disulfide (µmol/L)	19.61±2.79	25.39±4.67
Disulfide/NTHIOL (%)	6.81±0.71	6.53±1.75
Disulfide/TTHIOL (%)	5.84±0.53	5.39±1.15
NTHIOL/ TTHIOL (%)	88.33±1.06	89.23±2.30

Statistical significance is indicated by *$p<0.05$ and ***$p<0.001$.

DISCUSSION AND CONCLUSION

In this study, several biochemical and antioxidant parameters were evaluated in postpartum cows with subclinical hypocalcemia (SCH) and compared with those of healthy cows. The findings demonstrated that the decrease in serum calcium (Ca) levels in SCH cows was accompanied by a significant reduction in thiol groups, suggesting a potential link between hypocalcemia and increased oxidative stress.

The difference in Ca levels was an expected outcome and formed the basis of group classification. The normal serum total Ca concentration in dairy cows ranges from 8.5 to 10 mg/dL (Aiello and Moses 2016; Jessica et al. 2018). Various cutoff points ranging from 8.0 to 8.8 mg/dL have been reported to define subclinical hypocalcemia (Goff 2008; Venjakob et al. 2017; Caixeta et al. 2017). In our study, the mean Ca concentration on day 10 postpartum in the SCH group was 7.98±0.13 mg/dL, which is below the frequently used threshold of 8.5 mg/dL for SCH. Cows with serum Ca concentrations between 6–7 mg/dL generally remain standing, those between 4–5 mg/dL are recumbent, and at levels below 4 mg/dL most become comatose (Jessica et al. 2018). Importantly, the key biological question is why Ca remained lower in SCH cows than in healthy cows at day 10 postpartum. All cows were managed under the same feeding conditions and received the same calcium-containing diet (TMR: 0.7% Ca, 0.37% P on a dry matter basis) with free access to a mineral–vitamin lick bucket (7.5% Ca, 2.6% P). Thus, the between-group difference in serum Ca is unlikely to be explained by facility-level absence of dietary Ca sources, and the presence of normocalcemic controls under the same regimen suggests that SCH may reflect inter-individual differences in the adaptive response to early-lactation Ca demands rather than a simple dietary deficiency. However, individual feed and lick intake were not quantified, limiting inference regarding actual Ca intake at the animal level. Although serum phosphorus and magnesium concentrations did not differ between groups (Table 1), the persistence of low Ca may indicate delayed or insufficient restoration of calcium homeostasis during early lactation, when ongoing Ca export into milk continues to challenge regulatory capacity. Collectively, these findings indicate that cows with SCH at day 10 postpartum may represent a metabolically less resilient subgroup, in which the adaptive response required to re-establish normocalcemia appears to be compromised despite broadly comparable P and Mg status at the time of sampling.

In the current study, serum phosphorus (P) and magnesium (Mg) concentrations in the SCH group were statistically similar to those of the control group. This suggests that, at the time of sampling, SCH was not consistently accompanied by concurrent hypophosphatemia or hypomagnesemia in this cohort. Patel et al. (2021) similarly reported no significant differences in Mg and P levels between subclinically hypocalcemic and healthy cows. Therefore, our findings support the interpretation that reduced serum Ca can be observed even when circulating P and Mg concentrations remain comparable between groups. Because circulating mineral concentrations are influenced by multiple physiological and homeostatic mechanisms, the absence of between-group differences in P and Mg should be evaluated in this context. Overall, the present results are most consistent with SCH being primarily related to disturbances in calcium homeostasis rather than being driven by concurrent alterations in P or Mg concentrations at day 10 postpartum.

The role of oxidative stress in the development of diseases during the transition period in dairy cows is well known (Sordillo 2013; Abuelo et al. 2015), and in recent years, interest in the use of such biomarkers has increased (Abuelo et al. 2015; Tufarelli et al. 2023; Balkan et al. 2024). No statistically significant difference was found between SCH and healthy cows in terms of TAS and TOS levels. This finding suggests that subclinical hypocalcemia

diagnosed on day 10 postpartum did not significantly affect the overall oxidant–antioxidant balance. To date, no study has directly examined TAS and thiol levels in cows with clinical or subclinical hypocalcemia. However, a study conducted in transition cows reported that postpartum TAS values were lower than prepartum values, although the difference was statistically significant (Balkan et al. 2024). The lower TAS levels observed in the SCH group in our study are consistent with those findings reported during the transition period (Balkan et al., 2024).

Thiols are strong antioxidants based on amino acids and proteins containing sulfhydryl (-SH) groups; they protect the body by directly or indirectly neutralizing free radicals and reactive oxygen species (ROS) (Karoui et al. 1996; Erel and Neşelioğlu 2014; Balkan et al. 2024). In a study conducted on healthy humans, thiol groups were reported to contribute approximately 52.9% to the total serum antioxidant capacity (Erel 2004). In human medicine, studies have shown that native and total thiol levels are significantly lower in patients with preeclampsia (Ozler et al. 2015), prostatitis and prostate cancer (Solakhan et al. 2019), early-stage non-small cell lung cancer (Kavas et al. 2023), diabetic ketoacidosis (Otal et al. 2021), and in individuals with chronic kidney disease and those undergoing hemodialysis (Erdal et al. 2022). In these studies, disulfide levels were found to be increased in some (Ozler et al. 2015; Erdal et al. 2022; Kavas et al. 2023) and decreased in others (Solakhan et al. 2019; Otal et al. 2021). In veterinary medicine, increased NTHIOL and TTHIOL levels have been reported in animals with foot diseases (Deveci et al. 2022) and in dogs with parvoviral enteritis (Şenel et al. 2024). In contrast, decreased levels have been observed in calves with neonatal diarrhea (Terzi et al. 2023), sheep affected by sarcoptic mange (Çamkerten et al. 2019), sheep pox (Adıgüzel and Merhan 2024), trichophytosis (Bölükbaşı and Merhan 2024), and in animals subjected to thermal disbudding under general or local anesthesia and analgesia (Erdoğan et al. 2019). Regarding disulfide levels, increases were reported by Deveci et al. (2022), Terzi et al. (2023), Adıgüzel and Merhan (2024), and Bölükbaşı and Merhan (2024), whereas decreases were observed by Şenel et al. (2024) and Çamkerten et al. (2019). In the present study, the significantly lower native and total thiol levels observed in cows with subclinical hypocalcemia compared to healthy controls indicate the negative impact of metabolic stress induced by subclinical hypocalcemia. The absence of a statistically significant decrease in TAS, together with the significant reduction in thiol levels, suggests that thiols—an essential component of the antioxidant defense system—were more extensively utilized to neutralize the excessive free radicals generated during SCH.

In our study, no significant differences were observed in disulfide levels or thiol/disulfide ratios. It is well established that under conditions of increased oxidative stress, thiol groups are oxidized to form disulfide bonds, resulting in a decrease in circulating thiol concentrations (Erel and Neşelioğlu 2014; Balkan et al. 2024). However, despite increased thiol utilization in this study, no corresponding rise in disulfide levels was detected, suggesting the mechanism described by Otal et al. (2021). According to this mechanism, under severe oxidative stress, proteins undergo more advanced stages of oxidation beyond the classical thiol–disulfide cycle, leading to a disruption of thiol–disulfide homeostasis. Therefore, the decrease in thiol levels without an accompanying increase in disulfides observed in our study likely indicates the occurrence of further oxidative modifications of protein thiol groups. Subclinical hypocalcemia increases oxidative stress burden and disrupts thiol–disulfide homeostasis in dairy cows. Antioxidant defense systems, particularly thiol-based antioxidants, are consumed to counteract this excessive oxidative load, leading to their depletion. Therefore, maintaining calcium homeostasis may be important not only for mineral metabolism but also for controlling oxidative stress.

A further consideration is the limited number of subjects in this study, which may have constrained the detection of statistically significant variations in specific parameters. The lack of meaningful statistical differences in measures such as TAS and TOS, despite visible trends between the groups, could be a result of this constraint. In addition, this study focused on a single time point (day 10 postpartum).

In this study, the biochemical and redox-related profiles of cows with subclinical hypocalcemia were evaluated during the early postpartum period. SCH cows exhibited significantly reduced native and total thiol concentrations, which are key components of the antioxidant defense network and may reflect increased utilization of thiol-based antioxidants. Notably, these findings suggest that SCH cows do not exhibit a generalized increase in oxidative stress during early lactation; rather, a selective depletion of the thiol pool is observed, which may represent an adaptive response to persistently low circulating calcium concentrations.

CONFLICTS OF INTEREST

The authors report no conflicts of interest.

AUTHOR CONTRIBUTIONS

Idea/Concept: SA, KY
Supervision/Consultancy: KY, SA
Data Collection and/or Processing: SA, KY
Analysis and/or Interpretation: KY, SA
Writing the Article: SA
Critical Review: KY

REFERENCES

Abuelo A, Hernández J, Benedito JL, Castillo C (2015). The importance of the oxidative status of dairy cattle in the periparturient period: revisiting antioxidant supplementation. *J Anim Physiol Anim Nutr (Berl)*, 99(6), 1003-1016.

Adıgüzel S, Merhan O (2024). Determination of thiol/disulfide homeostasis and oxidative stress index in sheeppox virus. *Anim Health Prod Hyg*, 13(2), 21-25.

Aiello SE, Moses MA (Eds.) (2016). The Merck Veterinary Manual. 11th ed. Merck & Co., Inc., New Jersey, USA, pp. 998-991.

Balkan BM, Meral O, Cetintav B et al. (2024). Evaluation of thiol/disulphide and oxidant-antioxidant status of dairy cows in periparturient and post-partum period. *Vet Med Sci*, 10(6), e70023.

Bernabucci U, Ronchi B, Lacetera N, Nardone A (2005). Influence of body condition score on relationships between metabolic status and oxidative stress in periparturient dairy cows. *J Dairy Sci*, 88(6), 2017-2026.

Bölükbaşı L, Merhan O (2024). Lipid peroxidation and thiol/disulfide homeostasis in cattle with trichophytosis. *Dicle Üniv Vet Fak Derg*, 17(2), 161-164.

Caixeta LS, Ospina PA, Capel MB, Nydam DV (2017). Association between subclinical hypocalcemia in the first 3 days of lactation and reproductive performance of dairy cows. *Theriogenology*, 94, 1-7.

Castillo C, Hernandez J, Bravo A et al. (2005). Oxidative status during late pregnancy and early lactation in dairy cows. *Vet J*, 169(2), 286-292.

Chaudhary P, Janmeda P, Docea AO et al. (2023). Oxidative stress, free radicals and antioxidants: potential crosstalk in the pathophysiology of human diseases. *Front Chem*, 11, 1158198.

Çamkerten İ, Çamkerten G, Erdoğan H, et al. (2019). Serum thiol disulphide levels among sheep with sarcoptic mange. *Kafkas Univ Vet Fak Derg*, 25, 865-868.

Deveci MZY, Erdal H (2022). Determination of dynamic thiol-disulfide levels in dairy cattle with foot disease. *Vet Arhiv*, 92, 657–666.

Eddy RG (2004). Major Metabolic Disorders. In: Andrews AH, Blowey RW, Boyd H, Eddy RG (Eds). Bovine Medicine: Diseases and Husbandry of Cattle. 2nd ed. Blackwell Publishing Company, Ames, Iowa, USA.

Erdal H, Özcan O, Turgut F, Neşelioğlu S, Erel Ö (2022). Evaluation of dynamic thiol-disulfide balance and ischemia modified albumin levels in patients with chronic kidney disease. *MKÜ Tıp Derg*, 13(47), 237-242.

Erdoğan H, Çamkerten İ, Çamkerten G et al. (2019). The effect of hot-iron disbudding on thiol-disulphide homeostasis in calves. *Kafkas Univ Vet Fak Derg*, 25(3), 335-339.

Erel O (2004). A novel automated direct measurement method for total antioxidant capacity using a new generation, more stable ABTS radical cation. *Clin Biochem*, 37, 277–285.

Erel O, Neselioglu S (2014). A novel and automated assay for thiol/disulphide homeostasis. *Clin Biochem*, 47(18), 326-332.

Eren Y, Dirik E, Neşelioğlu S, Erel Ö (2015). Oxidative stress and decreased thiol level in patients with migraine: cross-sectional study. *Acta Neurol Belg*, 115, 643–649.

Ghasemi N, Amanlou H, Maheri-Sis N, Salamatdoust-Nobar R, Jozghasemi S (2024). Relationship between hypocalcemia immediately after calving with metabolic disorders and body condition score in Holstein cows. *Open Vet J*, 14(3), 805-813.

Goff JP (2008). The monitoring, prevention, and treatment of milk fever and subclinical hypocalcemia in dairy cows. *Vet J*, 176, 50-57.

Jessica AA McArt, Divers TJ, Peek SF (2018). Metabolic Diseases. In: Peek SF, Divers TJ (Eds). Rebhun's Diseases of Dairy Cattle. 3rd ed. Elsevier, Philadelphia, pp. 722–727.

Kavas M, Atınkaya Baytemir C, Alışık M et al. (2023). The effect of thiol-disulfide homeostasis on prognosis in patients with early-stage non-small cell lung cancer. *Online Turk J Health Sci*, 8(1), 122-126.

Kopáni M, Celec P, Danisovic L, Michalka P, Biró C (2006). Oxidative stress and electron spin resonance. *Clin Chim Acta*, 364(1-2), 61-66.

Martinez N, Risco CA, Lima FS et al. (2012). Evaluation of peripartal calcium status, energetic profile, and neutrophil function in dairy cows at low or high risk of developing uterine disease. *J Dairy Sci*, 95(12), 7158-7172.

Mirzaei A, Hajimohammadi A, Nasrian A et al. (2025). Oxidative stress biomarkers and metabolic parameters in healthy Holstein dairy cows and cows with left displacement abomasum during the transitional period. *Vet Med Sci*, 11(1), e70142.

Otal Y, Kahraman FA, Haydar FG, Erel Ö (2021). Dynamic thiol/disulfide homeostasis as oxidative stress marker in diabetic ketoacidosis. *Turk J Med Sci*, 51(2), 743-748.

Ozler S, Erel O, Oztas E et al. (2015). Serum thiol/disulphide homeostasis in preeclampsia. *Hypertens Pregnancy*, 34(4), 474-485.

Patel N, Baishya BC, Phukan A et al. (2021). Biochemical changes associated with subclinical hypocalcaemia in high producing crossbred dairy cows 15 days before the expected day of calving. *Pharma Innov J*, 10, 554-558.

Pizzino G, Irrera N, Cucinotta M et al. (2017). Oxidative stress: Harms and benefits for human health. *Oxid Med Cell Longev*, 2017(1), 8416763.

Reinhardt TA, Lippolis JD, McCluskey BJ, Goff JP, Horst RL (2011). Prevalence of subclinical hypocalcemia in dairy herds. *Vet J*, 188(1), 122-124.

Solakhan M, Cicek H, Orhan N, Yildirim M (2019). Role of native thiol, total thiol and dynamic disulphide in diagnosis of patients with prostate cancer and prostatitis. *Int Braz J Urol*, 45(3), 495-502.

Şenel Y, Terzi OS, Kara E et al. (2024). Alterations in serum thiol-disulfide homeostasis and ischemia-modified albumin concentrations in clinical canine parvoviral enteritis. *Turk J Vet Anim Sci*, 48(2), Article 2.

Terzi OS, Kara E, Şenel Y et al. (2023). Dynamic thiol-disulphide homeostasis and ischemia modified albumin levels in neonatal calf diarrhea. *Ankara Univ Vet Fak Derg*, 70(1), 81-86.

Tufarelli V, Colonna MA, Losacco C, Puvača N (2023). Biological health markers associated with oxidative stress in dairy cows during lactation period. *Metabolites*, 13(3), 405.

Venjakob PL, Borchardt S, Heuwieser W (2017). Hypocalcemia-cow-level prevalence and preventive strategies in German dairy herds. *J Dairy Sci*, 100(11), 9258-9266.

Van Veterinary Journal

https://dergipark.org.tr/tr/pub/vanvetj

Cite this article as: **Yavuz H, Kandemir Ö, Şimşek H, Akaras N, Kandemir FM (2026).** Investigation of the Effects of Carvacrol on Oxytetracycline-Induced Kidney Damage. *Van Vet J*, 37(1), 66-73. DOI: https://doi.org/10.36483/vanvetj.1819779

ISSN: 2149-3359 **Original Article** e-ISSN: 2149-8644

Investigation of the Effects of Carvacrol on Oxytetracycline-Induced Kidney Damage

Halil YAVUZ[1,*] Özge KANDEMİR[2] Hasan ŞİMŞEK[3] Nurhan AKARAS[4] Fatih Mehmet KANDEMİR[5]

[1] *Necmettin Erbakan University, Faculty of Veterinary Medicine, Department of Biochemistry, 42310, Konya, Türkiye*
[2] *Aksaray University, Aksaray Technical Sciences Vocational School, Department of Food Processing, 68100, Aksaray, Türkiye*
[3] *Aksaray University, Faculty of Medicine, Department of Physiology, 68100, Aksaray, Türkiye*
[4] *Aksaray University, Faculty of Medicine, Department of Histology and Embryology, 68100, Aksaray, Türkiye*
[5] *Aksaray University, Faculty of Medicine, Department of Medical Biochemistry, 68100, Aksaray, Türkiye*

Received: 07.11.2025 Accepted: 14.01.2026

ABSTRACT The main objective of this study was to assess the antioxidant capacity and the protective impact of carvacrol (CRV) against oxytetracycline (OXI)-mediated nephrotoxicity in albino rats. CRV, a naturally occurring phenolic compound found in various plant species, has significant antioxidant capacity, the ability to mitigate inflammatory processes, and tumor proliferation inhibiting properties. The study evaluated the efficacy of CRV in reducing oxidative stress-induced kidney damage in albino rats. Findings showed that CRV administration significantly reduced the kidney damage relative to the control group. Evaluation of the enzymatic antioxidant profile indicated a significant decrease in the activities of catalase (CAT), glutathione peroxidase (GPx), and superoxide dismutase (SOD) enzymes and GSH levels in the OXI-treated group compared to the CRV group. Furthermore, CRV treatment decreased malondialdehyde (MDA), a key biomarker of lipid peroxidation. The protective properties of CRV were confirmed by histological examination of the kidney. CRV treatment markedly suppressed pro-inflammatory molecules, specifically diminishing the expression of interleukin-1 beta (IL-1β) and mitigating nuclear factor kappa-B (NF-κB) activation. Furthermore, CRV administration attenuated OXI-induced increases in the proapoptotic proteins Bax and Caspase-3, while increasing the transcriptional activity of the antiapoptotic gene B-cell lymphoma-2 (Bcl-2). CRV diminished OXI-induced kidney tissue damage by decreasing Kidney Injury Molecule-1 (KIM-1) and increasing Aquaporin-2 (AQP-2) levels. The study results indicate that CRV administration can alleviate tissue damage in the kidney caused by OXI toxicity.

Keywords: *Albino rat, Antioxidant activity, Carvacrol, Kidney function, Lipid peroxidation, Oxytetracycline.*

ÖZ

Oksitetrasiklin Kaynaklı Böbrek Hasarı Üzerine Karvakrolün Etkilerinin Araştırılması

Bu çalışmanın amacı, albino sıçanlarda oksitetrasiklin (OXI) kaynaklı nefrotoksisiteye karşı karvakrolün (CRV) antioksidan potansiyelini ve koruyucu rolünü araştırmaktır. Çeşitli bitki türlerinde doğal olarak bulunan fenolik bir bileşik olan CRV'nin önemli antioksidan, anti-inflamatuar ve antikanser özellikleri vardır. Çalışmada, albino sıçanlarda oksidatif stres kaynaklı böbrek hasarını azaltmada CRV'nin etkinliği değerlendirilmiştir. Bulgular, CRV uygulamasının böbrek hasarını kontrol grubuna kıyasla önemli ölçüde azalttığını göstermiştir. OXI uygulanan grupta, CRV uygulanan gruba kıyasla süperoksit dismutaz (SOD), glutatyon peroksidaz (GPx) ile katalaz (CAT) da dâhil antioksidan etkinliği olan enzimlerin aktivitelerinde ve GSH seviyelerinde önemli bir azalma gözlenmiştir. Ayrıca, CRV tedavisi, lipid peroksidasyonunun önemli bir biyobelirteci olan malondialdehit (MDA) düzeyini düşürmüştür. CRV'nin koruyucu özellikleri, böbreğin histolojik incelemesiyle doğrulanmıştır. CRV tedavisi, nükleer faktör kappa-B (NF-κB) ile interlökin-1 beta (IL-1β) gibi inflamasyon medyatörleri önemli ölçüde azalttı. Ayrıca, CRV uygulaması, proapoptotik proteinler Bax ve Kaspaz-3'te OXI kaynaklı artışları azaltırken, antiapoptotik belirteç B hücreli lenfoma-2 (Bcl-2) ekspresyonunu artırdı. CRV, Böbrek Hasarı Molekülü-1'i (KIM-1) azaltarak ve Aquaporin-2 (AQP-2) seviyelerini artırarak OXI kaynaklı böbrek doku hasarını azalttı. Çalışma sonuçları, CRV uygulamasının OXI toksisitesinden kaynaklanan böbrek doku hasarını hafifletebileceğini göstermektedir.

Anahtar Kelimeler: *Albino sıçan, Antioksidan aktivite, Böbrek fonksiyonu, Karvakrol, Lipit peroksidasyonu, Oksitetrasiklin.*

✉ *Corresponding author: halil.yavuz@erbakan.edu.tr

INTRODUCTION

Oxytetracycline (OXI) is a broad-spectrum antibiotic widely used to control bacterial infections in humans and animals. Use of high doses of OXI without medical supervision has harmful effects on kidney and liver tissues (Abdel-Daim and Ghazy 2015).

OXI disrupts mitochondrial β-oxidation, consequently elevating the generation of free radicals and reactive oxygen species (ROS) (Gibson 2005). These harmful molecules, in turn, interact with cell membranes, causing lipid peroxidation and subsequent structural damage (Skakun and Vysotski 1982). Additionally, the decrease in tissue antioxidant biomarkers is associated with OXI overdose. A wide variety of antioxidants with different structures have been used against these side effects of OXI and their effects have been investigated.

Carvacrol (CRV) is found in the essential oils of aromatic plants. Besides, CRV (5-isopropyl-2-methylphenol) is a liquid monoterpenoid compound that is soluble in ethanol but insoluble in water. Its density at 20°C is approximately 0.976 g/mL, and its boiling point is between 236 and 237 °C (Mączka et al. 2023). The hydroxyl group (OH^-) in CRV's structure is what gives it its antioxidant qualities and its ability to scavenge radicals including hydrogen peroxide, nitric oxide, and superoxide radicals (Imran et al. 2022).

CRV has antimicrobial biological activity (Mączka et al. 2023). Its anti-inflammatory activity is primarily mediated through suppression of cyclooxygenase-2 (COX-2) expression and reduction of IL-1β levels (Akcılar et al. 2015).

There are also important studies on the anticancer properties of CRV (Ahmad et al. 2021; Bouhtit et al. 2021; Sampaio et al. 2021; Bansal et al. 2022; Gunes-Bayir et al. 2022; Tomsuk et al. 2024; Sathi-Devi et al. 2025; Yousef et al. 2025). CRV is documented to possess diverse biological properties, comprising anticancer, antimutagenic, inflammation-suppressing, acetylcholinesterase (AChE) inhibitory, analgesic, antioxidant, antihepatotoxic, antiparasitic, insecticidal, and antibacterial properties (Nostro and Papalia 2012).

The current research was designed to elucidate the protective efficacy of CRV against renal tissue injury induced by the commonly administered antibiotic OXI, employing a comprehensive suite of molecular, biochemical, and histopathological assessments.

MATERIAL AND METHODS

Research and Publication Ethics

This study was conducted with the permission of Konya Necmettin Erbakan University Animal Experiments Local Ethics Committee on 20.02.2025 with the number 2025-011.

Chemicals

Pioxy LA Injection Solution 100 ml (liter contains oxytetracycline dihydrate at a concentration corresponding to 200 mg of oxytetracycline base in each milliliter) by Pi Farma (Ankara, Türkiye) was purchased. CRV (CAS No: 499-75-2, with a purity of 98%) was purchased from Sigma-Aldrich.

The OXI dose was determined using the studies reported by Marza et al. (2020) and Oda et al. (2018). The study published by Şimşek et al. (2024) was used to determine the CRV dose.

Experimental design and animals

This study involved 28 albino rats of the Wistar, aged 10-12 weeks, each with a mean body weight of 235±15 g. All animals were maintained under standardized environmental conditions, including a steady temperature of 24-25 °C and a controlled 12-hour light-dark cycle (darkness commencing at 19:00 h). They had access to unlimited amounts of water and standard chow. After a week of resting in their cages, the rats were acclimated to their new surroundings, and the studies started. All animal procedures were carried out at the KONÜDAM Experimental Medicine Application and Research Center. A total of 28 rats were randomly divided into four experimental groups (n=7 per group). Literature was used to determine the dose of the active ingredients (Oda et al. 2018; Marza et al. 2020).

1. Control group (C): For seven days, 1 mL of physiological saline was administered intraperitoneally once daily.

2. Carvacrol group (CRV): For seven days, the treatment regimen involved daily oral delivery of CRV at 50 mg/kg by gavage.

3. Oxytetracycline group (OXI): OXI was delivered via a seven-day regimen of once-daily intraperitoneal injections at a fixed dose of 200 mg/kg.

4. Oxytetracycline+Carvacrol (OXI+CRV): Animals received OXI via daily intraperitoneal injection at a fixed dose of 200 mg/kg for 7 days, and at the same time 50 mg/kg of CRV was given orally by gavage once daily.

Tissue and Blood Collection

The rats were decapitated under light sevoflurane (Sevorane®; Queenborough, UK) anesthesia, which was conducted 24 hours after the final dose of CRV (on Day 8 of the protocol), and samples of kidney tissue and blood were taken. Kidney tissues were kept at -20 °C until they were subjected to molecular and biochemical investigations. Blood samples were transferred to vacuum tubes without anticoagulant and then centrifuged at 3000 rpm for 10 minutes at 4 °C. The separated serum was kept at -20 °C in a deep freezer until it was subjected to biochemical analysis.

Biochemical analysis

Kidney Function Tests

Renal function was evaluated by determining serum urea and creatinine concentrations, following the instructions provided by the commercial assay kit.

Determination of lipid peroxidation

Lipid peroxidation levels in the kidney tissues were determined via spectrophotometry. This method involves measuring the absorbance at 532 nm resulting from the chromogen formed by the reaction between MDA and thiobarbituric acid (TBA). Kidney samples were analyzed using a homogenizer. A potassium chloride (KCl) solution containing 1.15% was used to homogenize the tissues. Following homogenization, the resulting tissue suspensions underwent centrifugation at a force of 1,000 x g for 15 minutes at 4 °C. Centrifugation was followed by the use of the supernatant. MDA levels were calculated using the Placer et al. (1966) method.

Determination of Antioxidant Activity

Renal antioxidant capacity was assessed through the determination of the activities of the antioxidant enzymes CAT, GPx, and SOD using commercial ELISA kits. Supernatants were obtained using the same method used for lipid peroxidation to evaluate CAT, GPx, with SOD activities and GSH concentrations. The enzymatic activity of catalase (CAT) was measured following the established spectrophotometric procedure by Aebi (1984), SOD activity using the Sun et al. (1988) method, and GPx activity performing the method established by Lawrence and Burk (1976). GSH levels were also determined using the Sedlak and Lindsay (1968) method. The protein concentration of renal samples, needed for calculating enzyme assays, was performed using the Lowry et al. (1951) protocol.

Real Time PCR (RT-PCR)

At the conclusion of the research, mRNA expression grades of the genes were evaluated in kidney tissues using the RT-PCR technique (Table 1). RNA isolation was performed using commercially available QIAzol Lysis Reagent (Qiagen, 79306). Isolated total RNA was converted to cDNA with OneScript Plus cDNA Synthesis Kit (ABM, G236, Richmond, Canada). Then, the PCR mixture was prepared by adding BlasTaq™ 2X qPCR MasterMix (ABM, G891, Richmond, Canada) with primer sequences, and the reaction started. The procedures were carried out in appropriate temperature cycles in the Rotor-Gene Q (Qiagen) instrument according to the protocol specified by the producer.

Gene expressions obtained from the analysis were standardized with the β-Actin reference gene and assessed via the 2-ΔΔCT method (Livak and Schmittgen 2001).

Table 1: Primer sequences of genes analyzed in RT-PCR.

Gene	Sequences (5'-3')	(bp)	Accession No
NF-κB	F: AGTCCCGCCCCTTCTAAAAC R: CAATGGCCTCTGTGTAGCCC	106	NM_001276711.1
IL-1β	F: ATGGCAACTGTCCCTGAACT R: AGTGACACTGCCTTCCTGAA	197	NM_031512.2
Caspase-3	F: ACTGGAATGTCAGCTCGCAA R: GCAGTAGTCGCCTCTGAAGA	270	NM_012922.2
Bax	F: TTTCATCCAGGATCGAGCAG R: AATCATCCTCTGCAGCTCCA	154	NM_017059.2
Bcl-2	F: GACTTTGCAGAGATGTCCAG R: TCAGGTACTCAGTCATCCAC	214	NM_016993.2
KIM1	F: AGCACATTCTCCAGGAAGCC R: AGGCCAGCCCTCTAATGGTA	298	NM_173149.2
AQP2	F: AGCTGCCTTCTATGTGGCT R: GCGTTGTTGTGGAGAGCATT	120	NM_012909.2
β-Actin	F: CAGCCTTCCTTCTTGGGTATG R: AGCTCAGTAACAGTCCGCCT	360	NM_031144.3

Histopathological Examination for kidney

At the conclusion of the study, the rat kidney samples were immersed in 10% neutral-buffered formaldehyde solution for 2 days to ensure complete fixation. The tissues were submerged overnight to remove formalin. They were then dehydrated through ascending alcohols and then cleared in xylene. Following paraffin embedding, the samples were cut into 5 μm slices utilizing a microtome device. The obtained tissue sections were subjected to Hematoxylin-Eosin (H&E) staining for the observation of tissue morphology. The stained tissue sections were visualized and analyzed utilizing a binocular Olympus CX43 light microscope (Olympus Inc., Tokyo, Japan). They were subsequently captured using an EP50 digital camera.

Statistical Analysis

Statistical analysis of the dataset generated in this investigation was conducted utilizing IBM SPSS Statistics for Windows, Version 26.0 (IBM Corp., Armonk, NY, USA). Shapiro-Wilk and Kolmogorov-Smirnov normality tests and QQ plots were applied to determine the distributional properties of continuous variables. When the necessary assumptions for the parametric test were met, intergroup differences were assessed through a one-way analysis of variance (ANOVA). When significant differences were identified, subsequent pairwise comparisons were conducted using the Tukey post-hoc test. In the statistical analysis, the value ($p<0.05$) was considered significant.

RESULTS

Identification of creatinine and urea concentrations in OXI and CRV groups

To evaluate renal function, serum concentrations of urea and creatinine were quantified. These values are known as key biochemical indicators of kidney health. A significant increase in these parameters was observed in the OXI group compared to the control group ($p<0.05$). Rats that received CRV therapy had much lower concentrations of serum creatinine and urea compared to rats that only received OXI ($p<0.05$). However, CRV only slightly changed creatinine, a marker of kidney function, as seen in Figure 1.

Identification of antioxidant enzymes levels in the OXI and CRV groups

Kidney SOD, CAT and GPx activities were measured to evaluate oxidative stress. The effects of OXI and CRV on antioxidant enzyme activity are shown in Figure 2. CRV administration resulted in increased SOD, CAT, and GPx activities and increased GSH levels, while OXI treatment resulted in a reduction in these parameters. The status of lipid peroxidation, as indicated by the malondialdehyde (MDA) concentration, was measured, and an elevated level of MDA was detected in the OXI-treated group, compared to all the other experimental groups (Figure 2).

Identification of mRNA transcription levels in the OXI and CRV groups

The effects of OXI and CRV on mRNA transcription levels are shown in Figure 3. Transcriptional measures of pro-inflammatory mediators, including IL-1β and NF-κB, were assessed. OXI treatment resulted in a significant increase in NF-κB and IL-1β expression compared to the control group ($p<0.05$). However, CRV administration significantly attenuated the OXI-induced elevation in these proinflammatory markers ($p<0.05$, Figure 3).

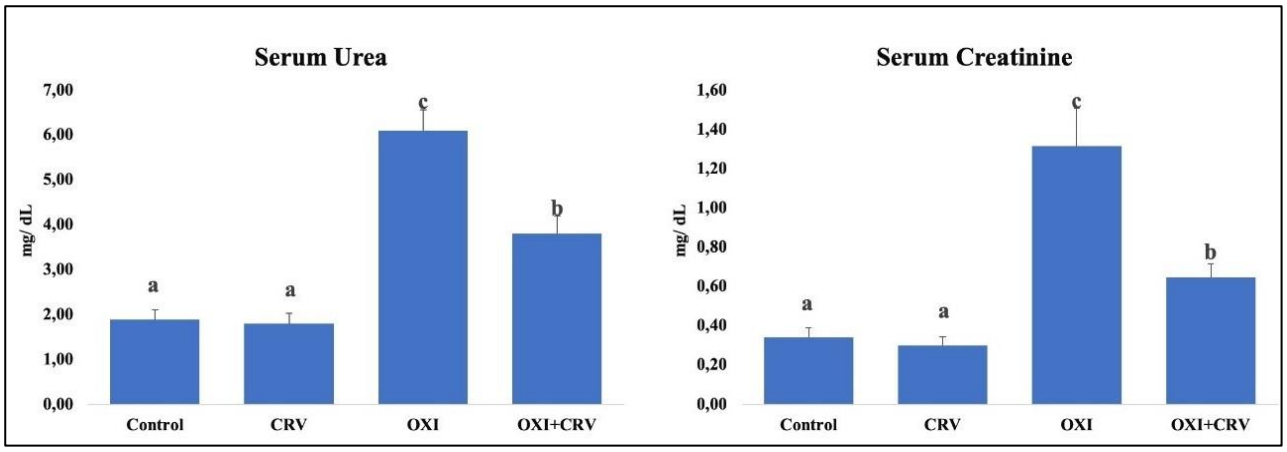

Figure 1: Effects of OXI and CRV on serum urea and serum creatinine levels. Values are given as mean±SD. Different letters indicate statistical difference: (a, b, c: p<0.05) (CRV: Carvacrol, OXI: Oxytetracycline).

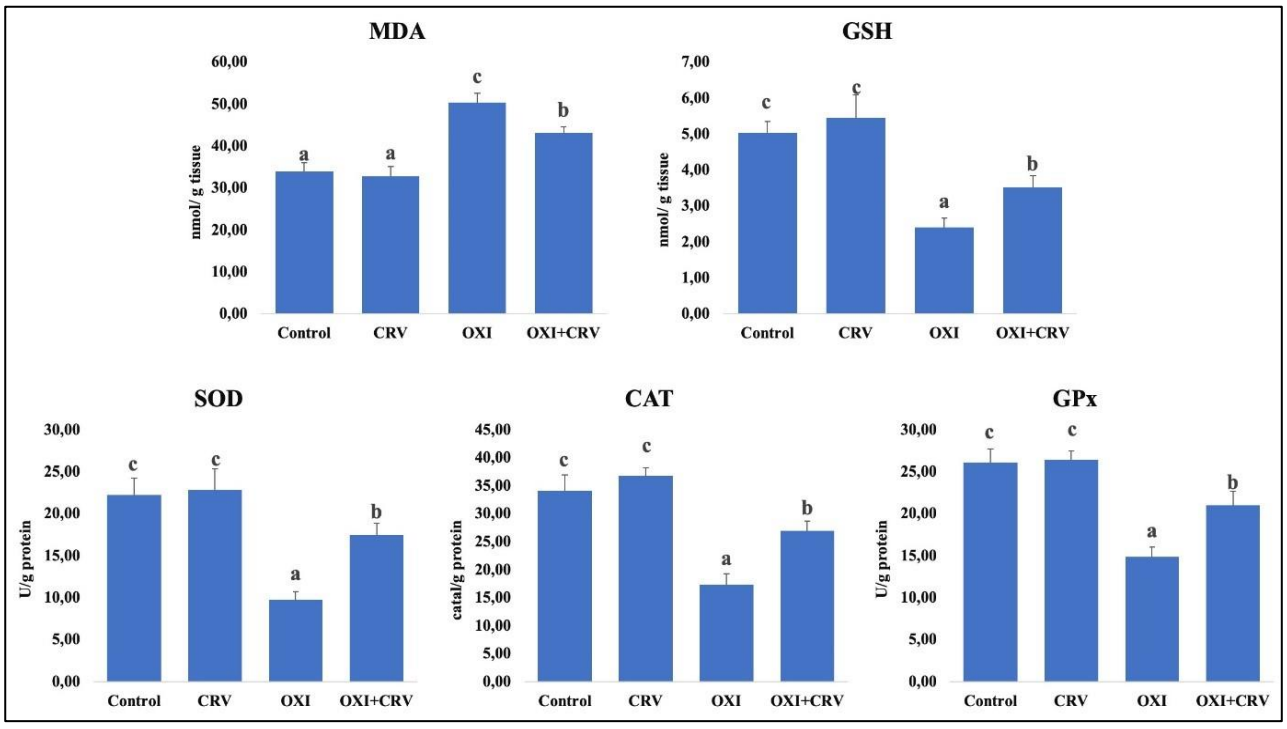

Figure 2: Effects of OXI and CRV on MDA and GSH levels and SOD, CAT, and GPx activities in rat kidney tissues. Values are given as mean±SD. Different letters indicate statistical difference: (a, b, c: p<0.05). (CRV: Carvacrol, OXI: Oxytetracycline, MDA: Malondialdehyde, GSH: Glutathione, SOD: Superoxide dismutase, CAT: Catalase, GPx: Glutathione peroxidase).

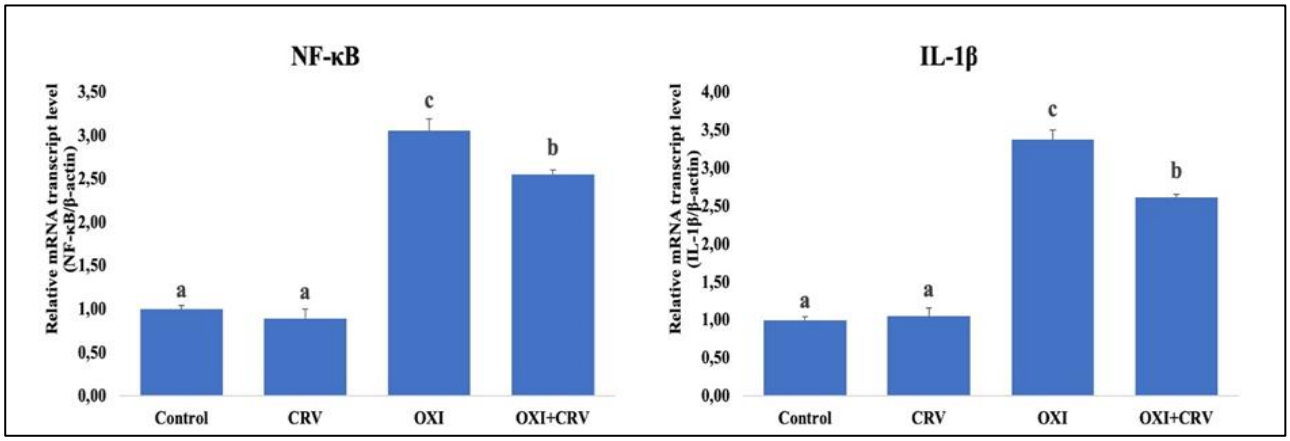

Figure 3: Effects of OXI and CRV on NF-κB and IL-1β (mRNA transcription levels) in rat kidney tissues. Values are given as mean±SD. Different letters indicate statistical difference: (a, b, c: p<0.05). (CRV: Carvacrol, OXI: Oxytetracycline, NF-κB: Nuclear factor kappa B, IL-1β: Interleukin 1β).

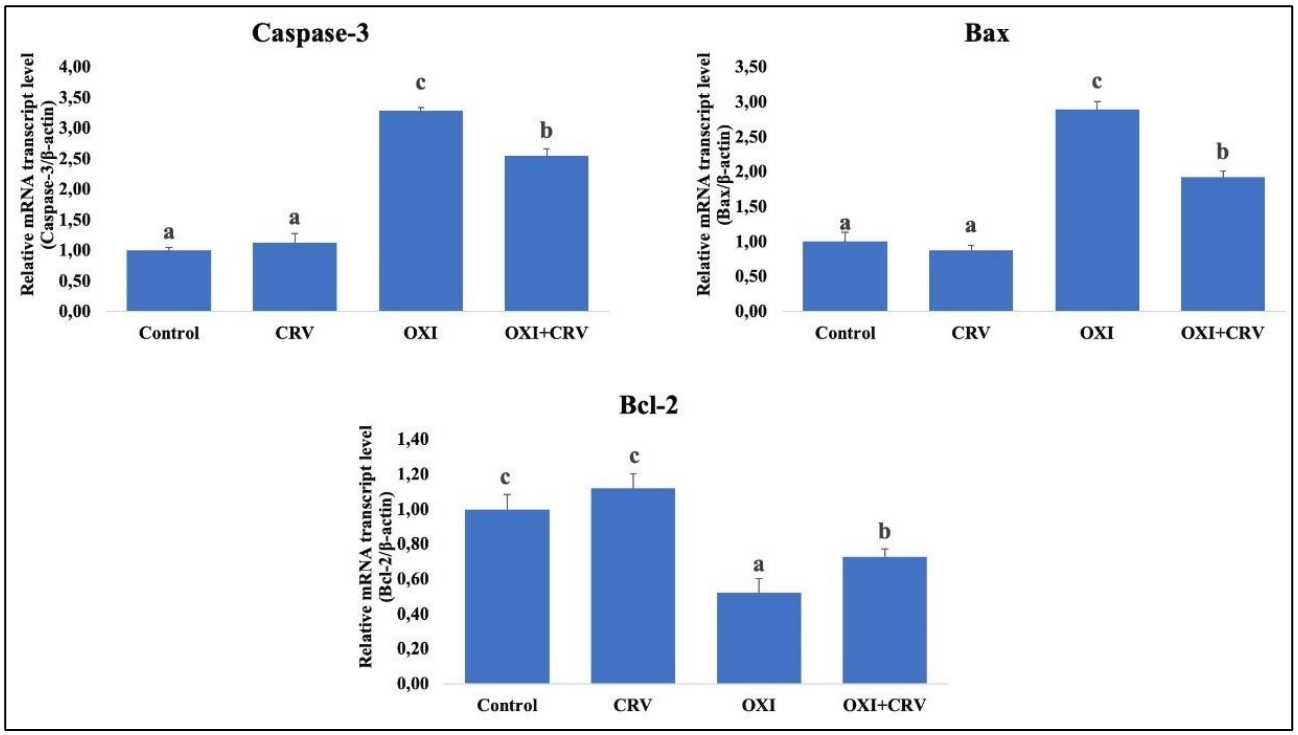

Figure 4: Effects of OXI and CRV on Caspase-3, Bax, and Bcl-2 (pro- and anti-apoptotic markers) in rat kidney tissues. Values are given as mean±SD. Different letters indicate statistical difference: (a, b, c: $p<0.05$). (CRV: Carvacrol, OXI: Oxytetracycline, Bcl-2: B-cell lymphoma-2).

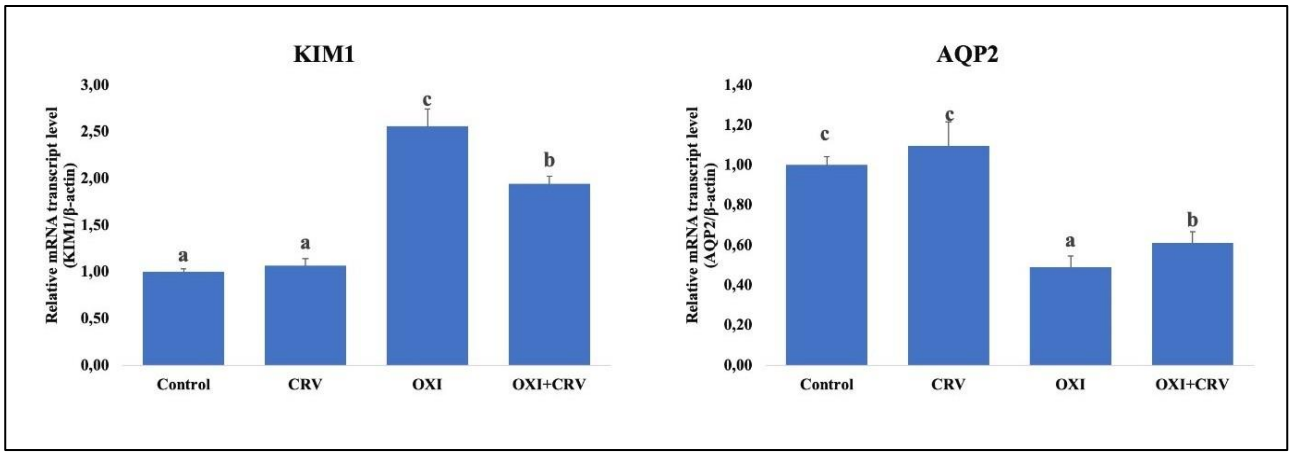

Figure 5: Effects of OXI and CRV on Kidney injury molecule-1 (KIM1) and AQP2 (mRNA transcription levels) in rat kidney tissues. Values are given as mean±SD. Different letters indicate statistical difference: (a, b, c: $p<0.05$). (CRV: Carvacrol, OXI: Oxytetracycline, KIM1: Kidney injury molecule-1, AQP2: Aquaporin-2).

Identification of apoptosis-related factors in the OXI and CRV groups

The effects of OXI and CRV on apoptosis-related factors are shown in Figure 4. As indicators of apoptosis, Caspase-3 and Bax activity were assessed. Pro- and anti-apoptotic indicators were assessed in relation to Bcl-2 levels. Animals given OXI had higher levels of Caspase-3 and Bax activity compared to the control group ($p<0.05$). Significantly reduced Bcl-2 levels were observed ($p<0.05$). Conversely, CRV administration dramatically increased Bcl-2 activity ($p<0.05$, Figure 4) and significantly decreased the higher levels of Caspase-3 and Bax ($p<0.05$) in the OXI-treated group.

Identification of nephrotoxicity biomarkers in the OXI and CRV groups

The effects of OXI and CRV on nephrotoxicity biomarkers are shown in Figure 5. Biomarkers of nephrotoxicity were found to be significantly lower in AQP-2 ($p<0.05$) and significantly higher in KIM-1 levels ($p<0.05$) in OXI-treated rats than in the control group. KIM-1 levels considerably decreased ($p<0.05$), and AQP-2 degree dramatically increased ($p<0.05$) during CRV treatment (Figure 5).

Light Microscopy Findings

Figure 6 shows the histopathological alterations in H&E-stained kidney tissue sections obtained from rats.

The results for the kidney samples in the CRV and control groups were comparable. The outcomes of the control, CRV, OXI, and OXI+CRV groups of kidney microscopic examinations are shown in Figure 6. Histological examination of kidney tissues in the control and CRV groups showed that the kidney bodies and tubular structures were of regular histological structure (Figures 6A, B). There was congestion in the glomerular capillaries and the vessels in the interstitial area in the OXI-

administered group. However, shedding and vacuolization in tubular epithelial cells, atrophy in the glomerular structure, dilatation in the Bowman's space, and inflammatory cell infiltration were noted (Figure 6 C). On the other hand, there was a significant improvement in kidney tissue in the group in which CRV was administered along with OXI. Congestion and bleeding decreased in both glomerular capillaries and interstitial vessels. Renal bodies and tubule structures were more normal (Figure 6 D).

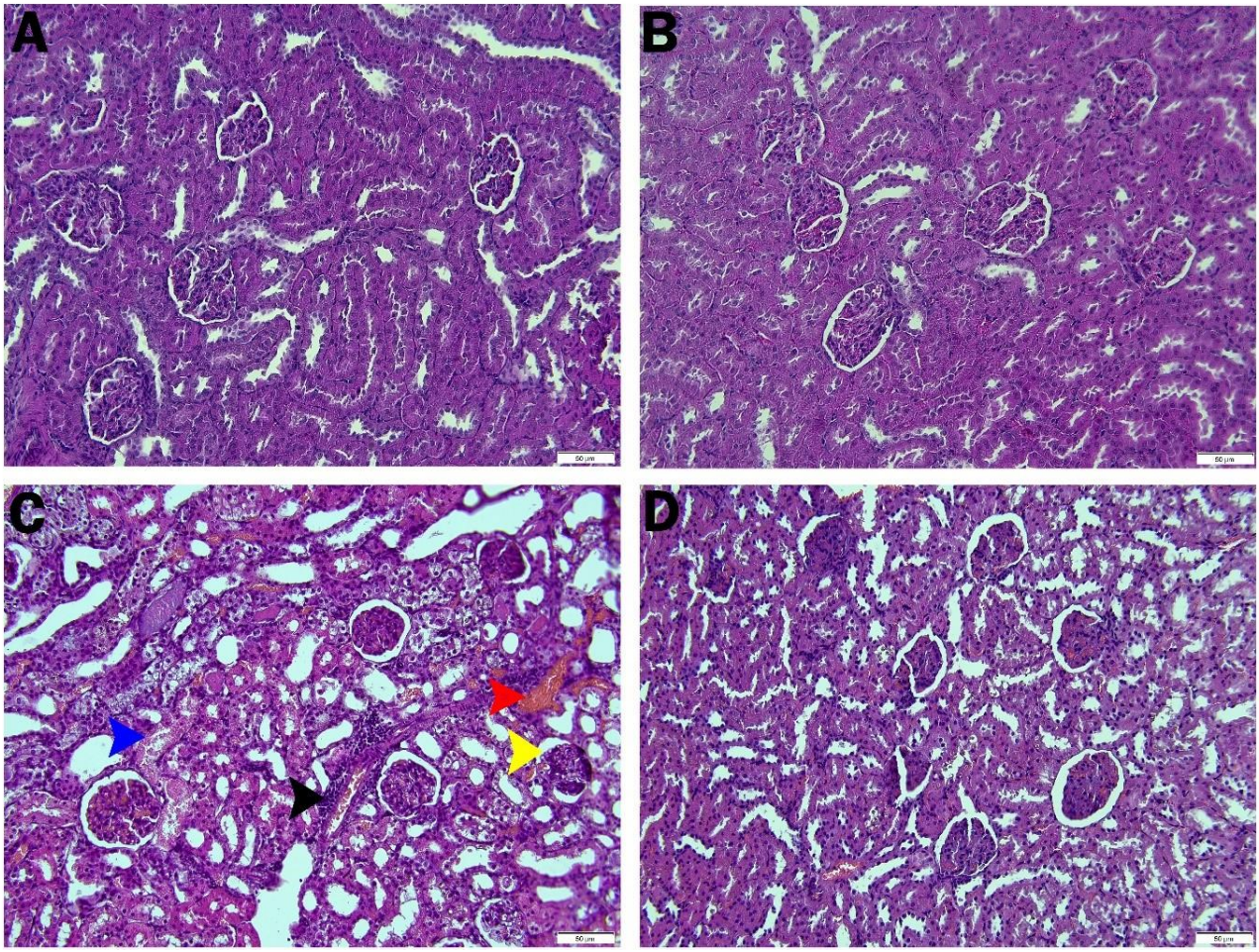

Figure 6: Photomicrographs of H&E-stained kidney sections. (H&E staining, 200x).

(A) control group, (B) CRV group, (C) OXI group, (D) OXI+CRV group. Red arrow: vascular congestion, yellow arrow: dilation in Bowman's space, black arrow: inflammatory cell infiltration, blue arrow: tubular epithelial cell loss.

DISCUSSION AND CONCLUSION

This study showed that CRV protects against kidney damage caused by OXI. The hypothesis that CRV may reduce the nephrotoxic effects of OXI was supported by its anti-inflammatory, interleukin-lowering, and antioxidant properties. OXI, a broad-spectrum antibiotic widely used in human and veterinary medicine, also has numerous side effects. High-dose OXI use without medical supervision has harmful effects on the kidneys and liver (Abdel-Daim and Ghazy 2015). The finding that OXI administration increased MDA levels and significantly inhibited the enzymatic antioxidants SOD, CAT, and GPx is consistent with EL-Akkad et al. (2022). Güvenç et al. (2019) reported in their research that CRV reduced MDA levels in kidney tissues. The results of this study revealed that OXI reduces renal function by causing histopathological changes in the glomerular capsule, accompanied by increased creatinine levels. Increased lipid peroxidation may deform membrane components, leading to changes in internal membrane properties such as enzyme activity and cell surface markers (Imbabi et al. 2024). The protective properties of CRV were confirmed by histological examination of the kidney. The OXI-treated group had higher concentrations of serum urea and creatinine than the control group. Rats that received CRV and OXI were shielded from this degradation. These findings also demonstrated the contribution of oral CRV administration to improving renal function. These results demonstrated a notable decline in urea and creatinine levels in rats treated with OXI+CRV, suggesting that CRV has an antioxidant effect as a free radical scavenger. Ahmadvand et al. (2016) reported a remarkable increase in urea and creatinine concentrations in rats treated with CRV for 12 days compared to the control group, showing a decrease in glomerular filtration in the kidneys. In the present study, high serum urea and creatinine levels resulting from OXI-induced kidney damage support the findings of previous studies (Ellero et al. 2020). Since lipids form the fundamental structure of cell membranes, increased ROS concentrations lead to the oxidative degradation of membrane lipids, a process known as lipid peroxidation (Şimşek et al. 2023). Serum MDA levels are used as a biomarker of lipid peroxidation (Yilgor and Demir 2024). ROS are neutralized by enzymatic antioxidants such as GPx, SOD, and CAT (Bhattacharyya et al. 2014). GSH, a non-enzymatic antioxidant, is a tripeptide compound that neutralizes free radicals and regenerates other antioxidants, maintaining the balance of oxidative stress in cells (Kurutas 2015).

Similar to our study, in the study conducted by Sharma et al. (2015), GSH reduction was observed in the kidneys of rats treated with OXI. Antioxidant defense systems in the body scavenge free radicals and protect against tissue damage (Akaras et al. 2023). In this study, antioxidant enzyme (SOD, CAT, and GPx) activities and non-enzymatic GSH levels decreased, while MDA levels increased in the OXI group. CRV administered in conjunction with OXI decreased these levels and also reduced the increased MDA levels. There are also some studies suggesting that CRV protects kidney health. CRV, with its antioxidant properties, protects kidney cells against free radical damage (Ram et al. 2022). Furthermore, thanks to its anti-inflammatory activities, CRV can alleviate renal inflammation and thus protect renal function (Riaz et al. 2023). Ram et al. (2022) demonstrated that CRV administration provided significant protection against experimentally induced renal injury in mice. Kidney damage has been correlated with increased levels of proinflammatory cytokines and the activation of systemic inflammation (Erdoğan et al. 2025). The pathophysiology of OXI-induced nephropathy is predicted to involve the release of proinflammatory cytokines and chemokines by macrophages, for instance, inducible nitric oxide synthase (iNOS), IL-1β, tumor necrosis factor alpha (TNF-α), macrophage migration inhibitory factor (MIF), NF-κB, and monocyte chemotactic protein-1 (MCP-1). Controlling the synthesis of proinflammatory cytokines that are useful in the inflammatory response is one of NF-κB's primary roles (Zhang et al. 2024). It has been demonstrated that oxidative stress activates the transcription factor NF-κB (Kankılıç et al. 2024). Tissue pathology is significantly influenced by inflammatory mediators including NF-κB and IL-1β (Gencer et al. 2025). Neutrophils, macrophages, monocytes, platelets, and mastocytes are inflammatory cells that are activated by these cytokines. These cells damage cells in a number of ways, such as by releasing ROS, causing lipid peroxidation in cell membranes, and oxidatively damaging proteins and DNA (Gür et al. 2022). It is known that DNA damage resulting from cancer treatment also activates NF-κB. For this reason, inhibiting NF-κB may be effective in reducing damage to the kidneys. Thus, inhibiting NF-κB may increase cellular protection against apoptosis. This study showed that the OXI-treated group resulted in higher levels of proinflammatory cytokines, especially NF-κB and IL-1β, in contrast to the control group. Additionally, higher KIM-1 and lower AQP-2 measures were detected in the OXI group in contrast with the control group. Conversely, the elevated KIM-1 levels were reduced, and the decreased AQP-2 levels increased in the OXI+CRV group compared to the control group. Ram et al. reported in 2022 that CRV administration significantly improved antioxidant proteins and kidney histological changes. They also reported that CRV lessened NF-κB (p65) phosphorylation and reduced IL-1β capacity. Consequently, CRV administration alleviates kidney fibrosis by targeting oxidative stress and inflammation (Ram et al. 2022). Additionally, Samarghandian et al. (2016) also reported renoprotective effects of CRV in rats exposed to oxidative stress. Apoptosis has an important role in maintaining homeostasis in the organism (Karaca et al. 2025). Caspases are members of the cysteine protease family and are key regulators of apoptosis, the tightly controlled cell death process crucial for the elimination of excess or unnecessary cells during development (Ozyigit et al. 2024). Execution caspases, including caspase-3, are triggered by initiator caspases and carry out most of the cellular destruction during apoptosis (Lestari et al. 2024). Doğu et al. (2022) reported that OXI not only reduces DNA damage but also reduces apoptosis. Overdosage of OXI without medical advice has harmful effects on the liver and kidney (Oda et al. 2018). Our study revealed increased apoptotic markers for Bax and Caspase-3 in the OXI group but diminished Bcl-2 levels. The opposite results were observed in the CRV+OXI group. Consequently, we concluded that OXI induces apoptosis.

In conclusion, CRV prevented OXI-induced kidney damage in rat kidney tissue. Furthermore, it inhibited lipid peroxidation by acting as an antioxidant against oxidative damage. Therefore, CRV can be considered an effective treatment method against nephrotoxicity by preventing OXI-induced oxidative stress in kidney tissues and the associated inflammation, apoptosis, and impairment of tissue integrity.

CONFLICTS OF INTEREST

The authors report no conflicts of interest.

AUTHOR CONTRIBUTIONS

Idea/Concept: FMK, HŞ, HY
Supervision/Consultancy: FMK, HŞ, HY
Data Collecting and/or Processing: HY, HŞ, OK, NA
Analysis and/or Interpretation: OK, NA, HŞ, HY
Writing the Article: HY, HŞ
Critical Review: FMK, HŞ, HY

REFERENCES

Abdel-Daim MM, Ghazy EW (2015). Effects of Nigella sativa oil and ascorbic acid against oxytetracycline-induced hepato-renal toxicity in rabbits. *Iran J Basic Med Sci,* 18(3), 221.

Aebi H (1984). Catalase in vitro. In: Methods Enzymol, Oxygen Radicals in Biological Systems 105, (pp 121-126) Academic Press, New York.

Ahmad A, Saeed M, Ansari IA (2021). Molecular insights on chemopreventive and anticancer potential of carvacrol: Implications from solid carcinomas. *J Food Biochem,* 45(12), e14010.

Ahmadvand H, Tavafi M, Asadollahi V et al. (2016). Protective effect of carvacrol on renal functional and histopathological changes in gentamicin-induced-nephrotoxicity in rats. *Z J Res Med Sci,* 18(4), e6446.

Akaras N, Gür C, Şimşek H, Tuncer SÇ (2023). Effects of quercetin on cypermethrin-ınduced stomach ınjury: the role of oxidative stress, ınflammation, and apoptosis. *GUJHS,* 12(2), 556-566.

Akcılar R, Akcılar A, Şimşek H et al. (2015). Hyperbaric oxygen treatment ameliorates lung injury in paraquat intoxicated rats. *Int J Clin Exp Pathol*, 8(10), 13034–13042.

Bansal A, Saleh-E-In MM, Kar P et al. (2022). Synthesis of carvacrol derivatives as potential new anticancer agent against lung cancer. *Molecules*, 27(14), 4597.

Bhattacharyya A, Chattopadhyay R, Mitra S, Crowe SE (2014). Oxidative stress: an essential factor in the pathogenesis of gastrointestinal mucosal diseases. *Physiol Rev*, 94(2), 329-354.

Bouhtit F, Najar M, Moussa Agha D (2021). New anti-leukemic effect of carvacrol and thymol combination through synergistic induction of different cell death pathways. *Molecules*, 26(2), 410.

Doğu Z, Şahinöz E, Aral F, Koyuncu I, Eğri K (2022). Effects of oxytetracycline supplementation on cryopreserved sperm quality of shabout (*Barbus grypus* Heckel 1843): Apoptotic analysis, DNA damage and oxidative stress. *Appl Ecol Environ Res*, 20(3), 2733-2746.

EL-Akkad NM, Sarwat MI, Ali NE, Sawy MS (2022). Protective effect of Nigella sativa seed extracts against oxytetracycline induced liver and kidney injuries in albino rats. *Al-Azhar J Agric Res,* 47(2), 186-197.

Ellero N, Freccero F, Lanci A et al. (2020). Rhabdomyolysis and acute renal failure associated with oxytetracycline administration in two neonatal foals affected by flexural limb deformity. *Vet Sci*, 7(4), 160.

Erdoğan E, Kandemir Ö, Akaras N, Şimşek H, Kandemir FM (2025). Protective and Preventive Role of Folic Acid Against Ivermectin-Induced Renal Toxicity. *FU Vet J Health Sci,* 39(2): 113-121.

Gencer S, Akaras N, Şimşek H (2025). The Protective Effects of Chrysin on Acrylamide-Induced Hepatotoxicity: Insights Into Oxidative Stress,

Inflammation, Apoptosis, Autophagy, and Histological Evaluation in Rats. *J Biochem Mol Toxicol*, 39(6), e70334.

Gibson BW (2005). The human mitochondrial proteome: oxidative stress, protein modifications and oxidative phosphorylation. *Int J Biochem Cell Biol,* 37(5), 927-934.

Gunes-Bayir A, Guler EM, Bilgin MG et al. (2022). Anti-inflammatory and antioxidant effects of carvacrol on N-methyl-N′-nitro-N-Nitrosoguanidine (MNNG) induced gastric carcinogenesis in Wistar rats. *Nutrients,* 14(14), 2848.

Gür C, Kandemir Ö, Kandemir FM (2022). Evaluation of the effects of chrysin on diclofenac-induced cardiotoxicity in rats by the markers of oxidative stress, endoplasmic reticulum stress and apoptosis. *Kocatepe Vet J,* 15(2), 151-160.

Güvenç M, Cellat M, Gökçek İ, Yavaş İ, Yurdagül Özsoy Ş (2019). Effects of thymol and carvacrol on sperm quality and oxidant/antioxidant balance in rats. *Arch Physiol Biochem,* 125(5), 396-403.

Imbabi TA, El-Sayed AIM, Radwan AA, Osman A, Abdel-Samad AM (2024). Prevention of aflatoxin B1 toxicity by pomegranate peel extract and its effects on growth, blood biochemical changes, oxidative stress and histopathological alterations. *J Anim Physiol Anim Nutr (Berl),* 108(1), 174-184.

Imran M, Aslam M, Alsagaby SA et al. (2022). Therapeutic application of carvacrol: A comprehensive review. *Food Sci. Nutr,* 10(11), 3544-3561.

Kankılıç NA, Küçükler S, Gür C et al. (2024). Naringin protects against paclitaxel-induced toxicity in rat testicular tissues by regulating genes in pro-inflammatory cytokines, oxidative stress, apoptosis, and JNK/MAPK signaling pathways. *J Biochem Mol Toxicol,* 38(7), e23751.

Karaca O, Akaras N, Şimşek H et al. (2025). Therapeutic potential of rosmarinic acid in tramadol-induced hepatorenal toxicity: Modulation of oxidative stress, inflammation, RAGE/NLRP3, ER stress, apoptosis, and tissue functions parameters. *Food Chem Toxicol,* 197, 115275.

Kurutas EB (2015). The importance of antioxidants which play the role in cellular response against oxidative/nitrosative stress: current state. *Nutr J*, 15(1), 71.

Lawrence RA, Burk RF (1976). Glutathione peroxidase activity in selenium-deficient rat liver. *Biochem Biophys Res Commun*, 71(4), 952-958.

Lestari B, Fukushima T, Utomo RY, Wahyuningsih MSH (2024). Apoptotic and non-apoptotic roles of caspases in placenta physiology and pathology. *Placenta*, 151, 37-47.

Livak KJ, Schmittgen TD (2001). Analysis of relative gene expression data using real-time quantitative PCR and the 2 (-Delta Delta C (T) Method. *Methods,* 25(4), 402–408.

Lowry OH, Rosebrough NJ, Farr AL, Randall RJ (1951). Protein measurement with the Folin phenol reagent. *J Biol Chem*, 193(1), 265–275.

Mączka W, Twardawska M, Grabarczyk M, Wińska K (2023). Carvacrol—A natural phenolic compound with antimicrobial properties. *Antibiotics,* 12(5), 824.

Marza AD, Murad HM, Ali MA, Faris JK, Khudhair AS (2020). Berberine effects on liver toxicity induced by oxytetracycline in albino rats. *Biochem Cell Arch*, 20(S2), 3411–3417.

Nostro A, Papalia T (2012). Antimicrobial activity of carvacrol: current progress and future prospectives. *Recent Pat Antiinfect Drug Discov*, 7(1), 28-35.

Oda SS, Waheeb RS, El-Maddawy ZK (2018). Potential efficacy of Coenzyme Q10 against oxytetracycline-induced hepatorenal and reproductive toxicity in male rats. *J Appl Pharm Sci,* 8(1), 098-107.

Ozyigit F, Deger AN, Kocak FE et al. (2024). Protective effects of hesperidin in gastric damage caused by experimental ischemia-reperfusion injury model in rats. *Acta Cir Bras*, 11:39: e391124.

Placer ZA, Cushman LL, Johnson BC. (1966). Estimation of product of lipid peroxidation (malonyl dialdehyde) in biochemical systems. *Anal Biochem*, 16(2), 359–364.

Ram C, Gairola S, Syed AM et al. (2022). Carvacrol preserves antioxidant status and attenuates kidney fibrosis via modulation of TGF-β1/Smad signaling and inflammation. *Food Func*, 13(20), 10587-10600.

Riaz M, Al Kury LT, Atzaz N et al. (2023). Carvacrol alleviates hyperuricemia-induced oxidative stress and inflammation by modulating the NLRP3/NF-κB pathwayt. *Drug Des Devel Ther*, 22(16), 1159-1170.

Samarghandian S, Farkhondeh T, Samini F, Borji A (2016). Protective effects of carvacrol against oxidative stress induced by chronic stress in rat's brain, liver, and kidney. *Biochem Res Int*, 2016(1), 2645237.

Sampaio LA, Pina LTS, Serafini MR, Tavares DDS, Guimarães AG (2021). Antitumor effects of carvacrol and thymol: a systematic review. *Front Pharmacol*, 7;12:702487.

Sathi-Devi L, Gigliobianco MR, Gabrielli S et al. (2025). Localized cancer treatment using thiol–ene hydrogels for dual drug delivery. *Biomacromolecules*, 26(5), 3234-3254.

Sedlak J, Lindsay RH (1968). Estimation of total, protein-bound, and nonprotein sulfhydryl groups in tissue with Ellman's reagent. *Anal Biochem*, 25(1), 192–205.

Sharma S, Singh, SP, Ahmad AH, Chaudhary GK. (2015). Acute toxicity study of oxytetracycline in rats. *J Vet Pharmacol Toxicol,* 14(1) 82-84.

Skakun NP, IIu Vysotskiĭ (1982). Effect of tetracycline antibiotics on lipid peroxidation. *Antibiotiki*, 27(9), 684-687.

Sun YI, Oberley LW, Li Y (1988). A simple method for clinical assay of superoxide dismutase. *Clin Chem,* 34(3), 497-500.

Şimşek H, Küçükler S, Gür C et al. (2023). Protective effects of zingerone against sodium arsenite-induced lung toxicity: A multi-biomarker approach. *Iran J Basic Med Sci*, 26(9), 1098.

Şimşek H, Gür C, Küçükler S (2024). Carvacrol reduces mercuric chloride-induced testicular toxicity by regulating oxidative stress, inflammation, apoptosis, autophagy, and histopathological changes. *Biol Trace Elem Res,* 202(10), 4605-4617.

Tomsuk Ö, Kuete V, Sivas H, Kürkçüoğlu M (2024). Effects of essential oil of Origanum onites and its major component carvacrol on the expression of toxicity pathway genes in HepG2 cells. *BMC Complement Med Ther*, 24(1), 265.

Yilgor A, Demi C (2024). Determination of oxidative stress level and some antioxidant activities in refractory epilepsy patients. *Sci Rep*, 14(1), 6688.

Yousef EH, El Gayar AM, Abo El-Magd NF (2025). Carvacrol potentiates immunity and sorafenib anti-cancer efficacy by targeting HIF-1α/STAT3/FGL1 pathway: in silico and in vivo study. *Naunyn Schmiedebergs Arch Pharmacol*, 398(4), 4335-4353.

Zhang C, Ma Y, Zhao Y et al. (2024). Systematic review of melatonin in cerebral ischemia-reperfusion injury: Critical role and therapeutic opportunities. *Front Pharmacol*, 15, 1356112.

Van Veterinary Journal

https://dergipark.org.tr/tr/pub/vanvetj

Cite this article as: **Çortu A, Ağaoğlu AR (2026).** Prevalence and Risk Factors of Complications in Canine Laparoscopic Ovariectomy and Ovariohysterectomy: A Meta-Analysis. *Van Vet J*, 37(1), 74-80. DOI: https://doi.org/10.36483/vanvetj.1823344

ISSN: 2149-3359 **Original Article** e-ISSN: 2149-8644

Prevalence and Risk Factors of Complications in Canine Laparoscopic Ovariectomy and Ovariohysterectomy: A Meta-Analysis

Atakan ÇORTU[1,*] Ali Reha AĞAOĞLU[1]

[1] *Burdur Mehmet Akif Ersoy University, Faculty of Veterinary Medicine, Department of Obstetrics and Gynaecology, 15000, Burdur, Türkiye*

Received: 13.11.2025 Accepted: 19.02.2026

ABSTRACT This meta-analysis investigated the pooled prevalence and risk factors of intra- and postoperative complications in dogs undergoing laparoscopic ovariectomy (LOVE) or laparoscopic ovariohysterectomy (LOVH). A comprehensive search of PubMed, Scopus, Web of Science, Science Direct, and Google Scholar was performed for studies published between January 2000 and October 2025. Eligible studies provided numerical data on intraoperative and/or postoperative complications and clearly reported the number of laparoscopic ports used. Forty-three studies comprising 45 analytical arms and 2.548 female dogs met the inclusion criteria. The pooled prevalence of total complications was 14.4% (95% CI 10.5–18.8) under the random-effects model, indicating high heterogeneity (I^2=87.1%). For LOVE, the pooled prevalence was 10.6% (95% CI 7.4–14.3), whereas for LOVH it was 31.6% (95% CI 21.3–42.9), both showing substantial heterogeneity (I^2>75%). The odds of complications were significantly lower for LOVE than for LOVH (OR=0.23, 95% CI 0.18–0.30, p<0.001), suggesting an approximately 4.3-fold higher risk during LOVH. When analysed by port configuration, the one-port approach was associated with a significantly higher complication risk than the two-port technique (OR=2.13, 95% CI 1.37–3.32, p<0.001), while no difference was found between one- and three-port procedures (OR=1.24, 95% CI 0.83–1.85, p=0.29). The two-port configuration showed the lowest odds of complications compared with the three-port approach (OR=0.58, 95% CI 0.44–0.77, p<0.001). In conclusion, LOVE was associated with a significantly lower prevalence of complications compared with LOVH. When analysed by port configuration, the two-port technique demonstrated a significantly lower odds of complications compared with the one- and three-port approaches. These findings indicate that both surgical procedure type and port number are important factors influencing complication risk in canine laparoscopic sterilization.

Keywords: *Complication, Dog, Meta-analysis, Laparoscopy, Ovariectomy, Ovariohysterectomy.*

ÖZ

Köpeklerde Laparoskopik Ovariektomi ve Ovariohisterektomi Sonrası Meydana Gelen Komplikasyonların Prevalansı ve Risk Faktörleri: Bir Meta-Analiz Çalışması

Bu meta-analizde, köpeklerde laparoskopik ovariektomi (LOVE) veya laparoskopik ovariohisterektomi (LOVH) uygulanan bilimsel çalışmalarda intraoperatif ve postoperatif komplikasyonların birleşik prevalansı ve risk faktörleri araştırılmıştır. Ocak 2000 ile Ekim 2025 tarihleri arasında yayımlanan çalışmalar için PubMed, Scopus, Web of Science, Science Direct ve Google Scholar veri tabanlarında kapsamlı bir tarama yapılmıştır. İntraoperatif ve/veya postoperatif komplikasyonlara ilişkin sayısal veriler ve kullanılan laparoskopik port sayısının açıkça bildirildiği çalışmalar araştırmaya dahil edilmiştir. Buna göre sunulan çalışma 43 çalışma, 45 analitik kol ve toplam 2.548 dişi köpeği kapsamıştır. Rastgele etkiler modeli altında toplam komplikasyonların birleşik prevalansı %14.4 (%95 GA %10.5-18.8) olarak hesaplanmış ve yüksek heterojenite (I^2=%87.1) gözlenmiştir. LOVE için birleşik prevalans %10.6 (%95 GA %7.4-14.3), LOVH için ise %31.6 (%95 GA %21.3–42.9) olarak bulunmuş, her iki analizde de belirgin heterojenite (I^2>%75) saptanmıştır. Komplikasyon olasılığı, LOVE'de LOVH'ye göre anlamlı derecede daha düşük bulunmuştur (OR=0.23, %95 GA 0.18-0.30, p<0.001). Buna göre LOVH sırasında yaklaşık 4.3 kat daha yüksek bir risk olduğu görülmektedir. Port konfigürasyonuna göre yapılan analizde, tek port yaklaşımı iki port tekniğine kıyasla anlamlı derecede daha yüksek komplikasyon riski ile ilişkili bulunurken (OR=2.13, %95 GA 1.37-3.32, p<0.001) tek port ile üç portlu yöntem arasında fark saptanmamıştır (OR=1.24, %95 GA 0.83-1.85, p=0.29). İki port konfigürasyonu, üç port yaklaşımına kıyasla en düşük komplikasyon olasılığını göstermiştir (OR=0.58, %95 GA 0.44-0.77, p<0.001). Sonuç olarak, LOVE prosedürü LOVH'ye kıyasla anlamlı derecede daha düşük komplikasyon prevalansı ile ilişkilidir. Port konfigürasyonuna göre yapılan analizde, iki port tekniğinin tek ve üç portlu yaklaşımlara kıyasla komplikasyon olasılığının anlamlı derecede daha düşük olduğu gösterilmiştir. Bu bulgular, köpeklerde laparoskopik sterilizasyon sırasında cerrahi prosedür tipi ve kullanılan port sayısının komplikasyon riski üzerinde belirleyici faktörler olduğunu ortaya koymaktadır.

Anahtar Kelimeler: *Komplikasyon, Köpek, Laparoskopi, Meta-analiz, Ovariektomi, Ovariohisterektomi.*

✉ *Corresponding author: atakancortu@mehmetakif.edu.tr

INTRODUCTION

In female dogs, surgical sterilization is one of the most frequently performed elective procedures, generally achieved by either ovariohysterectomy (OVH) or ovariectomy (OVE) (Reichler 2009; Sendag et al. 2025). Although these surgeries are considered routine, they can still induce postoperative complications and systemic inflammatory responses involving multiple organ systems (Siracusa et al. 2008). To minimize such risks, minimally invasive techniques have been developed, and laparoscopic surgery has become increasingly preferred over conventional open methods (Freeman et al. 2010). Laparoscopic ovariohysterectomy (LOVH) and laparoscopic ovariectomy (LOVE) have been associated with reduced tissue trauma, lower postoperative pain, and faster recovery compared with traditional celiotomy (Culp et al. 2009; Case et al. 2011). However, these techniques require specialized instrumentation and advanced surgical training, which may increase costs and limit widespread application (Culp et al. 2009). Laparoscopic sterilization can be performed using one, two, or three ports depending on the surgical technique and available equipment. Operative duration, complication rate, and postoperative pain may vary according to the number of ports used (Buote and Fransson 2022). Although the three-port approach has traditionally been the standard, two- and single-port techniques have recently gained attention for their potential to reduce surgical stress and improve cosmetic outcomes (Lacitignola et al. 2021; Buote 2022). However, the existing literature provides inconsistent findings regarding the impact of port number on complication rates. Therefore, this meta-analysis aimed to quantitatively assess intra- and postoperative complication risks associated with LOVE and LOVH in female dogs, comparing outcomes among one-, two-, and three-port techniques.

MATERIAL AND METHODS

Literature Search and Study Selection

This systematic review and meta-analysis was conducted according to the Preferred Reporting Items for Systematic Reviews and Meta-Analyses (PRISMA) guidelines (Moher et al. 2009). A comprehensive electronic search was performed in PubMed, Scopus, Web of Science, Science Direct, and Google Scholar for studies published between January 2000 and October 2025. "A combination of the following search terms was used: ("laparoscopy" or "laparoscopic" or "minimally invasive") and ("ovariohysterectomy" or "ovariectomy" or "spay" or "sterilization") and ("dog" or "bitch" or "canine"). Reference lists of relevant reviews and primary articles were also manually screened to identify additional eligible studies.

Inclusion and Exclusion Criteria

Studies were included if they (i) reported intraoperative and/or postoperative complications associated with LOVE or LOVH in dogs, (ii) provided numerical data on the number of operated animals and complications or adverse events, and (iii) clearly stated the number of laparoscopic ports used (single, dual, or triple). Studies were excluded if they (i) focused on ovarian remnant syndrome, hybrid or Natural Orifice Transluminal Endoscopic Surgery (NOTES) techniques, or combined surgeries, (ii) involved cadaveric or simulation models, or (iii) included fewer than ten animals.

Data Extraction and Complication Classification

From each eligible study, the following information was extracted: author and year of publication, procedure type (LOVE or LOVH), number of operated animals, number of ports, and counts of intraoperative and postoperative complications or adverse events. Complications were categorized as intraoperative (events occurring during surgery, such as splenic puncture, pedicle hemorrhage, or conversion to laparotomy) and postoperative (events occurring after surgery, including wound infection, seroma, hernia, or systemic signs such as vomiting or fever). For each analytical arm, the absolute numbers of intraoperative and postoperative complications were recorded, and the total complication rate (n, %) was calculated relative to the total number of operated animals.

Statistical Analysis

Each analytical arm was treated as an independent observational unit. Proportions were logit-transformed using a 0.5 continuity correction to stabilize variance. Pooled prevalence estimates were calculated using both the fixed-effects (inverse-variance) and DerSimonian–Laird random-effects models (DerSimonian and Laird 2015). Subgroup meta-analyses were conducted separately for procedure type and port number. Between-study heterogeneity was assessed using Cochran's Q statistic to quantify inconsistency among studies, its associated p-value, and Higgins' I^2 index with 95% confidence intervals (CIs) to quantify the degree of inconsistency. Egger's regression test (Egger et al. 1997) was applied to evaluate potential publication bias. In addition, odds ratio (OR) analyses were performed to compare the likelihood of complication events between laparoscopic techniques (LOVE vs. LOVH) and across all procedures according to port number (one-, two-, and three-port configurations combined). The analyses were based on the total numbers of complication and non-complication events, as multiple complications could occur in the same animal; thus, the OR reflects the odds of complication events rather than animals. All analyses were performed using MedCalc version 20.110 (MedCalc Software Ltd., Ostend, Belgium).

RESULTS

A total of 43 studies comprising 45 analytical arms and 2.548 female dogs undergoing laparoscopic sterilization were included in the quantitative synthesis (Figure 1). Across all study arms, 299 intraoperative or postoperative complications were reported (Table 1). The pooled prevalence of total complications (minor+major combined) was 9.95% (95% CI 8.82–11.16) under the fixed-effects model and 14.41% (95% CI 10.52–18.80) under the random-effects model. A high level of heterogeneity was observed (Q=341.0, df=44, p< 0.0001; I^2=87.13%, 95% CI 83.65–89.86).

Table 1: Summary of included studies reporting intraoperative and postoperative complications in laparoscopic ovariectomy (LOVE) and laparoscopic ovariohysterectomy (LOVH) in dogs.

No	Author and Year	Proc.	n	Ports	Intraop. Comp. (n)	Postop. Comp. (n)	Total Comp. (n, %)
1	Arntz 2019	LOVE	202	2	-	4	4 (%2)
2	Bianchi et al. 2021	LOVE	30	2	4	-	4 (13.3%)
3	Bydzovsky et al. 2019	LOVH	41	1	-	12	12 (29.3%)
4	Charlesworth and Sanchez 2019	LOVE	154	3	-	22	22 (14.3%)
5	Coutinho et al. 2018	LOVE	12	1	2	-	2 (16.7%)
6	Costa et al. 2025	LOVE	30	3	-	-	- (0%)
7	Culp et al. 2009	LOVE	10	2	3	-	3 (30%)
8	Davidson et al. 2003	LOVH	16	3	7	5	12 (75%)
9	Degani et al. 2023	LOVE	24	2	1	-	1 (4.2%)
10	Delaune et al. 2020	LOVE	30	2	6	-	6 (20%)
11	Devitt et al. 2005	LOVH	10	2	-	-	- (0%)
12	Dupré et al. 2009	LOVE	22	2	2	-	2 (9%)
			20	1	2	-	2 (10%)
13	Dutta et al. 2010	LOVE	20	3	3	-	3 (15.0%)
		LOVH	40		15	-	15 (37.5%)
14	Driessen et al. 2023	LOVE	21	3	3	0	3 (14.28%)
15	Espadas-González et al. 2022	LOVE	52	3	-	-	- (0%)
16	Espadas-González et al. 2023	LOVE	25	3	-	-	- (0%)
17	Forbes and Monnet 2023	LOVE	10	1	-	-	- (0%)
18	Fuertes-Recuero et al. 2024	LOVE	13	3	1	-	1 (7.69)
19	Freeman et al. 2010	LOVE	10	2	-	-	- (0%)
20	Guadalupi et al. 2025	LOVE	36	2	9	-	9 (25%)
21	Granados et al. 2017	LOVE	60	2	-	1	1 (1.66%)
22	Heblinski and Brückner 2018	LOVH	12	2	5	-	5 (41.7%)
23	Manassero et al. 2012	LOVE	40	1	5	-	5 (12.5%)
24	Martin et al. 2021	LOVE	18	3	8	-	8 (44.4%)
25	Matsunami 2022	LOVH	147	3	8	24	32 (21.8%)
26	Mayhew and Brown 2007	LOVH	30	3	16	-	16 (53.3%)
27	Moxon et al. 2025	LOVE	213	2	3	-	3 (1.4%)
28	Nylund et al. 2017	LOVE	161	2	24	-	24 (14.9%)
29	Öhlund et al. 2011	LOVE	10	3	1	-	1 (10.0%)
30	Paolini et al. 2022	LOVE	20	3	-	-	- (0%)
31	Pope and Knowles 2014	LOVE	618	3	13	12	25 (4.0%)
32	Romero et al. 2020	LOVE	16	2	-	1	1 (6.25%)
33	Runge and Mayhew 2013	LOVE	18	1	1	-	1 (5.6%)
34	Runge et al. 2014	LOVE	27	1	2	-	2 (7.4%)
35	Ruiz et al. 2008	LOVH	20	3	3	1	4 (20%)
36	Silva et al. 2015	LOVH	13	1	2	-	2 (15.4%)
37	Spillebeen et al. 2016	LOVE	22	3	4	-	4 (18.2%)
38	Tavares et al. 2023	LOVE	20	3	-	-	- (0%)
39	Tez et al. 2023	LOVE	46	2	9	-	9 (19.6%)
40	Tiosso et al. 2025	LOVH	26	1	7	-	7 (26.9%)
41	Van Goethem et al. 2012	LOVE	40	3	10	4	14 (14.3%)
42	Van Goethem et al. 2003	LOVE	103	3	11	12	23 (22.3%)
43	Van Nimwegen and Kirpensteijn 2007	LOVE	40	3	11	-	11 (27.5%)
TOTAL			2.548		201	98	299 (%11.8)

Comp.: Complication; Intraop.: Intraoperative; Postop.: Postoperative; Proc.: Procedure.

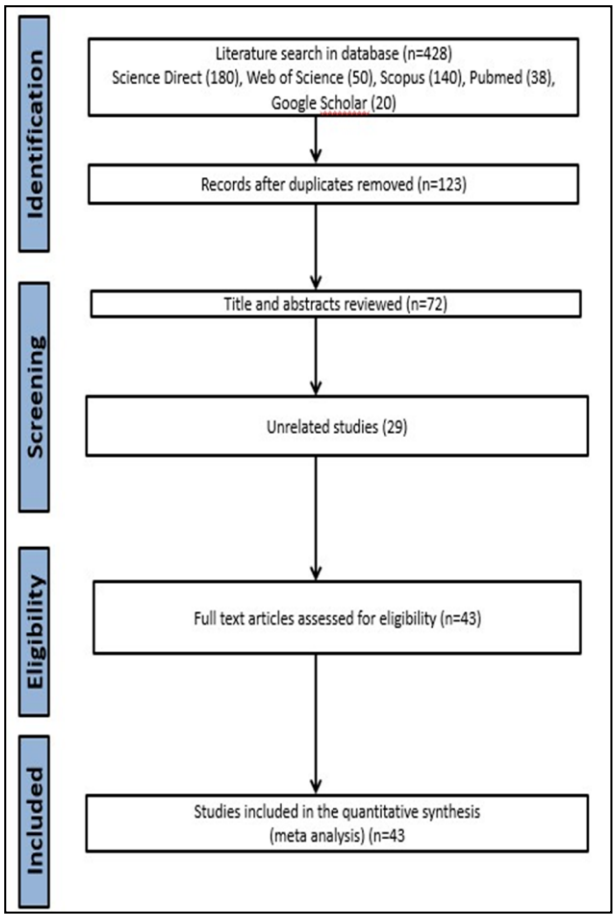

Figure 1: PRISMA flow diagram summarizing the identification, screening, eligibility, and inclusion of studies in the systematic review and meta-analysis of intra- and postoperative complications following LOVE and LOVH in female dogs.

For LOVE, the pooled prevalence of total complications was 7.63% (95% CI 6.56–8.81) under the fixed-effects model and 10.60% (95% CI 7.36–14.34) under the random-effects model, showing significant heterogeneity (Q=197.52, df=34, p<0.001; I^2=82.79%). For LOVH, the corresponding pooled prevalence was 29.22 % (95% CI 24.61–34.18) under the fixed-effects model and 31.60% (95% CI 21.31–42.89) under the random-effects model, also indicating high heterogeneity (Q=37.82, df=9, p<0.0001; I^2=76.21%). An odds ratio analysis comparing LOVE and LOVH showed that 194 complication events occurred in 2.193 procedures for LOVE and 105 in 355 procedures for LOVH. The odds of complications were significantly lower for LOVE than for LOVH (OR=0.23, 95% CI 0.18–0.30, p<0.001), indicating that complication events were approximately 4.3 times more likely during LOVH.

A total of 2.548 laparoscopic sterilization procedures were evaluated, comprising 207 one-port, 882 two-port, and 1.459 three-port surgeries. The numbers of reported complication events were 33, 72, and 194, respectively. One-port configuration was associated with a significantly higher likelihood of complication events compared with the two-port technique (OR=2.13, 95% CI 1.37–3.32, p<0.001). No significant difference was observed between the one-port and three-port approaches (OR = 1.24, 95% CI 0.83–1.85, p=0.29). In contrast, the two-port configuration showed a significantly lower odds of complications compared with the three-port technique (OR=0.58, 95% CI 0.44–0.77, p<0.001). The pooled estimates of intraoperative, postoperative, and total complications, stratified by surgical procedure (LOVE vs LOVH), are summarized in Figure 2, which illustrates individual study proportions and pooled prevalence under both fixed- and random-effects models.

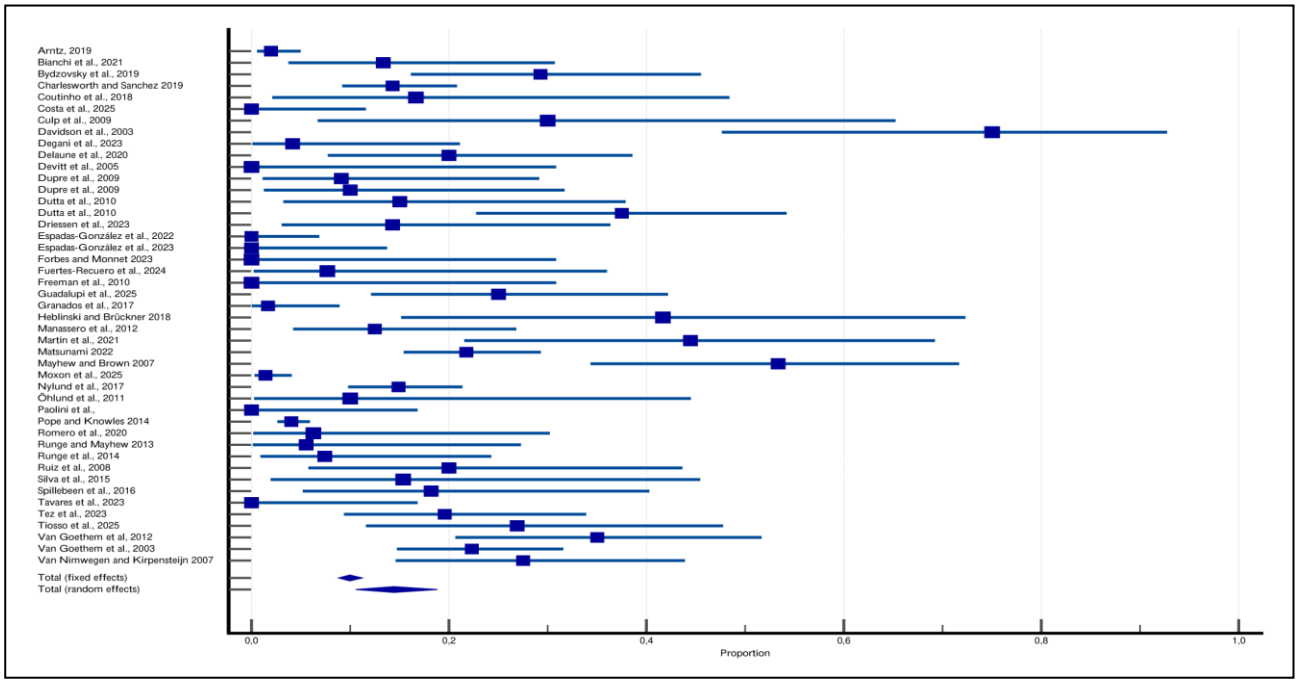

Figure 2: Forest plot illustrating the pooled prevalence of intraoperative or postoperative complications in dogs undergoing laparoscopic ovariectomy (LOVE) or ovariohysterectomy (LOVH). Each horizontal line represents an individual study with its corresponding 95% confidence interval, while the size of the blue square indicates the study weight. The diamond shapes denote the overall pooled estimates under fixed- and random-effects models.

DISCUSSION AND CONCLUSION

The most prominent finding of this meta-analysis was that LOVH in dogs carried a significantly higher complication risk compared with LOVE. This difference appears to arise primarily from the greater anatomical complexity, longer operative duration, and increased tissue manipulation inherent to LOVH. Ovariectomy confines surgical dissection to the ovarian pedicles and suspensory ligaments, while LOVH extends caudally to include the uterine body, necessitating traction, sealing, and transection of more vascular structures (Davidson et al. 2004; Freeman et al. 2010). These additional manipulations heighten the likelihood of hemorrhage, uterine tearing, or inadvertent visceral contact (Mayhew and Brown 2007; Corriveau et al. 2017). Moreover, the prolonged pneumoperitoneum and extended anesthetic duration required for LOVH may exacerbate physiological stress responses and impair postoperative recovery (Siracusa et al. 2008). Collectively, these factors explain the approximately fourfold higher complication risk observed with LOVH compared to LOVE, thereby supporting laparoscopic ovariectomy as the preferred technique for routine sterilization in bitches.

The technical simplicity of LOVE likely contributes to its superior safety profile. Because only ovarian vasculature requires sealing, the operative field remains limited and easily visualized. This simplicity reduces dependence on complex energy devices and advanced triangulation, resulting in shorter learning curves and more consistent outcomes (Culp et al. 2009; Runge and Mayhew 2013). In contrast, LOVH involves greater instrument coordination and tension on deep pelvic structures, which can challenge even experienced surgeons. Minor deviations in dissection angle or energy application may lead to incomplete coagulation or localized hemorrhage (Van Goethem et al. 2003; Ohlund et al. 2011). Indeed, multiple studies have demonstrated that complication frequency strongly correlates with surgeon experience, particularly for multi-step laparoscopic procedures (Pope and Knowles 2014; Runge et al. 2014; Nylund et al. 2017). As proficiency increases, complication rates decline sharply-emphasizing the importance of structured surgical training and mentorship in veterinary laparoscopy (Van Goethem et al. 2012).

The association between port configuration and complication risk also has clear mechanical and ergonomic explanations. Single-port approaches, while cosmetically advantageous, impose significant technical limitations: all instruments share a single access axis, leading to instrument collision, reduced triangulation, and compromised depth perception (Manassero et al. 2012; Lacitignola et al. 2021). These ergonomic constraints can cause excessive tissue traction, increased torque on the abdominal wall, and suboptimal angles during sealing, which may predispose to splenic punctures or pedicle slippage (Dupre et al. 2009; Bydzovsky et al. 2019). Dual-port configurations, in contrast, restore partial triangulation and permit more controlled manipulation, thereby minimizing iatrogenic trauma (Buote and Fransson 2022). The slightly higher complication tendency observed with triple-port techniques may reflect their preferential use in complex or pathological cases requiring extensive dissection (Corriveau et al. 2017; Degani et al. 2023). Furthermore, each additional trocar insertion increases the risk of bleeding, emphysema, or local pain (Freeman et al. 2010).

Obesity, high body weight, or abundant ovarian and uterine fat complicate tissue visualization and increase the difficulty of proper pedicle sealing (Runge and Mayhew 2013; Coutinho et al. 2018). In addition, high insufflation pressures and extended operative times can transiently impair venous return and splanchnic perfusion, thereby increasing postoperative discomfort or ileus (Siracusa et al. 2008). Variability in anesthetic and analgesic protocols may also influence complication recording; inadequate postoperative analgesia could result in over-reporting of pain-related complications, while under-detection may occur in heavily sedated patients (Degani et al. 2023). Such methodological discrepancies partly explain the high heterogeneity detected among studies. The considerable heterogeneity identified in this analysis reflects the multifactorial nature of laparoscopic outcomes in clinical populations. Variations in breed, age, reproductive status, and surgeon proficiency contribute substantially to this variability (Runge and Mayhew 2013; Charlesworth and Sanchez 2019). Furthermore, inconsistency in how complications are defined across studies, ranging from the inclusion of minor transient findings such as mild bleeding or emphysema (Case et al. 2011; Lacitignola et al. 2021) to the reporting of only major adverse events requiring intervention (Corriveau et al. 2017), hampers direct comparison.

Potential publication bias cannot be excluded, as smaller studies reporting low complication rates may be underrepresented (Egger et al. 1997; Moher et al. 2009). Early studies often prioritized demonstrating technical feasibility and innovation over comprehensive outcome reporting (Freeman et al. 2010). Future research should therefore emphasize prospective, multicenter designs with transparent and uniform complication documentation. Standardization of perioperative variables, combined with adequate sample sizes and detailed follow-up, will enable more accurate risk stratification and refinement of laparoscopic techniques in canine sterilization.

Several limitations of the present meta-analysis should be acknowledged. Substantial heterogeneity among the included studies reflects considerable variation in design, case selection, and perioperative management. Most data originated from retrospective or non-randomized clinical reports, increasing susceptibility to selection and reporting bias. Definitions of intraoperative and postoperative complications were inconsistent across studies, with some including minor events such as splenic puncture or emphysema and others reporting only major complications requiring intervention. This lack of standardization may have influenced pooled estimates and led to inaccurate reflections of true complication rates. Limited reporting of patient-related variables, anesthetic protocols, and surgical parameters also prevented adjustment for potential confounders. Because most studies were conducted in referral or academic centers, publication bias toward technically successful outcomes cannot be excluded. Furthermore, the present analysis was based on the total number of reported complication events rather than the number of affected animals, as multiple complications could occur in the same dog. This approach may have slightly overestimated the true incidence of complications at the individual level. Future prospective, multicenter investigations with standardized definitions and uniform reporting are needed to validate these findings and strengthen evidence-based recommendations for laparoscopic sterilization in dogs.

In conclusion, this systematic review and meta-analysis provides a comprehensive evaluation of intra- and

postoperative complications in canine laparoscopic sterilization. The pooled evidence shows that LOVE carries a substantially lower risk of complications than LOVH, likely due to the reduced tissue manipulation and shorter operative time. Among port configurations, the dual-port approach offers the best balance between minimal invasiveness, stability, and safety, while single-port techniques, although cosmetically advantageous, remain technically demanding and more prone to error. These results support LOVE as the preferred method for sterilization in healthy bitches. Standardized complication reporting, objective outcome assessment, and structured surgeon training are essential to enhance procedural consistency and patient safety.

CONFLICTS OF INTEREST

The authors report no conflicts of interest.

ACKNOWLEDGMENT

The authors would like to thank all researchers whose studies were included in this meta-analysis.

AUTHOR CONTRIBUTIONS

Idea/Concept: AÇ, ARA
Supervision/Consultancy: AÇ, ARA
Data Collection and/or Processing: AÇ, ARA
Analysis and/or Interpretation: AÇ, ARA
Writing the Article: AÇ, ARA
Critical Review: AÇ, ARA

REFERENCES

Arntz GJHM (2019). Transvaginal laparoscopic ovariectomy in 60 dogs: description of the technique and comparison with 2-portal-access laparoscopic ovariectomy. *Vet Surg,* 48(5), 726-734.

Bianchi A, Collivignarelli F, Vignoli M et al. (2021). A comparison of times taken for the placement of the first portal and complication rates between the Veress needle technique and the modified Hasson technique in canine ovariectomy laparoscopic surgery. *Animals (Basel),* 11 (10), 2936.

Bydzovsky ND, Bockstahler B, Dupré G (2019). Single-port laparoscopic-assisted ovariohysterectomy with a modified glove-port technique in dogs. *Vet Surg,* 48(5), 715-725.

Buote NJ (2022). Updates in laparoscopy. *Vet Clin North Am Small Anim Pract,* 52(2), 513-529.

Buote NJ, Fransson BA (2022). Small Animal Laparoscopy and Thoracoscopy. Fransson BA, Mayhew PD (Ed). Laparoscopic Ovariectomy, Ovariohysterectomy, and Hysterectomy (pp. 254-266). John Wiley & Sons, Hoboken.

Case JB, Marvel SJ, Boscan P, Monnet EL (2011). Surgical time and severity of postoperative pain in dogs undergoing laparoscopic ovariectomy with one, two, or three instrument cannulas. *J Am Vet Med Assoc,* 239(2), 203-208.

Charlesworth TM, Sanchez FT (2019). A comparison of the rates of postoperative complications between dogs undergoing laparoscopic and open ovariectomy. *Small Anim Pract,* 60(4), 218-222.

Corriveau KM, Giuffrida MA, Mayhew PD, Runge JJ (2017). Outcome of laparoscopic ovariectomy and laparoscopic-assisted ovariohysterectomy in dogs: 278 cases (2003-2013). *J Am Vet Med Assoc,* 251(4), 443-450.

Costa GL, Leonardi F, Licata P et al. (2025). Ovariectomy in Canine Surgical Medicine: A Comparative Analysis of Surgical Approaches and the Nociceptive, Inflammatory, and Oxidative Stress Responses. *Animals (Basel),* 15(16), 2336.

Coutinho AJ, Gasser B, Rodriguez MGK et al. (2018). Comparison between single port videolaparoscopy and miniceliotomy with snock hook ovariohysterectomy techniques in bitches. *Cienc Rural,* 48(10) e20180345.

Culp WT, Mayhew PD, Brown DC (2009). The effect of laparoscopic versus open ovariectomy on postsurgical activity in small dogs. *Vet Surg,* 38(7), 811-817.

Delaune T, Matres-Lorenzo L, Bernardé A, Bernard F (2021). Use of a T'LIFT transabdominal organ retraction device in two-portal laparoscopic ovariectomy in dogs. *Vet Surg,* 50(Suppl 1), O40-O48.

Davidson EB, Moll HD, Payton ME (2004). Comparison of laparoscopic ovariohysterectomy and ovariohysterectomy in dogs. *Vet Surg,* 33(1), 62-69.

Degani M, Di Franco C, Tayari H et al. (2023). Postoperative Analgesic Effect of Bilateral Quadratus Lumborum Block (QLB) for Canine Laparoscopic Ovariectomy: Comparison of Two Concentrations of Ropivacaine. *Animals (Basel),* 13(23), 3604.

Del Romero A, Cuervo B, Peláez P et al. (2020). Changes in Acute Phase Proteins in Bitches after Laparoscopic, Midline, and Flank Ovariectomy Using the Same Method for Hemostasis. *Animals (Basel),* 10(12), 2223.

DerSimonian R, Laird N (2015). Meta-analysis in clinical trials revisited. *Contemp Clin Trials,* 45(Pt A), 139-145.

Devitt CM, Cox RE, Hailey JJ (2005). Duration, complications, stress, and pain of open ovariohysterectomy versus a simple method of laparoscopic-assisted ovariohysterectomy in dogs. *J Am Vet Med Assoc,* 227(6), 921-927.

Driessen F, Marrero JD, Grinwis GCM, van Nimwegen SA (2023). Comparison of two advanced bipolar tissue sealer/dividers for laparoscopic ovariectomy in dogs: articulating enseal G2 versus Ligasure Maryland device. *Acta Vet Scand,* 65(1), 51.

Dupré G, Fiorbianco V, Skalicky M et al. (2009). Laparoscopic ovariectomy in dogs: comparison between single portal and two-portal access. *Vet Surg,* 38(7), 818-824.

Dutta A, Maiti S, Pillai AP, Kumar N (2010). Evaluation of different laparoscopic sterilization techniques in a canine birth control program. *Turk J Vet Anim Sci,* 34(4), 393-402.

Egger M, Davey Smith G, Schneider M, Minder C (1997). Bias in meta-analysis detected by a simple, graphical test. *BMJ,* 315 (7109), 629-634.

Espadas-González L, Usón-Casaús JM, Pastor-Sirvent N et al. (2022). Evaluation of the Two-Point Ultrasound-Guided Transversus Abdominis Plane Block for Laparoscopic Canine Ovariectomy. *Animals (Basel),* 12(24), 3556.

Espadas-González L, Usón-Casaús JM, Pastor-Sirvent N et al. (2023). Using complete blood count-derived inflammatory markers to compare postoperative inflammation in dogs undergoing open or laparoscopic ovariectomy. *Vet Rec,* 193(3), e2835.

Forbes JN, Monnet E (2023). A vessel sealing device and an ultrasonic dissector are equally effective and safe for single port laparoscopic ovariectomy in dogs. *Am J Vet Res,* 84(10), 1-6.

Freeman LJ, Rahmani EY, Al-Haddad M et al. (2010). Comparison of pain and postoperative stress in dogs undergoing natural orifice transluminal endoscopic surgery, laparoscopic, and open oophorectomy. *Gastrointest Endosc,* 72(2), 373-380.

Fuertes-Recuero M, de Segura IAG, López AS et al. (2024). Postoperative pain in dogs undergoing either laparoscopic or open ovariectomy. *Vet J,* 306, 106156.

Granados JR, Usón-Casaus J, Martínez JM, Sánchez-Margallo F, Pérez-Merino E (2017). Canine laparoscopic ovariectomy using two 3- and 5-mm portal sites: A prospective randomized clinical trial. *Can Vet J,* 58(6), 565-570.

Heblinski N, Bruckner M (2018). Vergleich zweier Instrumente zur Gefäßversiegelung bei der laparaskopisch-assistierten Ovariohysterektomie der Hündin. *Tierarztl Prax Ausg K Kleintiere Heimtiere,* 46(06), 363-369.

Lacitignola L, Guadalupi M, Massari F (2021). Single incision laparoscopic surgery (SILS) in small animals: a systematic review and meta-analysis of current veterinary literature. *Vet Sci,* 8(8), 144.

Manassero M, Leperlier D, Vallefuoco R, Viateau V (2012). Laparoscopic ovariectomy in dogs using a single-port multiple-access device. *Vet Rec,* 171(3), 69.

Martin KW, Karn K, Mickas MS, Fransson BA (2021). Comparison between intracorporeal and extracorporeal ligations in a laparoscopic ovariectomy model in dogs. *Vet Surg,* 50(3), 537-545.

Matsunami T (2022). Laparoscopic ovariohysterectomy for dogs under 5 kg body weight. *Vet Surg,* 51(Suppl 1), O92-O97.

Maurin MP, Mullins RA, Singh A, Mayhew PD (2020). A systematic review of complications related to laparoscopic and laparoscopic-assisted procedures in dogs. *Vet Surg,* 49(Suppl 1), O5-O14.

Mayhew PD, Brown DC (2007). Comparison of three techniques for ovarian pedicle hemostasis during laparoscopic-assisted ovariohysterectomy. *Vet Surg,* 36(6), 541-547.

Moher D, Liberati A, Tetzlaff J, Altman DG; PRISMA Group (2009). Preferred reporting items for systematic reviews and meta-analyses: the PRISMA statement. *PLoS Med,* 6(7), e1000097.

Moxon R, Yarwood E, Hawkins H, Came J, England GCW (2025). Laparoscopic ovariectomy provides favourable peri- and postoperative

outcomes compared with ovariohysterectomy via celiotomy in bitches. *J Small Anim Pract,* 10.1111/jsap.70013.

Nylund AM, Drury A, Weir H, Monnet E (2017). Rates of intraoperative complications and conversion to laparotomy during laparoscopic ovariectomy performed by veterinary students: 161 cases (2010-2014). *J Am Vet Med Assoc,* 251(1), 95-99.

Ohlund M, Hoglund O, Olsson U, Lagerstedt AS (2011). Laparoscopic ovariectomy in dogs: a comparison of the LigaSure™ and the SonoSurg™ systems. *J Small Anim Pract,* 52(6), 290-294.

Paolini A, Santoro F, Bianchi A et al. (2022). Use of transversus abdominis plane and intercostal blocks in bitches undergoing laparoscopic ovariectomy: a randomized controlled trial. *Vet Sci,* 9(11), 604.

Pope JF, Knowles TG (2014). Retrospective analysis of the learning curve associated with laparoscopic ovariectomy in dogs and associated perioperative complication rates. *Vet Surg,* 43(6), 668-677.

Reichler IM (2009). Gonadectomy in cats and dogs: a review of risks and benefits. *Reprod Domest Anim,* 44(Suppl 2), 29-35.

Ruiz IC, Acevedo CM, Rodriguez M (2008). Description and evaluation of a laparoscopic ovariohysterectomy technique in healthyfemale dogs. *Rev Colomb Cienc Pec,* 21, 546-558.

Runge JJ, Mayhew PD (2013). Evaluation of single port access gastropexy and ovariectomy using articulating instruments and angled telescopes in dogs. *Vet Surg,* 42(7), 807-813.

Runge JJ, Boston RC, Ross SB, Brown DC (2014). Evaluation of the learning curve for a board-certified veterinary surgeon performing laparoendoscopic single-site ovariectomy in dogs. *J Am Vet Med Assoc,* 245(7), 828-835.

Silva MAM, Toniollo GH, Flores FN et al. (2015). Surgical time and complications of total transvaginal (total-NOTES), single-port laparoscopic-assisted and conventional ovariohysterectomy in bitches. *Arq Bras Med Vet Zootec,* 67(3), 647-654.

Siracusa C, Manteca X, Cerón J et al. (2008). Perioperative stress response in dogs undergoing elective surgery: variations in behavioural, neuroendocrine, immune and acute phase responses. *Anim Welf,* 17(3), 259-273.

Spillebeen AL, Janssens SSDS, Thomas RE, Kirpensteijn J, van Nimwegen SA (2017). Cordless ultrasonic dissector versus advanced bipolar vessel sealing device for laparoscopic ovariectomy in dogs. *Vet Surg,* 46(4), 467-477.

Sendag S, Yildiz M, Conza T, Wehrend A (2025). Two-Portal Access Endoscopic Bilateral Ovariectomy in Bitches. *FU Vet J Health Sci,* 39(2), 85-89.

Tavares IT, Rivero R, Sales-Luís JP et al. (2023). Premedication with acetazolamide: Is its use for postoperative pain and stress control after laparoscopic ovariectomy in dogs ruled out?. *Vet Med Sci,* 9(3), 1114-1123.

Tez G, Kanca H, Ergul S (2023). Surgical Time for Laparoscopic Ovariectomy in Adult and Prepubertal Dogs. *Harran Univ Vet Fak Derg,* 12(2), 146-151.

Tiosso CF, Voorwald FA, Brun MV et al. (2025). Single-port video-assisted laparoscopic ovariohysterectomy using operative endoscope or SILS™ device in dogs. *Res Vet Sci,* 192, 105704.

Van Goethem BE, Rosenveldt KW, Kirpensteijn J (2003). Monopolar versus bipolar electrocoagulation in canine laparoscopic ovariectomy: a nonrandomized, prospective, clinical trial. *Vet Surg,* 32(5), 464-470.

Van Goethem B, van Nimwegen SA, Akkerdaas I, Murrell JC, Jolle K (2012). The effect of neuromuscular blockade on canine laparoscopic ovariectomy: a double-blinded, prospective clinical trial. *Vet Surg,* 41(3), 374-380.

Van Nimwegen SA, Kirpensteijn J (2007). Comparison of Nd: YAG surgical laser and Remorgida bipolar electrosurgery forceps for canine laparoscopic ovariectomy. *Vet Surg*, 36(6), 533-540.

Van Veterinary Journal

https://dergipark.org.tr/tr/pub/vanvetj

Cite this article as: **Okur DT, Bolat İ, Çiplak AY et al. (2026).** Corpus Luteum Presence as a Risk Factor for Endometrial Hyperplasia in Clinically Healthy Female Cats Undergoing Routine Ovariohysterectomy. *Van Vet J*, 37(1), 81-86. DOI: https://doi.org/10.36483/vanvetj.1833710

ISSN: 2149-3359 **Original Article** e-ISSN: 2149-8644

Corpus Luteum Presence as a Risk Factor for Endometrial Hyperplasia in Clinically Healthy Female Cats Undergoing Routine Ovariohysterectomy

Damla Tuğçe OKUR[1,*] İsmail BOLAT[2] Alper Yasin ÇİPLAK[1] Vefa TOHUMCU[1] Şifanur AYDIN[1] Betül ORHAN[2]

[1] *Atatürk University, Faculty of Veterinary Medicine, Department of Obstetrics and Gynecology, 25000, Erzurum, Türkiye*
[2] *Atatürk University, Faculty of Veterinary Medicine, Department of Pathology, 25000, Erzurum, Türkiye*

Received: 01.12.2025 Accepted: 06.01.2026

ABSTRACT In this prospective cross-sectional study, we investigated whether corpus luteum (CL) presence is associated with subclinical endometrial hyperplasia in clinically healthy female cats undergoing elective ovariohysterectomy. Fifty intact female cats (13-27 months, ASA I) presented for routine surgery were enrolled. Following ovariohysterectomy, uteri and ovaries were subjected to full-thickness histopathological examination, and uterine lesions and ovarian structures, including CL and cysts, were systematically recorded. Descriptive statistics were used to determine the prevalence of uterine and ovarian findings, and the association between CL presence (as a proxy for luteal-phase progesterone exposure) and endometrial hyperplasia (EH) was evaluated using Fisher's exact test with calculation of odds ratio (OR) and 95% confidence interval (CI). Despite the absence of reproductive complaints, EH and cystic endometrial hyperplasia (CEH) were identified in 36% (18/50) and 20% (10/50) of female cats, respectively, while mild endometritis and other hyperplastic lesions were detected in 12% and 8%. Ovarian cysts, predominantly follicular, were present in 34% of cats, and CLs were observed in 48% (24/50). Female cats with CL had a significantly higher prevalence of EH than those without CL (54.2% vs 19.2%; p=0.014), corresponding to an OR of 4.96 (95% CI 1.4-17.6), indicating that luteal-phase animals were nearly five times more likely to exhibit EH. These findings demonstrate that progesterone-associated endometrial changes are common and largely subclinical in young, clinically healthy female cats and support CL presence as a clinically relevant risk factor for early uterine remodeling, warranting further investigation into the long-term significance of these lesions.

Keywords: *Corpus luteum, Cystic endometrial hyperplasia, Endometrial hyperplasia, Feline, Ovariohysterectomy, Progesterone.*

ÖZ

Korpus Luteum Varlığının Rutin Ovariohisterektomi Uygulanan Klinik Olarak Sağlıklı Dişi Kedilerde Endometriyal Hiperplazi İçin Bir Risk Faktörü Olarak Değerlendirilmesi

Bu prospektif kesitsel çalışmada, rutin ovariohisterektomi geçiren klinik olarak sağlıklı dişi kedilerde korpus luteum (CL) varlığının subklinik endometriyal hiperplazi ile ilişkili olup olmadığı araştırılmıştır. Rutin cerrahi amacıyla getirilen, 13–27 aylık, ASA I sınıfında yer alan elli dişi kedi çalışmaya dahil edilmiştir. Ovariohisterektomi sonrasında uterus ve ovaryumlar histopatolojik incelemeye tabi tutulmuş; CL ve kistler dahil tüm ovaryum yapıları ile uterin lezyonlar sistematik şekilde kaydedilmiştir. Uterus ve ovaryum bulgularının prevalansı tanımlayıcı istatistiklerle belirlenmiş; CL varlığı (luteal faz progesteron maruziyetinin dolaylı göstergesi olarak) ile endometriyal hiperplazi (EH) arasındaki ilişki Fisher'ın kesin testi kullanılarak, olasılık oranı (OR) ve %95 güven aralığı (GA) hesaplanarak değerlendirilmiştir. Üreme ile ilgili herhangi bir klinik şikayet bulunmamasına rağmen kedilerin %36'sında (18/50) EH, %20'sinde (10/50) kistik endometriyal hiperplazi (CEH) tespit edilmiş; ayrıca %12'sinde hafif endometritis ve %8'inde diğer hiperplastik lezyonlar belirlenmiştir. Ovaryum kistleri, çoğunlukla foliküler tipte olup, kedilerin %34'ünde saptanmış; CL ise %48'inde (24/50) gözlenmiştir. CL bulunan kedilerde EH prevalansı CL bulunmayanlara göre anlamlı derecede daha yüksek olup (%54.2'ye karşı %19.2; p=0.014), bu fark OR 4.96 (GA %95, 1.4–17.6) ile luteal fazdaki hayvanların EH geliştirme olasılığının yaklaşık beş kat arttığını göstermektedir. Bu bulgular, progesteron ilişkili endometriyal değişikliklerin genç ve klinik olarak sağlıklı dişi kedilerde yaygın ve büyük ölçüde subklinik olduğunu ortaya koymakta; CL varlığını erken uterin yeniden şekillenme açısından klinik olarak önemli bir risk faktörü olarak desteklemektedir. Bu lezyonların uzun dönem klinik öneminin daha kapsamlı araştırılmasına ihtiyaç vardır.

Anahtar Kelimeler: *Endometriyal hiperplazi, Kedi, Kistik endometriyal hiperplazi, Korpus luteum, Ovariohisterektomi, Progesteron.*

✉ *Corresponding author: damla.tugce.okur@gmail.com

INTRODUCTION

Reproductive cyclicity in female cats is controlled by a hormonally dynamic system involving ovarian follicular activity, neuroendocrine regulation, and environmental cues such as photoperiod. Although traditionally classified as induced ovulators, emerging evidence indicates that spontaneous ovulation occurs far more frequently than once assumed, even in the absence of mating or overt coital stimulation (Binder et al. 2019). Consequently, many female cats experience repeated luteal phases throughout the breeding season, resulting in recurrent exposure of the endometrium to progesterone. This hormone plays a central role in post-ovulatory physiology and induces stromal proliferation, glandular remodeling, and secretory transformation-changes that may accumulate over time without producing clinical signs. The anatomical and physiological features of the feline reproductive system, including high follicular responsiveness and variable cyclicity modulated by season and light, further underscore the inherently sensitive endocrine environment of the female cats (Johnson 2022). Progesterone-driven regulation of the uterus exerts direct molecular effects that contribute to early, and often silent, endometrial alterations. Experimental studies demonstrate that feline endometrial epithelial cells express functional progesterone receptors and respond to physiological luteal-phase progesterone by increasing prostaglandin secretion through receptor-dependent genomic pathways, whereas stromal cells remain relatively unresponsive (Siemieniuch et al. 2010). Exogenous progestins magnify these effects: long-acting medroxyprogesterone acetate induces ovarian follicular cysts, pronounced endometrial hyperplasia, and marked mammary epithelial proliferation even after limited administration (Keskin et al. 2009; Enginler and Şenünver 2011). These findings collectively demonstrate that feline reproductive tissues are highly susceptible to both endogenous and synthetic progestational influences, supporting the concept that clinically inapparent endometrial remodeling may develop well before reproductive disease becomes detectable. The pathophysiology of cystic and non-cystic endometrial hyperplasia in female cats further emphasizes the pivotal role of luteal-phase progesterone. Schlafer and Gifford (2008) detailed how sustained progesterone exposure during diestrus promotes glandular proliferation, luminal secretion, and cystic dilation while reducing myometrial contractility, conditions favorable to endometrial hyperplasia. Complementary experimental data confirm that progesterone modulates key aspects of epithelial function in the female cats (Siemieniuch et al. 2010), while recent findings show that progesterone receptor expression varies markedly across the estrous cycle, with heightened sensitivity during diestrus (Nascimento et al. 2023). Molecular studies further indicate that interactions among progesterone signaling, oxidative stress pathways, and inflammatory mediators contribute to early endometrial remodeling even in clinically healthy cats (Okur et al. 2025). Together, these mechanistic insights suggest that even short luteal phases in induced-ovulators may be sufficient to initiate subclinical uterine changes. Despite the accumulating evidence linking repeated progesterone exposure to early endometrial remodeling, significant gaps remain in defining the true prevalence and characteristics of these lesions in healthy young female cats. Many available studies have examined heterogeneous or poorly documented populations, such as stray, shelter, or hormonally treated cats, where reproductive history and cycle status are unknown (Yaseen et al. 2022). Moreover, although the hormonal and molecular regulation of the feline endometrium has been increasingly described (Siemieniuch et al. 2010; Nascimento et al. 2023), few investigations have integrated these insights with systematic full-thickness histopathological assessment in well-defined cohorts of healthy, intact animals. The present study aimed to evaluate whether the presence of a corpus luteum represents a risk factor for the development of uterine and ovarian pathologies, including subclinical endometrial hyperplasia, in clinically healthy young female cats undergoing routine ovariohysterectomy.

MATERIAL AND METHODS

The study protocol was reviewed and approved by the Atatürk University Local Ethics Committee for Animal Experiments (Approval No: 68/2024). Before the initiation of the study, informed consent was obtained from all animal owners, who were thoroughly briefed on the objectives, procedures, and potential implications of the research. All procedures involving animals were conducted in strict accordance with national and institutional guidelines.

Animals

The study was conducted on 50 clinically healthy female cats (n=50, 13-27 months and weighing 3.3±1.2 kg) presented to the Atatürk University Animal Hospital for elective Ovariohysterectomy (OHE). Inclusion in the study required that all animals were classified as American Society of Anesthesiologists Physical Status Classification System (ASA) Physical Status I based on comprehensive physical and clinical examinations. Furthermore, all subjects were required to have blood biochemistry parameters within the established normal reference ranges for the species, confirming their overall healthy physiological status before surgical intervention.

Anesthesia and Surgery

Animals were premedicated intramuscularly with 20 µg/kg medetomidine (Domitor®, Zoetis Orion Corp, Finland) and 0.2 mg/kg butorphanol (Butomidor® 10 mg/mL, Richter Pharma, Austria). Fifteen minutes later, the skin over the left cephalic vein was aseptically prepared, a 22-gauge catheter was placed, and lactated Ringer's solution was infused at 5 mL/kg/h until extubation. Anesthesia was induced with intravenous propofol (Propofol 1%, Fresenius, Istanbul, Turkey) administered to effect to allow endotracheal intubation with an appropriately sized tube. The cats were then connected to a non-rebreathing circuit, and anesthesia was maintained with isoflurane (Forane 250 mL, Aesica Queenborough, England) vaporized in 100% oxygen delivered at 300 ml/kg/min. Spontaneous ventilation was permitted throughout the procedure. All anesthetic procedures were performed by the same experienced anesthetist. Animals were positioned in dorsal recumbency on a heated stainless-steel surgical table covered with cotton drapes; table heating was activated whenever rectal temperature fell below 37 °C. In both groups, ovariohysterectomy was performed via a midline approach. After the hair in the surgical area was clipped and the skin was prepared using standard aseptic and antiseptic techniques, a vertical skin incision approximately 2 cm in length was made midway between the last rib, the tuber coxae, and the vertebral column. The abdominal cavity was entered by bluntly penetrating all

muscle layers with curved hemostatic forceps. Both ovaries and uterine horns of the cats were ligated using 2-0 absorbable polyglycolic acid (PGA) suture. Immediately after the surgery, the excised ovaries and uterine tissues were placed into containers with 4% neutral buffered formaldehyde and stored at room temperature for 48 hours. The samples were subsequently submitted to the Department of Pathology, Faculty of Veterinary Medicine, Atatürk University for histopathological examination.

Histopathological Examination

A total of 50 uterine and ovarian samples were fixed in 10% neutral buffered formalin for 48 hours, routinely processed, and embedded in paraffin blocks. From each block, 4 µm-thick sections were prepared and stained with hematoxylin and eosin (H&E). All histological evaluations were performed by the same experienced veterinary pathologist, who was blinded to the clinical and gross findings. Microscopic examinations were carried out using a light microscope (Leica Microsystems, Germany) equipped with a Flexacam i5 digital camera, at magnifications of 4x, 10x, and 40x. In the uterine horns, the endometrium was systematically evaluated for the presence of endometrial hyperplasia, cystic endometrial hyperplasia, endometritis, and other hyperplastic lesions. Endometrial hyperplasia was defined as an increase in the number and size of endometrial glands, while cystic endometrial hyperplasia was characterized by glandular proliferation accompanied by cystic dilatation of glands. Endometritis was diagnosed based on inflammatory cell infiltration, predominantly neutrophils and lymphocytes, within the endometrial stroma. Hyperplastic lesions were identified by increased numbers of fibroblasts and fibrous connective tissue, cellular hyperchromasia, and architectural disorganization. Ovarian tissue sections were evaluated for the presence of corpus luteum (CL) and for cystic structures, which were classified as cysts originating from Wolffian or Müllerian duct remnants, follicular cysts, luteal cysts, combinations of different cyst types, and cystic rete ovarii. The histopathological classification and diagnostic criteria for ovarian cysts were based on previously published descriptions, particularly those reported by Binder et al. (2021). Wolffian or Müllerian duct cysts were identified by a single-layered cuboidal or low columnar, occasionally ciliated epithelium with a thin connective tissue wall. Follicular cysts were characterized by one or multiple layers of granulosa cells, sometimes showing degeneration, with variable thecal involvement. Luteal cysts were defined by the presence of luteinized theca cells lining the cyst wall.

Statistical Analysis

All statistical analyses were conducted using SPSS software (version 29.0, IBM SPSS Statistics). Descriptive statistics, presented as frequencies (n) and percentages (%), were used to summarize the prevalence of all histopathological lesions observed in the uterine and ovarian tissues. For the analytic phase, the association between progesterone exposure (indicated by the presence of the CL) and the occurrence of EH was investigated. Fisher's Exact Test was applied to the resulting 2x2 contingency table to determine statistical significance, with a p-value threshold set at $p<0.05$. The strength of this relationship was subsequently quantified by calculating the Odds Ratio (OR).

RESULTS

The descriptive statistical findings regarding the histopathological lesions encountered in the uteri and ovaries of the clinically healthy female cats included in this study are presented in Table 1.

Table 1: Prevalence of uterine and ovarian findings in cats (n=50).

Histopathological Finding	Positive Cases (n)	Prevalence (%)
Uterine Findings		
Endometrial Hyperplasia	18	36.0%
Cystic Endometrial Hyperplasia	10	20.0%
Endometritis	6	12.0%
Ovarian Findings		
Corpus Luteum (Active Luteal Phase)	24	48.0%
Follicular Cyst	8	16.0%
Luteal Cyst	3	6.0%
Hyperplastic Lesion	4	8.0%
Cystic Rete Ovarii	2	4.0%

The analytic statistics were performed to determine the relationship between hormonal activity and the observed uterine pathologies. The association between the presence of CL, which represents exposure to progesterone, and the occurrence of EH was evaluated using the Fisher's Exact Test (Table 2). Of the cats presenting with CL, 54.2% (13/24) were also diagnosed with EH, a rate considerably higher than the 19.2% (5/26) observed in cats without CL. This difference was found to be statistically significant ($p=0.014$). Furthermore, the calculated Odds Ratio (OR) was 4.96 (Cl 95% 1.4-17.6), indicating that cats in the luteal phase (CL present) were nearly five times more likely to develop endometrial hyperplasia compared to those without CL.

Table 2: Association between corpus luteum and endometrial hyperplasia.

Condition	Endometrial Hyperplasia Present (+)	Endometrial Hyperplasia Absent (-)	Total
C. Luteum Present (+)	13	11	24
C. Luteum Absent (-)	5	21	26
Total	18	32	50
Statistical Analysis			
p-value (Fisher's Exact Test)	0.014		
Odds Ratio (OR)	4.96		

Histopathological evaluation of the uterine tissues revealed a range of lesions among the examined cats. Endometrial hyperplasia was the most frequently observed finding, detected in 18 animals, followed by cystic endometrial hyperplasia in 10 cats. Mild endometritis was identified in 6 cases, while stromal hyperplastic lesions, predominantly involving fibroblast and fibrocyte proliferation without marked glandular epithelial involvement, were observed in 4 cats. No histopathological abnormalities were detected in the uterine tissues of the remaining 12 cats, which were considered histologically normal. A summary of uterine histopathological findings is presented in Table 1 and representative micrographs are shown in Figure 1.

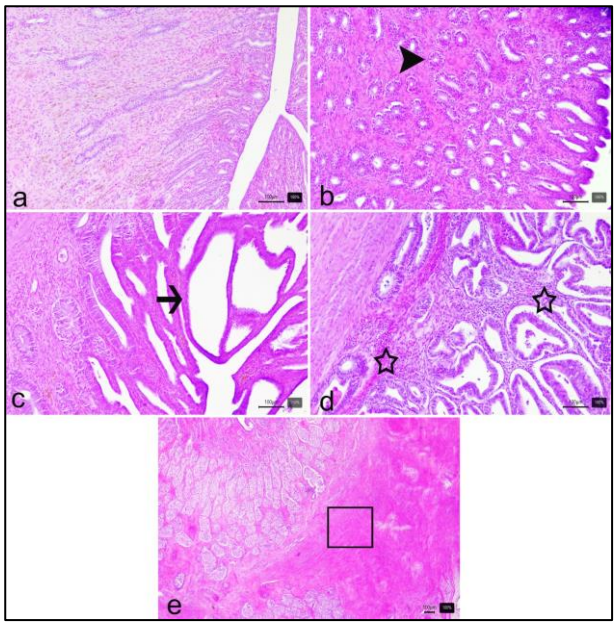

Figure 1: (a) Normal uterus (x10). (b) Endometrial hyperplasia (arrowheads, x10). (c) Cystic endometrial hyperplasia (arrows, x10). (d) Endometritis (asterisk, x10). (e) Stromal hyperplastic lesions highlighted within the boxed area (box, x10). Hematoxylin and eosin staining; scale bar: 100 µm.

Histopathological examination of the ovarian tissues revealed the presence of corpus luteum and various cystic alterations with variable frequencies among the examined cats. While a subset of ovaries showed different types of cystic structures, no histopathological abnormalities were detected in 9 cases. The distribution of ovarian findings is summarized in Table 1, and representative histological images are presented in Figure 2.

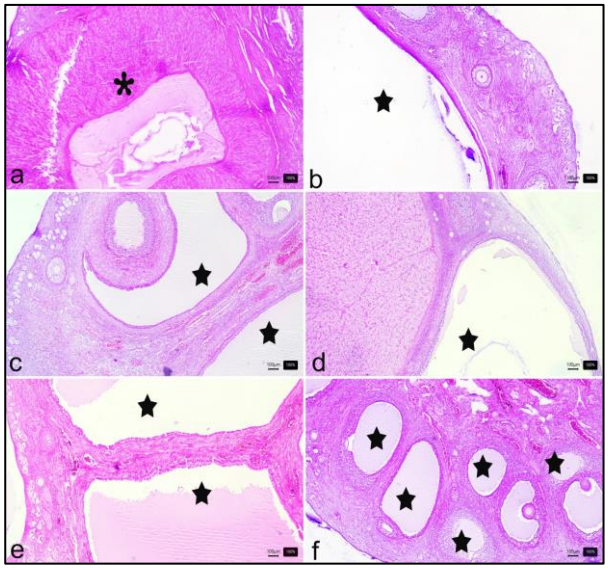

Figure 2: (a) Corpus luteum (asterisk, x4). (b) Cyst originating from Wolffian or Müllerian duct remnants (star, x4). (c) Follicular cyst (star, x4). (d) Luteal cyst (star, x4). (e) Cystic rete ovarii (star, x4). (f) Different combinations of ovarian cystic structures (star, x4). Hematoxylin and eosin staining; scale bar: 100 µm.

DISCUSSION AND CONCLUSION

In this study of 50 clinically healthy adult female cats, histopathological evaluation revealed a high prevalence of progesterone-associated endometrial alterations despite the absence of reproductive symptoms. EH and CEH were detected in 36% and 20% of uteri, respectively, and the presence of a CL was strongly associated with EH (54.2% vs. 19.2%; p=0.014; OR=4.96, 95% CI 1.4-17.6). Ovarian cysts, predominantly follicular, were identified in 34% of female cats. These findings indicate that subclinical progesterone-mediated uterine remodeling is common in intact female cats undergoing elective ovariohysterectomy.

The prevalence of EH and CEH in the present cohort (36% and 20%, respectively) is notable given the young age of the cats (13-27 months) and their clinically normal status. Similar subclinical lesions have been documented previously, with reported EH/CEH rates of 20-40% in asymptomatic female cats (Agudelo 2005; Younis et al. 2014). Comparative data from bitches also demonstrate subclinical EH rates of 28–45% (Schlafer and Gifford 2008; Woźna-Wysocka et al. 2021), underscoring that progesterone-driven endometrial proliferation is an early and frequent event across domestic carnivores. Such lesions commonly remain undetected in the absence of histopathological evaluation, highlighting the silent nature of early progesterone-related uterine remodeling.

The mechanistic basis for these findings is well established. In female cats, ovulation-induced luteal phases, even when brief, rapidly increase endometrial sensitivity to progesterone, stimulating glandular proliferation, secretory activity, and cystic dilation (Schlafer and Gifford 2008). Progesterone also enhances stromal and glandular epithelial responsiveness, with studies showing increased or sustained progesterone receptor expression in hyperplastic endometrium (De Bosschere et al. 2002). This creates a hormonally permissive environment that facilitates early subclinical cystic changes. Additionally, the proliferative effects of progesterone are pronounced in feline reproductive tissues: female cats exposed to synthetic progestins develop marked stromal and epithelial hyperplasia even without accompanying inflammation (Enginler and Şenünver 2011). These mechanisms support the present study's finding that luteal-phase female cats had nearly a five-fold increased likelihood of EH, reinforcing the pivotal role of endogenous or exogenous progesterone in early uterine remodeling.

Differences in population structure, reproductive history, and sampling methodology likely contributed to the higher prevalence of subclinical EH and CEH observed here compared with earlier reports. Studies of free-roaming or shelter-origin female cats, where estrous cycling patterns and ovulation frequency are poorly defined, describe wide morphological variability. For instance, Martí et al. (2021) reported substantial histological heterogeneity in 50 stray female cats, suggesting that repeated non-pregnant estrous cycles promote progesterone-associated endometrial changes even in the absence of clinical disease. Similarly, Yaseen et al. (2022) documented incidental ovarian follicular cysts and early hyperplastic changes in clinically normal female cats, underscoring that hormonally driven pathologies often arise independently of overt reproductive dysfunction. Considerable inter-study variability in reported CEH prevalence (12–20% up to ~40%) has also been attributed to differences in histopathological criteria, cycle-stage distribution, and tissue sampling depth (Maya-Pulgarin et al. 2017;

Bukowska et al. 2020). Comparable patterns in canine studies further illustrate that subclinical uterine pathology is common across species and frequently remains clinically silent. Thus, the elevated EH/CEH prevalence in this study likely reflects a combination of a young but heavily cycling population, a substantial proportion of female cats in the luteal phase, and the use of full-thickness histopathology capable of detecting subtle lesions overlooked in routine examinations.

These results are also supported by recent evidence demonstrating that subclinical uterine pathology is common even in clinically healthy female cats undergoing elective sterilization. Binder et al. (2021) identified CEH in 19.8% of 106 healthy cats, with more than one-quarter exhibiting ovarian or uterine abnormalities despite no reproductive complaints. Importantly, CLs were present in 15 of 29 cats with lesions, reinforcing the role of spontaneous ovulation and repeated luteal exposure in driving early endometrial remodeling. Similar findings in stray populations (Yaseen et al. 2022) and in clinically normal bitches (Maya-Pulgarín et al. 2017; Bukowska et al. 2020) further highlight the silent, hormonally mediated nature of early uterine pathology. Collectively, these data suggest that the comparatively high EH/CEH prevalence documented in the present study reflects the female cats reproductive physiology, characterized by repeated estrous cycling, spontaneous ovulation, and progesterone exposure, and the enhanced sensitivity afforded by comprehensive histopathological evaluation.

This study has several limitations that should be considered when interpreting the findings. First, the sample consisted exclusively of young, clinically healthy female cats presented for elective ovariohysterectomy, which may limit the generalizability of the results to older animals or those with known reproductive disorders. The cross-sectional design prevents determining temporal progression or causality between luteal-phase progesterone exposure and the development of endometrial lesions. Hormonal profiling was not performed, and luteal status was inferred from the presence of corpus luteum, which, while biologically reasonable in female cats, may not fully reflect dynamic endocrine fluctuations. Additionally, reproductive history, including the number of prior estrous cycles, frequency of spontaneous ovulations, and early pregnancies, could not be verified, introducing uncertainty regarding cumulative hormonal exposure. Finally, although full-thickness histopathology increases lesion detection, it may also identify subclinical changes of uncertain long-term relevance, and its sensitivity may not reflect what is achievable in routine clinical practice.

In conclusion, the present study provides novel evidence that clinically healthy young female cats undergoing routine ovariohysterectomy frequently harbor subclinical progesterone-associated uterine alterations, with endometrial hyperplasia emerging as a common and largely silent finding. By demonstrating a strong association between corpus luteum presence and endometrial hyperplasia, this study extends previous descriptive observations and supports the concept that even physiological luteal-phase progesterone exposure can act as a biologically relevant risk factor for early uterine remodeling in queens. Importantly, the inclusion of a well-defined, asymptomatic population and the use of systematic full-thickness histopathological evaluation enabled detection of subtle lesions that would otherwise remain undiagnosed in routine clinical settings. These findings underscore that the absence of clinical reproductive signs does not preclude underlying uterine pathology and highlight the cumulative impact of repeated estrous cycling and spontaneous ovulation on the feline endometrium. From a clinical and pathophysiological perspective, the results emphasize the value of early elective ovariohysterectomy not only as a population control measure but also as a means of preventing hormonally mediated uterine changes whose long-term consequences remain uncertain. Future longitudinal studies integrating hormonal profiling and follow-up data are warranted to clarify whether these subclinical lesions represent transient adaptive changes or early stages of progressive uterine disease.

CONFLICTS OF INTEREST

The authors report no conflicts of interest.

ACKNOWLEDGMENT

The authors would like to express their gratitude to Assoc. Prof. Sıtkıcan Okur for his support with the statistical analyses.

AUTHOR CONTRIBUTIONS

Idea/Concept: DTO
Supervision/Consultancy: DTO
Data Collecting and/or Processing: DTO, AYÇ, ŞA, VT
Analysis and/or Interpretation: İB
Writing the Article: DTO
Critical Review: DTO

REFERENCES

Agudelo CF (2005). Cystic endometrial hyperplasia-pyometra complex in cats: A review. *Vet Q,* 27(4), 173–182.

Binder C, Aurich C, Reifinger M, Aurich J (2019). Spontaneous ovulation in cats—uterine findings and correlations with animal weight and age. *Anim Reprod Sci*, 209, 106167.

Binder C, Reifinger M, Aurich J, Aurich C (2021). Histopathological findings in the uteri and ovaries of clinically healthy cats presented for routine spaying. *J Feline Med Surg*, 23(8), 770–776.

Bukowska B, Jurczak A, Tobolski D, Janowski T (2020). Prevalence of subclinical uterine pathologies diagnosed by biopsy, cytology and bacteriology in cyclic bitches. *Pol J Vet Sci*, 23, 595–603.

De Bosschere H, Ducatelle R, Vermeirsch H, Simoens P, Coryn M (2002). Estrogen-α and progesterone receptor expression in cystic endometrial hyperplasia and pyometra in the bitch. *Anim Reprod Sci*, 70, 251–259.

Enginler SÖ, Şenünver A (2011). The effects of progesterone hormone applications used for suppression of estrus on mammary glands in queens. *Kafkas Univ Vet Fak Derg*, 17, 277–284.

Johnson AK (2022). Normal feline reproduction: The queen. *J Feline Med Surg*, 24, 204–211.

Keskin A, Yılmazbas G, Yılmaz R, Ozyigit MO, Gümen A (2009). Pathological abnormalities after long-term administration of medroxyprogesterone acetate in a queen. *J Feline Med Surg*, 11, 518–521.

Martí A, Serrano A, Pastor J et al. (2021). Endometrial status in queens evaluated by histopathology findings and two cytological techniques: low-volume uterine lavage and uterine swabbing. *Animals*, 11, 88.

Maya-Pulgarin D, Gonzalez-Dominguez MS, Aranzazu-Taborda D et al. (2017). Histopathologic findings in uteri and ovaries from clinically healthy dogs at elective ovariohysterectomy: a cross-sectional study. *J Vet Sci,* 18, 407–414.

Nascimento AEJ, Santos LC, Santos BR et al. (2023). Estrogen and progesterone receptors and antioxidant enzymes are expressed differently in the uterus of domestic cats during the estrous cycle. *Theriogenology*, 203, 1–10.

Okur DT, Ozdemir S, Aydin S et al. (2025). Effects of melatonin implants on uterine inflammation and ovarian progesterone receptor expression in female cats: a histopathological and molecular analysis. *Theriogenology*, 238, 117368.

Schlafer DH, Gifford AT (2008). Cystic endometrial hyperplasia, pseudo-placentational endometrial hyperplasia, and other cystic conditions of the canine and feline uterus. *Theriogenology*, 70(3), 349-358.

Siemieniuch MJ, Bowolaksono A, Skarzynski DJ, Okuda K (2010). Ovarian steroids regulate prostaglandin secretion in the feline endometrium. *Anim Reprod Sci,* 120(1-4), 142-150.

Woźna-Wysocka M, Rybska M, Błaszak B et al. (2021). Morphological changes in bitches' endometrium affected by cystic endometrial hyperplasia–pyometra complex-the value of histopathological examination. *BMC Vet Res,* 17(1), 174.

Yaseen AA, Kareem DA, Waheed Z, Fahad TA (2022). Histopathological study of some abnormalities of infertility in queens. *Basrah J Vet Res,* 21(S1), 131-140.

Younis M, Mohammed FF, Abu-Seida AM, Ragab RS, Gohar HM (2014). Ultrasonography and pathological evaluation of cystic endometrial hyperplasia–pyometra complex in bitches and queens with related ovarian alterations. *Global Vet*, 13(1), 60-67.

Van Veterinary Journal

https://dergipark.org.tr/tr/pub/vanvetj

Cite this article as: **Gölgeli Bedir A, Baykal B, Orhun ÖT, Turgut F, Kocaman Y (2026).** Effects of Dexmedetomidine Alone and Combined with Tramadol on Intraocular Pressure, Pupil Size, and Tear Production in Cats: A Randomized Controlled Study. *Van Vet J*, 37(1), 87-91. DOI: https://doi.org/10.36483/vanvetj.1843931

ISSN: 2149-3359 **Original Article** e-ISSN: 2149-8644

Effects of Dexmedetomidine Alone and Combined with Tramadol on Intraocular Pressure, Pupil Size, and Tear Production in Cats: A Randomized Controlled Study

Ayşe GÖLGELİ BEDİR[1,*] Büşra BAYKAL[1] Ömer Tarık ORHUN[2] Ferda TURGUT[3] Yakup KOCAMAN[4]

[1] *Atatürk University, Faculty of Veterinary Medicine, Department of Surgery, 25240, Erzurum, Türkiye*
[2] *Necmettin Erbakan University, Faculty of Veterinary Medicine, Department of Surgery, 42310, Konya, Türkiye*
[3] *Çukurova University, Ceyhan Faculty of Veterinary Medicine, Department of Surgery, 01950, Adana, Türkiye*
[4] *Bozok University, Faculty of Veterinary Medicine, Department of Surgery, 66000, Yozgat, Türkiye*

Received: 18.12.2025 Accepted: 19.02.2026

ABSTRACT This present study was designed to evaluate the impact of intramuscular dexmedetomidine, alone or combined with subcutaneous tramadol, on intraocular pressure (IOP), pupil size (PS), and tear secretion (TS) in healthy cats. Thirty healthy cats (n=30) were randomly assigned to two groups (n=15/group). Cats received either dexmedetomidine alone (Dex; 25 µg/kg IM) or dexmedetomidine plus tramadol (Dex-Tra; tramadol 2 mg/kg SC + dexmedetomidine 25 µg/kg IM). IOP, PS, and TS were recorded at baseline (T_0) and 5, 15, and 30 minutes post-administration (T_5, T_{15}, T_{30}). Within the Dex group, IOP decreased significantly from T_0 to T_{30}, and PS increased from T_5 to T_{15}, returning to baseline by T_{30} ($p<0.05$). Between groups, IOP at T_5 was lower in Dex than Dex-Tra ($p<0.05$), with no between-group differences at T_{15} or T_{30} ($p>0.05$). No statistically significant differences were observed between groups for PS or TS at any measured time point ($p>0.05$). Both protocols reduced TS over time. Dexmedetomidine alone produced ocular hypotension and a transient increase in PS; co-administration with tramadol attenuated these effects. As both regimens decreased tear secretion, clinicians should consider potential impacts on tonometry, ocular surface integrity, and perioperative ophthalmic management when selecting sedation protocols.

Keywords: *Cat, Dexmedetomidine, Intraocular pressure, Pupil size, Tramadol.*

ÖZ

Dexmedetomidinin Tek Başına ve Tramadol ile Kombine Kullanımının Kedilerde İntraoküler Basınç, Pupilla Çapı ve Gözyaşı Üretimi Üzerine Etkileri: Randomize Kontrollü Bir Çalışma

Bu çalışmanın amacı, intramusküler deksmedetomidinin tek başına veya subkutan tramadol ile kombinasyon halinde uygulanmasının sağlıklı kedilerde intraoküler basınç (İOP), pupilla çapı (PS) ve gözyaşı sekresyonu (TS) üzerindeki etkilerini değerlendirmektir. Otuz sağlıklı kedi (n=30), rastgele iki gruba ayrıldı (n=15/grup). Kedilere ya yalnızca deksmedetomidin (Dex; 25 µg/kg IM) ya da deksmedetomidin + tramadol (Dex-Tra; tramadol 2 mg/kg SC + deksmedetomidin 25 µg/kg IM) uygulandı. İOP, PS ve TS ölçümleri başlangıçta (T_0) ve uygulamadan 5, 15 ve 30 dakika sonra (T_5, T_{15}, T_{30}) gerçekleştirildi. Dex grubunda, T_5-T_{30} zaman noktalarında İOP, T_0'a kıyasla anlamlı olarak azaldı ve PS T_5-T_{15}'te artarak T_{30}'da başlangıç değerlerine döndü ($p<0.05$). Gruplar arası karşılaştırmada, T_5'te İOP Dex grubunda Dex-Tra grubuna göre daha düşüktü ($p<0.05$); T_{15} ve T_{30}'da gruplar arasında fark gözlenmedi ($p>0.05$). PS ve TS açısından hiçbir zaman noktasında gruplar arasında anlamlı fark olmadığı görüldü ($p>0.05$). Her iki protokol de zamanla TS'yi azalttı. Deksmedetomidinin tek başına uygulanması oküler hipotansiyona ve pupilla çapında geçici bir artışa neden olurken, tramadol ile birlikte uygulanması bu etkileri zayıflattı. Her iki rejimin de gözyaşı sekresyonunu azaltması nedeniyle, sedasyon protokolleri seçilirken tonometri, oküler yüzey bütünlüğü ve perioperatif oftalmik yönetim üzerindeki olası etkiler klinisyenler tarafından dikkate alınmalıdır.

Anahtar Kelimeler: *Deksmedetomidin, İntraoküler basınç, Kedi, Pupilla çapı, Tramadol.*

INTRODUCTION

Dexmedetomidine (Dex), the dextrorotatory isomer of medetomidine, exhibits marked α2-adrenergic receptor selectivity and is widely applied in cats for sedation, analgesia, and muscle relaxation (Gómez and García 2023). It produces analgesic effects by activating α2-adrenergic receptors at both spinal and supraspinal levels, whereas tramadol (Tra), a synthetic codeine analog, acts through μ-opioid receptor agonism and monoamine reuptake

✉ *Corresponding author: aysegolgeli@atauni.edu.tr

inhibition, thereby providing multimodal central analgesia (Scott and Perry 2000; Valtolina et al. 2009; Slingsby et al. 2010). Since these two agents act through distinct mechanisms, their combination produces a synergistic effect, enabling effective pain control with lower drug doses. This synergism reduces the likelihood of adverse effects, such as cardiovascular depression or respiratory suppression, and enhances sedation quality, making the combination particularly advantageous in critically ill or systemically compromised patients (Valtolina et al., 2009; Slingsby et al. 2010). Furthermore, when dexmedetomidine is co-administered with opioids, it has been shown to decrease the requirement for postoperative rescue analgesics, underlining its role in multimodal analgesia (Slingsby et al. 2010).

Ocular physiology can be markedly influenced by anesthetic and sedative agents, which may alter intraocular pressure (IOP), pupil size (PS), and tear secretion (TS). In cats, the normal IOP ranges from 10 to 25 mmHg, with deviations from this range associated with vision-threatening conditions such as glaucoma or hypotony (Gelatt and Gelatt 2011; Gelatt et al. 2013; Levin and Albert 2021). Alpha-2 adrenoceptor agonists, including Dex, have been reported to decrease IOP in multiple species (Vartiainen et al. 1992; Okur et al. 2022; Yener et al. 2024). Similarly, changes in PS have been observed; pupil constriction has been reported in animals receiving α2-agonists, although in cats under anesthesia, pupil dilation is generally more common (Ghaffari et al. 2010; Mitchell and Oliver 2015; Aghababaei et al. 2021). TS is another critical ocular parameter, with normal Schirmer tear test (STT I) values in cats ranging from approximately 11 to 17 mm/min (Hartley et al. 2006; Stadtbäumer et al. 2006). Inadequate tear production, regardless of cause, predisposes to keratoconjunctivitis sicca and ocular surface disease (Hartley et al. 2006; Stadtbäumer et al. 2006; Maggs 2013; Sebbag et al. 2019).

In cats, a study of dexmedetomidine reported decreased IOP, increased PS, and reduced TS (Wolfran et al. 2022). In dogs, dexmedetomidine decreased IOP without altering PS or TS (Artigas et al. 2012; Aghababaei et al. 2021). Similarly, studies in rabbits, rats, and sheep also showed reduced IOP (Vartiainen et al. 1992; Okur et al. 2022; Yener et al. 2024). In cats, tramadol decreased IOP, while PS increased; in donkeys, a tramadol study reported no change in IOP (Hamed et al. 2018). In dogs, a combination of dexmedetomidine and tramadol was associated with a decrease in IOP (Mattos-Junior et al. 2021). Despite the widespread clinical use of dexmedetomidine (Dex) and tramadol (Tra), no published studies have specifically addressed the ocular effects of their simultaneous administration in cats. Therefore, this study was designed to examine the effects of dexmedetomidine (Dex) and tramadol (Tra), administered alone and in combination, on ocular variables (IOP, PS, and TS) in cats. We hypothesized that the co-administration of dexmedetomidine and tramadol would produce significant alterations in ocular physiology compared with their individual use, with potentially greater reductions in IOP and PS, and decreased TS.

MATERIAL AND METHODS

Ethical Statement

The study received approval from the Atatürk University Local Ethics Committee for Animal Experiments on (2025/11; Approval number: 231). All experimental procedures were conducted in accordance with the ethical principles defined by the Association for Research in Vision and Ophthalmology for animal-based vision research.

Animals

A total of thirty client-owned male cats, aged between 8 and 16 months and weighing 3.2±0.5 kg, were admitted to the Atatürk University Animal Hospital for elective castration. The study included cats with normal complete blood counts and serum chemistry, and were determined to be American Society of Anesthesiologists (ASA) physical status I. The cats were excluded if they had any disease, cardiac arrhythmias, were less than 6 months or more than 3 years old, or had an ASA status greater than I. Prior to the study, all animals were confirmed to be in good health based on results from physical assessments, complete blood counts, and comprehensive eye evaluations. These evaluations included direct and indirect ophthalmoscopy (Aesculap AC635 C, Braun, Tuttlingen, Germany), intraocular pressure measurement using rebound tonometry (Tonovet, Icare, Vantaa, Finland), Schirmer's tear testing, and fluorescein staining. Before the start of treatments, all cats fasted for 6 hours, except for water intake. The experiments were performed throughout the time frame of 8:00 a.m. to 11:00 a.m.

Study Design

The study population was randomly assigned to two treatment groups: Dex and Dex-Tra. To minimize emesis associated with α_2-agonists, maropitant (1 mg/kg, SC, Cerenia®, Pfizer Animal Health, New York, NY) was administered to cats in both groups 30 min prior to dexmedetomidine injection. In the Dex group, dexmedetomidine (25 µg/kg, IM, Dexdomitor®, Pfizer Animal Health Inc., NY, USA) was administered alone. In the Dex-Tra group, dexmedetomidine (25 µg/kg, IM) was administered 10 minutes after tramadol (2 mg/kg, SC, Tramosel, Haver Farma, Istanbul, TR). Prior to drug administration, all animals were given a 20-minute acclimatization period to the environmental conditions and lighting of the veterinary teaching hospital. Ocular variables were then randomly measured (randomization.org) in both eyes of each cat at time T0 (baseline). These variables were re-recorded at 5, 15, and 30 minutes after administration (T_5, T_{15}, and T_{30}). All injections were administered by the same individual using a 1 ml syringe with a 22 G needle, ensuring the total dose was 1 ml. Intramuscular injections were given into the quadriceps muscle of the left hind leg. Tramadol was administered subcutaneously in the interscapular region (dorsal cervical area) using the same needle/syringe protocol. After all measurements were obtained, intravenous propofol (2 mg/kg) was administered to the cats, and the castration was performed. The investigator performing ocular measurements was blinded to group allocation.

Measurement

IOP values were determined using a rebound tonometer (Tonovet, Icare, Vantaa, Finland), with six readings averaged for each measurement and the device set to "d". The tonometer was calibrated daily according to the manufacturer's recommendations, and an unused probe was assigned to each cat. The cats were restrained by calmly stabilizing the head and neck to avoid inaccurate IOP measurements. If blinking occurred or if an error message appeared due to significant deviation among the six readings, the IOP measurement was repeated. No topical anesthetic was applied to the cats' eyes. To minimize measurement-induced ocular irritation, the

measurement sequence was standardized as IOP first, then PS, and STT (TS) last at each time point. PS was measured by assessing the vertical pupil diameter with a Castroviejo caliper, ensuring no contact with the cornea. TS was obtained using a Schirmer tear test strip (STT1, Tear Touch, Madhu Instrument Pvt. Ltd., New Delhi, India). The strip was gently placed into the inferior conjunctival fornix, positioned laterally beneath the lower eyelid, and maintained in contact with the corneal surface for a duration of one minute per eye, ensuring no interference with the nictitating membrane. All variables were recorded while the cats were maintained in sternal recumbency.

Statistical Analysis

A power analysis (α=0.05, power=0.80) indicated that eight cats per group were required to detect a 20% difference in IOP (SD=1.40 mmHg) using PS Power and Sample Size (v3.1.2; Vanderbilt University) based on published feline IOP data (Stadtbäumer et al. 2006; Kovalcuka and Nikolajenko 2020). To increase robustness and account for potential variability/data loss, n=15 cats per group were included.

Analyses were performed in SPSS v25.0. Normality was assessed with the Shapiro–Wilk; data are presented as mean±SD. Baseline left-right eye values were compared with a paired t-test, and the mean of both eyes per cat was used for all subsequent analyses. Repeated measures (IOP, PS, TS) were analyzed using a two-way repeated-measures ANOVA (within-subject: time; between-subject: group), including the group×time interaction. Within-group comparisons vs. baseline (T_0) were performed using Dunnett's test; between-group comparisons at each time point were adjusted for multiple comparisons using Bonferroni. To reduce any impact of baseline variability, change-from-baseline values (Δ=Tx−T0) were also analyzed, yielding consistent results. Significance was set at $p<0.05$.

RESULTS

All measurements were completed uneventfully, and no vomiting, retching, or hypersalivation was observed in any of the animals. No significant difference was found in baseline IOP values between the Dex (15.87±4.2 mmHg) and Dex-Tra (17.2±5.5 mmHg) groups (p=0.46). In the Dex group, statistical analysis revealed significant differences in IOP at T_5, T_{15}, and T_{30} compared with T_0 ($p<0.05$). However, in the Dex-Tra group, there was no statistically significant difference at any time point compared to T_0 ($p>0.05$). Statistical analysis revealed a significant difference between the Dex and Dex-Tra groups only at the T_5 time point (p=0.023) (Table 1) (Figure 1).

There was no statistical difference in PS values at T_0 between the Dex (8.37±1.7) and Dex-Tra (8.8±2.5) groups (p=0.58). In the Dex group, there was a statistically significant increase in PS values at T_5 and T_{15} compared with T_0 ($p<0.05$), while there was no significant difference at T_{30} ($p>0.05$). In the Dex-Tra group, no statistically significant difference was observed at any time point compared with T_0 ($p>0.05$). PS values did not differ significantly between the Dex and Dex-Tra groups at any time point ($p>0.05$) (Table 1) (Figure 1).

Statistical analysis revealed no significant difference in TS values between the groups at baseline, T_5, T_{15}, and T_{30} ($p>0.05$). However, in both the Dex and Dex-Tra groups, statistically significant differences were observed at T_5, T_{15}, and T_{30} times compared with T_0 ($p<0.05$) (Table 1) (Figure 1).

Table 1: Mean±SD intraocular pressure (IOP), pupil size (PS), and tear secretion (TS) in cats receiving dexmedetomidine (Dex) or dexmedetomidine plus tramadol (Dex-Tra) at baseline (T_0) and 5, 15, 30 min (T_5-T_{30}) after drug administration (n=15/group).

		T_0	T_5	T_{15}	T_{30}
IOP	Dex	15.87±4.2[a]	13.3±3.1*[a]	13.3±3*[a]	12.97±2.8*[a]
	Dex-Tra	17.2±5.5[a]	15.3±3.3[b]	14.9±3[a]	14.3±2[a]
PS	Dex	8.37±1.7[a]	9.2±1.7*[a]	9.8±1.9*[a]	9±1.9[a]
	Dex-Tra	8.8±2.5[a]	9.7±0.6[a]	9.8±0.2[a]	9.6±0.9[a]
TS	Dex	10.63±5.2[a]	7.87±4.9*[a]	6.4±3.2*[a]	5.44±1.1*[a]
	Dex-Tra	13.2±5.5[a]	7.9±6*[a]	6.1±3.9*[a]	5.33±1.2*[a]

Significantly different from baseline within the group * ($p<0.05$). Significant differences between groups over time [a,b] ($p<0.05$). Intraocular pressure, IOP; pupil size, PS; tear secretion, TS.

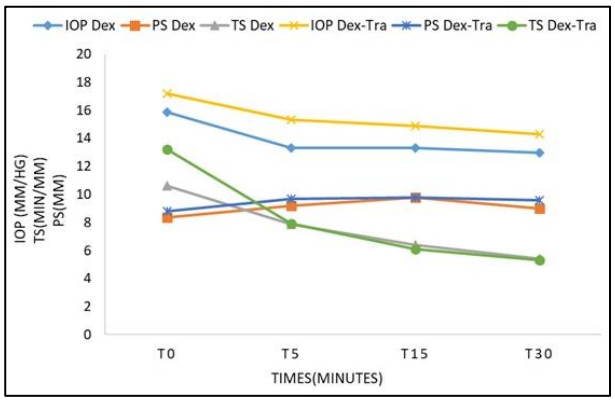

Figure 1: Time course of IOP, PS, and TS after Dex vs Dex-Tra sedation in cats (n=15/group).

DISCUSSION AND CONCLUSION

The principal outcome of the present study was that intramuscular administration of dexmedetomidine alone significantly decreased IOP and transiently increased PS, while its combination with tramadol attenuated these effects. Both protocols, however, significantly reduced tear secretion TS. Based on these results, our hypothesis that co-administration of Dex and Tra would produce greater alterations in ocular physiology than Dex alone was not supported, as the combination appeared to mitigate rather than enhance the changes observed with Dex monotherapy.

Wolfran et al. (2022) demonstrated a dose-dependent reduction in IOP in cats following Dex and methadone administration, due to α_2-adrenoceptor-mediated

suppression of aqueous humor secretion and reduced episcleral venous pressure. Similarly, Artigas et al. (2012) reported a significant decrease in IOP 20 minutes after intravenous Dex administration in dogs. These effects are believed to be mediated through both vascular and secretory mechanisms involving the ciliary body (Kaufman and Gabelt 1995; Reitsamer et al. 2006). However, in the current study, the Dex-Tra group showed no significant change in IOP. Notably, because subcutaneous tramadol may require a longer time to reach peak systemic effects in cats, early measurements may not have fully captured its contribution to ocular outcomes, potentially contributing to the absence of an IOP change at early time points. Through its centrally mediated effects on μ-opioid receptors and inhibition of norepinephrine reuptake, tramadol may influence systemic vascular tone or autonomic regulation, thereby attenuating the ocular hypotensive action of Dex (Scott and Perry 2000). This finding suggests a possible pharmacodynamic interaction, in line with Schroder et al. (2018), who reported tramadol-induced autonomic modulation in feline eyes (Schroder et al. 2018).

Wolfran et al. (2022) observed mydriasis with dexmedetomidine-methadone; in contrast, we observed mydriasis only with Dex alone, with no significant change in PS in the Dex-Tra group. This difference likely reflects opioid-specific pharmacodynamic interactions with α2-agonists (Wolfran et al. 2022). A frequently cited mechanism posits sympathetic inhibition with concomitant reductions in parasympathetic efferent activity; however, controversy persists, given reports that α2-adrenergic agonists can induce miosis in humans, potentially through augmentation of parasympathetic tone (Kato et al. 2018). Although Tra has been associated with mydriasis in cats (Schroder et al. 2018), this effect was not observed in this study. In light of these observations, variability in pupillary responses may be attributable to interspecies differences and to the distinct central and peripheral mechanisms engaged by individual opioids.

A significant decrease in TS was detected in both groups at all time points post-administration. This is consistent with prior reports showing that α2-agonists reduce tear production, potentially due to reduced lacrimal gland perfusion or sympathetic suppression (Gelatt and Gelatt 2011; Ruiz et al. 2014; Wolfran et al. 2022). Such reductions may predispose the ocular surface to desiccation and secondary complications in sedated animals. In a study by Ruiz et al. (2014) in dogs, intramuscular administration of tramadol at 4 and 6 mg/kg did not decrease tear production.

The most commonly observed adverse effect of dexmedetomidine in cats is vomiting and retching (Santos et al. 2011; Papastefanou et al. 2015; Gölgeli Bedir et al. 2025). These occur due to central stimulation of the area postrema by α2-adrenergic agonists (Maxwell et al. 2024). Vomiting can lead to an increase in intracranial and IOP and may result in retinal hemorrhage (Leite et al. 2022). In the present study, maropitant was administered to all animals 30 minutes prior to Dex to prevent its emetic effects, which likely explains why no adverse effects such as vomiting or retching were observed.

The current study is subject to a number of limitations. First, the observation period was short, which may have limited the detection of subtle or delayed ocular effects. In addition, the 10-15 min interval between subcutaneous tramadol administration and the early measurements may have been insufficient for peak tramadol plasma concentrations in cats; therefore, tramadol-related ocular effects at early time points may have been underestimated. Second, the study population comprised only healthy, young, male cats undergoing castration, restricting external validity and limiting generalisability to females, older animals, and cats with systemic or ocular disease. Moreover, a negative (saline/handling-only) control group was not included; thus, the contribution of handling and injection-related stress to changes in IOP and pupil size cannot be fully separated from drug effects, although inclusion of an untreated control was not considered feasible in this clinical population. Finally, each agent was assessed at a single dose with a limited set of ocular endpoints, potentially obscuring dose-response relationships and broader safety signals. Future studies with extended follow-up, varied dosing regimens, and additional outcome measures would better inform sedative protocol selection for feline ophthalmic safety.

In conclusion, intramuscular Dex in cats produced a significant decrease in IOP, transient mydriasis, and a decrease in TS. Co-administration with subcutaneous Tra attenuated the IOP-reducing effect, abolished significant changes in PS, and did not alter the reduction in TS. Clinically, this finding may be interpreted not as an "impairment" of Dex's effect, but rather as providing a more stable ocular profile during sedation in cats with normal baseline IOP. These findings warrant caution when combining Dex and Tra in ophthalmic patients, as altered ocular responses may influence diagnostic measurements and perioperative safety. Individualized sedative planning and close ocular monitoring are recommended, and further studies with extended follow-up and dose-response designs are needed to optimise feline ophthalmic sedation protocols.

CONFLICTS OF INTEREST

The authors declared that there is no conflict of interest.

ACKNOWLEDGMENT

The authors thank the clinical staff and technicians for their valuable assistance with animal handling and data collection.

AUTHOR CONTRIBUTIONS

Idea/Concept: AGB
Supervision/Consultancy: BB, YK
Data Collection and/or Processing: AGB, BB, ÖTO
Analysis and/or Interpretation: AGB, FT
Writing the Article: AGB, BB
Critical Review: FT, YK

REFERENCES

Aghababaei A, Ronagh A, Mosallanejad B, Baniadam A (2021). Effects of medetomidine, dexmedetomidine and their combination with acepromazine on the intraocular pressure (IOP), tear secretion and pupil diameter in dogs. *Vet Med Sci*, 7, 1090-1095.

Artigas C, Redondo JI, López-Murcia MM (2012). Effects of intravenous administration of dexmedetomidine on intraocular pressure and pupil size in clinically normal dogs. *Vet Ophthalmol*, 15(Suppl 1), 79-82.

Gelatt KN, Gelatt JP (Eds) (2011). Veterinary Ophthalmic Surgery. Elsevier/Saunders, St. Louis.

Gelatt KN, Gilger BC, Kern TJ (Eds) (2013). Veterinary Ophthalmology. 5th ed., Wiley-Blackwell, Ames.

Ghaffari MS, Malmasi A, Bokaie S (2010). Effect of acepromazine or xylazine on tear production as measured by Schirmer tear test in normal cats. *Vet Ophthalmol*, 13, 1-3.

Gölgeli Bedir A, Yanmaz LE, Okur S et al. (2025). The effect of maropitant, ondansetron and metoclopramide on dexmedetomidine-induced vomiting in cats. *Vet Med Sci*, 11(1), e70152.

Gómez de Segura IA, García-Fernández P (2023). Dexmedetomidine in cats: pharmacology and clinical applications. *Front Vet Sci*, 10, 1135124.

Hamed MA, Rizk MA, Hafez A, El-Mahdi AS, El-khodery SA (2018). Comparative effect of intravenous administration of medetomidine, tramadol, and medetomidine/tramadol combination on intraocular pressure in clinically healthy donkeys. *J Equine Vet Sci*, 69, 16-20.

Hartley C, Williams DL, Adams VJ (2006). Effect of age, gender, weight and time of day on tear production in normal dogs. *Vet Ophthalmol*, 9(1), 53-57.

Kato COS, Shimizu K, Kamiya K, Ishiwaka H, Igarashi A (2018). Effects of brimonidine tartrate 0.1% ophthalmic solution on the pupil, refraction, and light reflex. *Sci Rep*, 8, 9003.

Kaufman PL, Gabelt B (1995). Alpha2-adrenergic agonist effects on aqueous humor dynamics. *J Glaucoma*, 4(Suppl 1), S8-S14.

Kovalcuka L, Nikolajenko M (2020). Changes in intraocular pressure, horizontal pupil diameter and tear production during the use of topical 1% cyclopentolate in cats and rabbits. *Open Vet J*, 10(1), 59-67.

Leite J, Meireles A, Correia NA (2022). Valsalva retinopathy after a vomiting episode. *Case Rep Ophthalmol*, 13(3), 706-710.

Levin LA, Albert DM (2021). *Ocular Disease: Mechanisms and Management.* 2nd ed., Elsevier, London.

Maggs DJ (2013). *Slatter's Fundamentals of Veterinary Ophthalmology*. 5th ed., Elsevier, St. Louis.

Mattos-Junior E, Pypendop BH, Cabrini TM, Honsho CS, Nishimura LT (2021). Effects of dexmedetomidine alone or in combination with opioids on intraocular pressure in healthy Beagle dogs. *Vet Anaesth Analg*, 48(4), 541-544.

Maxwell KM, Odunayo A, Wissel C (2024). Use of orally administered dexmedetomidine to induce emesis in cats. *J Feline Med Surg*, 26(5), 1098612X241248980.

Mitchell N, Oliver J (2015). The cornea. In: *Feline Ophthalmology: The Manual* (pp. 103-128). Servet, Zaragoza.

Okur S, Yanmaz LE, Şenocak MG et al. (2022). Effects of medetomidine and dexmedetomidine on intraocular pressure, pupil size, and tear secretion in clinically normal Ghezel sheep. *Small Rumin Res*, 215, 106783.

Papastefanou AK, Galatos AD, Pappa E, Lymperis AG, Kostoulas P (2015). The effect of butorphanol on the incidence of dexmedetomidine-induced emesis in cats. *Vet Anaesth Analg*, 42, 608-613.

Reitsamer HA, Posey M, Kiel JW (2006). Effects of a topical α2-adrenergic agonist on ciliary blood flow and aqueous production in rabbits. *Exp Eye Res*, 82(3), 405-415.

Ruiz T, Peres TPS, Campos WNS, Sorte ECB, Ribeiro AP (2014). Effects of tramadol on tear production, intraocular pressure, and pupil size in dogs: clinical study. *Cienc Rural*, 45(4), 724-729.

Santos LCP, Ludders JW, Erb HN et al. (2011). A randomized, blinded, controlled trial of the antiemetic effect of ondansetron on dexmedetomidine-induced emesis in cats. *Vet Anaesth Analg*, 38, 320-327.

Schroder DC, Monteiro BG, Pytlak DB et al. (2018). Effects of tramadol and acepromazine on intraocular pressure and pupil diameter in young healthy cats. *Cienc Rural*, 48(3), e20170071.

Scott LJ, Perry CM (2000). Tramadol: a review of its use in perioperative pain. *Drugs*, 60(1), 139-176.

Sebbag L, Mochel JP, Romano E (2019). Tear film and ocular surface disorders in animals. *Vet Clin North Am Small Anim Pract*, 49(6), 1059-1073.

Slingsby LS, Murrell JC, Taylor PM (2010). Combination of dexmedetomidine with buprenorphine enhances the antinociceptive effect to a thermal stimulus in the cat compared with either agent alone. *Vet Anaesth Analg*, 37(2), 162-170.

Stadtbäumer K, Frommlet F, Nell B (2006). Measurements of tear production and intraocular pressure in clinically normal cats. *Vet Ophthalmol*, 9(4), 245-249.

Valtolina C, Robben JH, Uilenreef J et al. (2009). Clinical evaluation of the efficacy and safety of a constant rate infusion of dexmedetomidine for postoperative pain management in dogs. *Vet Anaesth Analg*, 36(4), 369-383.

Vartiainen J, MacDonald E, Urtti A, Rouhiainen H, Virtanen R (1992). Dexmedetomidine-induced ocular hypotension in rabbits with normal or elevated intraocular pressures. *Invest Ophthalmol Vis Sci*, 33(6), 2019-2023.

Wolfran L, Debiage RR, Lopes DM, Fukushima FB (2022). Ophthalmic effects of dexmedetomidine, methadone and dexmedetomidine-methadone in healthy cats and their reversal with atipamezole. *J Feline Med Surg*, 24(12), 1253-1259.

Yener K, Yavuz Ü, Hayat A et al. (2024). Effect of xylazine, midazolam and dexmedetomidine preanaesthetics on changes in intraocular pressure in rats. *Acta Sci Vet*, 52, 141948.

Van Veterinary Journal

https://dergipark.org.tr/tr/pub/vanvetj

Cite this article as: **Kocakaya A, Ünal N, Özbeyaz C, Dinç R (2026).** Morphometric Identification of Gemlik and Crossbreds. *Van Vet J*, 37(1), 92-97. DOI: https://doi.org/10.36483/vanvetj.1843971

ISSN: 2149-3359 **Original Article** e-ISSN: 2149-8644

Morphometric Identification of Gemlik Horse and Crossbreds

Afşin KOCAKAYA[1,*] Necmettin ÜNAL[1] Ceyhan ÖZBEYAZ[1] Recep DİNÇ[2,3]

[1] *Ankara University, Faculty of Veterinary Medicine, Department of Animal Breeding and Husbandry, 06070, Ankara, Türkiye*
[2] *Uludağ University, Graduate School of Health Science, 16059, Bursa, Türkiye*
[3] *Turkish Ministry of National Defense, Military Veterinary School and Training Center, Gemlik, Türkiye*

Received: 17.12.2025 Accepted: 23.02.2026

ABSTRACT This study aimed to morphometrically characterize Gemlik horses and their crossbreds, which originated from Holsteiner and KWPN lineages and have been bred since the early 2000s under the Turkish Ministry of National Defense. A total of 111 horses including pure Gemlik, Gemlik crossbred, and parental lines-were evaluated for various body measurements such as withers height, croup height, body length, chest depth, heart girth, neck length, and ear dimensions. Data were analyzed using the Kruskal-Wallis nonparametric test followed by Bonferroni-corrected post hoc comparisons due to the non-normal distribution of the data. Results revealed significant differences ($p<0.05$) among breeds for body length, heart girth, and interocular distance. Gemlik horses exhibited measurements generally aligned with their paternal Holsteiner and maternal KWPN lines, particularly in withers height (~166 cm) and live weight (~514 kg). Gender-based comparisons showed mares were significantly larger than stallions in several traits, including live weight, hind leg length, and chest width. Age also significantly influenced skeletal and muscular development, with older horses demonstrating greater withers height, body length, and heart girth. The findings suggest that Gemlik horses possess morphometric traits suitable for sport horse purposes, especially show jumping. The formal recognition of the Gemlik breed as a Turkish sport horse could support the development of national equestrian activities, accelerate its international competitiveness, and increase the recognition of equestrian sports among a wider audience.

Keywords: *Animal breeding, Body height, Body weight, Horse, Morphometry, Quantitative trait.*

ÖZ

Gemlik Atı ve Melezlerinin Morfometrik Olarak Tanımlanması

Bu çalışma, 2000'li yılların başından beri Türk Millî Savunma Bakanlığı çatısı altında Holsteıner X KWPN ırklarının melezlenmesiyle geliştirilen Gemlik ve Gemlik melezi atların morfometrik özelliklerini tanımlamayı amaçlamıştır. Toplam 111 baş attan (saf Gemlik, melezler ve ebeveyn ırklar) alınan veriler; cidago yüksekliği, sağrı yüksekliği, vücut uzunluğu, göğüs derinliği, göğüs çevresi, boyun uzunluğu ve kulak ölçüleri gibi morfometrik özellikler açısından incelenmiştir. Verilerin normal dağılım göstermemesi nedeniyle Kruskal-Wallis nonparametrik testi ve Bonferroni düzeltmeli çoklu karşılaştırmalar kullanılmıştır. Irk özelliklerine göre vücut uzunluğu, göğüs çevresi ve gözler arası mesafe açısından istatistiksel olarak anlamlı farklılıklar ($p<0.05$) saptanmıştır. Gemlik atları, özellikle ~166 cm cidago yüksekliği ve ~514 kg canlı ağırlık ile Holsteıner ve KWPN ırklarına benzer özellikler taşımaktadır. Cinsiyet analizlerinde dişilerin, erkeklerden canlı ağırlık, arka bacak uzunluğu ve göğüs genişliği gibi birçok ölçümde daha yüksek değerlere sahip olduğu görülmüştür. Yaş arttıkça iskelet ve kas gelişimine bağlı olarak cidago yüksekliği, vücut uzunluğu ve göğüs çevresinde artışlar kaydedilmiştir. Bulgular, Gemlik atının engel atlama spor dalı için uygun morfometrik yapıya sahip olduğunu göstermektedir. Gemlik atının bir Türk spor atı olarak tescil edilmesi, ulusal binicilik faaliyetlerinin gelişimini desteklemek ve uluslararası rekabet gücünü artırılmasını hızlandırarak binicilik sporunun daha geniş kitlelerce tanınmasını sağlayabilecektir.

Anahtar Kelimeler: *At, Hayvan ıslahı, Kantitatif özellik, Morfometri, Vücut ağırlığı, Vücut yüksekliği.*

INTRODUCTION

Horses, which have helped people in food, transportation, agriculture, trade, and warfare throughout history, were domesticated by the Turks in the Botai (Northern Kazakhstan) region of Turkestan about 5.500 years ago (Henner et al. 2002; Ünver 2006; Gücüyener Hacan and Akçapınar 2011; Neves et al. 2017; Özbeyaz 2019; Bailey and Brooks 2020; Akçapınar and Özbeyaz 2021; Durmuş 2021; Grilz-Seger et al. 2021; Klecel and Martyniuk 2021; Librado and Orlando 2021; Olsen 2025). Archaeological

✉ *Corresponding author: akocakaya@ankara.edu.tr

excavations in the Botai region have uncovered evidence of human-controlled management practices, including harnessing, tethering, milking, and sheltering (Outram et al. 2009; Librado and Orlando 2021; Olsen 2025).

In the early days, people who relied on horses for food, such as milk and meat, later discovered additional benefits and began using them for transportation, agriculture, and trade (Taşkın 2012; Durmuş 2021; Kocakaya et al. 2023). Horses rapidly emerged on the battlefield, demonstrating their speed and strength (Ünver 2006; Taşkın 2012; Durmuş 2020; Durmuş 2021; Kocakaya et al. 2023).

Turkish civilization, originating in the wide steppes of Turkestan and referred to as "steppe culture," expanded through the domestication of the horse (Ünver 2006; Durmuş 2021). By 800 BC, Turkish culture transformed the function of the horse, advancing it from a basic provider of sustenance, agriculture, and trade to a riding animal, thereby conclusively undermining the supremacy of adjacent cultures dependent on horse-drawn chariots through their adept horse archers and spear cavalry (Ünver 2006; Durmuş 2020; Durmuş 2021). By 700 BC, the horse-drawn carriage had entirely diminished in military significance and was repurposed as a racing vehicle in the ancient Olympic Games (Ünver 2006; Mann and Scharff 2020).

According to reports, Hiao, the Turkish-born emperor of the Chou dynasty in 900 BC, participated in equestrian sports (Ünver 2006). In this case, the Turks became the first nation to use horses for sporting purposes, about 200–300 years before the Olympics, in addition to their skillful use as a means of warfare (Ünver 2006; Durmuş 2020; Durmuş 2021; Durmuş 2023).

The Turks held competitions in equestrian sports; cirit (javelin), çöğen (polo), and gökbörü were held as equestrian sports (Ünver 2006; Taşkın 2012; Durmuş 2021; Durmuş 2023; Acar 2024). Horse carriage races and horse races with and without riders, held in Greece, Rome, and Eastern Rome (Byzantium), which started with the Olympics, continued for many years. With the Renaissance, equestrianism and horse training were considered a science and even an art in Italy and France, and equestrian schools started to be opened in these countries (Ünver 2006). The use of horses in war and sports developed and changed until 1896, when the Olympics, which were banned in 394 AD due to church pressure, resumed. Cavalry units were formed in different styles, and horses suitable for these styles were raised.

In the modern era, horse competitions are organized in branches such as dressage, jumping, three-day eventing, horse endurance, horse racing, horse gymnastics, and pony (Ünver 2006; Taşkın 2012; OSC 2017; TBF 2025). Although many Turkish riders have achieved success in various contests, particularly "Atatürk's Cavalry" (ASEM 2025), interest in equestrian sports remains low owing to a lack of a Turkish sport horse breed and insufficient public awareness of the sport.

The present study aims to determine the morphometric characteristics of Gemlik horses and Gemlik hybrid horses, which are the progeny of the breeding and crossbreeding of the "Gemlik Horse" (Holsteiner X KWPN) breed, which commenced in the early 2000s at the Military Veterinary School and Training Center Command of the Land Forces Command, with the objective of developing a native sport horse breed for participation in national and international show jumping competitions and other sport events.

MATERIAL AND METHODS

The Ankara University Animal Experiments Local Ethics Committee assessed the conformity of this research with ethical regulations, issuing a decision on 16.10.2024, numbered 2024-15-120.

The 111 horses included in the study comprised Gemlik, Gemlik crossbred, and parent line horses, all reared under the auspices of the Ministry of National Defense. The horses were weighed in kilograms (kg) using a scale that could detect half-kilogram increments. We measured the horses' Withers Height (WH), Croup Height (CrH), Front Leg Length (FLL), Hind Leg Length (HLL), Body Length (BL), Back Length (BaL), Chest Depth (CD), and Chest Width (CW) using a measuring cane. A tape measure was used to measure HG (Heart Girth), HL (Head Length), FL (Face Length), NL (Neck Length), DBE (Distance Between Eyes), DBEa (Distance Between Ears), EL (Ear Length), EW (Ear Width), SC (Shank Circumference), CrW (Croup Width), and CrL (Croup Length) in centimeters (Figure 1).

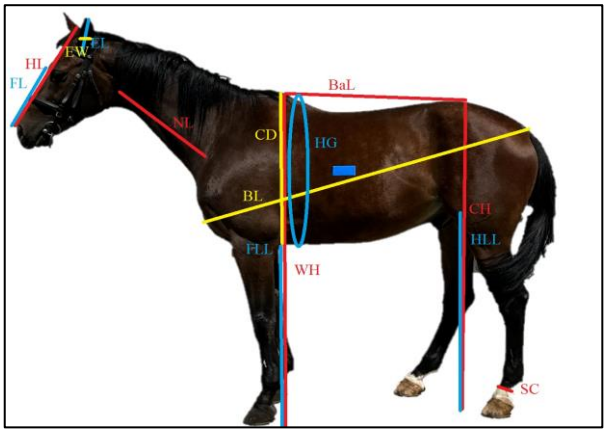

Figure 1: Some Body Dimensions on Gemlik horse.

Statistical Analysis

Power analysis was not performed, as the study was descriptive in nature and based on the available population.

The Shapiro-Wilk normality test was applied to the data obtained from 111 heads of horses for the morphometric identification of the Gemlik, and it was determined that the majority of the data did not comply with the normal distribution. For this reason, the Kruskal-Wallis non-parametric test was used to analyze the differences in morphometric characters between breed and age and the Mann-Whitney U test for the gender groups for the data obtained from 111 horses, which were the subject of the study. As a result of Kruskal-Wallis test, Bonferroni corrections were made for the characters whose differences were significant, and the analyses were finalized. All analyses were conducted using SPSS 30.0.

RESULTS

A normality test was applied to the data obtained as a result of the measurements. Since it was determined that the majority of the data did not comply with the normal distribution, the Kruskal-Wallis nonparametric test was applied, and differences in morphometric characters between breed (Table 1), gender (Table 2), and age (Table 3) groups were analyzed. Bonferroni correction was used to identify the groups with significant differences. In the comparisons performed according to breed and crossbreeding type (Table 1), statistically significant differences were identified in body length (BL), heart girth

(HG), and distance between eyes (DBE) ($p<0.05$). No significant breed-related differences were observed for the remaining morphometric traits. Although some crossbred combinations tended to exhibit relatively higher values in body size and thoracic measurements, these differences were limited to specific traits and did not indicate a consistent overall superiority pattern across all parameters. Gender-based comparisons (Table 2) revealed significant differences in live weight (LW), front leg length (FLL), body length (BL), back length (BaL), chest depth (CD), heart girth (HG), face length (FL), and shank circumference (SC) ($p<0.05$). In general, mares demonstrated higher values in traits associated with body mass and thoracic development. However, no statistically significant differences were found between stallions and mares for withers height, croup height, neck length, distance between eyes, distance between ears, or ear measurements. These findings suggest that sexual dimorphism in the studied population is more evident in body mass and musculoskeletal robustness than in linear height traits. Age-related analyses (Table 3) demonstrated significant differences in withers height (WH), croup height (CrH), front leg length (FLL), croup length (CrL), body length (BL), back length (BaL), chest width (CW), heart girth (HG), neck length (NL), distance between eyes (DBE), distance between ears (DBEa), and ear length (EL) ($p<0.05$). These measurements generally showed an increasing tendency with advancing age, reflecting skeletal growth and muscular development. In contrast, live weight, hind leg length, several cranial measurements, ear width, and shank circumference did not differ significantly among age groups. Overall, the morphometric variation observed in the study population was primarily associated with specific body length and thoracic traits across breeds, body mass-related characteristics across genders, and skeletal growth-related parameters across age groups.

Table 1: Body measurements of Gemlik horse and crossbreeds according to breed and crossbreeding type.

BD		LW (kg)		WH (cm)		CrH (cm)		FLL (cm)		CrL (cm)		HLL (cm)		CrW (cm)	
Breed	**N**	**Mean**	**SE**	**Mean**	**SE**	**Mean**	**SE**	**Mean**	**SE**	**Mean**	**SE**	**Mean**	**SE**	**Mean**	**SE**
GG	49	478.66	11.23	162.99	0.86	161.86	0.73	109.19	1.22	44.19	0.68	148.38	0.75	53.74	0.69
GH	21	488.52	15.34	166.71	0.96	163.82	0.84	113.86	1.52	46.76	1.04	150.43	1.15	57.02	1.07
GK	14	457.96	6.22	164.50	0.75	160.86	0.98	114.14	0.84	43.68	0.56	146.68	2.62	56.21	1.49
HolG	10	516.25	27.05	165.10	1.05	163.40	1.49	112.00	2.24	47.20	1.66	151.40	1.74	57.60	1.01
HolK	7	514.29	39.20	166.00	0.91	162.71	1.06	113.43	2.59	45.86	1.62	149.86	1.40	56.14	2.30
KG	5	555.60	50.71	167.00	0.71	165.20	0.86	111.80	5.44	48.40	1.17	148.10	1.81	58.60	3.31
KWPN	5	477.50	40.98	166.90	2.52	163.40	2.38	113.60	1.36	46.20	2.06	151.20	2.24	53.20	1.24
p		0.177		0.095		0.236		0.311		0.083		0.321		0.056	
BD		**BL (cm)**		**BaL (cm)**		**CW (cm)**		**CD (cm)**		**HG (cm)**		**HL (cm)**		**FL (cm)**	
Breed	**N**	**Mean**	**SE**	**Mean**	**SE**	**Mean**	**SE**	**Mean**	**SE**	**Mean**	**SE**	**Mean**	**SE**	**Mean**	**SE**
GG	49	157.92	0.97	65.76	1.76	41.60	0.82	71.58	0.75	186.00	1.61	52.86	0.44	36.30	0.47
GH	21	161.58	0.63	61.54	2.30	40.54	0.55	73.52	1.00	189.83	1.64	53.23	0.53	35.55	0.57
GK	14	159.54	1.07	56.86	1.01	37.64	0.83	72.29	0.62	185.48	0.99	52.68	0.38	36.21	0.58
HolG	10	160.65	1.34	63.40	2.92	41.70	2.14	75.20	1.23	191.30	2.78	52.55	0.96	37.60	0.70
HolK	7	166.64	2.51	64.57	3.77	42.36	2.15	74.00	2.16	189.93	4.00	54.71	1.04	37.43	1.34
KG	5	161.80	1.96	70.60	6.98	41.80	2.31	76.40	5.56	197.60	2.91	54.80	0.58	37.70	0.94
KWPN	5	159.50	3.91	64.60	5.44	41.40	1.11	72.60	2.73	191.00	4.59	50.90	0.68	35.80	1.02
p		0.041		0.169		0.119		0.339		0.022		0.071		0.312	
BD		**NL (cm)**		**DBE (cm)**		**DBEa (cm)**		**EL (cm)**		**EW (cm)**		**SC (cm)**			
Breed	**N**	**Mean**	**SE**	**Mean**	**SE**	**Mean**	**SE**	**Mean**	**SE**	**Mean**	**SE**	**Mean**	**SE**		
GG	49	56.22	0.84	18.13	0.21	15.35	0.32	16.67	0.20	5.64	0.08	19.97	0.17		
GH	21	54.31	0.88	17.10	0.30	14.88	0.28	16.29	0.39	5.71	0.12	20.31	0.20		
GK	14	53.43	1.21	17.64	0.34	14.29	0.45	16.93	0.22	5.93	0.16	20.00	0.15		
HolG	10	52.85	1.16	17.70	0.54	14.60	0.54	17.55	0.55	6.30	0.34	20.20	0.39		
HolK	7	57.43	1.09	19.00	0.31	16.00	0.58	17.21	0.71	6.00	0.38	21.07	0.41		
KG	5	52.40	1.17	19.10	0.40	14.30	0.37	16.90	0.40	6.20	0.37	21.70	0.77		
KWPN	5	56.00	1.45	18.80	0.73	14.00	0.42	16.60	0.51	6.00	0.00	20.20	0.66		
p		0.05		0.006		0.108		0.503		0.110		0.058			

Kruskal-Wallis was performed and $\alpha = 0.05$, Mean: Mean value, SE: Standard Error, GG: Gemlik, GH: Gemlik X Holsteiner, GK: Gemlik X KWPN, Holg: Holsteiner X Gemlik, Holk: Holsteiner X KWPN (Gemlik), KG: KWPN X Gemlik, KWPN: KWPN. BD: Body Dimensions, LW: Live Weight, WH: Withers Height, CrH: Croup Height, FLL: Front Leg Length, CrL: Croup Length, HLL: Hind Leg Length, CrW: Croup Width, BL: Body Length, BaL: Back Length, CW: Chest Width, CD: Chest Depth, HG: Heart Girth, HL: Head Length, FL: Face Length, NL: Neck Length, DBE: Distance Between Eyes, DBEa: Distance Between Ears, EL: Ear Length, EW: Ear Width, SC: Shank Circumference.

Table 2: Body measurements of Gemlik horses and crosses by gender.

BD		LW (kg)		WH (cm)		CrH (cm)		FLL (cm)		CrL (cm)		HLL (cm)		CrW (cm)	
SEX	**N**	**Mean**	**SE**	**Mean**	**SE**	**Mean**	**SE**	**Mean**	**SE**	**Mean**	**SE**	**Mean**	**SE**	**Mean**	**SE**
Stallion	48	454.10	4.01	165.25	0.68	162.73	0.59	114.34	0.91	45.35	0.64	148.59	0.75	54.72	0.73
Mares	63	512.00	11.79	164.14	0.67	162.35	0.61	109.40	1.01	45.21	0.60	149.37	0.82	55.87	0.65
p		0.001		0.283		0.463		<0.001		0.969		0.279		0.124	
BD		**BL (cm)**		**BaL (cm)**		**CW (cm)**		**CD (cm)**		**HG (cm)**		**HL (cm)**		**FL (cm)**	
SEX	**N**	**Mean**	**SE**	**Mean**	**SE**	**Mean**	**SE**	**Breed**	**N**	**Mean**	**SE**	**Mean**	**SE**	**Mean**	**SE**
Stallion	48	158.53	0.82	60.21	1.37	40.31	0.64	70.91	0.62	185.02	0.89	53.31	0.39	37.27	0.34
Mares	63	160.88	0.77	66.38	1.48	41.45	0.68	74.21	0.71	190.51	1.41	52.75	0.34	35.69	0.39
p		0.034		0.001		0.251		0.002		0.001		0.282		0.001	
BD		**NL (cm)**		**DBE (cm)**		**DBEa (cm)**		**EL (cm)**		**EW (cm)**		**SC (cm)**			
SEX	**N**	**Mean**	**SE**	**Mean**	**SE**	**Mean**	**SE**	**Mean**	**SE**	**Mean**	**SE**	**Mean**	**SE**		
Stallion	48	55.43	0.81	17.87	0.22	15.00	0.28	16.67	0.23	5.73	0.08	20.46	0.13		
Mares	63	54.85	0.57	18.04	0.18	14.99	0.23	16.81	0.17	5.88	0.09	20.03	0.17		
p		0.876		0.650		0.850		0.567		0.359		0.010			

Mann-Whitney U was performed and $\alpha = 0.05$, Mean: Mean value, SE: Standard Error. GG: Gemlik, GH: Gemlik X Holsteiner, GK: Gemlik X KWPN, Holg: Holsteiner X Gemlik, Holk: Holsteiner X KWPN (Gemlik), KG: KWPN X Gemlik, KWPN: KWPN. BD: Body Dimensions, LW: Live Weight, WH: Withers Height, CrH: Croup Height, FLL: Front Leg Length, CrL: Croup Length, HLL: Hind Leg Length, CrW: Croup Width, BL: Body Length, BaL: Back Length, CW: Chest Width, CD: Chest Depth, HG: Heart Girth, HL: Head Length, FL: Face Length, NL: Neck Length, DBE: Distance Between Eyes, DBEa: Distance Between Ears, EL: Ear Length, EW: Ear Width, SC: Shank Circumference.

Table 3: Body measurements of Gemlik horse and crosses according to their age.

BD		LW (kg)		WH (cm)		CrH (cm)		FLL (cm)		CrL (cm)		HLL (cm)		CrW (cm)	
Age	**N**	**Mean**	**SE**	**Mean**	**SE**	**Mean**	**SE**	**Mean**	**SE**	**Mean**	**SE**	**Mean**	**SE**	**Mean**	**SE**
1	**5**	402.30	28.33	153.80	5.01	153.80	3.69	98.00	5.13	34.80	2.44	145.40	3.78	47.50	2.57
2	**7**	461.71	10.68	159.86	1.08	159.43	0.97	101.00	2.05	45.43	2.65	149.14	1.16	51.57	1.78
3	**11**	466.45	15.00	162.00	0.80	158.36	0.78	112.27	1.58	44.36	0.62	147.23	1.24	55.09	0.91
4	**12**	472.75	6.12	166.58	0.57	164.25	0.83	115.33	0.94	43.88	0.77	148.75	3.21	58.25	1.61
5	**11**	466.64	23.20	163.09	1.19	161.64	1.19	111.36	1.87	45.36	0.75	147.09	1.30	54.36	1.11
6	**8**	473.50	10.67	167.38	1.19	165.94	1.36	116.19	2.36	45.75	0.92	150.25	1.94	55.75	1.72
7	**11**	526.36	28.52	166.82	1.31	164.52	1.03	111.45	2.55	45.14	1.13	150.41	2.14	56.09	1.02
8	**6**	505.58	24.14	169.08	1.94	165.83	0.91	111.83	3.60	48.00	1.29	150.00	2.59	54.33	1.78
9	**8**	514.25	27.75	163.19	0.77	162.13	0.95	111.63	2.34	45.00	1.13	149.38	1.07	55.25	1.11
10	**7**	485.14	36.99	165.79	1.91	162.21	1.54	113.43	2.57	45.43	1.13	149.00	1.70	55.71	1.43
11	**6**	555.42	48.23	166.58	1.19	165.25	1.03	109.00	2.38	45.50	2.20	149.83	1.47	57.17	2.56
12	**5**	459.70	7.41	165.40	1.03	163.10	1.29	118.70	1.00	50.00	1.82	148.00	2.93	60.30	3.95
13	**5**	529.00	58.25	166.80	1.33	164.00	2.30	113.20	3.02	48.00	1.76	152.00	2.63	56.40	2.62
14	**9**	497.22	35.06	166.11	1.22	163.53	1.27	112.50	1.89	47.56	1.86	150.61	1.19	55.22	1.64
p		0.218		<0.001		<0.001		0.003		0.013		0.682		0.115	

BD		BL (cm)		BaL (cm)		CW (cm)		CD (cm)		HG (cm)		HL (cm)		FL (cm)	
Age	**N**	**Mean**	**SE**	**Mean**	**SE**	**Mean**	**SE**	**Mean**	**SE**	**Mean**	**SE**	**Mean**	**SE**	**Mean**	**SE**
1	**5**	144.40	2.94	67.70	1.93	38.10	1.38	62.40	3.59	170.60	6.52	50.30	0.30	39.40	0.60
2	**7**	156.29	1.44	82.00	2.93	44.57	3.35	72.86	1.28	180.43	2.07	52.14	0.83	37.14	2.14
3	**11**	156.86	1.29	55.55	1.32	36.77	1.07	72.18	0.60	185.43	1.41	52.32	0.69	36.18	0.71
4	**12**	161.33	0.91	60.58	1.54	39.79	1.09	73.25	0.73	188.92	1.29	52.71	0.50	36.42	0.72
5	**11**	159.00	1.11	59.41	3.58	40.27	1.12	72.73	2.07	185.86	2.25	52.86	1.09	35.91	0.77
6	**8**	161.31	0.80	58.38	1.52	39.25	0.80	72.31	0.75	186.88	3.14	54.00	1.10	36.75	1.18
7	**11**	159.89	1.55	69.18	3.56	41.02	1.60	75.00	1.89	191.86	2.62	53.23	0.86	36.50	1.12
8	**6**	163.67	0.84	68.83	3.78	44.67	3.80	72.17	2.36	186.17	4.20	55.83	1.51	35.67	0.88
9	**8**	159.81	1.48	63.88	3.91	41.38	1.15	74.13	1.13	191.63	3.26	52.13	1.08	34.88	0.77
10	**7**	160.21	2.11	58.71	4.18	41.43	0.79	72.57	1.46	193.14	3.79	53.21	0.85	35.79	0.92
11	**6**	162.75	1.28	69.17	6.21	43.58	1.67	76.25	2.14	197.17	4.19	53.00	0.82	35.00	0.68
12	**5**	160.70	2.19	60.40	4.52	40.30	1.20	70.60	2.38	188.10	0.64	53.00	0.61	36.80	0.87
13	**5**	167.60	3.03	64.80	3.23	43.80	3.32	75.60	2.64	192.40	6.30	55.80	1.36	38.40	1.69
14	**9**	163.19	2.30	62.69	4.59	42.47	1.28	73.06	2.15	191.39	3.11	52.47	0.70	36.17	0.72
p		<0.001		<0.001		0.026		0.114		0.010		0.065		0.421	

BD		NL (cm)		DBE (cm)		DBEa (cm)		EL (cm)		EW (cm)		SC (cm)	
Ageed	**N**	**Mean**	**SE**	**Mean**	**SE**	**Mean**	**SE**	**Mean**	**SE**	**Mean**	**SE**	**Mean**	**SE**
1	**5**	64.50	3.52	20.20	0.20	19.20	1.19	16.53	0.14	5.67	0.12	19.60	0.68
2	**7**	57.57	3.26	18.71	0.68	15.79	0.96	17.12	0.74	6.02	0.57	20.43	0.43
3	**11**	52.82	0.85	17.27	0.24	13.64	0.31	17.18	0.42	5.73	0.14	19.73	0.30
4	**12**	52.79	1.45	17.50	0.48	14.58	0.54	16.96	0.28	6.08	0.15	20.00	0.25
5	**11**	54.64	1.18	17.91	0.37	15.00	0.38	16.86	0.27	5.55	0.16	19.73	0.51
6	**8**	54.38	1.05	17.88	0.13	15.13	0.69	17.13	0.40	5.69	0.16	20.17	0.48
7	**11**	54.00	0.94	17.45	0.57	14.55	0.52	15.86	0.39	5.68	0.12	19.73	0.20
8	**6**	54.17	2.73	18.75	0.44	15.17	0.46	16.92	0.80	6.00	0.37	20.67	0.40
9	**8**	56.00	1.43	16.88	0.35	14.00	0.46	15.88	0.67	5.75	0.16	20.19	0.19
10	**7**	54.71	1.80	17.71	0.27	15.21	0.24	17.36	0.32	5.86	0.26	20.60	0.37
11	**6**	55.50	0.96	18.67	0.61	15.00	0.63	17.50	0.67	6.17	0.21	21.00	0.52
12	**5**	53.10	1.21	17.00	0.99	14.40	0.66	15.00	0.88	5.40	0.25	21.00	0.55
13	**5**	58.60	0.83	19.00	0.32	16.20	0.20	18.40	0.51	6.60	0.40	21.00	0.45
14	**9**	55.39	1.22	18.50	0.50	14.89	0.61	16.17	0.41	5.56	0.18	20.56	0.47
p		0.047		0.002		0.018		0.038		0.160		0.142	

Kruskal-Wallis was performed and α = 0.05 Mean: Mean value, SE: Standard Error. GG: Gemlik, GH: Gemlik X Holsteiner, GK: Gemlik X KWPN, Holg: Holsteiner X Gemlik, Holk: Holsteiner X KWPN (Gemlik), KG: KWPN X Gemlik, KWPN: KWPN. BD: Body Dimensions, LW: Live Weight, WH: Withers Height, CrH: Croup Height, FLL: Front Leg Length, CrL: Croup Length, HLL: Hind Leg Length, CrW: Croup Width, BL: Body Length, BaL: Back Length, CW: Chest Width, CD: Chest Depth, HG: Heart Girth, HL: Head Length, FL: Face Length, NL: Neck Length, DBE: Distance Between Eyes, DBEa: Distance Between Ears, EL: Ear Length, EW: Ear Width, SC: Shank Circumference.

DISCUSSION AND CONCLUSION

The objective of the study was descriptive morphometric characterization rather than hypothesis testing of treatment or group effects, and since the sample size was constrained by population availability, power analysis was not conducted.

Size and morphometry are critical characteristics in practically all horse breeds. Numerous breed registries evaluate horses based on functional criteria and promote the breeding of horses with body types best suited for certain roles (Paksoy and Ünal 2019; Kaya et al. 2024).

When the body measurements of Gemlik and Crosses were evaluated according to their breed and crossbreeding type, KWPNXGemlik cross horses had higher values than Gemlik, KWPN, and other GEMLİK cross horses in terms of LW, WH, CH, CL, CW, BaL, CD, HG, HL, FL, HLL, and SC. The Gemlik (HolsteinerXKWPN) horse had greater values in terms of FLL, BL, CW, NL, and DBEa than the KWPN and other Gemlik crosses. HolsteinerxGemlik cross horses, on the other hand, had higher values in terms of HLL, DBEa, and EW than Gemlik, KWPN, and other Gemlik crosses.

The LW (514.29) of Gemlik horses, resulting from the crossbreeding of Holsteiner (Kelley 2002; Pitts and Shang 2016) and KWPN (Pitts and Shang 2016), both of which are half-blood and medium-weight breeds, varied from 449.00 to 800.50 kg, as recorded for Holsteiner; however, it was low to the 549.00-599.00 kg range reported for KWPN. The LWs of Gemlik horses were higher than the mean LW (Table 1) determined for KWPN in the same study. It was found to be higher than the weights reported by Taşkın (2012) for KWPN at the ages of 12 months (345.08 kg) and 24 months (468.86 kg), but similar to the average weight of 516.66 kg at the age of 36 months.

The average wither height (WH) of 166.00 cm in Gemlik horses is comparable to the Holsteiner breed (163–173 cm), which represents the paternal lineage. This measurement exceelineage andously reported values of 145.13–161.3 cm and 163.00 cm for the KWPN breed,

which is the maternal lineage, and aligns closely with the average value of 166.90 cm established in this study. In addition, the height of the stallion was found to be similar to the values reported by the Turkish Patent and Trademark Office for the Gemlik horse in 2002 (145.0-170.00 cm) (Türk Patent 2025).

The average croup height of Gemlik horses, measured at 162.71 cm, was found to be lower than the 163.40 cm recorded for KWPN in the same research and comparable to previously published figures for the KWPN breed (Taşkın 2012).

The heart girth (HG) of Gemlik horses was determined to be 189.93 cm in this research. This value was close to the 191.00 cm measurement established for KWPN in this research; however, it was smaller, similar to the 158.59–190.48 cm range documented for the KWPN breed (Taşkın 2012) and comparable to the 150.00–200.00 cm range (Türk Patent 2025) previously noted for the Gemlik horse.

The study revealed that the mean chest width (CW) of Gemlik horses was 42.36 cm, comparable to the 41.40 cm recorded for the maternal line KWPN within the same research. However, this measurement was significantly lower than the previously documented value of 47.63 cm for the father line Holsteiner breed (Alagić et al. 2002). The chest depth of 74.00 cm observed in Gemlik horses exceeds the 72.60 cm recorded for KWPN, which serves as the primary reference in the same study. The values observed were comparable to the 73.50–74.35 cm range reported for the Holsteiner breed, which represents the paternal lineage (Alagić et al. 2002). The study found that the shank circumference value of 21.07 cm for Gemlik horses aligns with previously reported values of 19–21 cm. Additionally, the value of 20.20 cm for the KWPN, a primary line, is consistent with earlier reports of 19.23–21.03 cm for the KWPN breed (Brown and Carton 2021). In the same study, the body length of 166.64 cm for Gemlik horses was found to exceed the 159.50 cm recorded for the maternal line KWPN (Brown and Carton 2021), while being lower than the 172.32-173.14 cm values reported for the HOLSTEINER breed, which was previously the paternal line (Alagić et al. 2002).

The Kruskal-Wallis test was conducted on the data from Gemlik and Gemlik cross horses, with Bonferroni correction used for multiple comparisons. It was concluded that the statistical differences between Gemlik and Crosses were substantial ($p<0.05$) for BL, HG, and DBE traits. The body length (BL) differed significantly between Gemlik and Gemlik Cross horses. The post hoc test revealed significant differences among KWPN-Gemlik horses, GG-GK crosses, GG-Gemlik horses, and KG-GH crosses ($p<0.05$). Upon using the Bonferroni correction, the comparisons yielded insignificant results ($p>0.05$).

Upon evaluating the body measurements of Gemlik and Crosses by gender, it was noted that mares had superior LW values in comparison to stallions. End-gestational live weight in mares is 13-14% more than the beginning-gestational LW (Paksoy and Güngör, 2023). This differential is attributed to the mares' greater use for breeding rather than competing. Upon evaluating Table 2, it is evident that mares exhibit superior values in HLL, CW, BL, BaL, CD, SC, HL, DBE, DBEa, and EW characteristics compared to stallions. The Mann-Whitney U test findings indicated significant variations in body structure-related characteristics, including LW, FLL, BL, BaL, CD, HG, FL, and SC, based on gender ($p<0.05$).

When the body measurements of Gemlik and Crosses were evaluated according to their genders, the differences between the age groups in the characters of WH, CH, FLL, CW, BL, BaL, CW, HG, NL, DBE, DBEa, and EL were significant ($p<0.05$). Measurements such as BL, WH, CH, and FLL are usually related to skeletal growth, so they are expected to increase with age. The results obtained in the study confirm this expectation (Table 3). Heart Girth (HG) is related to respiratory capacity and muscle development. There is a significant increase in groups that have reached adulthood at the age of six and above (Table 3). In general, significant differences in certain characteristics are observed among age groups, which is believed to be due to the use of the Holsteiner breed as the paternal line.

The body measures of the Gemlik horse analyzed in the study were compared with those of the Holsteiner paternal line and the KWPN maternal line. The breeds, including both the paternal and maternal lineages of the Gemlik horse, are used as jumping sport horses. The body dimensions of the Gemlik horse closely reflect those of the Holsteiner lineage, which is its paternal line. Further research is required on the Gemlik horse, now competing in events organized by the Turkish Equestrian Federation as a show jumper, particularly about its paternal and maternal lineage, and it should be officially classified as a Turkish sports horse. This aspect is expected to elevate and promote Turkish equestrian sport, augmenting its worldwide prominence. This acknowledgment may result in greater investment in breeding programs and training facilities, hence enhancing competitive stature internationally. As interest in the Gemlik horse increases, chances for cooperation and interaction among equestrian enthusiasts globally may also expand.

CONFLICTS OF INTEREST

The authors report no conflicts of interest.

ACKNOWLEDGMENT

We thank Turkish Ministry of National Defense for their permission, assistance and hospitality in conducting the study.

AUTHOR CONTRIBUTIONS

Idea/Concept: AK, NÜ, CÖ
Supervision/Consultancy: NÜ, CÖ
Data Collecting and/or Processing: AK, RD
Analysis and/or Interpretation: AK
Writing the Article: AK
Critical Review: NÜ, CÖ

REFERENCES

Acar G (2024). Forgotten Heritage in Turks: An Analysis on Equestrianism and Horse Breeding. *Iğdır University Journal of Sports Sciences*, 7(1), 18-26.

Akçapınar H, Özbeyaz C (2021). Animal Husbandry (Basic Knowledge). 2nd Ed. Medisan, Ankara.

Alagić D, Seleš J, Seleš I, Meštrović M (2002). Body measures and indexes of the Holstein horses reared in Krizevci. *Acta Agr Kapos*, 6(2), 125-130.

ASEM (2025). History. Available from: 04 December 2025. Access Address: https://kho.msu.edu.tr/spor/ASEM/ASEM_tarihce.html.

Bailey E, Brooks SA (2020). Horse genetics. 3. Edition. CABI, Wallingford, Oxfordshire, UK.

Brown S, Carton S (2021). Horses and Ponies. I. Edition. DK Penguin Random Houses. NY, USA.

Durmuş E (2020). Military Structure in Ancient Turks. *Asya Araştırmaları USBD*, 4(1), 87-102.

Durmuş İ (2021). Horse in Turkish Culture Region. *Asya Araştırmaları USBD*, 5(1), 1-12.

Durmuş İ (2023). Formation and Development of Turkish Personality in the Steppe Culturel Environment. *ASYAR*, 7 (Cumhuriyet'in 100. Yılına Armağan Özel Sayısı), 7-18.

Grilz-Seger G, Mesarič M, Brem G, Cotman M (2021). Characterization of coat color in the Slovenian Posavje horse. *Slov Vet Res,* 58(2), 77 – 84.

Gücüyener Hacan O, Akçapınar H (2011). Some phenotypic and genetic parameters of purebred Turkish Arabian horses raised in different stud farms I. body measurements and heritabilities. *Livestock Studies*, 1(2), 55-70.

Henner J, Poncet PA, Guerin G, et al. (2002). Genetic mapping of the (G) - locus, responsible or the coat color phenotype "progressive greying with age" in horses (Equus caballus). *Mamm Genome,* 13, 535-537.

Kaya ZK, Paksoy Y, Koluman N (2024). The Effect of Age, Gender and Feeding Method on Some Body Measurements in Pony Horses. *Journal of Animal Production*, 65(1), 59-65.

Kelley B (2002). The Horse Library. Horse Breeds of the World. I. Edition. Chelsea House Publishers, USA.

Klecel W, Martyniuk E (2021). From the Eurasian Steppes to the Roman Circuses: A Review of Early Development of Horse Breeding and Management. *Animal,*11, 1859.

Kocakaya A, Paksoy Y, Özbeyaz C (2023). Color and marking distribution in Arabian and Thoroughbred horses. *Vet Hekim Der Derg*, 94(2), 110-118.

Librado P, Orlando L (2021). Genomics and the Evolutionary History of Equids. *Annu Rev Anim Biosci,* 9, 81-101.

Mann C, Scharff S (2020). Horse Races and Chariot Races in Ancient Greece: Struggling for Eternal Glory, *IJHS*, 37(3-4), 163-182.

Neves AP, Schwengber EB, Albrecht FF, Isola JV, Van der Linden LS (2017). Beyond Fifty Shades: The Genetics of Horse Colors. Abubakar M (Ed). Trends and Advances in Veterinary Genetics. (pp. 75-100) IntechOpen. Sage, London, UK.

Olsen S (2025). The Early Horse Herders of Botai, Available from: 04 December 2025. Access Address: https://biodiversity.ku.edu/archaeology/research/early-horse-herders.

OSC (2017). History of equestrian sport at the Olympic games in OSC (The Olympic Studies Centre) Reference Collection. Available from: 04 December 2025. Access Address: https://stillmed.olympic.org.

Outram AK, Stear NA, Bendrey R et al. (2009). The earliest horse harnessing and milking. *Science*, 323(5919), 332-35.

Özbeyaz C (2019). Horse breeding. Yarsan E (Ed). Equine Medicine (pp.19-52). Güneş Tıp Kitapevleri, Ankara.

Paksoy Y, Ünal (2019). Multivariate analysis of morphometry effect on race performance in Thoroughbred horses. *R. Bras. Zootec,* 48: e20180030.

Paksoy Y, Güngör ÖF (2023). Some Parturition and Birth-Related Traits and Foal Behaviors of Thoroughbred Horses. *KSU J Agric Nat,* 27(3), 727-734.

Pitts G, Shang K (2016). The Horse Encyclopedia. I. Edition. DK Penguin Random Houses. NY, USA.

Taşkın D (2012). Factors Affecting Live Weight, Body Measurements, Incidence of Disease, Vitality and Fecundity in Concubine Horses. PhD Thesis, Afyon Kocatepe University, Institute of Health Sciences, Afyonkarahisar, Türkiye.

TBF (2025). Branches. Available from: 04 December 2025. Access Address: https://www.binicilik.org.tr/.

Türk Patent (2025). Gemlik horse. Certificate of registration of geographical indication. Available from: 04 December 2025. Access Address: https://ci.turkpatent.gov.tr/cografi-isaretler/detay/37901.

Ünver AF (2006). Equestrian sports from antiquity to modern Olympics and Olympic development of Turkish equestrianism. Available from: 04.12.2025. Access Address: https://www.binicilik.org.tr/Anasayfa/EYayinlar.

Van Veterinary Journal

https://dergipark.org.tr/tr/pub/vanvetj

Cite this article as: **Akgöz S, Nuhay Ç, Adalıoğlu Çimenlidağ EÇ et al. (2026).** Molecular Identification, Biofilm Formation Ability and Antimicrobial Resistance of *Staphylococcus Warneri* Isolates Obtained from Mastitic Cows in the Aegean Region. *Van Vet J*, 37(1), 98-103. DOI: https://doi.org/10.36483/vanvetj.1849676

ISSN: 2149-3359 **Original Article** e-ISSN: 2149-8644

Molecular Identification, Biofilm Formation Ability and Antimicrobial Resistance of *Staphylococcus warneri* Isolates Obtained from Mastitic Cows in the Aegean Region

Serhan AKGÖZ[1, *] Çağatay NUHAY[1] Emine Çiler ÇİMENLİDAĞ ADALIOĞLU[1] Aliye Ebru ÇELİK[1] Ceren HALICI DEMİR[1] Aslı GÖNÜLKIRMAZ[1] Nizamettin YÜCEDAĞ[1]

[1]*İzmir Bornova Veterinary Control Institute, Bacteriology Laboratory, 35040, İzmir, Türkiye*

Received: 26.12.2025 Accepted: 9.02.2026

ABSTRACT *Staphylococcus warneri* is a species belonging to the coagulase-negative *staphylococci* (CoNS) group and is commonly found as a commensal organism on the skin and mucosal surfaces of humans and animals. In recent years, the increasing isolation rates of CoNS from milk and dairy products have highlighted their significance in terms of both food safety and livestock production. This study aimed to confirm *S. warneri* isolates obtained from milk samples using molecular methods, to evaluate their biofilm-forming ability through the Congo Red Agar (CRA) method, and to determine their phenotypic antimicrobial resistance profiles. For this purpose, 650 milk samples were examined, the presence of *S. warneri* was investigated using phenotypic identification methods, and suspected isolates were confirmed by Polymerase Chain Reaction (PCR). The biofilm-forming ability of isolates identified as *S. warneri* was assessed on CRA medium. In addition, the susceptibility of the isolates to eight different antibiotics was determined by the Kirby-Bauer disk diffusion method according to CLSI standards. Among the 650 samples analyzed, 21 isolates were found to be positive for *S. warneri*, and all isolates demonstrated biofilm-forming capacity. According to the antibiotic susceptibility results, the isolates exhibited resistance to oxacillin (90.5%), trimethoprim–sulfamethoxazole (81.0%), penicillin (47.6%), tetracycline (38.1%), chloramphenicol (23.8%), erythromycin (14.3%), and doxycycline (14.3%), while all isolates were fully susceptible to gentamicin (100%). In conclusion, the presence of *S. warneri*, a CoNS species, in dairy cattle within the sampling region was confirmed; their biofilm-forming abilities were determined; and the most appropriate antibiotic options for treatment were evaluated phenotypically based on resistance profiles.

Keywords: *Antibiotic resistance, Biofilm, Staphylococcus warneri.*

ÖZ

Ege Bölgesindeki Mastitisli Sığırlardan İzole Edilen *Staphylococcus warneri* Suşlarında Moleküler Tanımlama, Biyofilm Oluşturma Yeteneği ve Antimikrobiyal Direncin Değerlendirilmesi

Staphylococcus warneri, koagulaz-negatif stafilokoklar (KNS) arasında yer alan ve insan ile hayvanların deri ve mukozalarında kommensal olarak bulunan bir türdür. Son yıllarda süt ve süt ürünlerinde KNS türlerinin artan oranlarda izole edilmesi, bu bakterilerin hem gıda güvenliği hem de hayvansal üretim açısından önemini artırmıştır. Bu çalışma, süt örneklerinden izole edilen *Staphylococcus warneri* suşlarının moleküler yöntemlerle doğrulanması, biyofilm oluşturma kapasitelerinin Congo Red Agar (CRA) yöntemiyle değerlendirilmesi ve antimikrobiyal direnç profillerinin fenotipik olarak ortaya konması amacıyla yürütülmüştür. Bu amaçla 650 süt örneği incelenmiş, fenotipik yöntemlerle *S. warneri* varlığı araştırılmış ve şüpheli izolatlar PCR ile doğrulanmıştır. *S. warneri* olarak tanımlanan izolatların biyofilm oluşturma yeteneği CRA besiyeri kullanılarak değerlendirilmiştir. Ayrıca izolatların sekiz farklı antibiyotiğe karşı duyarlılığı CLSI standartlarına göre Kirby-Bauer disk difüzyon yöntemi ile belirlenmiştir. Çalışmada 650 örnekten elde edilen 21 izolatın *S. warneri* yönünden pozitif olduğu ve tüm izolatların biyofilm oluşturma yeteneğine sahip olduğu tespit edilmiştir. Antibiyotik duyarlılık sonuçlarına göre izolatlarda %90.5 oksasilin, %81.0 trimetoprim-sülfametoksazol, %47.6 penisilin, %38.1 tetrasiklin, %23.8 kloramfenikol, %14.3 eritromisin ve doksisiklin direnci görülürken; tüm izolatların gentamisine karşı %100 duyarlı olduğu belirlenmiştir. Sonuç olarak, örnekleme bölgesindeki süt sığırlarında KNS türlerinden *S. warneri* varlığı ortaya konulmuş, biyofilm oluşturma kapasiteleri belirlenmiş ve tedavide kullanılabilecek en uygun antibiyotik seçenekleri fenotipik olarak değerlendirilmiştir.

Anahtar Kelimeler: *Antibiyotik direnci, Biyofilm, Staphylococcus warneri.*

✉ *Corresponding author: akgozserhan@gmail.com

INTRODUCTION

The family Staphylococcaceae comprises the genus *Staphylococcus*, a diverse group of Gram-positive bacteria that colonize humans and warm-blooded animals as commensals. These species are traditionally classified as coagulase-negative or coagulase-positive depending on their ability to clot rabbit plasma (Locatelli et al. 2023). Coagulase-negative *staphylococci* (CoNS) are among the bacteria most frequently isolated from clinical and subclinical mastitis in dairy cows (Phophi et al. 2019). Although they have long been regarded as "minor pathogens" (Hamel et al. 2020; Ryman et al. 2021), intramammary infections caused by CoNS often tend to resolve spontaneously; however, clinical mastitis cases requiring antimicrobial treatment have also been reported (Taponen et al. 2006; Phophi et al. 2019). In the specific context of Türkiye, the etiology of mastitis has been shown to involve a spectrum of pathogens, ranging from *Corynebacterium pseudotuberculosis* (Nuhay 2025) to major agents like *Staphylococcus aureus* (Sezener et al. 2019). Among these species, *Staphylococcus warneri* (*S. warneri*) is a coagulase-negative staphylococcal species that is increasingly being identified in dairy cattle and attracts attention with its distinct phenotypic characteristics (Getahun et al. 2024).

The name *S. warneri* was given after the bacterium was first isolated in 1975 by Wesley E. Kloos and Karl H. Schleifer from a patient named Arthur Warner Jr. In their collection of 38 isolates, Kloos and Schleifer described in detail the main morphological and phenotypic features of *S. warneri*. The bacterial cells measure approximately 0.5–1.2 µm in diameter and are usually observed singly or in pairs, and less frequently in tetrads. This non-motile, non-spore-forming species are resistant to lysozyme and slightly resistant to lysostaphin, with weak or absent hemolytic activity and variable bacteriolytic activity among isolates. In terms of colony morphology, *S. warneri* forms small, entire, circular, smooth and slightly sticky colonies. Approximately 80% of the isolates produce bright yellow-orange pigment, while the remaining 20% form non-pigmented, white-grey colonies. These features are important phenotypic criteria that help distinguish *S. warneri* from other coagulase-negative staphylococcal species (Kloos and Schleifer 1975; Ravaioli et al. 2024).

S. warneri has been detected in approximately 50% of healthy humans and is considered a common saprophyte and component of the normal skin microbiota (Balows et al. 1991). It can also be found on mucosal surfaces such as the nasal and oral cavities (Rasmussen et al. 2000; Regecová et al. 2022). In addition, the presence of *S. warneri* has been reported in foods of animal origin, including raw milk and dairy products, poultry, pork, beef and wild rabbit meat (Regecová et al. 2022; Sivaraman et al. 2022; Yilmaz and Berik 2024). As an opportunistic pathogen, this species can act as an etiological agent of a wide range of infections (Alves et al. 2015). Indeed, *S. warneri* has been reported in association with clinical conditions such as native-valve endocarditis, vertebral osteomyelitis, discitis, urinary tract infections, neonatal sepsis, meningitis related to ventriculoperitoneal shunts, subdural empyema and bacteremia in humans (Ravaioli et al. 2024). In veterinary medicine, *S. warneri* has also been implicated in various conditions, including abortion in cattle (Barigye et al. 2007), mastitis (de Oliveira et al. 2022) and meningoencephalitis in dogs (Espino et al. 2006). Moreover, it has been detected as a commensal species in rainbow trout, where, under suitable conditions, it may act as an indirect pathobiont facilitating the colonization and growth of pathogens such as *Vibrio anguillarum* (Musharrafieh et al. 2014). The ability of *S. warneri* to cause severe systemic infections such as bacteremia and septicemia, combined with high rates of antibiotic resistance and biofilm production, highlights the need for more comprehensive investigation of this species. Nevertheless, current knowledge on the molecular epidemiology of *S. warneri* and the mechanisms underlying its pathogenicity remains incomplete (Azimi et al. 2020).

Therefore, the present study was conducted to determine the molecular identification, biofilm-forming capacity and phenotypic antimicrobial resistance characteristics of *S. warneri* isolates obtained from mastitic dairy cows in the Aegean region of Türkiye.

MATERIAL AND METHODS

For the implementation of the study, an application was submitted to the Animal Experiments Ethics Committee of the Bornova Veterinary Control Institute. The Committee stated in its decision dated 18.12.2025 and numbered 2025/6 that ethical approval was not required for this research.

Sample Collection and *S. warneri* Identification

The material of the study consisted of milk samples obtained from 650 mastitic cows submitted to the Bornova Veterinary Control Institute for routine microbiological diagnosis from various commercial dairy farms located in the Aegean region of Türkiye between 2020 and 2025. After arrival at the laboratory, all milk samples were processed following the laboratory procedures recommended by the National Mastitis Council (National Mastitis Council 2017).

Milk samples were streaked onto blood agar plates and incubated for 24 hours. Colony morphology was evaluated, and suspicious colonies were subjected to Gram staining. Isolates displaying Gram-positive cocci morphology were further examined by catalase testing. Catalase-positive isolates were considered consistent with Staphylococcus species. These isolates were subsequently analyzed for species-level identification using the VITEK-2 Compact automated system (bioMérieux, France).

DNA Extraction and Molecular Identification

Genomic DNA was extracted using the High Pure PCR Template Preparation Kit (Roche, Germany), and the samples were stored at -20 °C until further analysis. Molecular confirmation of *S. warneri* was performed using primer targeting the *sodA* gene (F:5'-GTAACAAAATTAAATGCAGCTG-3'; R:5'-TCTTACTGCAGTTTGAATATCAGA-3') (Kim et al. 2018). A synthetic *S. warneri* (Letgen Biyoteknoloji, Türkiye) positive control was included in each PCR run.

PCR reactions were prepared in a final volume of 20 µL, containing 12.5 µL Xpert Fast Hotstart Mastermix (2x, GRiSP, Portugal), 2 µL forward primer, 2 µL reverse primer, 3.5 µL nuclease-free water and 5 µL template DNA. Amplification was carried out in a Techne TC-412 thermal cycler (Keison Products, UK) under the following cycling conditions: initial denaturation at 94 °C for 3 min; 40 cycles of denaturation at 94 °C for 15 s, annealing at 57 °C for 30 s, and extension at 72 °C for 15 s; followed by a final extension at 72 °C for 3 min. PCR analysis yielded a specific 110-bp amplicon in all isolates phenotypically identified as *S. warneri*, confirming species-level identification (Kim et al. 2018).

Determination of Biofilm Formation by Congo Red Agar

Biofilm-forming capacity was assessed using the Congo Red Agar (CRA) method described by Freeman et al. (1989). Isolates were streaked onto CRA (Sigma-Aldrich, USA) plates and incubated at 37 °C for 24–48 h. Colonies exhibiting black, dry, and rough morphologies were classified as biofilm-positive, whereas those forming red, burgundy, or pink, smooth and shiny colonies were considered biofilm-negative. Biofilm production on CRA was evaluated in duplicate for each isolate.

Antibiotic Susceptibility Test

Antimicrobial susceptibility of the isolates was determined using the Kirby–Bauer standard disk diffusion method. Eight antibiotics representing commonly used antimicrobial classes were tested using commercial disks (Bioanalyse, Türkiye): penicillin (P; 10 µg), gentamicin (CN; 10 µg), chloramphenicol (C; 30 µg), tetracycline (TE; 30 µg), erythromycin (E; 15 µg), trimethoprim–sulfamethoxazole (SXT; 1.25/23.75 µg), doxycycline (DO; 30 µg), and oxacillin (OX; 1 µg). Susceptibility results were interpreted according to the Clinical and Laboratory Standards Institute (CLSI, 2024) guidelines. All antibiotic susceptibility tests were performed in duplicate to ensure reproducibility.

Statistical Analysis

The data obtained in this study were analyzed using descriptive statistical methods. The prevalence of *S warneri* among mastitic milk samples was expressed as percentages. Biofilm production results and antimicrobial susceptibility profiles were evaluated based on the proportion of positive, intermediate and resistant isolates. No comparative or inferential statistical tests were applied, as the study was designed to provide a descriptive evaluation of isolation frequency, biofilm-forming ability and antimicrobial resistance patterns of *S. warneri* isolates.

RESULTS

Isolation and Identification of *S. warneri*

A total of 650 milk samples obtained from mastitic cows in the Aegean region were examined, and 21 isolates (3.2%) were identified as *S. warneri* based on colony morphology, Gram staining, catalase activity, and species-level identification using the VITEK-2 Compact system.

Molecular Confirmation of *S. warneri* Isolates

All 21 isolates were confirmed as *S. warneri* by *sodA*-targeted PCR, which consistently produced the characteristic 110-bp amplicon (Figure 1).

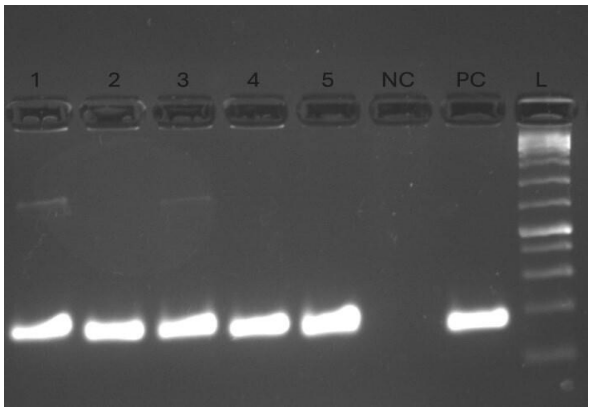

Figure 1: PCR confirmation of *S. warneri*.

L=100 bp DNA ladder, PC=positive control, NC=negative control, lanes 1-5= *S. warneri* isolates.

Determination of Biofilm Formation by Congo Red Agar

All 21 *S. warneri* isolates demonstrated biofilm-forming capacity on Congo Red Agar (CRA). Following incubation, all isolates developed black, dry, and rough colonies, which are characteristic of biofilm-positive staphylococci. No isolate exhibited red, burgundy, or pink, smooth colonies, which are indicative of biofilm-negative phenotypes (Figure 2).

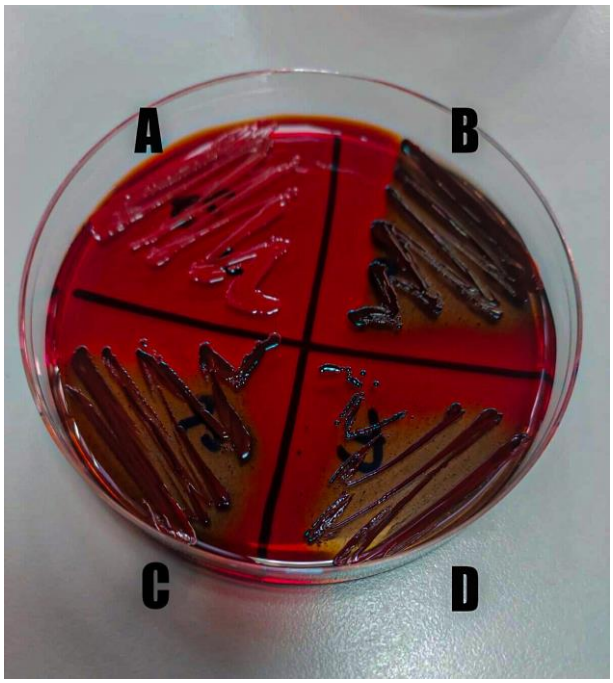

Figure 2: Biofilm formation of *Staphylococcus warneri* on Congo Red Agar.

A=Negative Control, B=Positive Control, C-D=Representative isolates.

Antibiotic Susceptibility Test

In this study, the antibiotic susceptibility of 21 *Staphylococcus warneri* isolates which were obtained from mastitic bovine milk samples was evaluated using the disk diffusion method. The results are presented in Table 1.

Table 1: Antibiotic resistance of *S. warneri* isolates obtained from bovine milk samples.

Isolate	P	CN	E	DO	SXT	C	TE	OX
1	S	S	S	S	R	S	R	R
2	R	S	R	S	S	S	S	S
3	R	S	S	S	S	S	R	S
4	S	S	S	S	S	S	S	R
5	S	S	S	S	R	R	S	R
6	S	S	S	S	R	S	S	R
7	S	S	S	S	R	R	S	R
8	R	S	S	S	R	S	S	R
9	R	S	S	S	R	R	S	R
10	R	S	S	S	R	S	S	R
11	R	S	S	S	R	R	R	R
12	R	S	R	S	R	S	S	R
13	R	S	R	S	R	S	R	R
14	S	S	S	S	R	S	S	R
15	R	S	S	S	R	R	S	R
16	S	S	S	S	R	S	R	R
17	S	S	S	S	R	S	R	R
18	S	S	S	S	R	S	R	R
19	R	S	S	R	S	S	R	R
20	S	S	S	R	R	S	S	R
21	S	S	S	R	R	S	S	R

According to CLSI (2024), all S. *warneri* isolates were susceptible to gentamicin (100%). High susceptibility rates were also observed for erythromycin and doxycycline (85.7%), followed by chloramphenicol (76.2%). Susceptibility rates were 61.9% for tetracycline and 52.4% for penicillin. The lowest susceptibility rates were recorded for oxacillin (9.5%) and trimethoprim–sulfamethoxazole (19.0%). Among the 21 *S. warneri* isolates, resistance profiles varied considerably. One isolate was resistant to a single antibiotic, four isolates were resistant to two antibiotics, ten isolates were resistant to three antibiotics, four isolates were resistant to four antibiotics, and two isolates showed resistance to five different antibiotics (Table 2).

Table 2: Antibiotic susceptibility profile of *S. warneri* isolates.

Antibiotic	Resistant n (%)	Susceptible n (%)
Penicillin	10 (47.6%)	11 (52.4%)
Gentamicin	0 (0%)	21 (100%)
Erythromycin	3 (14.3%)	18 (85.7%)
Doxycycline	3 (14.3%)	18 (85.7%)
Trimethoprim-sulfamethoxazole	17 (81%)	4 (19%)
Chloramphenicol	5 (23.8%)	16 (76.2%)
Tetracycline	8 (38.1%)	13 (61.9%)
Oxacillin	19 (90.5%)	2 (9.5%)

DISCUSSION AND CONCLUSION

In the present study, *Staphylococcus warneri* was isolated from 3.2% (21/650) of milk samples obtained from mastitic cows in the Aegean region of Türkiye. Non-aureus staphylococci (NAS), including coagulase-negative staphylococci (CoNS), are now recognized as some of the most frequently isolated pathogens from bovine milk worldwide and are increasingly implicated in both clinical and subclinical intramammary infections (Hamel et al. 2020; De Buck et al. 2021). Although NAS have historically been regarded as "minor pathogens", their impact on udder health, somatic cell count and milk quality has become more evident in recent years (Traversari et al. 2019; Addis et al. 2024). Within this group, *S. warneri* is generally less prevalent than species such as *S. chromogenes*, *S. haemolyticus* or *S. epidermidis*, but several studies have confirmed its presence in bovine milk and mastitis cases (Hosseinzadeh and Saei 2014). For example, Mello et al. (2020) reported *S. warneri* in 3.3% of staphylococcal isolates from subclinical bovine mastitis, a proportion comparable to the 3.2% observed in our study. These data suggest that, although *S. warneri* is not among the most dominant NAS species in dairy herds, it represents a consistent component of the mastitis-associated staphylococcal flora. The relatively low isolation rate (3.2%) observed in this study may be attributed to the ecological dominance of other major pathogens or potentially to the widespread empirical use of broad-spectrum antimicrobials in the region, which might limit the detection of susceptible CoNS species like *S. warneri* in clinical samples.

Our isolates were first identified phenotypically using colony morphology on blood agar, Gram staining, catalase testing and species-level identification by VITEK-2, and subsequently confirmed by *sodA*-based PCR. The use of molecular methods targeting housekeeping genes such as *sodA*, *tuf* or *gap* has been widely recommended to overcome the limited discriminatory power of 16S rRNA sequencing and phenotypic tests for CoNS species (Kooken et al. 2014; Kim et al. 2018). Kim et al. (2018) developed *sodA*-specific multiplex PCR primers that allowed rapid and accurate identification of multiple CoNS species, demonstrating higher accuracy than conventional phenotypic identification. Our findings are consistent with this approach, as all 21 isolates that were phenotypically identified as *S. warneri* were confirmed by sodA-based PCR, underscoring the value of integrating molecular tools into routine milk microbiology, particularly when dealing with closely related CoNS species.

One of the most notable results of this study is that all *S. warneri* isolates (21/21, 100%) were classified as biofilm producers on Congo Red Agar (CRA). Biofilm formation is considered a key virulence trait in staphylococci, contributing to persistence in the mammary gland, survival on milking equipment surfaces and reduced susceptibility to antimicrobials. Reported biofilm positivity rates among staphylococci vary depending on the method used (CRA, tube method, microtiter plate assay) and the examined species. Studies on CoNS from clinical samples have reported biofilm formation in approximately 60–70% of isolates (Shrestha et al. 2017; Abdel Halim et al. 2018). In this context, the 100% CRA-positivity observed in our *S. warneri* collection appears unusually high and suggests that this species may possess an intrinsically strong tendency to form biofilms under the tested conditions, or that our selection of isolates (all derived from mastitic quarters) enriched for particularly adapted, biofilm-competent strains.

Biofilm formation by *S. warneri* has also been documented in other clinical and veterinary settings. A recent review emphasized biofilm formation, internalization into host cells and antimicrobial resistance as key features associated with invasive infections (Ravaioli et al. 2024). Experimental studies have also shown that proteases such as aureolysin may contribute to biofilm persistence on abiotic surfaces (Yokoi et al. 2016). Furthermore, research on methicillin-resistant CoNS, including *S. warneri*, has demonstrated substantial biofilm-forming capacity in both hospital and community environments (Seng et al. 2017; Al-Mousawi et al. 2022). The uniformly positive CRA results obtained in our study therefore support the notion that *S. warneri* isolated from mastitic milk should not be dismissed as a harmless contaminant but may instead represent a biofilm-adapted organism capable of persisting in the udder and milking environment.

Regarding antimicrobial susceptibility, our isolates exhibited a heterogeneous resistance pattern. According to CLSI (2024) criteria, all isolates were susceptible to gentamicin (100%). High susceptibility rates were also observed for erythromycin (85.7%), doxycycline (85.7%), and chloramphenicol (76.2%). Susceptibility rates were determined as 61.9% for tetracycline and 52.4% for penicillin. The lowest susceptibility rate was observed for oxacillin (9.5%), followed by trimethoprim–sulfamethoxazole (19.0%). When resistance profiles across all antibiotics were examined, most isolates (76.2%) were resistant to three or more antibiotics, fulfilling common definitions of multidrug resistance (MDR). Comparable MDR frequencies have been reported in CoNS characterized using *sodA*-based methods; Kim et al. (2018) found that 60% of isolates were resistant to

three or more antibiotics and over 90% were resistant to at least one.

Comparative findings on *S. warneri* show substantial variability, likely influenced by host species, sample origin and geography. A study on bloodstream isolates reported multiple resistance genes and high resistance to β-lactams and macrolides (Szczuka et al. 2016). Another investigation using a murine mastitis model identified a multidrug-resistant strain carrying a diverse set of resistance determinants, suggesting that *S. warneri* may readily develop complex resistance profiles under antimicrobial pressure (Hoque et al. 2024). Research analyzing *S. warneri* from food and clinical samples also described high resistance to macrolides and gentamicin, which contrasts with the complete gentamicin susceptibility observed in our isolates (Ravaioli et al. 2024). Collectively, these findings indicate that while antimicrobial resistance is common in *S. warneri*, the exact phenotype varies considerably by ecological niche and antimicrobial exposure patterns.

Our penicillin resistance rate (47.6%) was somewhat lower than the 55–60% reported for staphylococci (including CoNS) in dairy and food studies, whereas our tetracycline resistance rate (38.1%) aligned with or slightly exceeded values from large-scale surveys (Raspanti et al. 2016; Wang et al. 2019). Oxacillin resistance (90.5%) was remarkably high, raising concerns about potential methicillin-resistant *S. warneri* (MR-*S. warneri*) strains circulating in the region. High β-lactam resistance rates in NAS have often been linked to widespread intramammary antibiotic use (Raspanti et al. 2016; Addis et al. 2024). In contrast, the full gentamicin susceptibility (100%) suggests that aminoglycosides remain highly effective in vitro. This preservation of susceptibility is likely attributable to the limited use of this antimicrobial class in the region's dairy herds, driven by strict avoidance of long withdrawal periods and nephrotoxicity risks, which has consequently prevented the development of significant selective pressure.

Trimethoprim–sulfamethoxazole (SXT) resistance was also notably high in our isolates (81.0%). Although SXT is not among the most frequently used antimicrobials for bovine mastitis therapy in many countries, increasing resistance to this drug combination has been reported in staphylococci isolated from both human and animal sources (Wang et al. 2019; Garbacz et al. 2021). Our findings therefore indicate that empirical use of SXT against NAS-associated mastitis in the studied region would likely have limited therapeutic success. The variable susceptibility rates observed for penicillin and tetracycline, together with the high prevalence of MDR phenotypes, further emphasize the necessity of susceptibility-guided treatment strategies and prudent antimicrobial stewardship practices within the dairy sector.

From an epidemiological standpoint, the detection of *S. warneri* in mastitic cows, all displaying strong biofilm formation and significant antimicrobial resistance, has important implications for udder health. Biofilm-producing NAS can persist in the teat canal or udder parenchyma and may act as reservoirs of resistance genes transferable to other staphylococci, including *S. aureus* (De Buck et al. 2021; Addis et al. 2024). That all isolates originated from mastitic cows, rather than healthy ones, supports considering *S. warneri* a potential intramammary pathogen.

This study has certain limitations that should be considered. The sampling was geographically restricted to the Aegean region, and the exact distribution of samples per province was not available due to the retrospective nature of the study. A critical limitation is that biofilm formation was evaluated solely using the qualitative Congo Red Agar (CRA) method. While CRA is a standard screening tool, the 100% positivity rate observed in our study should be interpreted with caution. This method relies on phenotypic colony morphology, which can be subjective and may lead to an overestimation of biofilm production compared to quantitative methods like the Microtiter Plate Assay (MPA) (Kaiser et al., 2013; Shrestha et al., 2017). Although the high prevalence likely reflects the clinical origin of the isolates, the lack of quantitative validation suggests that these results represent a screening potential rather than a quantified biofilm mass. Finally, only mastitic cows were examined, precluding comparisons with healthy animals or environmental reservoirs.

Despite these limitations, this study provides one of the few detailed descriptions of *S. warneri* isolated from bovine mastitis in Türkiye, combining phenotypic and *sodA*-based identification with biofilm detection and a comprehensive antimicrobial susceptibility profile. The findings emphasize that *S. w*arneri should be recognized as a mastitis-associated NAS species with strong biofilm-forming ability and notable multidrug resistance. Future studies incorporating resistance gene characterization and herd-level risk analyses are essential for improved understanding and control.

CONFLICTS OF INTEREST

The authors report no conflicts of interest.

AUTHOR CONTRIBUTIONS

Idea/Concept: SA, ÇN
Supervision/Consultancy: SA, ÇN
Data Collection and/or Processing: SA, ÇN, EÇÇA, AEÇ, CHD, AG, NY
Analysis and/or Interpretation: SA, ÇN
Writing the Article: SA
Critical Review: SA, ÇN, EÇÇA, AEÇ, CHD, AG, NY

REFERENCES

Abdel Halim RM, Kassem NN, Mahmoud BS (2018). Detection of biofilm producing staphylococci among different clinical isolates and its relation to methicillin susceptibility. *Open Access Maced J Med Sci*, 6(8), 1335-1341.

Addis MF, Locatelli C, Penati M et al. (2024). Non-aureus staphylococci and mammaliicocci isolated from bovine milk in Italian dairy farms: A retrospective investigation. *Vet Res Commun*, 48(1), 547-554.

Al-Mousawi AH, Chessab RM, Alquraishy MK (2022). Inhibition of biofilm formation by methicillin-resistant *Staphylococcus warneri* using *Citrus limon* oil. *Caspian J Environ Sci*, 20(1), 197-201.

Alves E, Esteves AC, Correia A et al. (2015). Protein profiles of Escherichia coli and *Staphylococcus warneri* are altered by photosensitization with cationic porphyrins. *Photochem Photobiol Sci*, 14, 1169-1178.

Azimi T, Mirzadeh M, Sabour S et al. (2020). Coagulase-negative staphylococci (CoNS) meningitis: A narrative review of the literature from 2000 to 2020. *New Microbes New Infect*, 37, 100755.

Balows A, Hausler WJ Jr, Herrmann KL et al. (1991). Manual of Clinical Microbiology. V. Edition. American Society for Microbiology, Washington DC, USA.

Barigye R, Schaan L, Gibbs PS, Schamber E, Dyer NW (2007). Diagnostic evidence of *Staphylococcus warneri* as a possible cause of bovine abortion. *J Vet Diagn Invest*, 19, 694-696.

Clinical and Laboratory Standards Institute (2024). Performance Standards for Antimicrobial Susceptibility Testing. 34. Edition. Clinical and Laboratory Standards Institute, Malvern, USA.

De Buck J, Ha V, Naushad S et al. (2021). Non-aureus *Staphylococci* and bovine udder health: Current understanding and knowledge gaps. *Front Vet Sci*, 8, 658031.

de Oliveira RP, da Silva JG, Aragão BB et al. (2022). Diversity and emergence of multi-resistant *Staphylococcus* spp. isolated from subclinical mastitis in cows in the state of Piauí, Brazil. *Braz J Microbiol*, 53(4), 2215-2222.

Espino L, Bermudez R, Fidalgo LE et al. (2006). Meningoencephalitis associated with *Staphylococcus warneri* in a dog. *J Small Anim Pract*, 47, 598-602.

Freeman DJ, Falkiner FR, Keane CT (1989). New method for detecting slime production by coagulase-negative staphylococci. *J Clin Pathol*, 42(8), 872-874.

Garbacz K, Wierzbowska M, Kwapisz E et al. (2021). Distribution and antibiotic resistance of different *Staphylococcus* species identified by matrix assisted laser desorption ionization–time of flight mass spectrometry (MALDI-TOF MS) isolated from the oral cavity. *J Oral Microbiol*, 13(1), 1983322.

Getahun YA, Abey SL, Beyene AM et al. (2024). Coagulase-negative staphylococci from bovine milk: Antibiogram profiles and virulence gene detection. *BMC Microbiol*, 24, 263.

Hamel J, Zhang Y, Wente N et al. (2020). Non-S. aureus staphylococci (NAS) in milk samples: Infection or contamination? *Vet Microbiol*, 242, 108594.

Hoque MN, Faisal GM, Das ZC et al. (2024). Genomic features and pathophysiological impact of a multidrug-resistant *Staphylococcus warneri* variant in murine mastitis. *Microbes Infect*, 26(3), 105285.

Hosseinzadeh S, Saei HD (2014). Staphylococcal species associated with bovine mastitis in the North West of Iran: Emerging of coagulase-negative staphylococci. *Int J Vet Sci Med*, 2(1), 27-34.

Kaiser TD, Pereira EM, Dos Santos KR et al. (2013). Modification of the Congo red agar method to detect biofilm production by *Staphylococcus epidermidis*. *Diagn Microbiol Infect Dis*, 75(3), 235-239.

Kim J, Hong J, Lim JA, Heu S, Roh E (2018). Improved multiplex PCR primers for rapid identification of coagulase-negative staphylococci. *Arch Microbiol*, 200(1), 73-83.

Kloos WE, Schleifer KH (1975). Isolation and characterization of staphylococci from human skin II. Descriptions of four new species: *Staphylococcus warneri*, *Staphylococcus capitis*, *Staphylococcus hominis* and *Staphylococcus simulans*. *Int J Syst Bacteriol*, 25, 62-79.

Kooken J, Fox K, Fox A et al. (2014). Identification of staphylococcal species based on variations in protein sequences (mass spectrometry) and DNA sequence (*sodA* microarray). *Mol Cell Probes*, 28(1), 41-50.

Locatelli C, Gattolin S, Monistero V et al. (2023). *Staphylococcus aureus* coa gene sequence analysis can prevent misidentification of coagulase-negative strains and contribute to their control in dairy cow herds. *Front Microbiol*, 14, 1120305.

Mello PL, Riboli DFM, Martins LA et al. (**2020**). *Staphylococcus* spp. isolated from bovine subclinical mastitis in different regions of Brazil: Molecular typing and biofilm gene expression analysis by RT-qPCR. *Antibiotics (Basel)*, 9(12), 888.

Musharrafieh R, Tacchi L, Trujeque J, LaPatra S, Salinas I (2014). *Staphylococcus warneri*, a resident skin commensal of rainbow trout (Oncorhynchus mykiss) with pathobiont characteristics. *Vet Microbiol*, 169, 80-88.

National Mastitis Council (2017). Laboratory handbook on bovine mastitis, III. Edition. Verona, WI: National Mastitis Council.

Nuhay C (2025). Investigation of *Corynebacterium pseudotuberculosis* and its antimicrobial susceptibility in subclinical mastitis cattle in the Aegean Region. *J Anatol Env Anim Sci,* 10(2), 202-207.

Phophi L, Petzer IM, Qekwana DN (2019). Antimicrobial resistance patterns and biofilm formation of coagulase-negative *Staphylococcus* species isolated from subclinical mastitis cow milk samples submitted to the Onderstepoort Milk Laboratory. *BMC Vet Res*, 15(1), 420.

Rasmussen TT, Kirkeby LP, Poulsen K, Reinholdt J, Kilian M (2000). Resident aerobic microbiota of the adult human nasal cavity. *APMIS*, 108, 663–675.

Raspanti CG, Bonetto CC, Vissio C et al. (2016). Prevalence and antibiotic susceptibility of coagulase-negative *Staphylococcus* species from bovine subclinical mastitis in dairy herds in the central region of Argentina. *Rev Argent Microbiol*, 48(1), 50-56.

Ravaioli S, De Donno A, Bottau G et al. (2024). The opportunistic pathogen *Staphylococcus warneri*: Virulence and antibiotic resistance, clinical features, association with orthopedic implants and other medical devices, and a glance at industrial applications. *Antibiotics (Basel)*, 13(10), 972.

Regecová I, Výrostková J, Zigo F et al. (2022). Detection of resistant and enterotoxigenic strains of *Staphylococcus warneri* isolated from food of animal origin. *Foods*, 11, 1496.

Ryman VE, Kautz FM, Nickerson SC (2021). Case study: Misdiagnosis of nonhemolytic *Staphylococcus aureus* isolates from cases of bovine mastitis as coagulase-negative staphylococci. *Animals (Basel)*, 11, 252.

Seng R, Kitti T, Thummeepak R et al. (2017). Biofilm formation of methicillin-resistant coagulase-negative staphylococci (MR-CoNS) isolated from community and hospital environments. *PLoS One*, 12(8), e0184172.

Sezener MG, Findik A, Erguden VE et al. (2019). Investigation of antibiotic resistance and some virulence genes in mastitis isolate *Staphylococcus aureus* strains. *J Anatol Env Anim Sci*, 4(2), 182-187.

Shrestha LB, Bhattarai NR, Khanal B (2017). Antibiotic resistance and biofilm formation among coagulase-negative staphylococci isolated from clinical samples at a tertiary care hospital of eastern Nepal. *Antimicrob Resist Infect Control*, 6, 89.

Sivaraman GK, Vijayan AA, Visnuvinayagam S et al. (2022). Incidence of multidrug-resistant coagulase-negative *Staphylococci* from seafood samples, Veraval, Gujarat. *Indian J Anim Health*, 61, 65-70.

Szczuka E, Krzymińska S, Kaznowski A (2016). Clonality, virulence and the occurrence of genes encoding antibiotic resistance among *Staphylococcus warneri* isolates from bloodstream infections. *J Med Microbiol*, 65(8), 828-836.

Taponen S, Simojoki H, Haveri M, Larsen HD, Pyörälä S (2006). Clinical characteristics and persistence of bovine mastitis caused by different species of coagulase-negative staphylococci identified with API or AFLP. *Vet Microbiol*, 115, 199-207.

Traversari J, van den Borne BHP, Dolder C et al. (2019). Non-aureus *Staphylococci* species in the teat canal and milk in four commercial Swiss dairy herds. *Front Vet Sci*, 6, 186.

Wang YT, Lin YT, Wan TW et al. (2019). Distribution of antibiotic resistance genes among *Staphylococcus* species isolated from ready-to-eat foods. *J Food Drug Anal*, 27(4), 841-848.

Yilmaz DK, Berik N (2024). Phenotypic and genotypic antibiotic resistance of *Staphylococcus warneri* and *Staphylococcus pasteuri* isolated from stuffed mussels. *Aquat Sci Eng*, 39, 172-178.

Yokoi KJ, Kuzuwa S, Iwasaki SI et al. (2016). Aureolysin of *Staphylococcus warneri* M accelerates its proteolytic cascade and participates in biofilm formation. *Biosci Biotechnol Biochem*, 80(6), 1238-1242.

Van Vet J, 2026, 37(1) 104-108

Van Veterinary Journal

https://dergipark.org.tr/tr/pub/vanvetj

Cite this article as: **Yeşilyurt M, Gülaydın Ö (2026).** Detection of Some *Mycoplasma* Species in Sheep Lung Samples by PCR. *Van Vet J*, 37(1), 104-108. DOI: https://doi.org/10.36483/vanvetj.1863229

ISSN: 2149-3359 **Araştırma Makalesi** e-ISSN: 2149-8644

Koyun Akciğer Örneklerinden Bazı *Mycoplasma* Türlerinin PCR ile Tespiti

Muazzez YEŞİLYURT[1,*] Özgül GÜLAYDIN[1]

[1] *Siirt University, Faculty of Veterinary Medicine, Department of Microbiology, 56100, Siirt, Türkiye*

Geliş Tarihi: 13.01.2026 Kabul Tarihi: 12.03.2026

ÖZ

Koyun yetiştiriciliği kırsal alanda verimsiz meraların değerlendirilmesi ve kaliteli hayvansal protein elde edilmesi ile önemli geçim kaynakları arasında yer almaktadır. Sürülerde karşılaşılan çeşitli enfeksiyöz hastalıklar, sürü sağlığını ve ekonomik geliri olumsuz yönde etkilemektedir. *Mycoplasma* kaynaklı pnömoni olguları da verim düşüklüğü, yüksek ölüm oranları, tedavi masrafları nedeniyle koyun yetiştiriciliğinde önemli sorunlara yol açmaktadır. Bu çalışmada, koyun akciğer örneklerinden bazı *Mycoplasma* türlerinin polimeraz zincir reaksiyonu (PCR) ile araştırılması amaçlandı. Bu doğrultuda Siirt belediye mezbahasında kesimi yapılan ve postmortem muayene sonucunda pnömonik lezyonlar gözlenen 159 koyun akciğer örneği kullanıldı. PCR analizi sonucunda incelenen örneklerin 8 (%5.03)'inde *Mycoplasma* spp. tespit edildi. Tespit edilen 8 örnekten sırasıyla %37.5 ve %25'inde *Mycoplasma ovipneumoniae* (*M. ovipneumoniae*) ve *Mycoplasma agalactiae* (*M. agalactiae*) identifiye edildi. Akciğer örneklerinin 1'inde ise *M. arginini* ve *M. ovipneumoniae* birlikte belirlendi. Sonuç olarak çalışmada Siirt bölgesinde koyunların solunum sistemi hastalıklarında *M. ovipneumoniae*, *M. agalactiae* ve *M. arginini* etkenlerinin de rol oynayabileceği belirlenmiştir. Ancak elde edilen düşük prevalans değerleri, bu etkenlerin mevcut enfeksiyonlardaki primer rolünün kısıtlı olabileceğine işaret etmektedir. Bu nedenle bölgede uygulanacak tedavi ve koruma-kontrol programlarının bu sınırlı yaygınlık verileri ışığında ve diğer olası patojenler de dikkate alınarak planlanması daha rasyonel bir yaklaşım olacaktır.

Anahtar Kelimeler: *Koyun, Mycoplasma, PCR, Pnömoni.*

ABSTRACT

Detection of Some *Mycoplasma* Species in Sheep Lung Samples by PCR

Sheep farming is an important source of livelihood in rural areas, utilizing unproductive pastures and providing high-quality animal protein. Various infectious diseases observed in herds negatively affect herd health and economic returns. *Mycoplasma*-induced pneumonia cases also cause significant problems in sheep farming due to reduced productivity, high mortality rates, and treatment costs. This study aimed to detect some *Mycoplasma* species in sheep lung samples using polymerase chain reaction (PCR). For this purpose, lung samples were used from 159 sheep that were identified with pneumonic lesions during postmortem examination at the Siirt municipal slaughterhouse. *Mycoplasma* spp. was detected in 8 (5.03%) of the samples examined as a result of PCR analysis. Of the 8 samples detected as *Mycoplasma* spp., *Mycoplasma ovipneumoniae* (*M. ovipneumoniae*) and *Mycoplasma agalactiae* (*M. agalactiae*) were identified in 37.5% and 25%, respectively. In one of the lung samples, *M. arginini* and *M. ovipneumoniae* were identified together. As a result, the study determined that *M. ovipneumoniae*, *M. agalactiae*, and *M. arginini* may also play a role in respiratory system diseases in sheep in the Siirt region. However, the low prevalence values obtained indicate that the primary role of these agents in current infections may be limited. Therefore, it would be a more rational approach to plan treatment and protection-control programs to be implemented in the region in light of these limited prevalence data and taking other possible pathogens into account.

Keywords: *Mycoplasma, PCR, Pneumonia, Sheep.*

GİRİŞ

Küçükbaş hayvanlarda görülen solunum sistemi hastalıkları, birçok ülkede önemli ekonomik kayıplara yol açmaktadır. (Adehan ve ark. 2006; Öztürkler ve Otlu 2020). Solunum sistemi hastalıklarının oluşumunda birçok faktör rol oynamaktadır (Maksimović ve ark. 2022). Bu faktörler arasında, bakteriler, virusler, parazitler ve mantarlar gibi enfeksiyöz etkenler ile stres ve iklim koşulları gibi enfeksiyöz olmayan etkenler yer almaktadır (Ali ve Abdullah 2024). Koyunlarda sıklıkla izole edilen bakteriyel etkenler arasında *Mycoplasma* spp., *Pasteurella*

✉ *Corresponding author: muazzez.yesilyurt@siirt.edu.tr

spp., *Mannheimia haemolytica*, *Staphylococcus* spp., *Actinomyces* spp., ve *Streptococcus* türleri yer almaktadır (Kılıc ve ark. 2013; Öztürkler ve Otlu 2020). Koyunlarda pnömoni olgularına yol açan çeşitli mikroorganizmalar arasında yer alan *Mycoplasma* türleri, akciğer dokusunda neden oldukları spesifik lezyonlar ve klasik antibiyotik tedavilerine karşı gösterdikleri direnç potansiyeli ile klinik ve ekonomik açıdan öncelikli bir öneme sahiptir (Gautier-Bouchardon 2018; Nadhim ve ark. 2025). Önemli *Mycoplasma* türlerinden biri olan *M. ovipneumoniae*; koyunlarda atipik pnömoni, bronkopnömoni ve eksudatif pnömoniye yol açmaktadır. Ayrıca bu etken, hayvanları *M. haemolytica* ve Parainfluenza-3 (PI-3) virüsü kaynaklı enfeksiyonlara karşı daha duyarlı hale getirerek hastalığın şiddetini artırmaktadır (Kılıc ve ark. 2013; Udhayavel ve ark. 2025). *M. ovipneumoniae*, hasta hayvanların burun, akciğer ve trakeasından izole edilebildiği gibi sağlıklı hayvanlardan da izole edilmektedir. *M. arginini* ise atipik pnömoni vakalarında genellikle *M. ovipneumoniae* ile birlikte izole edilmektedir (Lin ve ark. 2008). Mikoplazmaların teşhisi amacıyla kullanılan konvansiyonel bakteriyolojik yöntemler tanı için altın standart olarak kabul edilse de oldukça güç ve zaman alıcı olmasından dolayı pek tercih edilmemektedir. Bunun yerine spesifik, hassas ve karışık kültürlerin de tanımlanmasını sağlayan PCR yöntemi daha çok tercih edilmektedir (Awan ve ark. 2012; Weiser ve ark. 2012).

Bu çalışmada; koyunlarda başta atipik pnömoni kompleksi ve bulaşıcı agalaksi olmak üzere önemli solunum sistemi enfeksiyonlarına ve ekonomik verim kayıplarına yol açan *M. ovipneumoniae*, *M. arginini* ve *M. agalactiae* varlığının, akciğer örneklerinden direkt PCR ile tespit edilmesi amaçlanmıştır.

MATERYAL VE METOT

Etik kurul onayı Siirt Üniversitesi Hayvan Deneyleri Yerel Etik Kurulu'nun 25.12.2025 tarih ve 2025.12.74 sayılı kararı ile alınmıştır.

Bu çalışmada, Kasım 2023-Ağustos 2024 tarihleri arasında Siirt Belediye mezbahasında kesilen koyunlardan alınan ve yapılan makroskobik incelemeler sonucunda pnömoni lezyonları tespit edilen 159 akciğer örneği kullanıldı. Bu çalışmanın örnek genişliğini hesaplamada, her değişken için Power (Testin Gücü) en az 0.80 ve 1. Tip Hata 0.05 alınarak belirlenmiştir.

Koyun Akciğer Örneklerinin Alınması

Siirt Belediye mezbahasında kesimi yapılan koyunların akciğerleri makroskobik olarak incelendi ve pnömoni lezyonları tespit edilen akciğerlere enine kesitler atılarak el ayası genişliğinde örnekler alındı. Alınan örnekler %20 gliserinli PBS içeren örnek toplama kaplarına aktarıldı ve soğuk zincir koşulları sağlanarak Siirt Üniversitesi, Veteriner Fakültesi, Mikrobiyoloji Anabilim Dalı Laboratuvarı'na getirildi.

PCR ile Mikoplazma Türlerinin Tespit Edilmesi

DNA Ekstraksiyonu

Koyun akciğer örneklerinden DNA ekstraksiyonu, ticari bir DNA ekstraksiyon kiti (EcoTech Biotecnology, Tissue genomic DNA Kit, E1070, Türkiye) kullanılarak gerçekleştirildi. Üretici firmanın talimatları doğrultusunda elde edilen DNA'lar kullanılıncaya kadar -20 °C'de saklandı.

Amplifikasyon

Örneklerde PCR ile *Mycoplasma* spp., *M. ovipneumoniae*, *M. arginini* ve *M. agalactia* tespiti için kullanılan cins ve tür spesifik primerler ve amplifikasyon koşulları Tablo 1'de sunulmuştur.

PCR karışımı üretici firmanın protokolü temel alınarak hazırlanmıştır. Toplamda 25 µl hacme sahip reaksiyon karışımı: 12.5 µl mastermix (EcoTaq 2x PCR Master Mix, ET-1, Türkiye), 5 µl genomik DNA, 1.5 µl (10µM) primer ve 4.5 µl PCR suyu ilave edilerek oluşturulmuştur.

PCR sonucu elde edilen amplikonlar, %1.5'lik agaroz jelde elektroforeze tabi tutuldu ve jel görüntüleme sistemi (Gene-Box FX, ER Biotech, Türkiye) kullanılarak görüntülendi. Negatif kontrol olarak DNA içermeyen PCR suyu kullanıldı.

Sekans Analizi

Mycoplasma spp. için spesifik bant profiline sahip PCR ürünlerinden 1'i (50 µl), her bir primer ile birlikte, dizi analizinin gerçekleştirilmesi amacıyla BM Laboratuvar Sistemleri (Ankara, Türkiye) firmasına gönderildi. Sanger sekanslama yöntemi ile elde edilen dizi verileri, GenBank veri tabanındaki nükleotid dizileriyle (NCBI BLAST) karşılaştırıldı.

Tablo 1: *Mycoplasma* cins ve türlerinin identifikasyonunda kullanılan primer dizileri ve PCR amplifikasyon koşulları.

Table 1: Primer sequences and PCR amplification conditions used in the identification of *Mycoplasma* genus and species.

Etken	Hedef Gen	Oligonukleotid (5'-3')	Amplikon Büyüklüğü (bp)	Denatürasyon/Bağlanma Sıcaklığı/ Uzama (35 Siklus)	Referans
Mycoplasma spp.	*16SrRNA*	F: GCTGGCTGTGTGCCTAATACA R:TGCACCATCTGTCACTCTGTTAACCTC	1013	94°C/1 dk. 65°C/1 dk. 72°C 1 dk.	Lierz ve ark., 2007.
Mycoplasma ovipneumoniae	*LMFI* *LMRI*	F: TGAACGGAATATGTTAGCTTR R: GACTTCATCCTGCACTCTGT	361	94°C/1 dk. 51°C 1 dk. 72°C 1 dk.	McAuliffe ve ark., 2003.
Mycoplasma arginini	*MAG* *GP4*	F: GCATGGAATCGCATGATTCCT R: GGTGTTCTTCCTTATATCTACGC	545	94°C/1 dk. 57°C 1 dk. 72°C 1 dk.	Timenetsky ve ark., 2006.
Mycoplasma agalactiae	*p80*	F: AAAGGTGCTTGAGAAATGGC R: GTTGCAGAAGAAAGTCCAATCA	375	94°C/1 dk. 57°C 1 dk. 72°C 1 dk.	Tola ve ark., 1994.

İstatistiksel Analiz

Çalışmadaki değişkenler için tanımlayıcı istatistikler; "sayı (n) ve yüzde (%)," olarak ifade edilmiştir. Kategorik değişkenler arasındaki ilişkileri belirlemede "iki oranlı Z-testi" hesaplanmıştır. Hesaplamalarda istatistik anlamlılık düzeyi %5 olarak alınmış ve analiz için SPSS (IBM SPSS for Windows, ver.27) ve Minitab ver.17 (Statistical Software LLC) istatistik paket programları kullanılmıştır.

BULGULAR

Çalışmada incelenen 159 koyun akciğer örneğinin 8 (%5.03)'inde cins spesifik primer ile 1013 bp'lik bant görüntülendi (Şekil 1).

Sekans analizi sonucunda elde edilen nükleotid dizisi, GenBank veri tabanında NCBI BLAST kullanılarak analiz edildi. Analiz sonucunda elde edilen nükleotid dizisinin CP144381.1 erişim numaralı *Mycoplasma agalactiae* strain 2463 nükleotid dizisiyle %100 uyum gösterdiği belirlendi. Sekans analizi sonucunda elde edilen dizi, PV929007 erişim numarası ile GenBank veri tabanına yüklenerek çalışmada pozitif kontrol olarak kullanıldı.

Mycoplasma spp. yönünden pozitif olduğu tespit edilen 8 örneğin 3 (%37.5)'ü *M. ovipneumoniae*, 2'si (%25) *M. agalactiae* olarak tanımlanırken, 1 (%12.5) örnekte hem *M. arginini* hem de *M. ovipneumoniae* tespit edildi (Şekil 1).

PCR ile *Mycoplasma* spp. tespit edilen 2 örnekte kullanılan tür spesifik primer ile tür düzeyinde identifikasyon yapılamadı.

Tablo 2: Farklı çalışmalardaki PCR sonuçlarına göre *Mycoplasma* spp. görülme oranlarının karşılaştırmalı analizi ve dağılımları.

Table 2: Comparative analysis and distribution of Mycoplasma spp. prevalence rates according to PCR results from different studies.

	N	*Mycoplasma* spp. Pozitiflik Sayısı	Pozitiflik Oranı	*p.
Bu çalışmada	159	8	%5.03	**0.001**
Sayed ve ark. 2025	50	36	%72.00	**0.001**
Bottinelli ve ark. 2017	115	25	%21.73	**0.001**
Daee ve ark. 2020	50	12	%24.00	**0.001**
Öztürkler ve Oltu 2020	250	26	%10.40	**0.001**
Deepika ve ark. 2023	49	32	65.30	**0.001**

* İki oranlı Z-testi sonuçlarına göre anlamlılık düzeyleri.

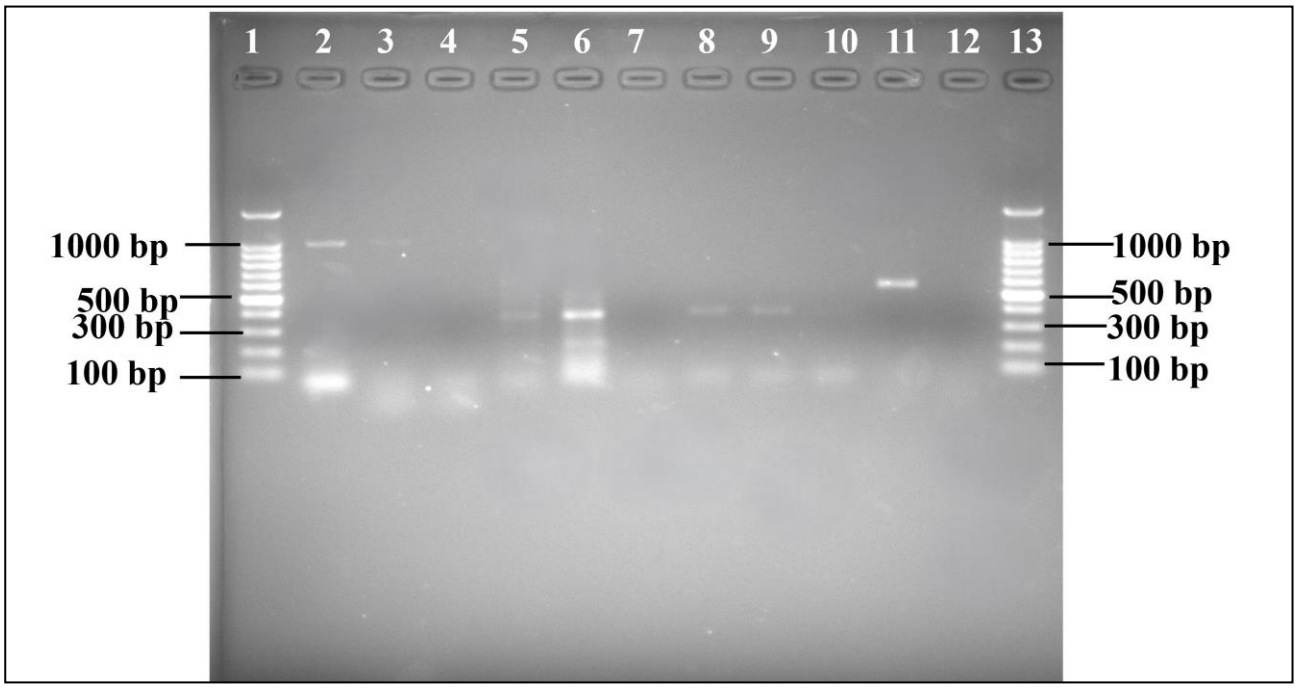

Şekil 1: PCR ile *Mycoplasma* spp. tespit edilen örneklerden elde edilen amplikonların agaroz jel görüntüsü. M (1,13): 100 bp DNA marker, 2: *Mycoplasma* spp. pozitif kontrol; 3: *Mycoplasma* spp. pozitif izolat; 4: *Mycoplasma* spp. negatif kontrol; 5-6: *M. ovipneumoniae* pozitif izolat; 7: *M. ovipneumoniae* negatif kontrol; 8: *M. agalactia* pozitif kontrol; 9: *M. agalactia* pozitif izolat; 10: *M. agalactia* negatif kontrol; 11: *M. arginini* pozitif izolat; 12: *M. arginini* negatif izolat.

Figure 1: Agarose gel image of amplicons obtained from samples in which *Mycoplasma* spp. was detected by PCR. M (1,13): 100 bp DNA marker, 2: *Mycoplasma* spp. positive control (1013 bp); 3: *Mycoplasma* spp. positive isolate (1013 bp); 4: *Mycoplasma* spp. negative control; 5-6: *M. ovipneumoniae* positive isolate (361 bp); 7: *M. ovipneumoniae* negative control; 8: *M. agalactia* positive control (375 bp); 9: *M. agalactia* positive isolate; 10: *M. agalactia* negative control; 11: *M. arginini* positive isolate (545 bp); 12*: M. arginini* negative isolate.

Pozitif örnekler arasında en yüksek prevalansa sahip olan *M. ovipneumoniae* (%37.5) ile *M. agalactiae* (%25) oranları ''iki oranlı Z-testi'' ile karşılaştırılmıştır. Yapılan analiz sonucunda, iki alt türün görülme sıklığı arasındaki fark istatistiksel olarak anlamlı bulunmamıştır (Z=0.535, p=0.593). Bu durum, örneklem grubunda her iki türün de benzer yaygınlıkta olduğunu göstermektedir.

TARTIŞMA VE SONUÇ

Küçük ruminantlarda meydana gelen solunum sistemi hastalıkları birçok ülkede önemli verim kayıplarına neden olmaktadır. Solunum sistemi hastalıklarına neden olan ajanlar arasında birçok bakteriyel etken bulunmakla birlikte, *Mycoplasma* türleri en önemli etkenler arasında yer almaktadır (Öztürkler ve Otlu 2020; Mousa ve ark. 2021). Konu ile ilgili ulusal ve uluslararası alanda çeşitli çalışmaların yapıldığı ve moleküler yöntemler kullanılarak etken identifikasyonun yapıldığı belirlenmiştir. Bu kapsamda, Bottinelli ve ark. (2017) İtalya'da yapmış oldukları bir çalışmada 115 pnömonik kuzu akciğer örneğini incelemişlerdir. Çalışma sonucunda PCR ile %21.73 oranında *Mycoplasma* spp. tespit etmişlerdir. Daee ve ark. (2020)'nın İran'da yapmış oldukları bir çalışmada 50 akciğer örneğinin %24'ünü (n=12) *Mycoplasma* spp. yönünden pozitif olarak belirlemişlerdir. Kars yöresinde yapılan bir çalışmada ise araştırmacılar 250 pnömonik akciğer örneğinin %10.4'ünde (n=26) *Mycoplasma* spp. izole ettiklerini ve yapılan PCR analizi sonucunda da izolatların tamamını *Mycoplasma* spp. olarak identifiye ettiklerini rapor etmişlerdir (Öztürkler ve Otlu 2020). Deepika ve ark. (2023) Hindistan'da yapmış oldukları bir çalışmada koyun akciğer örneklerinden %65.3 (32/49) oranında *Mycoplasma* spp. bildirmişlerdir. Sayed ve arkadaşları 2025 yılında Mısır'da yaptıkları bir çalışmada 50 pnömonik akciğer örneğini incelediklerini ve PCR ile %72 (n=36) oranında *Mycoplasma* spp. bulduklarını beyan etmişlerdir.

Bu çalışma kapsamında koyun akciğer örneklerinden PCR ile %5.03 (8/159) oranında *Mycoplasma* spp. tespit edildi. Elde edilen bu verilerin, Bottinelli ve ark. (2017), Daee ve ark. (2020), Öztürkler ve Otlu (2020), Deepika ve ark. (2023) ile Sayed ve ark. (2025)'nın elde ettiği verilere göre daha düşük olduğu tespit edildi. Farklı ülkelerde yapılan çalışma sonuçlarının *Mycoplasma* spp. varlığı yönünden değişkenlik göstermesi enfeksiyonun coğrafi dağılımının, hayvanların yetiştirilme koşullarının ve sürü yönetim politikalarının farklı olmasından kaynaklandığı düşünülmektedir.

Farklı çalışmalarda koyun akciğer örneklerinde PCR yöntemi ile saptanan *Mycoplasma* spp. görülme oranlarının karşılaştırmalı analizlerine bakıldığında, "iki oranlı Z-testi" sonuçları, literatürdeki çalışmalar ile mevcut çalışma arasındaki prevalans farklarının istatistiksel olarak yüksek derecede anlamlı (p=0.001) olduğunu ortaya koymaktadır. Mevcut çalışmada saptanan %5.03'lük pozitiflik oranı, karşılaştırılan diğer tüm çalışmalara kıyasla biyoistatistiksel açıdan en düşük prevalans değeridir.

Literatürdeki veriler incelendiğinde *Mycoplasma* spp. görülme oranlarının %10.4 ile %72 gibi çok geniş bir yelpazede dağıldığı görülmektedir. Özellikle Sayed ve ark. (2025) tarafından bildirilen %72 ve Deepika ve ark. (2023) tarafından bildirilen %65.3 oranları, mevcut çalışmanın bulgularından istatistiksel olarak anlamlı derecede yüksektir. En düşük literatür verisi olan Öztürkler ve Oltu (2020) çalışması %10.4 ile bu çalışmadaki pozitiflik oranının yaklaşık iki katı seviyesindedir. Bottinelli ve ark. (2017) (%21.73) ile Daee ve ark. (2020)'nın (%24) verileri de mevcut çalışma sonuçlarından anlamlı derecede farklılık göstermektedir (Tablo 2).

Sonuç olarak biyoistatistiksel veriler, *Mycoplasma* spp. yaygınlığının çalışılan popülasyonlar arasında belirgin bir heterojenlik sergilediğini kanıtlamaktadır. Bu karşılaştırmalı analiz mevcut çalışmanın bulgularının literatürdeki yaygın prevalans verilerinden negatif yönde anlamlı derecede ayrıştığını doğrulamaktadır.

Önemli *Mycoplasma* türleri arasında yer alan *M. ovipneumoniae*, koyunlarda meydana gelen pnömoni olgularından sıklıkla izole edilmektedir. *M. arginini* ise tek başına hem koyun hem de keçilerden izole edilen bir mikroorganizma olmasına rağmen, *Mannheimia haemolytica* ile birlikte seyrettiğinde akciğerde meydana gelen hasarın şiddetini artırmaktadır (Kılıc ve ark., 2013).

Bu çalışmada 159 koyun akciğer örneğinin PCR ile incelenmesi sonucunda %1.88 (n=3) oranında *M. ovipneumoniae*, %0.62 oranında da *M. arginini* tespit edildi. Elde edilen yaygınlık oranlarının Pavone ve ark. (2023)'nın *M. ovipneumoniae* ve *M. arginini* için sırasıyla belirlediği %9.9 (20/202) ve %8.91'lik (18/202) oran, Mousa ve ark. (2021) tarafından bildirilen %3.8 (4/104) ve %4.8'lik (5/104) oran, Daee ve ark. (2020)'nın belirlediği % 4 (2/50) ve %14'lük (7/50) oran ile Öztürkler ve Otlu (2020)'nun bildirdiği %4.8 (12/250) ve 1.6'lık (4/250) oranlara göre düşük olduğu tespit edildi.

Elde edilen sonuçlar arasındaki farklılıkların çalışmaların yapıldığı ülkelerin ve iklim koşullarının farklı olması, örneklem büyüklüğü ve örneklem şekline bağlı olabileceği düşünülmektedir.

M. agalactiae çoğunlukla sütten izole edilmesine rağmen mastitis, artritis, keratokonjonktivitis, pnömoni ve septisemi (MAKePS sendromu) olgularından da izole edilmiştir (Göçmen 2019). Koyunların *M. agalactiae* kaynaklı solunum sistemi enfeksiyonları ile ilgili yapılan çalışma sayısı sınırlıdır. Marmara bölgesinde yapılan bir çalışmada araştırmacılar 4 akciğer doku örneğinden %25 (n=1) oranında *M. agalactiae* tespit ettiklerini rapor etmişlerdir (Göçmen 2019). Deepika ve arkadaşlarının 2023 yılında yapmış oldukları çalışmada ise 49 koyun akciğer örneğinin %24.48'inde (n=12) *M. agalactiae* bulduklarını bildirmişlerdir. Yapılan bu çalışmada 159 akciğer örneğinin %1.25'inden *M. agalactiae* tespit edildi. Çalışma kapsamında elde edilen veriler Göçmen (2019) ile Deepika ve ark. (2023)'nın elde ettiği sonuçlara göre daha düşük olarak değerlendirildi.

Sonuçlar arasındaki farklılıkların örneklem büyüklüğü, akciğerdeki *M. agalactiae* yükünün düşük olmasından kaynaklı olabileceği düşünülmektedir.

Sonuç olarak Siirt yöresinde yetiştiriciliği yapılan koyunlarda meydana gelen solunum sistemi enfeksiyonlarında *M. ovipneumoniae*, *M. arginini* ve *M. agalactaie*'nin etiyolojik ajan olarak rol oynayabileceği görüldü. Ayrıca *M. ovipneumoniae* ve *M. arginini*'nin eş zamanlı olarak tespit edilmesi ile birlikte etkenlerin, enfeksiyonun şiddetini ve hastalığın kronikleşme potansiyelini artırabileceği düşünülerek etkenlere karşı koruma-kontrol stratejilerinin oluşturulması gerektiği kanaatine varıldı.

ÇIKAR ÇATIŞMASI

Yazarlar bu çalışma için herhangi bir çıkar çatışması olmadığını beyan ederler.

YAZAR KATKILARI

Fikir/Kavram: MY
Denetleme/Danışmanlık: ÖG
Veri Toplama ve/veya İşleme: MY
Analiz ve/veya Yorum: MY
Makalenin Yazımı: MY
Eleştirel İnceleme: ÖG

KAYNAKLAR

Adehan RK, Ajuwape ATP, Adetosoye AI, Alaka OO (2006). Characterization of Mycoplasmas isolated from pneumonic lungs of sheep and goats. *Small Rumin Res*, 63(1-2), 44-49.

Ali BA, Abdullah MA (2024). Pathologıcal study of pnumonia in sheep and goat in abttoitr at Duhok province. *Iraqi J Agric Sci*, 55(4), 1367-1380.

Awan MA, Ferhat A, Masoom YZ et al. (2012). Prevalence of *Mycoplasma* species by polymerase chain reaction (PCR) directly from the nasal swab samples of goats. *Pak J Life Soc Sci*, 10(1), 5–12.

Bottinelli M, Schnee C, Lepri E et al. (2017). Investigation on *Mycoplasma* populations in pneumonic dairy lamb lungs using a DNA microarray assay. *Small Rumin Res*, 147, 96-100.

Daee AA, Khodakaram-Tafti A, Derakhshandeh A, Seyedin M (2020). Identification of *Mycoplasma ovipneumoniae* and *Mycoplasma arginini* in sheep with pneumonia in North East of Iran. *Iran J Vet Res*, 21(1), 15-9.

Deepika R, Vijayalakshmi S, Reddy N (2023). Molecular detection of Non-*Mycoplasma mycoides* cluster organisms in respiratory infections of sheep and goats. *J Pharm Innov*, SP-12(8), 300-304.

Gautier-Bouchardon, AV (2018). Antimicrobial resistance in *Mycoplasma* spp. *Microbiol Spectr*, 6(4), 10-1128.

Göçmen H (2014). Marmara Bölgesinde Koyun ve Keçilerde *Mycoplasma agalactiae*'nin Bakteriyolojik ve Moleküler Yöntemler ile Araştırılması. Doktora Tezi, Bursa Uludag Universitesi, Sağlık Bilimleri Enstitüsü, Bursa, Türkiye.

Kılıc A, Kalender H, Eroksuz H, Muz A, Tasdemir B (2013). Identification by culture, PCR, and immunohistochemistry of mycoplasmas and their moleculer typing in sheep and lamb lungs with pneumonie in Eastren Turkey. *Trop Anim Health Prod,* 45(7), 1525-1531.

Lierz M, Hagen N, Harcourt-Brown N et al. (2007). Prevalence of mycoplasmas in eggs from birds of prey usingculture and a genus-specific *Mycoplasma* polymerase chain reaction. *Avian Pathol*, 36(2), 145-150.

Lin YC, Miles RJ, Nicholas RA J, Kelly DP, Wood AP (2008). Isolation and immunological detection of *Mycoplasma ovipneumoniae* in sheep with atypical pneumonia, and lack of a role for *Mycoplasma arginini*. *Res Vet Sci*, 84(3), 367-373.

Maksimović Z, Rifatbegović M, Loria GR, Nicholas RA (2022). *Mycoplasma ovipneumoniae*: a most variable pathogen. *Pathogens*, 11(12), 1477.

McAuliffe L, Hatchell FM, Ayling RD (2003). *Mycoplasma ovipneumoniae* detection of. *The Vet Rec*, 153, 687-688.

Mousa WS, Zaghawa AA, Elsify AM., et al. (2021). Clinical, histopathological, and molecular characterization of *Mycoplasma* species in sheep and goats in Egypt. *Vet world*, 14(9), 2561.

Nadhim RS, Al-Mashhadani ZI, Obead SA et al. (2025). Prevalence and control measures of mycoplasma infections in small ruminants. *J Anim Health Prod*, 13(s1), 136-143.

Öztürkler O, Otlu S (2020). A phylogenetic analysis of *Mycoplasma* strains circulating in sheep pneumonia in the Kars region of Turkey. *Turk J Vet Anim Sci*, 44(4), 805-813.

Pavone S, Crotti S, D'Avino N et al. (2023). The role of *Mycoplasma ovipneumoniae* and *Mycoplasma arginini* in the respiratory mycoplasmosis of sheep and goats in Italy: correlation of molecular data with histopathological features. *Res Vet Sci*, 163, 104983.

Sayed AE, Hafez A, Ateya , Darwish, A, Tahoun A (2025). Single nucleotide polymorphisms, gene expression and evaluation of immunological, antioxidant, and pathological parameters associated with bacterial pneumonia in Barki sheep. *Irish Vet J*, 78(1), 11.

Timenetsky J, Santos LM, Buzinhani M, Mettifogo E (2006). Detection of multiple *Mycoplasma* infection in cell cultures by PCR. *Brazilian J Med Biol Res*, 39, 907-914.

Tola S, Rizzu P, Leori G (1994). A species-specific DNA probe for the detection of Mycoplasma agalactiae. *Vet microbiol*, 41(4), 355-361.

Udhayavel S, Sukumar K, Senthilkumar K, Srinivasan P, Elango A (2025). Isolation and molecular characterization of *Mycoplasma ovipneumoniae* associated with respiratory infection in sheep and goats in South India. *Braz J Microbio*, 56, 2087-2095.

Weiser GC, Drew ML, Cassirer EF, Ward AC (2012). Detection of *Mycoplasma ovipneumoniae* and *M. arginini* in bighorn sheep using enrichment culture coupled with genus-and species-specific polymerase chain reaction. *J Wildl Dis*, 48(2), 449-453.

Van Veterinary Journal

https://dergipark.org.tr/tr/pub/vanvetj

Cite this article as: **Takcı L, Uslu S, Orhan İ, Alan S, Taş Kepenek EN (2026).** Investigations on the Light and Scanning Electron Microscopic Structure of Tongue Papillae of Kangal Sheep: Taste and Mechanical. *Van Vet J*, 37(1), 109-114.
DOI: https://doi.org/10.36483/vanvetj.1872262

ISSN: 2149-3359 **Original Article** e-ISSN: 2149-8644

Investigations on the Light and Scanning Electron Microscopic Structure of Tongue Papillae of Kangal Sheep: Taste and Mechanical

Lutfi TAKCI[1, *] Sema USLU[2] İmdat ORHAN[3] Sariye ALAN[1] Elif Nur TAŞ KEPENEK[2]

[1] *Sivas Cumhuriyet University, Faculty of Veterinary Medicine, Department of Anatomy, 58140, Sivas, Türkiye*
[2] *Sivas Cumhuriyet University, Faculty of Veterinary Medicine, Department of Histology and Embryology, 58140, Sivas, Türkiye*
[3] *Erciyes University, Faculty of Veterinary Medicine, Department of Anatomy, 38039, Kayseri, Türkiye*

Received: 26.01.2026 Accepted: 9.03.2026

ABSTRACT This study was conducted to examine the morphological, histological, and ultrastructural structure of the tongue papillae in Kangal sheep, which is the largest local type of the Akkaraman sheep breed, raised in Central Anatolia and especially in the Sivas region. After the tissues were prepared according to the necessary tissue processing protocols, they were examined using light (LM) and scanning electron microscopy (SEM). Histological examination revealed that the dorsal surface of the tongue was covered with stratified squamous keratinized epithelium, and the underlying layers contained lamina propria, submucosa, well-developed skeletal muscle bundles running in various directions, and serous/seromucous glands. SEM examinations revealed that the filiform papilla consisted of a main body and a pair of secondary papillae located on either side. Two types of lentiform papilla, pyramidal and irregularly shaped, were distinguished. Two types of taste papillae were identified: fungiform papilla and circumvallate papilla. It was observed that the fungiform papillae were typically mushroom-shaped and contained taste pores on their surfaces. It was determined that the circumvallate papillae were surrounded by a trench and contained taste pores. Although the tongue papilla structure of the Kangal sheep generally shows similarities with other ruminant species, specific morphological differences were identified, such as the consistent presence of a single pair of secondary extensions in the filiform papilla. These findings provide descriptive data for Kangal sheep and may serve as a basis for future comparative and functional studies.

Keywords: *Tongue, Light microscopy, Kangal sheep, Papilla, Scanning electron microscopy.*

ÖZ

Kangal Koyununun Dil Papillalarının Işık ve Taramalı Elektron Mikroskobik Yapısı Üzerine Araştırmalar: Tat ve Mekanik Papillalar

Bu çalışma, Orta Anadolu'da ve özellikle Sivas bölgesinde yetiştirilen Akkaraman koyun ırkının en büyük yerel tipi olan Kangal koyunlarında dil papillalarının morfolojik, histolojik ve ultrastrüktürel yapısını incelemek amacıyla yapılmıştır. Doku örnekleri gerekli doku işleme protokollerine göre hazırlandıktan sonra ışık mikroskobu (LM) ve taramalı elektron mikroskobu (SEM) ile incelenmiştir. Histolojik olarak, dilin dorsal yüzeyinin çok katlı yassı keratinize epitel ile kaplı olduğu ve altta yatan tabakaların lamina propria, submukoza, çeşitli yönlerde uzanan iyi gelişmiş iskelet kas demetleri ve seröz/seromuköz bezler içerdiği belirlenmiştir. SEM incelemeleri, papilla filiformisin bir ana gövde ve her iki yanında bulunan bir çift sekonder papilladan oluştuğunu ortaya koymuştur. Piramidal ve düzensiz şekilli olmak üzere iki tip papilla lentiformis ayırt edilmiştir. İki tip tat papillası tanımlanmıştır: papilla fungiformis ve papilla vallata. Papilla fungiformis'in tipik olarak mantar şeklinde olduğu ve yüzeylerinde tat alma gözenekleri içerdiği gözlemlenmiştir. Papilla vallata'nın ise bir hendekle çevrili olduğu ve tat alma tomurcukları içerdiği belirlenmiştir. Kangal koyununun dil papilla yapısı genel olarak diğer geviş getiren türlerle benzerlik gösterse de, papilla filiformis'te tek bir çift ikincil uzantının sürekli varlığı gibi belirli morfolojik farklılıklar tespit edilmiştir. Bu bulgular, Kangal koyunları için tanımlayıcı veriler sağlamakta olup, gelecekteki karşılaştırmalı ve fonksiyonel çalışmalar için bir temel oluşturabilir.

Anahtar Kelimeler: *Dil, Işık mikroskobu, Kangal koyunu, Papilla, Taramalı elektron mikroskobu.*

INTRODUCTION

Kangal sheep, which is the largest local type of the Akkaraman sheep breed in terms of size, is a sheep breed raised in Central Anatolia, especially in the Sivas Region (Aydin et al. 2024).

How food is masticated into a bolus in domestic mammals, whether the taste of the food is perceived, where the

✉ *Corresponding author: ltakci@cumhuriyet.edu.tr

receptors for taste sensation are located, and the effect of feeding conditions on taste sensation have been subjects of scientific research from the past to the present. It is reported that feeding type and diet are two important factors determining an organism's adaptation to its environment (Erdoğan and Sağsöz 2018). The tongue is the organ that enables the perception of taste sensation and the grinding of food taken into the mouth to form a bolus (Dyce et al. 2009; König and Liebich 2020). Specialized papillae are located on the surface of the tongue to perform these functions. Those that enable the mechanical grinding of food are called mechanical papillae (papilla mechanica), and those that enable the perception of taste sensation are called taste papillae (papilla gustatori). The number, shape, and presence of these papillae vary among species in domestic mammals. Ruminants have three mechanical papillae, namely filiform papilla, lentiform papilla, and conic papilla, and two taste papillae called fungiform papilla and circumvallate papilla. The foliate papilla, which is present in other domestic mammals, is absent in ruminants (Dyce et al. 2009; König and Liebich 2020). Numerous studies have been conducted to reveal the morphological and ultrastructural organization of the lingual papillae in sheep and goats. While surface scanning was performed using scanning electron microscopy, the histology of these structures was revealed using light microscopy. These studies have even been reduced to the breed level, attempting to determine the relationships between the environment in which sheep and goat breeds live and the structure of their lingual papillae. Karacabey Merino (Can et al. 2016), Morkaraman (Demircioğlu et al. 2024), Hamdani (Güzel et al. 2025), Norduz (Delibaş et al. 2023), Rahmani (Madkour and Mohammed 2021; Madkour et al. 2023a; Madkour et al. 2023b), and Egyptian Ossimi sheep (Abumandour et al. 2023) are some of the sheep breeds currently studied. Egyptian goat (Mahdy et al. 2021), Saanen (Kurtul and Atalgın 2008), and Angora goat (Toprak 2023) are the goat breeds where such studies have been conducted. Furthermore, these studies have also been performed on lambs to investigate the development of lingual papillae (Tadjalli and Pazhoomand 2004; Güzel et al. 2025). A literature search revealed no such study on the Kangal sheep. This study aims to examine the lingual papillae in Kangal sheep using light and scanning electron microscopy and to identify their morphological characteristics in comparison with those reported for other sheep breeds and ruminant species.

MATERIAL AND METHODS

Tongue samples belonging to 10 adult Kangal sheep slaughtered in abattoirs in the Sivas region were washed with physiological saline, and then the necessary procedures were applied to the samples taken from determined regions of the dorsal surface of the tongue for examination under light and electron microscopes. This study was approved by the Sivas Cumhuriyet University Local Ethics Committee for Animal Experiments with decision number 65202830-050.04.04-126 dated 26/12/2025.

Light Microscopy

Histological evaluation was performed at the Department of Histology and Embryology, Faculty of Veterinary Medicine, Cumhuriyet University. Tissues determined from 6 regions of the tongue in sheep were taken in 1 cm^3 size, and the tissues were fixed in 10% buffered formalin for 24-48 hours. Following washing under running water, routine histological tissue processing was applied (dehydration in 70%, 80%, 96%, 100% alcohols). After clearing in xylene, the tissues were blocked in paraplast. Sections 4-5 µm thick were cut and mounted on slides using a microtome (Leica RM2125RTS) from the resulting blocks. The sections mounted were stained with trichrome staining and evaluated under a microscope (Zeiss Axio 500), and photographs of the necessary areas were taken (Bancroft and Cook 1984).

Scanning Electron Microscopy (SEM)

Samples taken for scanning electron microscopy were kept in 10% formaldehyde solution for 24 hours. After washing twice for ten minutes in Phosphate Buffered Saline (0.1M PBS) solution, they were kept in glutaraldehyde (2.5%) for 5-6 hours. Following 5 repeated washes with buffer solution, they were kept in 70%, 80%, 96%, and 100% alcohol series for dehydration. The resulting samples were dried in a critical point dryer at the Erciyes University Nanotechnology Application and Research Center in Kayseri, then gold-coated and examined under a Zeiss Evo LS10 scanning electron microscope.

RESULTS

Light Microscopy

Tissues taken from the 6 determined regions of the tongue were examined. Generally, without regional distinction, the dorsal surface of the tongue was determined to be covered with stratified squamous keratinized epithelium. The epithelium was distinguished as covering the upper surface of the papillae located on the dorsal surface, with varying thicknesses depending on the regions taken from the tongue. Filiform papilla, conic papilla, lentiform papilla (Figure 1 A, B, C), fungiform papilla, and circumvallate papilla (Figure 2 A, B) were distinguished by their shapes and locations.

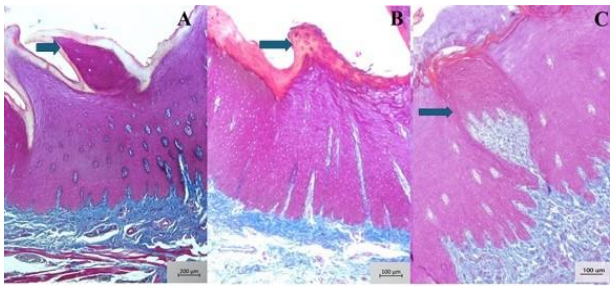

Figure 1: Light microscopic appearance of the mechanical lingual papillae in Kangal sheep. (A) Filiform papilla. (B) Conical papilla. (C) Lentiform papilla. Arrows indicate the papillae. Masson's trichrome staining. Scale bars: A = 200 µm; B = 100 µm; C = 100 µm.

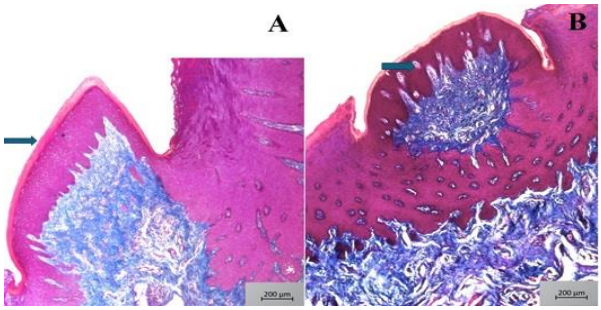

Figure 2: Light microscopic appearance of the gustatory lingual papillae in Kangal sheep. (A) Fungiform papilla. (B) Circumvallate papilla. Arrows indicate the papillae. Masson's trichrome staining. Scale bars: A = 200 µm; B = 200 µm.

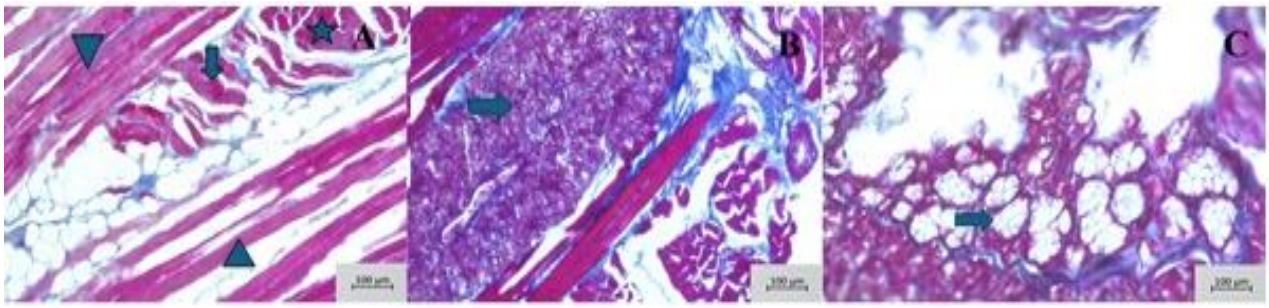

Figure 3: Light microscopic appearance of the deeper structures of the tongue in Kangal sheep. (A) Skeletal muscle bundles running in different directions beneath the papillae (arrowhead, longitudinal; arrow, vertical; star, transverse). (B) Serous glands between muscle bundles (arrow). (C) Seromucous glands (arrow). Masson's trichrome staining. Scale bars: A = 100 µm; B = 100 µm; C = 100 µm.

Taste pores were determined to be located on the vallate papillae. The standard layers of this epithelium covering the entire surface of the tongue and the upper parts of the papillae, showing stratified keratinization-stratum basale, stratum spinosum, stratum granulosum, and stratum corneum-were observed separately. It was determined that the stratum basale had a single layer of prismatic cell structure, the stratum spinosum was formed by polygonal cells, the stratum granulosum consisted of several layers of flattened cells containing keratohyalin granules, and the keratin layer was distinct and varied in thickness in places. Below the lamina epithelialis, the lamina propria and the submucosa, composed of looser connective tissue, were observed. It was determined that the lamina propria sent extensions into the epithelial layer, forming microscopic papillae, and these microscopic papillae were distinguished as clusters within the epithelium. Skeletal muscles running in various directions, sometimes intertwined, were detected beneath the submucosa (Figure 3 A). These muscles were identified as skeletal muscles responsible for voluntary movement in the tongue, running longitudinally, vertically, and horizontally, and forming bundles of varying thicknesses. Lingual glands were photographed among the muscles (Figure 3 B, C).

Scanning Electron Microscopy

In photographs examined by scanning electron microscopy of the Kangal sheep tongue, it was determined to possess three different mechanical papillae: filiform papilla, lentiform papilla, and conic papillae. Furthermore, two different types of taste papillae, named fungiform papilla and circumvallate papilla, were distinguished.

Filiform papillae were found densely on the dorsal surface of the tongue, especially in regions close to the apex, other regions of the dorsum although not as densely as at the apex. Furthermore, it was determined that the lengths of these papillae were longer and sharper at the apex lingua, but shorter and blunter in the corpus lingua. The filiform papillae were observed to be arranged as a main papilla (Mfp) emerging from the center and smaller secondary papillae (Sfp) emerging from both sides of this papilla. It was determined that the secondary papillae did not reach the main papilla in terms of either length or width. It was determined that both lentiform papilla and fungiform papillae were irregularly distributed among these papillae (Figure 4).

The pyramidal shaped lentiform papillae were generally observed leaning on one another. It was determined that the irregularly shaped ones were more independent than the others (Figure 5). It was determined that fungiform papillae were distributed among these papillae.

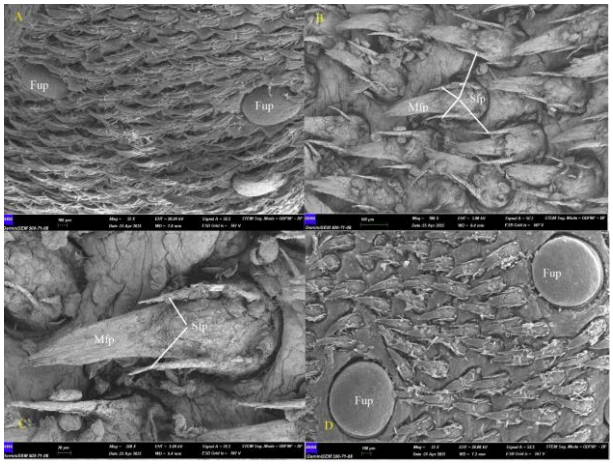

Figure 4: Scanning electron microscopic appearance of filiform and fungiform papillae on the dorsal surface of the tongue in Kangal sheep. (A) Fungiform papillae (Fup) interspersed among densely arranged filiform papillae at the apex linguae. (B) Filiform papillae showing a main filiform papilla (Mfp) and paired secondary papillae (Sfp). (C) Higher-magnification view of a filiform papilla showing the main papilla (Mfp) and secondary papillae (Sfp). (D) Fungiform papillae (Fup) distributed among filiform papillae. Scale bars: A = 100 µm; B = 100 µm; C = 20 µm; D = 100 µm.

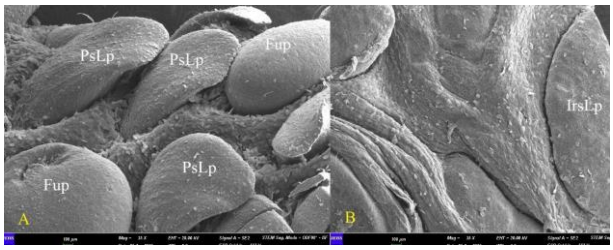

Figure 5: Scanning electron microscopic appearance of lentiform papillae in Kangal sheep. (A) Pyramidal-shaped lentiform papillae (PsLp) located among fungiform papillae (Fup). (B) Irregular-shaped lentiform papilla (IrsLp). Scale bars: A = 100 µm; B = 100 µm.

Papillae conicae were primarily found scattered in the lateral parts of the torus linguae and on the caudal surface of the radix linguae. It was determined that the distribution of Conic papillae on the tongue surface was not as dense as that of filiform papilla, and they were found more sparsely. It was determined that their shape resembled a blunt cone at the apex (Figure 6).

Circumvallate papillae were observed to exhibit a round structure surrounded by a trench and their surfaces were smooth. They were generally located on both sides of the radix lingua, behind the torus lingua (Figure 6).

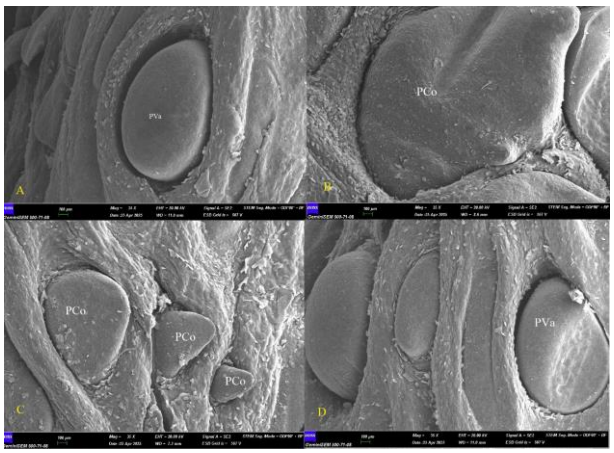

Figure 6: Scanning electron microscopic appearance of circumvallate and conical papillae in Kangal sheep. (A, D) Circumvallate papillae (PVa) surrounded by a trench. (B, C) Conical papillae (PCo). Scale bars: A = 100 µm; B = 100 µm; C = 100 µm; D = 100 µm.

Fungiform papilla typically exhibited a mushroom shape, a structure connected to the tongue by a round or oval head and a narrow neck. Taste pores (openings), where taste pores open, were observed on the surface of their heads (Figure 7).

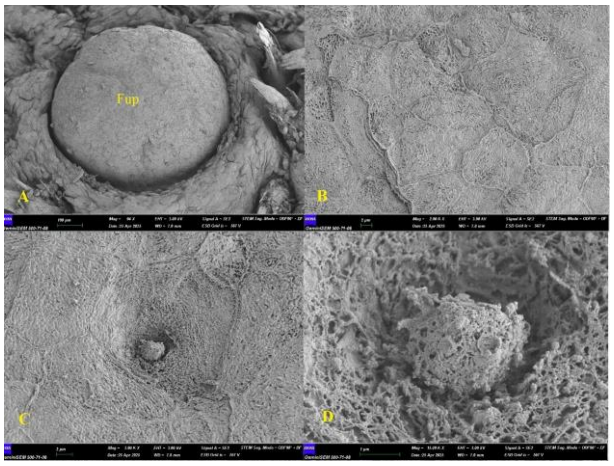

Figure 7: Scanning electron microscopic appearance of a fungiform papilla and its surface features in Kangal sheep. (A) Fungiform papilla (Fup). (B) Surface micromorphology of the fungiform papilla. (C) Taste pore on the surface of the fungiform papilla. (D) Higher-magnification view of the taste pore. Scale bars: A = 100 µm; B = 2 µm; C = 2 µm; D = 1 µm.

DISCUSSION AND CONCLUSION

This study provides descriptive morphological and ultrastructural data on the lingual papillae of Kangal sheep and allows comparison with previous reports in other ruminant breeds. Previous studies have suggested that pasture characteristics, diet, and climatic conditions may influence papillary morphology; however, the present study was not designed to test these relationships directly (Erdoğan and Sağsöz 2018).

Filiform papilla: It was stated that in Morkaraman sheep, they are densely located throughout the tongue, and secondary papillae are also present alongside the main papilla (Demircioğlu et al. 2024). In Karacabey Merino, it was determined that two secondary papillae emerge from the right and left sides of every main filiform papilla, and 3 or 4 smaller secondary papillae branch off from these secondary papillae, that secondary papillae are not found on the lateral surface of the tongue, that the lengths of the secondary papillae do not reach the length of the main papilla, and that the surface layer of the epithelium is keratinized, especially in the anterior parts of the papillae (Can et al. 2016). In Norduz sheep, primary papillae originating from a single stem and secondary papillae emerging from their right and left sides were observed. It was determined that smaller papilla extensions, varying in number between 1-2, were present on the sides of the secondary papillae (Delibaş et al. 2023). In another study, it was stated that 2-6 secondary extensions emerge from the sides of the main papillae, that the number of secondary papillae increases at the back of the tongue, that these projections exhibit a longer and fringed appearance on the sides of the corpus lingua, and that secondary papillae are absent in front of the torus lingua and surrounding the fossa lingua (Erdoğan and Sağsöz 2018). In the study conducted on Ossimi sheep, it was reported that the directions of the filiform papilla vary according to the region they are in, that they can have different shapes, that there are 5 subtypes, and that the subtypes show shape differences according to their location (Abumandour et al. 2023). In our study, the filiform papilla also exhibited the characteristics demonstrated in these studies. However, the number of secondary papillae did not change in our study and was observed as a single pair everywhere (Figure 4B, C, D). This aspect can be seen as a difference between our findings and the sheep species mentioned above. These differences may reflect breed-related or population-level morphological variation; however, direct associations with feeding habits, climate, environment, or pasture conditions cannot be established on the basis of the present descriptive findings alone (Erdoğan and Sağsöz 2018).

Lentiform papilla: It has been reported that in Morkaraman sheep, two types of lentiform papilla are located on the torus of the tongue: pyramid-shaped and irregularly rounded (Demircioğlu et al. 2024). In Karacabey Merino, it was determined that they were found only on the torus lingua, having two types-pyramidal and rounded-where the pyramid-shaped ones had pointed tips and the rounded ones had a blunt apex (Can et al. 2016). In Norduz sheep, they were found densely on the torus of the tongue, and the presence of pores at their tips was detected under high magnification (Delibaş et al. 2023). In another study conducted on sheep, it was found that these papillae were both larger and terminated in bifurcated tips, especially in the anterior half of the torus lingua compared to those located laterally on the corpus (Erdoğan and Sağsöz 2018). Different shapes of these papillae were not mentioned in Ossimi sheep (Abumandour et al. 2023). In our study, two types of lentiform papilla, pyramidal and irregular, were distinguished, similar to those in Morkaraman sheep (Figure 5).

Conic papilla: It has been stated that they are located in the lateral region of the tongue in Morkaraman sheep (Demircioğlu et al. 2024); in Karacabey Merino, they have a rounded base and a blunt tip on the torus and its lateral side, and their surface areas are covered with squamous epithelium (Can et al. 2016); in Norduz sheep, they resemble a typical cone (Delibaş et al. 2023); and in Ossimi sheep, those on the tongue are smaller and wider than the paralingual ones (Abumandour et al. 2023). In our study, conic papillae were observed on the torus lingua consistent with the literature (Figure 6 B, C). The findings

in the studies mentioned above are consistent with the findings in our study.

Fungiform papilla: In a similar study conducted on Morkaraman sheep, it was stated that the fungiform papilla appeared like shriveled peas in some regions (Demircioğlu et al. 2024). The sparse presence of fungiform papilla on the dorsal part of the tongue and their rare presence on the radix in Morkaraman sheep is consistent with the findings of our study (Demircioğlu et al. 2024). In Karacabey Merino, it was determined that they were scattered among the filiform papillae on the apex, corpus, and radix of the tongue, that they were rounded, mushroom-like structures, that their number per cm2 area decreased from the apex towards the radix, and that crater-like pores were present under high magnification (Can et al. 2016). In Norduz sheep, it was detected that they were distributed starting from the apex of the tongue along its body, that their number per cm^2 area decreased from the apex towards the radix, and that Taste pores were present on them (Delibaş et al. 2023). In another study, it was reported that the convex surfaces of these papillae were quite prominent, some were spherical, and others were outwardly conical, that a shallow groove was present on their surfaces, and that taste pores could be distinguished under high magnification (Erdoğan and Sağsöz 2018). In the study conducted on Ossimi sheep, it was found that these papillae had two subtypes, oval and rounded, that they were surrounded by a circular trench, and that they possessed taste pores (Abumandour et al. 2023). In our study, the fungiform papilla did not present a shriveled pea appearance in any of the scanned regions (Figure 5 A, 7). In all SEM photographs, this papillae were determined to have a very regular rounded mushroom appearance (Figure 5 A, 7). Furthermore, the trench surrounding this papilla and the taste pores located on it were also detected in our study (Figure 7).

Circumvallate papilla: In Morkaraman Sheep, they were large and small papillae of round-oval shape arranged in two rows behind the torus of the tongue (Demircioğlu et al. 2024); in Karacabey Merino, they were arranged in varying sizes on the sides of the torus (Can et al. 2016); in Norduz Sheep, they were shown to be arranged in two rows on the radix of the tongue and composed of three parts: the mucosal vallum, the parietal trench, and the ring-shaped cushion (Delibaş et al. 2023). Similar findings were also detected in the study conducted on Ossimi sheep (Abumandour et al. 2023). In another study, it was found that 6-10 circumvallate papillae were arranged laterally in the caudal half of the torus lingua, that the pedicle surrounding the papillae were not continuous, that some lacked a surrounding pedicle, and that the taste pores and the rough appearance of the epithelium were noticeable under high magnification (Erdoğan and Sağsöz 2018). In our study, the circumvallate papilla exhibited the mucosal vallum, parietal trench, and ring-shaped cushion, similar to those in Norduz and Ossimi sheep (Figure 6 A, D).

When the light microscopic findings in the examined mechanical and taste papillae were reviewed based on general structural characteristics, the epithelial feature being stratified squamous epithelium and the variation in thickness according to the papillae and their locations, observed in cattle (Ding et al. 2016), camels (Nabipour 2011), goats (Kurtul and Atalgın 2008), and sheep (Murad 2011), were similarly observed in the Kangal sheep breed. Muscles, connective tissue vascular arrangement, Ebner's glands, and excretory duct structures in the lamina propria were determined to be parallel in cattle (Ding et al. 2016), buffaloes (Prakash and Rao 1980), camels (Nabipour 2011), goats (Kurtul and Atalgın 2008), and many sheep breeds (Murad 2011; Delibaş et al. 2023; Demircioğlu et al. 2024; Güzel et al. 2025) and in Kangal sheep.

With the introduction of the electron microscope into the scientific world, numerous studies have been conducted and are still ongoing to reveal the surface anatomy of organs and tissues at macro and micro levels. Many studies have also been carried out to reveal the lingual papillae at macro and micro levels. In our study, the lingual papillae of the Kangal Sheep, an endemic subspecies in our country, were revealed both histologically and using an electron microscope. In the present study, the lingual papillae of Kangal sheep were described histologically and by scanning electron microscopy, and some minor morphological differences were noted in comparison with previous reports on other sheep breeds. These findings provide baseline descriptive data on the lingual papillae of Kangal sheep and may be useful for future comparative and functional studies. Future studies should evaluate whether variations such as the number of secondary extensions of the filiform papillae or the continuity of the cushion surrounding the circumvallate papillae are associated with functional features of the tongue. In conclusion, the present findings may serve as a reference for future studies in this field.

CONFLICTS OF INTEREST

The authors report no conflicts of interest.

AUTHOR CONTRIBUTIONS

Idea/Concept: LT, SU, İO
Supervision/Consultancy: LT, SU
Data Collecting and/or Processing: LT, SA, SU
Analysis and/or Interpretation: LT, SU, İO, SA, EK
Writing the Article: LT, SU
Critical Review: LT, SU, İO

REFERENCES

Abumandour MM, Morsy K, Elghoul M (2023). Morphological features of the Egyptian Ossimi sheep tongue: New scanning electron microscopic insights into its papillary system adaptations to Egyptian ecological conditions. *Anat Histol Embryol,* 52(2), 262-278.

Aydin KB, Bi Y, Brito LF, Ulutas Z, Morota G (2024). Review of sheep breeding and genetic research in Türkiye. *Front Genet*, *15*, 1308113.

Bancroft JD, Cook HC (1984). Manual of Histological Techniques. 1. Edition. Churchill Livingstone, Edinburgh.

Can M, Atalgın S, Ates S, Takci L (2016). Scanning electron microscopic study on the structure of the lingual papillae of the Karacabey Merino sheep. *Eurasian J Vet Sci, 32(3), 130-135*

Delibas V, Soyguder Z, Cakmak G, Gunduz MS (2023). Morphological Examination of Tongue Papillae in Norduz Sheep: A Scanning Electron Microscopic Study. *Van Vet J*, *34*(1), 75-80.

Demircioglu M, Dortbudak MB, Karaavcı FA, Guzel BC, Demircioglu I (2024). Investigations on the Light and Scanning Electron Microscopic Structure of Tongue Papillae of Morkaraman Sheep: Taste and Mechanical. *Manas J Agric Vet Life Sci*, *14*(2), 167-175.

Dyce KM, Sack WO, Wensing CJG (2009). Textbook of veterinary anatomy. 4. Edition. Saunders Elsevier, Missouri.

Erdogan S, Sagsoz H (2018). Papillary architecture and functional characterization of mucosubstances in the sheep tongue. *Anat Rec*, *301*(8), 1320-1335.

Guzel BC, Isbilir I, Yavas SE, Isbilir F (2025). Lingual Papillae in Hamdani Sheep During Foetal Periods: Gross, Scanning Electron Microscopy, Histochemical and Immunohistochemical Analysis. *Vet Med Sci 11*(4), e70403.

Konig HE, Liebich HG (2020). Veterinary anatomy of domestic animals: Textbook and colour atlas. 7. Edition. Thieme, Stuttgart.

Kurtul I, Atalgın S (2008). Scanning electron microscopic study on the structure of the lingual papillae of the Saanen goat. *Small Rumin Res*, *80*(1-3), 52-56.

Madkour FA, Mohamed AA, Mohammed ES, Choudhary OP (2023a). Sublingual floor of Rahmani sheep (Ovis aries): A scanning electron microscopy and histomorphology analysis. *Anat Histol Embryol, 52*(6), 907-918.

Madkour FA, Mohammed ES (2021). Histomorphological investigations on the lips of Rahmani sheep (Ovis aries): A scanning electron and light microscopic study. *Microsc Res Tech*, *84*(5), 992-1002.

Madkour FA, Soliman SA, Abd-elhafeez HH, Elmansi A (2023b). Morphometrical and Scanning Electron Microscopic Investigations on the Rahmani Sheep's Tongue: Adaptive Strategies for Feeding Behaviors. *Preprints 2023,* 2023061376.

Mahdy MA, Abdalla KE, Mohamed SA (2021). Morphological and scanning electron microscopic studies of the lingual papillae of the tongue of the goat (Capra hircus). *Microsc Res Tech*, *84*(5), 891-901.

Murad NA (2011). Anatomical and histological study of the tongue in adult Awassi rams *(Ovis ovis)* M. Sc. thesis, University of Al-Qadisiya, Iraq.

Nabipour A (2011). Gross and histological study on the minor salivary glands of camel (Camelus dromedarius). *J Camel Pract Res*, *18*(1), 123-129.

Prakash P, Rao G (1980). Anatomical and neurohistological studies on the tongue of the Indian buffalo (Bubalus bubalis). *Cells Tissues Organs*, *107*(4), 373-383.

Tadjalli M, Pazhoomand R (2004). Tongue papillae in lambs: a scanning electron microscopic study. *Small Rumin Res, 54*(1-2), 157-164.

Toprak B (2023). Investigations on the light and scanning electron microscopic structure of the lingual papillae in the angora goat (Capra hircus): II. Mechanical papillae. *Anat Histol Embryol, 52*(2), 327-335.

Ding Y, Yu S, Shao B. (2016). Anatomical and histological characteristic of the tongue and tongue mucosa linguae in the cattle-yak (Bos taurus× Bos grunniens). *Front Biol*, *11*(2), 141-148.

Van Veterinary Journal

https://dergipark.org.tr/tr/pub/vanvetj

Cite this article as: **Eğdir SH, Pekcan Z (2026).** A Review of Diagnostic and Therapeutic Options for Patent Ductus Arteriosus in Dogs. *Van Vet J*, 37(1), 115-122. DOI: https://doi.org/10.36483/vanvetj.1841166

ISSN: 2149-3359 **Review Article** e-ISSN: 2149-8644

A Review of Diagnostic and Therapeutic Options for Patent Ductus Arteriosus in Dogs

Saliha Hazal EĞDİR[1,*] Zeynep PEKCAN[1]

[1] *Kirikkale University, Faculty of Veterinary Medicine, Department of Surgery, 71450, Kirikkale, Türkiye*

Received: 12.12.2025 Accepted: 09.03.2026

ABSTRACT Patent ductus arteriosus (PDA) is a congenital cardiovascular disorder that can be seen in all species but is most frequently encountered in dogs. Despite being one of the most common cardiac diseases, diagnosis and treatment can still be challenging due to the diversity in vascular morphology. Physical examination findings and imaging modalities (e.g., radiography, echocardiography, and advanced imaging techniques) play a critical role in the diagnosis of the disease and in determining the severity of the shunt. Treatment options include standard surgical applications as well as transcatheter occlusion methods, which are more widely preferred today. Early diagnosis and appropriate intervention for PDA are of critical importance in reducing mortality and preserving cardiac function in dogs. In untreated cases, progressive cardiac remodeling and permanent functional impairment occur; indeed, even if the PDA is closed in late-intervention cases, systolic dysfunction and persistent ventricular enlargement may continue. Following successful operations, complications such as left ventricular dysfunction, arrhythmia, pulmonary edema, and residual shunts must be carefully monitored. Although patients treated at an early stage generally have a normal life expectancy, long-term medical support and follow-up may be required in chronic cases. This review aims to contribute to the clinical decision-making process by summarizing current evidence regarding PDA management in dogs, focusing on anesthetic protocols, surgical and transcatheter techniques, and perioperative outcomes.

Keywords: *Cardiovascular, Congenital, Ductus arteriosus, Heart defects.*

ÖZ

Köpeklerde Patent Duktus Arteriyozus için Tanı ve Tedavi Seçeneklerinin Gözden Geçirilmesi

Patent ductus arteriosus (PDA), her türlü hayvanda görülebilen ancak en çok köpeklerde görülen doğuştan gelen bir kardiyovasküler bozukluktur. En yaygın kalp hastalıklarından biri olmasına rağmen, vasküler morfolojideki çeşitlilik nedeniyle teşhis ve tedavi edilmesi hâlâ zor olabilir. Fiziksel muayene ve görüntüleme yöntemleri (örneğin, radyografi, ekokardiyografi, ileri görüntüleme yöntemleri) hastalığın tanısında ve şant şiddetinin belirlenmesinde önemli rol oynamaktadır. Tedavi seçenekleri arasında, standart cerrahi uygulamaların yanı sıra günümüzde daha fazla tercih edilen transkateter oklüzyon yöntemleri yer almaktadır. PDA'nın erken tanısı ve uygun müdahale yöntemi, köpeklerde mortaliteyi azaltmak ve kalp fonksiyonlarını korumak açısından kritik bir önem taşır. Müdahale edilmeyen vakalarda ilerleyici kardiyak remodelling ve kalıcı fonksiyonel bozulma meydana gelir; nitekim geç müdahale edilen vakalarda PDA kapatılsa dahi sistolik disfonksiyon ve kalıcı ventriküler genişleme devam edebilmektedir. Başarılı operasyonlar sonrası ise sol ventrikül disfonksiyonu, aritmi, pulmoner ödem ve rezidüel şantlar gibi komplikasyonlar dikkatle takip edilmelidir. Erken dönemde tedavi edilen hastalar genellikle normal bir yaşam beklentisine sahip olsa da uzun süreli tıbbi destek ve takip gerekebilir. Bu derleme, köpeklerde PDA yönetimine ilişkin güncel kanıtları; anestezi protokolleri, cerrahi ve transkateter teknikler ile perioperatif sonuçlar odağında özetleyerek klinik karar verme sürecine katkı sağlamayı amaçlamaktadır.

Anahtar Kelimeler: *Duktus arteriyozus, Kalp defektleri, Kardiyovasküler, Konjenital.*

INTRODUCTION

Patent ductus arteriosus (PDA) is one of the most common congenital heart diseases in dogs and typically presents as a left-to-right shunt. It is a fetal vessel connecting the pulmonary artery to the descending aorta. During intrauterine life, it remains open due to the low oxygen tension in fetal blood and the effects of prostaglandins. At birth, the sudden increase in blood oxygen content and the decrease in circulating prostaglandin levels stimulate ductal closure, and the smooth muscle fibers within the ductal wall begin to contract. In genetically predisposed

✉ *Corresponding author: hazalertas@hotmail.com

animals, these smooth muscle fibers are partially replaced by elastic tissue within the ductus arteriosus wall. These segments are unable to contract, preventing normal ductal closure. The ductus arteriosus normally closes within the first week of life; if it remains patent beyond the first few days after birth, it is termed patent ductus arteriosus (Hsu et al. 2021; Grimes and Thieman Mankin 2022; Bussadori 2023). This disease is more commonly observed in large breeds such as German Shepherds, Belgian Shepherds, Border Collies, and Australian Shepherds, as well as in small breeds including Poodles, Maltese dogs, Chihuahuas, and Pomeranians. Females are affected more frequently than males. In contrast, PDA is relatively rare in brachycephalic breeds (Brambilla et al. 2020; Bussadori 2023). The cardiac abnormalities associated with PDA vary according to the magnitude and direction of blood flow through the defect, which depend on ductal size, pulmonary vascular resistance, left ventricular (LV) function, and patient age. In PDA, the presence of a continuous left-to-right shunt from the aorta to the pulmonary artery leads to marked volume overload in the pulmonary circulation and the left side of the heart. This results in volume overload of the left heart, causing enlargement of the left atrium (LA), hypertrophy and dilation of the left LV, increased end-diastolic pressure, mitral regurgitation, and the development of left-sided congestive heart failure (CHF) signs such as exercise intolerance, progressing to pulmonary congestion/edema, arrhythmias, and ultimately death in advanced cases (Saunders et al. 2014; Takahashi et al. 2019). Severe pulmonary hypertension may reverse the direction of PDA shunt flow, resulting in right-to-left shunting when pulmonary vascular resistance exceeding systemic resistance, ultimately leading to hypoxemia and cyanosis (Greet et al. 2021). Consequently, occlusion via surgical ligation or transcatheter intervention is recommended to eliminate the shunt and resolve the volume-overload state in appropriate case.

This review was designed to summarize current evidence regarding the management of PDA in dogs, with particular emphasis on anesthetic considerations, surgical and transcatheter techniques, and perioperative outcomes.

Review Methodology

This study aims to systematically evaluate the current literature on the diagnostic and therapeutic approaches to patent ductus arteriosus in dogs and to provide a comprehensive resource to enhance diagnostic and therapeutic success in clinical practice. A structured literature search was conducted using the PubMed and Google Scholar databases with the following keywords: “patent ductus arteriosus,” “dog,” “canine,” “surgical ligation,” “transarterial occlusion,” and “prognosis.” To ensure clinical relevance, the search primarily included studies published between 2020 and 2025; however, publications from 2010 to 2020 were also considered if they were deemed to be of fundamental importance and made significant contributions to the literature. The inclusion criteria comprised English-language original research articles, prospective and retrospective clinical studies, and case series focusing on the diagnosis, treatment, or prognosis of PDA in dogs. Additionally, research articles conducted in cats and humans, as well as up-to-date textbooks, were included when they provided essential pathophysiological insights or supported comparative clinical evaluation. Studies focusing on congenital cardiac anomalies other than PDA, publications with insufficient methodological rigor, articles published before 2010, and non-English-language studies were excluded.

The study selection process was performed in two stages: initially, titles and abstracts were screened to exclude publications not relevant to the topic; subsequently, full-text articles were assessed according to the predefined inclusion and exclusion criteria. The included studies were categorized and analyzed under the following headings: general disease characteristics and pathophysiology, diagnostic methods, surgical and minimally invasive treatment options, postoperative follow-up and care, and prognosis.

Diagnosis

Multiple diagnostic modalities are available for the detection of PDA. In clinical practice, many cases are identified incidentally during routine physical examination. The most characteristic finding is a loud, continuous murmur (typically grade III/VI or higher) auscultated at the left cardiac base. A systolic murmur over the mitral valve area may also be present. Additional findings can include a palpable cardiac thrill, strong femoral pulses, cyanosis, and polycythemia (Martin et al. 2022; Bussadori 2023).

Thoracic radiographs remains a valuable initial imaging tool. In dogs with left-to-right shunting, radiographs commonly demonstrate dilation of the descending aorta, enlargement of the LA and LV, prominence of the aortic arch, and left-sided cardiomegaly. Pulmonary venous and arterial dilation may be evident on lateral views, often accompanied by pulmonary congestion or edema. In rare cases where the PDA is small, the cardiac silhouette may appear normal (Broaddus and Tillson 2010; Orton 2018; Bussadori 2023; Dukes-McEwan 2024).

In dogs with reverse PDA, typically exhibit right-sided cardiac enlargement and dilation of the main pulmonary artery. Inadequate perfusion of lung areas may be evident (hypovascular pattern and hyperlucent lung fields) (Dukes-McEwan, 2024). Additionally, radiographic images may also reveal a ductal aneurysm, a pathognomonic finding indicating dilation of the aorta and the aortic portion of the PDA (Broaddus and Tillson 2010; Ro et al. 2022).

Echocardiography is considered the gold standard for definitive diagnosis. It allows detailed assessment of ductal morphology, measurement of ductal dimensions. In most patients, the ductus arteriosus is always clearly visible in both left and right parasternal views. LV myocardial failure, which is often present in PDA, can be assessed using M-mode echocardiography. In left-to-right shunting, typical findings include LA enlargement, LV hypertrophy and dilation, and enlargement of the aorta and pulmonary artery. Secondary valvular regurgitations involving the aortic, pulmonary, tricuspid, and mitral valves may also occur due to hemodynamic alterations. A slight increase in flow velocity (but usually <2.5 m/s) may be measured in the left ventricular outflow tract. Doppler imaging demonstrates continuous high-velocity turbulent flow from the aorta into the pulmonary artery, often producing the characteristic “sawtooth” pattern within the pulmonary artery. In reverse PDA, a dilated main pulmonary artery and concentric right ventricular hypertrophy are commonly seen. Computed tomography (CT) may be recommended when atypical ductal morphology that could complicate closure is suspected (Buranakarl et al. 2015; Bussadori 2023; Dukes-McEwan 2024). Althouhgh, angiography is now rarely used solely for diagnostic purposes, it remains essential during

transarterial occlusion procedures accurately to measure and evaluate the ductus (Brewer 2017).

In summary, while multimodal imaging has substantially improved diagnostic accuracy and procedural planning in PDA, limitations in available evidence and the need for prospective comparative studies highlight important areas for future research.

Anesthesia Considerations

In patients undergoing thoracic surgery for PDA correction, anesthetic management should be planned carefully. Anesthetic agents with minimal cardiovascular effects should be preferred in patients undergoing PDA occlusion. In dogs with left-to-right shunting, various drug combinations have been used for anesthetic induction, including opioids, benzodiazepines, propofol, alfaxalone, and etomidate. Anesthesia may be maintained with inhalational agents alone or combined with intravenous infusions (Medina-Serra et al. 2021). However, opioid dosing must be carefully calculated to minimize adverse effects on ventilation (Broaddus and Tillson 2010). In dogs anesthetized for correction of a left-to-right shunting PDA, there is general agreement that α2-agonists should be excluded from the anesthetic protocol. These agents decrease cardiac output and increase systemic vascular resistance, potentially exacerbating shunt flow and increasing the risk of hydrostatic pulmonary edema (Medina-Serra et al. 2021). Stress free preoxygenation is recommended prior to induction. Thoracic entry inevitably induces pneumothorax. Although spontaneous ventilation may persist initially, paradoxical respiration and atelectasis can develop, leading to ventilation-perfusion mismatch. Therefore, manual or mechanical ventilation is required until the procedure is completed and the pleural space is evacuated (Pascoe 2016). Selected anesthetic agents may contribute to perianesthetic hypotension, particularly inhalational anesthetics, which reduce systemic vascular resistance and myocardial contractility. For this reason, their use is generally discouraged in patients with right-to-left shunting (Ban et al. 2022). In dogs with left-to-right shunts, management of intraoperative hypotension can also be challenging due to continuous blood flow from the aorta to the pulmonary artery (Medina-Serra et al. 2021).

Overall, anesthetic management in PDA patients must be individualized according to shunt direction and cardiovascular status, with the primary goal of maintaining hemodynamic stability while minimizing alterations in systemic and pulmonary vascular resistance.

Preoperative Evaluation and Risk Factors

Preoperative evaluation should include a comprehensive assessment of the patient's clinical status, pathophysiological stage, and the extent of left ventricular anatomical and functional remodeling. The degree of remodeling is influenced by the age of the affected animals, preoperative LV size, and systolic function. Conditions that may require patient stabilization before PDA closure should be identified, include congestive heart failure, systolic dysfunction, and arrhythmias. Discontinuation of angiotensin-converting enzyme inhibitors may be considered preoperatively, as these drugs can increase the risk of hypotension. Dogs with pulmonary edema should be stabilized with appropriate diuretic therapy before undergoing interventional or surgical procedures (Araos et al. 2021; Bussadori 2023). Dogs aged 8-16 weeks without concurrent cardiac disease are considered ideal candidates for surgical correction of left-to-right PDA (Saunders et al. 2014). In older dogs, correction is often not performed because of anesthetic risk. However, subsequent clinical improvement has also been reported in this population. Older dogs may exhibit more remodeling and scar tissue in the region due to chronic changes from altered blood flow. This often results in structural vessel alterations, more difficult dissection, and a significantly increased risk of rupture. Higher body weight may be associated with larger ductal diameter, thereby raising the risk of rupture by enlarging the weak surface area of the medial wall. Additionally, the use of larger surgical instruments may reduce dissection precision (Broaddus and Tillson 2010; Boutet et al. 2017; Grimes and Thieman Mankin 2022).

In summary, older age, high body weight, large ductal diameter, severe cardiomegaly, and arrhythmias associated with impaired cardiac remodeling and increased perioperative risk. Therefore, early ductal closure is recommended whenever feasible, particularly in medium and large breed dogs. Nonetheless, advanced age alone should not be considered a contraindication, as persistent shunting may lead to congestive heart failure, arrhythmias, or sudden death. It should also be recognized that irreversible remodeling and residual functional impairment may persist even after successful closure (Ro et al. 2022; Bussadori 2023; Papa et al. 2023).

Treatment Options

In dogs, PDA management includes medical therapy, intravascular transcatheter occlusion, and extravascular surgical ligation (Markovic et al. 2022). Surgical or transcatheter closure is contraindicated in cases of reverse PDA or bidirectional shunting, as well as in congenital cardiac defects that depend on right-to-left shunting for systemic perfusion (e.g. Tetralogy of Fallot). In these situations, intervention may precipitate acute hemodynamic decompensation. Therefore, management is conservative and guided by clinical signs rather than definitive ductal closure (Broaddus and Tillson 2010; Bussadori 2023).

Although both interventional and surgical approaches are effective in eliminating left-to-right shunting, treatment selection is largely determined by shunt direction, hemodynamic status, patient size, and the presence of concurrent cardiac abnormalities.

Management of Right-to-Left Shunting

According to Bussadori (2023), reverse PDA, also known as right-to-left shunting, lowers the risk of progressive left heart failure but increases polycythemia, causes exercise intolerance, and results in systemic hypoxemia (Piantedosi et al. 2019). If a reverse PDA is closed, right ventricular afterload increases abruptly. This often results in acute right heart failure and death. Therefore, treatment focuses on alleviating the clinical signs of hypoxemia and correcting polycythemia through phlebotomy to reduce blood viscosity and improve tissue perfusion. Management of secondary polycythemia is considered the cornerstone of therapy in dogs with reverse PDA. The objective is to reduce the PCV to below 65%. However, the effect of phlebotomy is transient and may lead to iron deficiency. For this reason, it is recommended for the short-term relief of hyperviscosity symptoms rather than for strict hematocrit control. Frequent repetition of the procedure may be challenging for some animals and may raise concerns regarding owner-perceived quality of life (Greet et al. 2021). Sildenafil has been used in dogs with PDA associated with pulmonary hypertension to promote pulmonary vasodilation and improve hemodynamics. Some studies have reported improved clinical signs and

prolonged survival in treated patients (Greet et al. 2021; Sugimoto et al. 2025). However, the number of studies involving animals with right-to-left shunting is limited, and further research is needed to better define clinical outcomes in this population.

Standard Surgical Ligation

The surgical approach is typically reserved for dogs weighing less than 2.5 kg or for cases in which ductal morphology precludes the use of transcatheter occlusion devices. Surgical ligation is performed using either a standard dissection techniques (extrapericardial or intrapericardial technique) or the Jackson and Henderson approach.

The intrapericardial technique represents an alternative surgical approach for PDA ligation, offering a distinct dissection plane. It is particularly advantageous in redo procedures following ductal rupture, as it avoids manipulation of the previous tear site and circumvents fibrotic adhesions that may develop after the extrapericardial approach. Access is typically achieved via a left fourth intercostal thoracotomy. The left cranial lung lobe is carefully retracted caudally, to allowing visualization of the left cardiac base, the ductus arteriosus and adjacent neurovascular structures (Broaddus and Tillson 2010; Selmic et al. 2013; Grimes and Thieman Mankin 2022). Preservation of the left vagus nerve and the recurrent laryngeal nerve is essential during dissection to prevent postoperative complications. Dissection of the cranial portion of the ductus arteriosus is performed within the anatomical space formed by the aortic arch and the pulmonary artery, using a gentle, controlled approach to create adequate room for ligature placement. Once adequate dissection has been achieved, two ligatures are placed around the ductus. The ligature closest to the aorta is typically tightened first, followed by the second ligature. The pulsation palpated in the pulmonary artery before ligation should disappear completely after ligation. Standard thoracic closure follows, including placement of a thoracostomy tube (Monnet 2014; Orton 2018).

Ductal rupture remains one of the most significant intraoperative complications. Hemorrhage, particularly from the medial aspect of the ductus arteriosus, can often be controlled with gentle tamponade. However, simple ligation is not feasible in cases of ductal rupture. In such situations, surgical alternatives including digital pressure, hemostatic agents, vascular clips, or tampon-supported U-sutures should be used to control the hemorrhage (Orton 2018; Grimes and Thieman Mankin 2022).

If residual ductal flow persists after surgical ligation, transcatheter occlusion with an ACDO or coil may be performed, or repeat surgical ligation using the Jackson-Henderson technique can be considered (Bussadori 2023).

Modified Jackson-Henderson Technique

In extrapericardial techniques, the PDA is exposed and isolated without opening the pericardium. A non-absorbable suture is placed circumferentially for ligation. The Jackson-Henderson modification of the extrapericardial technique, alters the direction of dissection by working around the dorsal aorta, allowing the suture to be passed dorsally and cranially without advancing instruments medial to the ductus. The Jackson-Henderson technique is particularly useful following a rupture, as it eliminates the need to pass an instrument medial to the PDA. This is critical because the muscular wall is thinnest at this location, making it the most common site for tears. Although the technique was developed to reduce the risk of intraoperative rupture, it may carry a higher likelihood of residual flow, likely due to the inclusion of periductal tissue within the ligature (Selmic et al. 2013; Grimes and Thieman Mankin 2022).

During placement of the first ligature, a reflex bradycardia may occur due to an increase in aortic pressure. This phenomenon, known as the Branham sign, can be managed with anticholinergic agents such as atropine. Gradual tightening of the ligature over 2–3 minutes has been suggested to mitigate the severity of this reflex. In rare cases, severe vagal stimulation may progress to cardiopulmonary arrest following ductal occlusion, a complication thought to be associated with an exaggerated Branham reflex (Broaddus and Tillson 2010; Saunders et al. 2014).

Hemostatic Clip Method

In PDA treatment, hemostatic clips reduce the risk of bleeding by avoiding unnecessary medial dissection of the shunt (Ozai et al. 2022). However, this technique carries a higher risk of residual ductal flow due to the interposition of connective tissue within the clip. Transesophageal echocardiography can be used to detect residual ductal flow. If present, additional clips or sutures may be applied to achieve complete occlusion. Unlike traditional techniques, this approach provides a smaller operative field and shorter operative time (Takeuchi et al. 2020). Minimally invasive surgical ligation techniques are also available. In these approaches, titanium clips are placed via thoracoscopy or video-assisted minithoracotomy (Selmic et al. 2013).

The primary disadvantage of thoracotomy is its invasive nature; however, puppies in particular appear to recover rapidly and are typically discharged within 24-48 hours. Recent studies have demonstrated that hospital discharge rates are similar among techniques. However, serious complications are reported more frequently with surgical ligation. The primary complications of surgical ligation include hemorrhage, laryngeal dysfunction, iatrogenic lung injury, myocardial hypoxia, arrhythmias, hypotension and cardiac arrest associated with ductal closure. Among these, fatal hemorrhage is the most serious surgical complication. Reported incidence rates range from 1% to 17%, with associated mortality rates between 0% to 7% (Ranganathan et al. 2018; Claretti et al. 2019; Markovic et al. 2022). In one study, residual flow was observed in 9.4% of dogs undergoing PDA ligation, regardless of rupture. The incidence of residual flow varies according to surgical techniques. One study reported rates of 21% with standard technique and 53% with the Jackson-Henderson technique (Grimes and Thieman Mankin 2022). While trivial residual flow may resolve spontaneously, moderate to severe flow suggests inadequate ligation. Surgeons must aim for complete occlusion to eliminate blood flow, despite the risk of suture-induced rupture and hemorrhage. The success of surgery depends on several risk factors. The most favorable outcomes are observed in patients younger than 2 years of age and without atrial fibrillation or clinical signs of CHF (Broaddus and Tillson 2010).

Surgical ligation has long been used and remains a commonly performed treatment modality in many centers. However, the wide variation in reported complication and residual flow rates in the literature is noteworthy. Reported hemorrhage rates ranging from 1-17%, mortality rates between 0-7%, and residual flow rates of 9-53% suggest that these outcomes are not solely attributable to the procedure itself, but may also be influenced by factors such as surgical experience, patient selection, ductal morphology, and appropriate choice of surgical

instruments. Consequently, although surgical ligation continues to represent an indispensable option (particularly in patients weighing less than 2.5 kg or in cases where ductal anatomy is unsuitable for transcatheter closure) its success appears to be largely operator-dependent.

Interventional Interventions

Currently, transcatheter closure of PDA has largely replaced surgical ligation in most centers, except in very small patients or when ductal size or morphology is unsuitable. It has also been performed in cases where surgical repair was not feasible due to hemorrhage, increased flow, or inability to identify the ductus. In catheter-based occlusion, the choice between venous and arterial access, as well as device selection, depends on species, patient size, vessel caliber, and ductal morphology and dimensions. In dogs with severe volume overload and congestive heart failure, medical stabilization followed by urgent transcatheter closure should be considered (Markovic et al. 2022). Coils, the Amplatzer plug, and the Amplatzer duct occluder are the main devices used in catheter-based occlusion techniques. Currently, transarterial occlusion using the Amplatzer Canine Duct Occluder (ACDO) is one of the most widely used methods for closing PDA defects with a left-to-right shunt (Piantedosi et al. 2019; Craciun et al. 2024; Mcmullen et al. 2024). Echocardiographic or angiographic measurements are used to determine the appropriate ACDO device size. The selected device is generally 1.5-2 times the minimum ductal diameter. After induction of anesthesia, the vascular access site is selected according to the animal's size and the occlusion technique. The most common access sites the femoral artery, carotid artery, or jugular vein (Bussadori 2023). According to the procedure described by Martin et al. (2022), the selected coil or occluder is deployed under fluoroscopic guidance following the visualization of the PDA shunt with contrast medium. The smallest size ACDO device is generally unsuitable for femoral artery access in dogs weighing less than 2 kg. Therefore, treatment options for very small dogs are limited to open-chest surgery or the alternative catheter-based devices (Hogan and Goldfeder 2021). This limitation in arterial access has prompted veterinary cardiologists to explore venous approaches. The femoral and jugular veins provide a larger diameter and greater wall compliance, facilitating vascular access. The jugular vein is often preferred for a percutaneous procedures. Transvenous coil embolization has been shown to be effective in dogs weighing less than 3.0 kg. The carotid artery may also be used in very small patients. However, the transvenous approach is technically challenging and requires cardiac catheterization. Various techniques, including coils and vascular plugs, have been described in the literature (Hogan and Goldfeder 2021; Bagardi et al. 2022; Ostenkamp et al. 2022; Cala et al. 2024). In one study, transarterial PDA occlusion was successful in most dogs with a 98% success rate at the 24-hour follow-up. Complete flow cessation achieved in 95% of patients at this time point. At medium-term follow-up, complete flow cessation was observed in 91.5% of cases (Ciccozzi et al. 2025). Transarterial ductal closure using a low-profile vascular plug has been described for dogs with small femoral arteries. These devices expand treatment options in patients with limited arterial access. New devices, such as the low-profile vascular plug, are broadening the range of endovascular PDA occlusion techniques (Hogan and Goldfeder 2021; Martin et al. 2022). A recent retrospective study has shown that transvenous PDA closure using the Nit-Occlud PDA occlusion system is feasible and can be successfully performed in dogs weighing less than 3 kg (Cala et al. 2024). Thromboembolic coils (TCEs) is ideal for dogs small, funnel-shaped PDAs measuring 2-3 mm in diameter. Dogs with large PDAs are better candidates for ACDO placement. Because multiple coils within the ductal ampulla may lead to displacement and residual shunting. The advantages of transcatheter occlusion include a high success rate, ease of deployment, low morbidity (7.1% vs. up to 28% with surgical ligation), rapid recovery, early discharge, and a low complication rate (2-12%) (Ranganathan et al. 2018; Medina-Serra et al. 2021; Markovic et al. 2022). Major complications associated with transarterial procedures occur in 0% to 4% of dogs. These include arrhythmias, femoral artery hemorrhage, residual ductal shunt, aortic regurgitation, femoral artery dissection, aortic perforation, device embolization or migration, pulmonary artery dissection, ductal arteritis, infection, bacterial endocarditis, septicemia, and hemolysis. Device embolization is considered the most significant complication (Lavennes et al. 2018; Ranganathan et al. 2018; Parisi et al. 2020; Grimes and Thieman Mankin 2022; Ro et al. 2022). Residual ductal flow may occur after uneventful surgical ligation or transcatheter closure. This is generally attributed to incomplete closure or recanalization of the PDA (Markovic et al. 2022). Reported residual flow rates for alternative closure devices, such as coils or vascular plugs, range from 0% to 44% (Belachsen et al. 2022; Hildebrandt et al. 2022).

Studies comparing surgical ligation and transarterial coil occlusion shown that surgical ligation has a higher success rate (94%). However, it is associated with a higher major complication rate (12%). In contrast, coil occlusion has a lower success rate (84%) but a safer profile, with fewer complications (4%). Mortality rates range from 0% to 6% for surgical ligation and from 0% to 3% for transarterial procedures (Saunders et al. 2014; Ranganathan et al. 2018; LeBlanc et al. 2019; Martin et al. 2022). Although surgical ligation has long been considered the standard treatment and demonstrates high efficacy, it carries a greater risk of complications and mortality. In contrast, transcatheter occlusion is a safe, effective, and less invasive alternative. However, this approach is generally more expensive than ligation (Grimes and Thieman Mankin 2022). And all treatment modalities are presented in a comparative format in Table 1.

Transcatheter closure is currently the preferred approach due to its minimally invasive nature and lower reported morbidity; however, device embolization remains the most significant complication. Moreover, much of the available evidence is based on retrospective and non-randomized studies, limiting direct comparisons with surgical ligation and introducing potential selection bias. Data in very small breeds (<2-3 kg) remain insufficient, as vascular access limitations increase procedural complexity. In addition, long-term data regarding cardiac remodeling, durability of occlusion, and postoperative follow-up outcomes are limited. Therefore, prospective and comparative studies are needed to better define patient selection criteria and optimize device choice.

Table 1: Comparative Summary of Treatment Options for Canine PDA.

Method	Indication	Success Rate	Major Complications	Residual Flow	Mortality	Ideal Candidate
Standard Surgical Ligation	Dogs <2-2.5 kg; unsuitable duct morphology; limited catheter access	~94%	Hemorrhage, laryngeal dysfunction, lung injury, arrhythmias, hypotension, cardiac arrest	9.4-21% (up to 53% depending on technique)	0-7%	Dogs aged 8-16 weeks and free of concomitant heart disease
Jackson–Henderson Technique	Redo ligations; high rupture risk cases	Comparable to standard ligation	Reduced rupture risk; possible higher residual flow	Up to 53% reported	0-7%	Dogs at risk of ductal rupture; redo procedures
Hemostatic Clip Method	Alternative surgical approach	High (varies by study)	Residual ductal flow, hemorrhage	Variable	0-7%	Small–medium dogs; thoracoscopic capability
Transarterial ACDO	Adequate femoral artery size; Dogs with large PDAs	95-98% (short term); ~91.5% medium term	Embolization, arrhythmias, femoral artery complications, aortic regurgitation	Low	0-3%	Dogs >2 kg with suitable duct morphology
Transarterial Coil Occlusion	Small, funnel-shaped PDA (2-3 mm)	~84%	Coil displacement, embolization, residual shunt	0-44%	0-3%	Dogs with small PDA diameter
Transvenous Coil / Vascular Plug	Very small dogs; limited arterial access	High feasibility; varies	Technical difficulty; embolization; residual shunt	0-44%	0-3%	Dogs <3 kg; small femoral arteries

ACDO: Amplatzer Canine Duct Occluder, CHF: congestive heart failure, PDA: Patent ductus arteriosus

Postoperative Follow-up and Care

Closure of the PDA should result in the disappearance of the continuous murmur. Patients undergoing surgical or minimally invasive procedures require postoperative follow-up This follow-up includes radiography, echocardiography, and auscultation (Broaddus and Tillson 2010). PDA closure may cause sudden hemodynamic changes. Reflex bradycardia after closure is mild in small and medium-sized ductus arteriosus. In large ductus arteriosus, however, bradycardia occurs immediately and may persist for several hours. In dogs with very large ductus arteriosus and concurrent systolic dysfunction, bradycardia may further reduce cardiac output after closure. Dogs with limited cardiac remodeling are risk of perioperative complications. These include pulmonary edema, arrhythmia, or cardiac death following ductal closure. The risk is higher in these patients compared with others. Furthermore, mismatch between the left ventricle and the aorta after PDA closure may increase residual volume. This can further impair ventricular expansion and lead to pulmonary congestion. These hemodynamic changes increase the risk of pulmonary edema, arrhythmia, CHF and sudden death. Affected dogs require treatment with vasodilators and positive inotropic agent. This therapy may be necessary intraoperatively, during intensive care, and long term. PDA closure reduces preload and increased afterload. This results in decreased left chamber volume and may lead to a decline in contractility. Consequently, LV size and wall tension decrease (Piantedosi et al. 2019; Grimes and Thieman Mankin 2022; Bussadori 2023; Papa et al. 2023). This phenomenon, often referred to as 'afterload mismatch', may cause LV systolic dysfunction in both dogs and humans. It is characterized by reduced fractional shortening (FS%) and ejection fraction (EF)% (Hou et al. 2019). However, FS% and EF% are not considered the gold standard for assessing systolic function in dogs. Speckle-tracking echocardiography is recommended as a more accurate method for evaluating myocardial contractility in dogs with PDA (Spalla et al. 2016).

Therefore, careful perioperative monitoring and individualized medical management are essential, and further prospective studies using imaging modalities are needed to better clarify the mechanisms, clinical significance, and long-term impact of post-closure systolic dysfunction in dogs with PDA.

Prognosis

Correction of PDA within the first year of life is associated with excellent procedural outcomes (Buranakarl et al. 2015). A recent study demonstrated that the medium-term prognosis is very good, particularly in dogs without pre-existing heart failure or pulmonary hypertension. Sudden death is uncommon. Most medium- and long-term mortalities are attributed to refractory chronic heart failure (Martin et al. 2022). The long-term prognosis after surgical ligation or transarterial occlusion is generally favorable. However, outcomes are poor in dogs with advanced heart failure or atrial fibrillation. Dogs responses

differently to ductal closure depending on body size. Small breeds show a greater reduction in indexed ventricular diameters than large breeds. In contrast, large breeds exhibit larger LV dimensions and lower shortening fractions during follow-up compared with small and mixed breeds (Hou et al. 2019; Piantedosi et al. 2019). This difference may be explained by increased wall stress in large-breed dogs. A larger LV diameter results in higher wall stress, which limits myocardial adaptation. Even long after surgery, LV volumes may remain elevated and contractile indices may stay below reference ranges. In such cases, the LV remains dilated and hypokinetic but is still capable of maintaining adequate cardiac output. These dogs typically maintain a normal quality of life, normal life expectancy, and good exercise tolerance. Nevertheless, the relationship between age at intervention and degree of cardiac remodeling after PDA occlusion remains controversial (Saunders et al. 2014; Grimes and Thieman Mankin 2022; Papa et al. 2023).

In conclusion, successful management of PDA requires accurate assessment of the patient's hemodynamic status, careful evaluation of shunt direction, appropriate selection of the closure technique in eligible candidates, and effective control of perioperative cardiovascular fluctuations. However, current evidence is largely retrospective and heterogeneous, with limited long-term standardized data. The effect of age at intervention on cardiac remodeling remains controversial, and the clinical relevance of persistent ventricular dilation is not fully understood. Further studies are needed to clarify the roles of age, body size, and preoperative remodeling in long-term outcomes.

In this review, treatment modalities were compared with respect to short- and long-term complications as well as recovery outcomes. We believe that these comparisons may facilitate clinical decision-making among the available therapeutic options.

CONFLICTS OF INTEREST

The authors report no conflicts of interest.

AUTHOR CONTRIBUTIONS

Idea/Concept: SHE
Supervision/Consultancy: ZP
Data Collection and/or Processing: SHE
Analysis and/or Interpretation: SHE, ZP
Writing the Article: SHE
Critical Review: ZP

REFERENCES

Araos J, Kenny JES, Rousseau-Blass F, Pang DS (2021). Dynamic prediction of fluid responsiveness during positive pressure ventilation: a review of the physiology underlying heart–lung interactions and a critical interpretation. *Vet Anaesth Analg*, 47(1), 3-14.

Bagardi M, Domenech O, Vezzosi T et al. (2022). Transjugular Patent Ductus Arteriosus Occlusion in Seven Dogs Using the Amplatzer Vascular Plug II. *Vet Sci*, 9(8), 431-435.

Ban K, Bini G, Herrold E, Stavri A, Winter R (2022). Anaesthetic management of a dog with a bidirectionally shunting patent ductus arteriosus and concurrent pulmonary hypertension. *Vet Rec Case Rep*, 10(4), e501.

Belachsen O, Sargent J, Koffas H, Schneider M, Wagner T (2022). The use of Amplatzer vascular plug II in 32 consecutive dogs for transvenous occlusion of patent ductus arteriosus. *J Vet Cardiol*, 41, 88-98

Boutet BG, Saunders AB, Gordon SG (2017). Clinical Characteristics of Adult Dogs More Than 5 Years of Age at Presentation for Patent Ductus Arteriosus. *J Vet Intern Med*, 31(3), 685-690.

Brambilla PG, Polli M, Pradelli D et al. (2020). Epidemiological study of congenital heart diseases in dogs: Prevalence, popularity, and volatility throughout twenty years of clinical practice. *PLoS ONE*, 15(7), 1-17.

Brewer BP (2017). Angiography. Durham HE (Ed). Cardiology for Veterinary Technicians and Nurses (pp. 199-224) Wiley-Blackwell, USA.

Broaddus K, Tillson M (2010). Patent ductus arteriosus in dogs. *Compend Contin Educ Vet*, 32(9), E1-E14.

Buranakarl C, Kijtawornrat A, Udayachalerm W et al. (2015). Intervention technique using transvenous patent ductus arteriosus (PDA) occluder in a dog. *Thai J Vet Med*, 45(4), 593-602.

Bussadori CM (2023). Congenital cardiovascular diseases with a systemic-to-pulmonary shunt. Bussadori CM (Ed). Textbook of Cardiovascular Medicine in Dogs and Cats (pp. 341-362). Edra Publishing, USA

Cala A, Ferasin L, Ferasin H, Domenech O (2024). Transvenous closure of patent ductus arteriosus with Nit-Occlud PDA occlusion system in 13 dogs weighing less than 3 kg. *J Vet Cardiol*, 56(3), 23-34.

Ciccozzi M, Stauthammer CD, Coats C et al. (2025). Transcatheter Amplatz canine duct occluder placement for patent ductus arteriosus occlusion: A retrospective analysis of outcomes and complications in 200 dogs. *J Vet Cardiol*, 60, 36-45.

Claretti M, Lopez BS, Boz E et al. (2019). Complications during catheter-mediated patent ductus arteriosus closure and pulmonary balloon valvuloplasty. *J Small Anim Pract*, 60(10), 607-615.

Craciun I, Silva J, Dutton LC, Loureiro J (2024). Two- and three-dimensional transesophageal echocardiographic assessment and successful occlusion of a window-like patent ductus arteriosus in two dogs. *J Vet Cardiol*, 51, 214-219.

Dukes-McEwan J (2024). The heart and major vessels. Schwarz T, Scrivani P (Ed.) Manual of Canine and Feline Thoracic Imaging (pp. 172-275). BSVA, England.

Greet V, Bode EF, Dukes-McEwan J et al. (2021). Clinical features and outcome of dogs and cats with bidirectional and continuous right-to-left shunting patent ductus arteriosus. *J Vet Intern Med*, 35(2), 780-788.

Grimes JA, Thieman Mankin KM (2022). Surgical ligation of patent ductus arteriosus in dogs: Incidence and risk factors for rupture. *Vet Surg*, 51(4), 592-599.

Hildebrandt N, Stosic A, Henrich E et al. (2022). Transvenous embolization of moderate to large patent ductus arteriosus in dogs using the Amplatzer vascular plug II. *J Vet Intern Med*, 36(1), 20-28.

Hogan DF, Goldfeder GT (2021). Transarterial correction of patent ductus arteriosus in small dogs with the Amplatz Vascular Plug II. *J Vet Cardiol*, 35, 48-54.

Hou M, Qian W, Wang B et al. (2019). Echocardiographic Prediction of Left Ventricular Dysfunction After Transcatheter Patent Ductus Arteriosus Closure in Children. *Front Pediatr*, 7, 409-414.

Hsu HW, Lin TY, Liu YC, Yeh JL, Hsu JH (2021). Molecular mechanisms underlying remodeling of ductus arteriosus: Looking beyond the prostaglandin pathway. *Int J Mol Med Sci,* 22(6), 1-18.

Lavennes M, Chetboul V, Passavin P et al. (2018). Successful transcatheter retrieval of embolized Amplatz Canine Duct Occluders in two dogs. *J Vet Cardiol*, 20(6), 451-457.

LeBlanc NL, Agarwal D, Menzen E et al. (2019). Prevalence of major complications and procedural mortality in 336 dogs undergoing interventional cardiology procedures in a single academic center. *J Vet Cardiol*, 23, 45-57.

Martin M, Pedro B, Dickson D et al. (2022). Outcome clinical audit: Analyses of interventional closure of patent ductus arteriosus in dogs. *J Vet Cardiol*, 43, 27-40.

Mcmullen M, Maneval KL, Ferrel, CS, Holland M, Winter RL (2024). Unilateral pulmonary edema in a dog with a large, left-to-right shunting patent ductus arteriosus. *J Vet Cardiol*, 56, 111-115.

Medina-Serra R, Palacios C, McMillan M (2021). Alternative anaesthetic management in a reintervention for correction of a left-to-right shunting patent ductus arteriosus (PDA) in a dog. *Vet Rec Case Rep*, 9(1), 25-30.

Monnet E (2014). Cardiovascular and Lymphatic. Borjab MJ (Ed), Current Techniques In Small Animal Surgery (pp. 642–643). Teton NewMedia.

Orton E (2018). Patent Ductus Arteriosus. Orton E, Monnet E (Ed), Small Animal Thoracic Surgery (pp. 177-181). USA: Wiley Blackwell.

Ostenkamp SM, Bell SC, Hogan DF (2022). Transvenous correction of patent ductus arteriosus in two toy-breed dogs with the Amplatzer Vascular Plug 4. *J Vet Cardiol*, 44, 13-17.

Ozai Y, Uemura A, Tanaka R et al. (2022). Clip ligation for treatment of patent ductus arteriosus occlusion in three cats. *J Vet Sci*, 23(4), 39-44.

Papa M, Scarpellini L, Pradelli D et al. (2023). Retrospective cohort evaluation of left ventricular remodeling, perioperative complications and outcome in medium and large size dogs with patent ductus arteriosus after percutaneous closure. *Vet Sci*, 10(12), 669.

Parisi C, Phillips V, Ferreira J, Linney C, Mair A (2020). Anaesthetic management and complications of transvascular patent ductus arteriosus occlusion in dogs. *Vet Anaesth Analg*, 47(5), 581-587.

Pascoe PJ (2016). Intrathoracic surgery and interventions. Duke-Novakovski T, de Vries M, Seymour C (Ed). BSAVA Manual of Canine and Feline Anaesthesia and Analgesia (pp. 329-342). BSAVA, England

Piantedosi D, Piscitelli A, De Rosa A et al. (2019). Evaluation of left ventricular dimension and systolic function by standard transthoracic echocardiography before and 24-hours after percutaneous closure of patent ductus arteriosus in 120 dogs. *PLoS ONE*, 14(10), 1-12.

Ranganathan B, Leblanc NL, Scollan KF et al. (2018). Comparison of major complication and survival rates between surgical ligation and use of a canine ductal occluder device for treatment of dogs with left-to-right shunting patent ductus arteriosus. *J Am Vet Med Assoc*, 253(8), 1046-1052.

Ro WB, Park HM, Song DW et al. (2022). Case Report: Aortic Regurgitation of Postocclusion and Long-Term Outcome Following PDA Correction in an Adult Dog. *Front Vet Sci*, 9(5), 1-7.

Saunders AB, Gordon SG, Boggess MM, Miller MW (2014). Long-term outcome in dogs with patent ductus arteriosus: 520 Cases (1994-2009). *J Vet Intern Med,* 28(2), 401-410.

Selmic LE, Nelson DA, Saunders AB, Hobson HP, Saunders WB (2013). An intrapericardial technique for pda ligation: Surgical description and clinical outcome in 35 dogs *J Am Anim Hosp Assoc,* 49(1), 31-40.

Spalla I, Locatelli C, Zanaboni AM, Brambilla P, Bussadori C (2016). Echocardiographic Assessment of Cardiac Function by Conventional and Speckle-Tracking Echocardiography in Dogs with Patent Ductus Arteriosus. *J Vet Intern Med*, 30(3), 706-713.

Sugimoto K, Mochizuki Y, Itoi T et al. (2025). Successful treatment of patent ductus arteriosus and severe pulmonary hypertension using sildenafil and beraprost sodium in two dogs. *J Vet Med Sci*, 87(7), 798-803.

Takahashi K, Nii M, Takigiku K et al. (2019). Development of suction force during early diastole from the left atrium to the left ventricle in infants, children, and adolescents. *Heart Vessels*, 34(2), 296-306.

Takeuchi A, Uemura A, Goya S et al. (2020). The utility of patent ductus arteriosus closure with hemostatic clip in dogs. *Pol J Vet Sci*, 23(2), 255–260.

Van Veterinary Journal

https://dergipark.org.tr/tr/pub/vanvetj

Cite this article as: **Bozkurt MF, Zafar M, Karakurt E (2026).** Feline Tuberculosis and Non-Tuberculous Mycobacterioses: An Updated Veterinary Perspective. *Van Vet J*, 37(1), 123-130. DOI: https://doi.org/10.36483/vanvetj.1874107

ISSN: 2149-3359 **Review** e-ISSN: 2149-8644

Feline Tuberculosis and Non-Tuberculous Mycobacterioses: An Updated Veterinary Perspective

Mehmet Fatih BOZKURT[1] Mudassar ZAFAR[1,*] Emin KARAKURT[2]

[1] *Afyon Kocatepe University, Faculty of Veterinary Medicine, Department of Pathology, 03204, Afyonkarahisar, Türkiye*
[2] *Kafkas University, Faculty of Veterinary Medicine, Department of Pathology, 36100, Kars, Türkiye*

Received: 28.01.2026 Accepted: 17.03.2026

ABSTRACT Traditionally considered to be an uncommon illness in domestic cats, feline tuberculosis (TB) is now recognized as an emerging infection with significant consequences for both public health and veterinary practice. Cats are susceptible to multiple members of the Mycobacterium tuberculosis complex, especially Mycobacterium bovis and Mycobacterium microti, which can produce a variety of clinical and epidemiological patterns, according to advances in molecular diagnostics and surveillance over the past three decades. Concurrently, non-tuberculous mycobacteria (NTM) infections are increasingly being reported, which makes diagnostic and treatment choices in feline practice even more difficult. In rural and peri-urban settings, contact with wildlife or livestock, consumption of contaminated prey, inhalation of contaminated aerosols, or traumatic inoculation of wounds are the most common ways that the disease is spread. Concurrent diseases, pathogen virulence, and host immunological state all affect how rapidly and severely a disease worsens. Clinical signs and symptoms vary greatly, from respiratory illness and widespread multi-organ involvement to localized skin lesions and lymphadenopathy. Despite not being key reservoirs for tuberculosis, cats are relevant in a One Health framework due to their close interaction with humans and susceptibility to infection. The length of therapy, possible zoonotic hazards, regulatory limitations, and the scarcity of licensed anti-mycobacterial medications for companion animals make treatment difficult. The etiology, pathophysiology, epidemiology, clinical features, diagnostic techniques, treatment choices, and preventive measures of feline tuberculosis and non-tuberculous are all covered in this study, which offers an updated synthesis of global and regional data.

Keywords: *Feline tuberculosis, Mycobacterium bovis, Mycobacterium microti, Mycobacterium tuberculosis complex, Non-tuberculous mycobacteria.*

ÖZ

Kedi Tüberkülozu ve Non-Tüberküloz Mikobakteriyozlar: Güncel Bir Veteriner Hekimlik Perspektifi

Evcil kedilerde uzun yıllar nadir görülen bir hastalık olarak kabul edilen tüberküloz, günümüzde hem veteriner hekimlik hem de halk sağlığı açısından önem kazanan, ortaya çıkan bir enfeksiyon hastalığı olarak değerlendirilmektedir. Son otuz yılda moleküler tanı yöntemleri ve epidemiyolojik sürveyans alanındaki gelişmeler, kedilerin başta Mycobacterium bovis ve Mycobacterium microti olmak üzere Mycobacterium tuberculosis kompleksine (MTBC) ait çeşitli türlere duyarlı olduğunu ve hastalığın farklı klinik ve epidemiyolojik özellikler gösterebildiğini ortaya koymuştur. Bununla birlikte, non-tüberküloz mikobakteri (NTM) enfeksiyonlarının bildiriminde de belirgin bir artış gözlenmekte olup, bu durum kedi pratiğinde tanı ve tedavi yaklaşımlarını daha karmaşık hale getirmektedir. Hastalığın bulaşmasında özellikle kırsal ve yarı kentsel bölgelerde yaban hayatı veya çiftlik hayvanlarıyla temas, kontamine avların tüketilmesi, enfekte aerosollerin inhalasyonu ve travmatik yaralar yoluyla inokülasyon önemli rol oynamaktadır. Hastalığın seyri ve şiddeti; etkenin virülansı, eşlik eden hastalıklar ve konağın immün durumu gibi faktörlere bağlı olarak değişkenlik göstermektedir. Klinik bulgular solunum sistemi tutulumundan yaygın multiorgan enfeksiyonlarına, lokalize deri lezyonlarından lenfadenopatiye kadar geniş bir yelpazede ortaya çıkabilmektedir. Kediler tüberküloz için primer rezervuarlar arasında yer almamakla birlikte, insanlarla yakın temasları ve enfeksiyona duyarlılıkları nedeniyle Tek Sağlık yaklaşımı kapsamında önemli kabul edilmektedir. Uzun tedavi süreleri, potansiyel zoonotik riskler, yasal düzenlemeler ve evcil hayvanlar için ruhsatlı antimikobakteriyel ilaçların sınırlı olması tedaviyi güçleştiren başlıca etmenlerdir. Bu derleme, kedi tüberkülozu ve non-tüberküloz mikobakteriyozların etiyolojisi, patogenezi, epidemiyolojisi, klinik özellikleri, tanı yöntemleri, tedavi yaklaşımları ve korunma stratejilerini güncel literatür ışığında kapsamlı olarak ele almayı amaçlamaktadır.

Anahtar Kelimeler: *Kedi tüberkülozu, Mycobacterium bovis, Mycobacterium microti, Mycobacterium tuberculosis kompleksi, Non-tüberküloz mikobakteriler.*

✉ *Corresponding author: mudassarjanjua4321@gmail.com

INTRODUCTION

The chronic, granulomatous diseases known as tuberculosis (TB), which affects a range of animals worldwide, are caused by members of the *Mycobacterium tuberculosis* complex (MTBC) and other non-tuberculous mycobacteria (NTM) (Dutra et al. 2025; Commandeur et al. 2025). Domestic cats (Felis catus) used to have a low incidence of TB, but more confirmed cases have been documented due to increased clinical awareness and broader use of accurate diagnostics (Commandeur et al. 2025). In the past, most cases of tuberculosis in cats were diagnosed after death. (Clifton-Hadley et al. 1993). The low number of reported cases may be the consequence of underreporting rather than true rarity, according to systematic retrospective research and the development of genetic testing tools (O'Halloran and Gunn-Moore 2017). Geographical differences in prevalence are a reflection of differences in animal reservoirs, wildlife TB control, and human TB prevalence. The disease can spread through ingestion of contaminated prey, inhalation of aerosolized bacilli, percutaneous inoculation (such as bites or scratches), or environmental exposure (Commandeur et al. 2025). Histopathology typically shows granulomatous inflammation with localized caseous necrosis and acid-fast bacilli on Ziehl-Neelsen, and the disease typically manifests as cutaneous (Lalor et al. 2012), respiratory (Sykes 2025), alimentary, lymphatic, or widespread symptoms (Commandeur et al. 2025).

Mycobacterial infections caused by *Mycobacterium avium* and *Mycobacterium tuberculosis* in companion animals are underreported. A Brazilian case series highlighted diagnostic challenges, severe clinical outcomes, and One Health implications, emphasizing the epidemiological role of cats and dogs and the need for enhanced surveillance, particularly in rural regions (Dutra et al. 2025). Evidence-based approaches promote ongoing cooperation between the human and animal health sectors despite the low incidence of cat-to-human transmission (O'Halloran et al. 2019). This review, which is based on thirty years of published research, looks at the origins, epidemiology, pathogenesis, clinical and pathological characteristics, diagnostic methods, treatment options, and prevention initiatives of feline tuberculosis.

ETIOLOGY

The genus Mycobacterium contains rod-shaped, aerobic, acid-fast bacteria that have a remarkable ability to live inside cells, particularly in macrophages. While early taxonomic systems mostly relied on colony appearance and development rate in culture, molecular genetic approaches have revolutionized classification. In addition to laboratory factors, these advancements have enabled scientists to distinguish between species based on their evolutionary relationship and potential for disease (Brites and Gagneux 2017). As summarized in Table 1, the genus Mycobacterium comprises two principal groups: the MTBC and the heterogeneous group of NTM.

Mycobacterium tuberculosis-Complex

The closely interconnected pathogenic species that make up the MTBC have approximately 99% genetic similarity, despite differences in host preferences and geographic distribution. This group includes *M. tuberculosis, M. bovis, M. africanum, M. microti, M. caprae, M. canettii, M. pinnipedii, M. orygis, M. mungi,* and *M. suricattae* (O'Halloran and Gunn-Moore 2017). *M. tuberculosis* is the primary agent in human medical care, whereas *M. bovis* and *M. microti* are most commonly seen in feline illnesses. There have only been a few isolated occurrences of *M. tuberculosis* in cats, typically following intimate contact with an infected individual, indicating that cats are not especially vulnerable to contracting the disease (O'Halloran and Gunn-Moore 2017). However, *M. bovis* has the largest host range of any MTBC (Commandeur et al. 2025).

Although *M. bovis* and *M. microti* tend to cause feline tuberculosis in many places, its occurrence in companion animals has declined in societies where milk pasteurization is popular. There are multiple ways of transmission. Cats may eat infected prey while hunting small mammals outside, particularly rodents carrying *M. microti* or *M. bovis*. Less common methods include inoculation by scratches, bite wounds, or contaminated surgical sites. Once established, an infection can spread through the circulation and result in respiratory or systemic illness. Additionally, there have been signs of environmental pollution and possible invasive (in-clinic) transmission (Commandeur et al. 2025). The regional spread of feline tuberculosis usually reflects the geographic locations of wildlife reservoirs. Europe, North America, Japan, Australia, and New Zealand have all reported cases of *M. bovis* infections. *M. microti* is most commonly seen in the United Kingdom, especially in regions where rodent reservoirs have been identified (O'Halloran et al. 2019), while examples have also been reported in Switzerland. The majority of infected cats are adults, with an average age of 3 years for *M. bovis* and 8 years for *M. microti*, according to UK data (O'Halloran et al. 2019). Even while the majority of infected cats test negative for feline leukemia virus (FeLV) and feline immunodeficiency virus (FIV), many have reduced serum vitamin D concentrations, which may affect macrophage function and alter susceptibility to disease (Lalor et al. 2012).

Non-Tuberculous Mycobacteria

NTM contain a broad range of environmental microbes with different growth rates and pathogenic potential. Slow-growing organisms include *Mycobacterium avium* complex (MAC), *Mycobacterium genavense, Mycobacterium kansasii,* and *Mycobacterium malmoense*; fast-growing organisms include the *M. fortuitum* group, *Mycobacterium chelonae,* and *Mycobacterium abscessus* (Pekkarinen et al. 2018). Other species observed in cat include *M. goodii, M. mucogenicum, M. septicum, M. ulcerans, M. szulgai, M. peregrinum, M. simiae, M. thermoresistibile, M. flavescens, M. xenopi, M. alvei, M. smegmatis, M. phlei, M. massiliense,* and members of the *M. terrae* complex (O'Halloran and Gunn-Moore 2017). Among them, MAC organisms particularly *M. avium* are recognized to be the most clinically significant in animals, causing avian tuberculosis. In contrast to other members of the Mycobacterium avium complex (MAC) that are frequently linked to feline mycobacteriosis, Mycobacterium avium subsp. paratuberculosis (MAP) is primarily identified as the causative agent of paratuberculosis (Johne's disease) in ruminants. There are still few and inconsistent reports of clinical illness linked to MAP in cats (Palmer et al. 2005; Pekkarinen et al. 2018).

Cat infections caused by other NTM species are usually more opportunistic, non-specific, or sporadic. The most frequent mechanisms that environmental exposure through soil, water, or organic waste causes transmission are infection following traumatic inoculation, wound contamination, or mucosal colonization (O'Brien et al.

2017a). NTMs can manifest clinically in a variety of ways. Many function as opportunistic cutaneous pathogens or produce localized wound infections. "Feline leprosy syndrome" (FLS) is a characteristic feline manifestation that usually results in alopecic or ulcerated, painless, and freely mobile nodules on the head and limbs, however any part of the body might be afflicted (O'Brien et al. 2017a; O'Brien et al. 2017b; O'Halloran and Gunn-Moore 2017). Numerous clinical manifestations of NTMs are possible. Many cause localized wound infections or act as opportunistic cutaneous pathogens. A common sign of feline leprosy is "feline leprosy syndrome" (FLS), which typically appears as alopecic or ulcerated, painless, and freely moving nodules on the head and limbs, however it can affect any part of the body (O'Halloran and Gunn-Moore 2017). Histopathological examination of these nodules often reveals granulomatous panniculitis, sometimes involving local lymph nodes and draining tracts (Commandeur et al. 2025). Systemic NTM infections are most commonly caused by MAC pathogens, while they are uncommon in cats (Pekkarinen et al. 2018). Disseminated instances are typically associated with severe immunosuppression, such as FIV infection, chronic renal illness, myelodysplasia, or reduced interferon-gamma production. The documented cases are disproportionately African, and older cats appear to be more vulnerable (O'Brien et al. 2017c). Clinical signs of systemic sickness include lethargy, lymphadenopathy, pyrexia, anorexia, and involvement of multiple organ systems (Pekkarinen et al. 2018).

The pathogenesis and clinical spectrum vary according to the infecting species. *M. avium* is believed to be more dangerous than the majority of NTMs. In addition to cutaneous signs, it can result in granulomatous panniculitis, disseminated disease, and subcutaneous nodules. However, *M. fortuitum* has been linked to a greater range of symptoms, including cutaneous disease, pneumonia, systemic lymphadenopathy, gastrointestinal symptoms, vestibular dysfunction, brain infection, and extensive involvement (Pekkarinen et al. 2018). An overview of MTBC and NTM species reported in feline tuberculosis, including associated clinical manifestations and diagnostic approaches, is presented in Table 1.

HISTOPATHOLOGICAL CHANGES

Pathogenesis and Clinical Signs

Numerous factors can lead to cat infections, and the early stages of an illness usually dictate how it will develop. According to Clifton-Hadley et al. (1993), a hunting cat consumes an infected rodent may have gastrointestinal tract lesions, and a cat that is in close proximity to contaminated aerosols may develop bacilli in its lungs. Less frequently, the organism penetrates through skin injuries; battle wounds and unintentional mishaps are common instances. Before any systemic transmission takes place, this results in a localized skin target. After entering macrophages, the infection weakens the host's resistance to death, enabling it to spread covertly for weeks or months (Brites and Gagneux 2017). After that, the infection may either remain localized or spread to the lymphatic and blood systems. Propagation can cause lesions in the kidneys, lungs, liver, spleen, and other organs (O'Brien et al. 2017a).

The immune capacity of each cat and the traits of the bacteria determine how the pattern manifests clinically (Lalor et al. 2012; O'Halloran and Gunn-Moore 2017). Skin disease diagnosis is a typical initial step. Veterinarians frequently observe solid nodules, poorly healing wounds, or draining tracts particularly on the head, distal limbs, or tail base. A primary inhalational infection or, more frequently, blood might be the source of respiratory symptoms. O'Halloran et al. (2019), thoracic radiography in affected cats may occasionally simply reveal enlargement of the mediastinal lymph nodes, but other times it may reveal extensive or interstitial changes. According to a review of clinical cases, about 70% of the afflicted cats had respiratory abnormalities ranging from mildly elevated breathing rate to severe, forced respiration (O'Halloran et al. 2019). The alimentary variant, albeit less common, has a major impact on the condition; afflicted cats may experience diarrhea and vomiting, lose weight, or develop anemia.

Palpable abdominal masses and mesenteric lymphadenopathy frequently coexist with systemic lymph node enlargement (Dagar et al. 2024; Barandiaran 2025). Weight loss, organomegaly, and a prolonged fever possibly accompanied by fluid in the thoracic or pericardial cavities are indicators of systemic disease (Pekkarinen et al. 2018). Although not common, granulomatous lesions of the choroid, retina, sclera, and conjunctiva have been discovered in some nations, such as Australia, indicating ocular involvement (O'Halloran et al. 2019). Mycobacterial arthritis is much less common but nevertheless significant; in many cases, it has resulted in limb amputation. These patients' histological examinations revealed synovitis and panniculitis with acid-fast organisms (Lalor et al. 2012). Under a microscope, feline tuberculosis is characterized by granulomatous inflammation with central necrosis, surrounded by epithelioid macrophages, lymphocytes, plasma cells, and multinucleated giant cells. With Ziehl-Neelsen staining, acid-fast bacilli are visible in macrophages and, in more advanced lesions, freely in the surrounding tissue. Periportal fibrosis, bile duct proliferation, and lymphohistiocytic infiltration may be present in hepatic disease (Haligur et al 2007; Eroksuz et al. 2019).

DIAGNOSIS

Since clinical symptoms often overlap between species, it is critical to accurately diagnose feline mycobacterial infections at the species level. However, zoonotic repercussions and treatment strategies may differ dramatically (Commandeur et al. 2025). A reasonable first step is to perform histopathological investigation on samples taken from lesions that are problematic, such as swollen peripheral lymph nodes, abscesses that only partially respond to treatments, or persistent, non-healing ulcers. Both incisional and excisional methods are used, depending on the lesion's location and size (O'Halloran and Gunn-Moore 2017; Stavinohova et al. 2019). For solitary masses, cytology may provide a rapid and minimally intrusive assessment, particularly if neoplasia is on the differential list. Both histology and cytology can reveal granulomatous inflammation that is suggestive of mycobacteriosis, but neither method can pinpoint the exact mycobacterial species that is active (O'Halloran and Gunn-Moore 2017; Lalor et al. 2012).

Table 1: Mycobacterium tuberculosis complex (MTBC) and nontuberculous mycobacteria (NTM) species reported in feline tuberculosis, associated clinical signs and diagnostic methods.

Group	Species/ subgroup	Reported clinical signs in cats / zoonotic relevance	Diagnostic methods used	References
MTBC	*Mycobacterium bovis*	Chronic weight loss, respiratory distress, lymphadenopathy, nasal discharge, nodular and ulcerative skin lesions	Acid-fast staining (Ziehl–Neelsen), histopathology, culture, PCR assays, interferon-gamma release assays	O'Halloran et al. 2019
MTBC	*Mycobacterium microti*	Mild respiratory signs, head and neck subcutaneous swellings, cutaneous ulceration	Histopathology, culture, PCR, spoligotyping	O'Halloran et al. 2019
MTBC	*Mycobacterium tuberculosis*	Chronic cough, weight loss, lethargy, ocular involvement	Histopathology, culture, PCR (RD9 region), thoracic radiography	O'Halloran et al. 2019
MLC	*Candidatus Mycobacterium lepraefelis*	Nodular cutaneous lesions progressing to ulceration	Histopathology, acid-fast staining, PCR (16S rRNA), gene sequencing	O'Brien et al. 2017a
MLC	*Candidatus Mycobacterium tarwinense*	Localized cutaneous nodules	Histopathology, PCR, sequencing	O'Brien et al. 2017b
MAC	*Mycobacterium avium* complex	Fever, diarrhea, hepatosplenomegaly, weight loss, generalized lymphadenopathy	Histopathology, culture, PCR, mycobacterial serology (AGID)	Han and Gunn-Moore 2023
Slow-growing NTM (Photochromogens)	*Mycobacterium marinum*	Cutaneous lesions, nodules and ulcers in cats; sporotrichoid cutaneous infection in humans following cat bite/scratch and aquarium exposure	Culture at 30 °C, PCR, histopathology, skin biopsy	Malik et al. 2002; Duval et al. 2009
Slow-growing NTM (Scotochromogens)	*Mycobacterium kansasii*	Cutaneous lesions, subcutaneous masses, osteolytic lesions, pulmonary pathology; rare systemic disease	Histopathology, culture, PCR (FNA and biopsy), interferon-gamma release assay	Malik et al. 2002; Černá et al. 2020
Rapid-growing NTM	*Mycobacterium fortuitum*	Draining tracts, non-healing wounds, localized cutaneous abscesses	Rapid culture, PCR, histopathology	Malik et al. 2002
Rapid-growing NTM (zoonotic transmission)	*Mycobacterium chelonae*	Cats implicated as source via scratches; persistent granulomatous cutaneous lesions in humans	Histopathology, acid-fast staining, tissue culture, PCR	Shah et al. 2023
Novel/unclassified slow-growing NTM	**Mycobacterium visibilis (proposed)**	Chronic nodular and ulcerative cutaneous lesions; abundant filamentous bacteria visible on H and E; granulomatous dermatitis	Histopathology (H and E), PCR amplification of Mycobacterium-specific DNA, 16S rRNA gene cloning and sequencing, phylogenetic (parsimony) analysis	Appleyard and Clark 2002

Culture is still the gold standard for confirmation since it offers definitive identification and susceptibility testing. However, it can take weeks or even months to get results, and it is more expensive than many molecular procedures. The Animal and Plant Health Agency (APHA) in the UK offers free culture for feline submissions when suspected *M. bovis* exposure may have occurred in sensitive animals. To facilitate national *M. bovis* surveillance programs, all animal samples in Scotland and Wales are routinely free-cultured (Barandiaran 2025). When instant results are required, interferon-gamma release assays (IGRAs) can be useful. There have been reports of nearly all infections caused by the MTBC and about half of *M. avium* cases (Han and Gunn-Moore 2023). The polymerase chain reaction (PCR) is another helpful technique that can be used on a variety of materials, including fresh tissue, formalin-fixed paraffin-embedded tissues, and unstained cytology slides (Table 2). PCR can enable species-level identification in addition to expediting diagnosis, which is crucial for assessing zoonotic risk and tailoring treatment plans (Lalor et al. 2012; O'Halloran and Gunn-Moore 2017).

TREATMENT

Treatment for feline TB is difficult because to its chronic nature, zoonotic danger, and various drug resistance patterns. Unlike human tuberculosis, recognized methods for cats are still evolving, therefore veterinarians must adjust their treatments based on the type of mycobacteria and the severity of the infection (O'Halloran and Gunn-Moore 2019). The cornerstone of treatment to stop recurrence is long-term multidrug combinations (6-12 months). Clarithromycin (5-10 mg/kg twice a day) is chosen over previous macrolides due to its superior tissue penetration and reduced gastrointestinal side effects (O'Halloran and Gunn-Moore 2019). It results in less gastrointestinal ailments. Although rifampicin (10-15 mg/kg once daily) is effective against *Mycobacterium bovis*, hepatotoxicity risks necessitate frequent monitoring of liver enzymes. One of its side effects is hepatotoxicity, which affects over 20% of cats (Mitchell et al. 2023). Renal function must be assessed before using fluoroquinolones, including Pradofloxacin, as an additional treatment for resistant bacteria (Table 3).

Table 2: Diagnostic approaches for feline mycobacterial infections.

Diagnostic method	Sample type	Purpose / usefulness	Advantages	Limitations	References
Histopathology (biopsy)	Incisional or excisional tissue biopsies from lesions or lymph nodes	Initial diagnostic screening; detection of granulomatous inflammation	Widely available; useful for chronic non-healing lesions	Cannot identify species; requires invasive sampling	Stavinohova et al. 2019; O'Halloran and Gunn-Moore 2017
Cytology (FNA, impression smears)	Fine-needle aspirates, lesion smears	Rapid, minimally invasive evaluation; rule out neoplasia	Quick, inexpensive; useful for solitary masses	Cannot reliably identify species; low sensitivity	O'Halloran and Gunn-Moore 2017; Lalor et al. 2012
Culture (gold standard)	Fresh tissue, aspirates, exudates	Definitive diagnosis; species identification and antimicrobial susceptibility testing	High specificity; epidemiological value	Slow (weeks–months); costly; requires biosafety facilities	O'Halloran and Gunn-Moore 2017; Barandiaran. 2025
Interferon-gamma release assay (IGRA)	Whole blood	Detection of cell-mediated immune response to MTBC	Rapid results; useful for screening	Lower sensitivity for *M. avium*; not species definitive	Lalor et al. 2012; Han and Gunn-Moore 2023
PCR (molecular detection)	Cytology slides, FFPE tissue, fresh tissue	Species-level identification; zoonotic risk assessment	Fast; highly specific; works on archived samples	Requires molecular facilities; false negatives possible	O'Halloran and Gunn-Moore 2017; Lalor et al. 2012

Table 3: Treatment recommendations for feline mycobacterial infections.

Infection group	Disease pattern	Recommended antimicrobial regimen	Typical duration	Key references
MTBC	Localised or disseminated; pulmonary and/or systemic involvement	Rifampicin + fluoroquinolone (pradofloxacin or moxifloxacin) + macrolide (clarithromycin or azithromycin)	6–9 months; extended triple therapy ≥4 months (≥6 months if pulmonary); continue 2–3 months beyond clinical/radiographic resolution	Gunn-Moore et al. 1996; Major et al. 2018; Albuquerque et al. 2021
NTM: MAC, slow- and rapid-growing species	Localised or disseminated; panniculitis common	Clarithromycin + clofazimine or rifampicin ± doxycycline or pradofloxacin	Continue 1–2 months beyond clinical resolution; up to 12 months for disseminated disease	Jordan et al. 1994; Govendir et al. 2011; Manou et al. 2021; Han and Gunn-Moore 2023
Fastidious NTM	Localised cutaneous or subcutaneous nodules	Surgical excision ± clarithromycin, rifampicin, fluoroquinolone (pradofloxacin or moxifloxacin) and/or clofazimine	3–6 months (shorter courses occasionally effective)	Ghielmetti et al. 2021; O'Brien et al. 2017a; O'Brien et al. 2017b; O'Brien et al. 2017c

Mycobacterium tuberculosis Complex Treatment

Long-term combination antibiotic therapy is necessary to treat feline infections brought on by the MTBC. For six to nine months, double or triple therapy with rifampicin, a macrolide (clarithromycin or azithromycin), and a fluoroquinolone (ideally pradofloxacin or moxifloxacin) is recommended. More recent approaches support prolonged triple therapy for at least four months, or six months in cases of pulmonary involvement, with continuation beyond clinical or radiographic resolution (O'Halloran and Gunn-Moore 2017; Major et al. 2018; Albuquerque et al. 2021). Previous protocols involved an initial two-month phase of triple therapy followed by dual therapy (Gunn-Moore et al. 1996). This approach, which aims to lower antibiotic resistance, is similar to the concepts of human tuberculosis treatment. Pradofloxacin and moxifloxacin are examples of newer fluoroquinolones that seem to work better than earlier medications. While combination therapy should be initiated right away to reduce relapse and resistance, pradofloxacin may be used initially in localized disease pending species confirmation. Regular monitoring is necessary because to the frequent adverse effects, especially hepatic and cutaneous responses. Rifampicin is still essential for successful MTBC treatment, even with the availability of second-line medications like isoniazid and ethambutol (Table 3).

Treatment of Non-Tuberculous Mycobacterial Infections

Treatment for NTM infections in cats is difficult and relies on the kind of infection and severity of the illness. Older fluoroquinolones are frequently unsuccessful for treating widespread *Mycobacterium avium* complex (MAC) infections (Jordan et al. 1994; Manou et al. 2021). Based on documented effective outcomes, clarithromycin is the recommended first-line medication, frequently in combination with clofazimine or rifampicin, and where feasible, doxycycline or pradofloxacin (O'Halloran and Gunn-Moore 2019). Although *M. avium* isolates frequently exhibit resistance to fluoroquinolones and aminoglycosides (Manou et al. 2021), limited clinical experience indicates that pradofloxacin is more effective than older fluoroquinolones, especially against rapidly growing NTM species (Govendir et al. 2011). Since antibiotic sensitivity varies greatly among NTM species

and strains, culture and antimicrobial susceptibility tests should ideally direct treatment (Manou et al. 2021; Han and Gunn-Moore 2023). Dual or triple therapy, using regimens specific to the species in question, is advised when testing is not practical. After clinical remission, therapy should continue for one to two months; for disseminated disease, it may take up to 12 months. In cases of severe panniculitis, surgical resection may be a useful adjuvant.

Treatment of Fastidious Non-Tuberculous Mycobacteria

Localized cutaneous or subcutaneous lesions are usually the result of fastidious NTM linked to feline leprosy-like disorders. There have been reports of spontaneous lesion remission in certain cases, and surgical excision of isolated nodules may be curative (Ghielmetti et al. 2021). Dual or triple antibiotic regimens, typically consisting of clarithromycin, rifampicin, and a fluoroquinolone (pradofloxacin or moxifloxacin) and/or clofazimine, are advised when medical therapy is necessary and are given for three to six months (O'Halloran and Gunn-Moore 2019). Sometimes shorter treatment regimens work; one patient responded to a four-week course of clarithromycin and rifampicin (Ghielmetti et al. 2021). Extensive analyses of feline leprosy-like syndromes show that treatment efficacy varies significantly based on the infecting species, highlighting the significance of species identification wherever feasible. (O'Brien et al. 2017a; O'Brien et al. 2017b; O'Brien et al. 2017c). Overall, prognosis is generally favorable with appropriate surgical and/or antimicrobial management. Treatment recommendations for feline mycobacterial infections are summarized in table 3.

Table 4: Zoonotic considerations and biosafety measures for suspected mycobacterial infections in veterinary practice.

Risk situation	Potential zoonotic exposure	Recommended protective measures (PPE and biosafety)	References
Handling cats with respiratory signs (coughing, dyspnea)	Inhalation of aerosolized mycobacteria	Wear fitted FFP3/N95 facemask; use protective clothing; minimize close facial contact; perform procedures in well-ventilated rooms	Haydock et al. 2022
Handling draining skin lesions or open wounds	Direct contact with infectious organisms through skin breaks	Gloves, protective clothing; cover open wounds on personnel; strict asepsis	Murray et al. 2015
Collecting clinical samples (FNAs, biopsies, BALs)	Aerosolization or cutaneous inoculation	Gloves, gowns, eye protection; FFP3/N95 mask during airway procedures; sedation during lymph node aspiration	Haydock et al. 2022
Needle-stick injuries or skin cuts during sampling	Cutaneous inoculation leading to localized or systemic disease	Avoid needle recapping; use sedation; proper sharps disposal; staff training	Murray et al. 2015
Anaesthesia and intubation of suspected cases	Aerosol exposure during airway manipulation	FFP3/N95 mask; limit personnel; disposable breathing circuits and endotracheal tubes	Haydock et al. 2022
Necropsy of suspected mycobacterial cases	Aerosol generation from tissue cutting (e.g., electric saws)	Perform necropsy in isolation unit; avoid aerosolizing tools; use powered air-purifying respirators (PAPR)	Posthaus et al. 2011
Surgical procedures in suspected TB cases	Exposure to blood and aerosols	Full PPE including filtered airflow helmet respirator (e.g., powered respirator systems)	Haydock et al. 2022
Environmental contamination	Indirect transmission via clothing, hands, equipment	Disinfectants (60–90% alcohol, iodine, halogenated amines); avoid 4% chlorhexidine	Murray et al. 2015
Disposal of contaminated equipment	Ongoing environmental exposure	Double-bagging of clinical waste; dispose breathing systems and tubes	Haydock et al.2022
Post-euthanasia management	Environmental persistence of organisms	Recommend cremation rather than burial	Haydock et al. 2022

Surgical Intervention

Excision of granulomas improves outcomes for localized tuberculosis. When isolated skin lesions can be removed, surgery is recommended; more diffuse lesions may be treated with surgical debridement followed by antibiotic therapy (Mitchell et al. 2023).

Public Health Implications

Every member of the MTBC, including *M. microti*, has the potential to be zoonotic (O'Connor et al. 2019). However, because cats and dogs are overflow hosts, the danger of transmission from them to humans is extremely low (Public Health News and Reports 2014). In Texas, USA, there was a suspicion of cat-to-human transfer (Ramdas et al. 2015). The danger of *M. bovis* spreading from cats to their human contacts increased from insignificant to extremely low in the UK following the documented evidence of cat-to-human transmission (Public Health England 2013). Before treatment is initiated, cats exhibiting clinical signs consistent with disseminated disease are thought to be the most dangerous to humans. This is probably due to ingestion from a contaminated environment, handling discharges from exudative tuberculous lesions, or aerosols from cats exhibiting respiratory signs or aerosol-generating procedures. It is also feasible to inoculate humans through cuts or skin breaks after handling mycobacterial secretions. No transmission to owners was noted in the documented outbreaks of *M. bovis* infection in cats who were probably infected after consuming tainted raw food. However, there is worry about the possibility that owners could become infected if they handle tainted raw food while preparing meals. The primary cause of tuberculosis in humans is *M. tuberculosis*.

According to O'Halloran et al. (2025), dogs are more likely than cats to contract *M. tuberculosis*, and when they do, it is more frequently acquired from sick humans than the other way around. In fact, in one instance of a dog with disseminated *M. tuberculosis* disease (Posthaus et al. 2011), zoonotic *M. tuberculosis* infection was reported in three veterinary pathologists who performed necropsy on the dog, but none of the humans (including the owners) in contact with the dog. Although there have not been any reports of cat-to-human cases, MAC species, especially M. *avium* subsp. *hominissuis*, have the ability to spread from cat to person. An Australian case report (Phan and Relic 2010) describes a local skin illness caused by *Mycobacterium marinum*, an NTM pathogen of fish, in a human who had been scratched by her cat. It is possible that the cat spread *M. marinum* by coming into contact with the water from the house's fish tank and then scratching the human, but there is also a chance that the scratch made the human more susceptible to being inoculated with fish tank water later on while the tank was being cleaned (Phan and Relic 2010). Since *M. kansasii* is a human NTM pathogen, it is also a possible zoonotic agent. According to one report, an isolate from an indoor-only cat in Japan was genetically identical to human isolates (Fukano et al. 2021) (Table 4).

Infection Control in Suspected Feline Mycobacterial Disease

When working with cats in clinical settings, especially in endemic areas, the zoonotic potential of mycobacterial infections must be carefully acknowledged (Murray et al. 2015). Humans can contract the disease by breathing in aerosols from cats exhibiting respiratory symptoms or by coming into touch with organisms in draining lesions through open skin wounds (Murray et al. 2015). Appropriate personal protective equipment (PPE) is therefore crucial. When treating cats with draining skin lesions, staff members should cover any open wounds and wear gloves and protective clothes to prevent the disease from spreading to other animals and workers (Posthaus et al. 2011).

PPE is also necessary for gathering or handling clinical samples, such as bronchoalveolar lavage (BAL) specimens and fine-needle aspirates (FNAs). When in close proximity to cats displaying respiratory symptoms, especially during operations like intubation, FNAs, or BAL collection, a fitting FFP3 (N95-equivalent) face mask should be worn. Because NTM infection can result from unintentional skin penetration, veterinarians must avoid needlestick injuries and cutaneous inoculation. To lower danger, sedation is advised when aspirating lymph nodes from cats with unexplained lymphadenopathy (Murray et al. 2015).

Aerosol formation must be avoided during necropsy; pathologists exposed to aerosols produced during post-mortem procedures utilizing electric saws have been documented to contract zoonotic *Mycobacterium tuberculosis* (Posthaus et al. 2011). Strict asepsis is essential since nosocomial transmission, including *M. bovis* infection linked to contaminated staff hands and clothing, has been reported in veterinary clinics (Murray et al. 2015). Halogenated tertiary amines, 60–90% alcohols, and 3% iodine solutions are effective. Investigations should be conducted in well-ventilated rooms, and breathing circuits and endotracheal tubes used for suspected cases should be disposed of as clinical waste. Powered respirators are advised if surgery is necessary. According to Haydock et al. (2022), necropsies should be carried out in special isolation facilities with improved PPE and personnel logging. To avoid contaminating the environment after euthanasia, cremation is preferred over burial.

CONFLICTS OF INTEREST

The authors report no conflicts of interest.

AUTHOR CONTRIBUTIONS

Idea/Concept: MFB
Supervision/Consultancy: MFB
Data Collecting and/or Processing: MZ
Analysis and/or Interpretation: MFB, EK, MZ
Writing the Article: MFB, EK, MZ
Critical Review: MFB, EK, MZ

REFERENCES

Albuquerque CS, Černá P, Gunn-Moore DA (2021). Repeated bouts of pulmonary tuberculosis in a hunting cat: reinfection or recrudescence? *JFMS Open Rep,* 7(1), 2055116921990292.

Appleyard GD, Clark EG (2002). Histologic and genotypic characterization of a novel *Mycobacterium* species found in three cats. *J Clin Microbiol,* 40(7), 2425-2430.

Barandiaran S, Marfil MJ, Yaafar N et al. (2025). *Mycobacterium bovis* infection in cats: Zoonotic transmission. *Zoonoses Public Health,* 72(7), 683-689.

Brites D, Gagneux S (2017). The nature and evolution of genomic diversity in the *Mycobacterium tuberculosis* complex. *Adv Exp Med Biol,* 1019,1-26.

Černá P, Mitchell JL, Lodzinska J et al. (2020). Systemic *Mycobacterium kansasii* infection in two related cats. *Pathogens,* 9(11), 959.

Clifton-Hadley RS, Wilesmith JW, Stuart FA (1993). *Mycobacterium bovis* in the European badger (*Meles meles*): Epidemiological findings in tuberculous badgers from a naturally infected population. *Epidemiol Infect,* 111(1), 9-19.

Commandeur S, Vander M, Koomen J et al. (2025). *Mycobacterium bovis* infected domestic cats in an officially bovine tuberculosis free country resulting in human infection. *One Health,* 20, 101048.

Dagar O, Ateş MB, Ortatatlı M, Öztürk FM (2024). Congenital feline tuberculosis: The first case report. *Vet Res Forum,* 15(4), 203-205.

Dutra BCM, Trindade-Gerardi AB, Da-Cruz-Schaefer G et al. (2025). Mycobacterial infections in cats and a dog: A case series from Southern Brazil and one health implications. *Vet Res Commun,* 49, 336.

Duval A, Adehossi E, Parola P (2009). *Mycobacterium marinum* infection. *BMJ Case Rep*, bcr12. 2008. 1311.

Eroksuz Y, Baydar E, Otlu B et al. (2019). Case report: Systemic tuberculosis caused by *Mycobacterium bovis* in a cat. *BMC Vet Res,* 15(1), 9.

Fukano H, Terazono T, Hirabayashi A et al. (2021). Human pathogenic *Mycobacterium kansasii* (former subtype I) with zoonotic potential isolated from a diseased indoor pet cat, Japan. *Emerg Microbes Infect,* 10(1), 220-222.

Ghielmetti G, Schmitt S, Friedel U, Guscetti F, Walser-Reinhardt L (2021). Unusual presentation of feline leprosy caused by *Mycobacterium lepraemurium* in the Alpine region. *Pathogens,* 10(6), 687.

Govendir M, Norris JM, Hansen T et al. (2011). Susceptibility of rapidly growing mycobacteria and *Nocardia* isolates from cats and dogs to pradofloxacin. *Vet Microbiol,* 153(3-4), 240-245.

Gunn-Moore DA, Jenkins PA, Lucke VM (1996). Feline tuberculosis: a literature review and discussion of 19 cases caused by an unusual mycobacterial variant. *Vet Rec,* 138(3), 53-58.

Haligür M, Vural S, Şahal M et al. (2007). Generalised tuberculosis in a cat. *Bull Vet Inst Pulawy*, 51(4), 531-534.

Han HS, Gunn-Moore D (2023). First report of *Mycobacterium avium* complex (*Mycobacterium intracellulare*) in a cat from Southeast Asia. *JFMS Open Rep,* 9(2), 20551169231194311.

Haydock LAJ, Abrams-Ogg ACG, Weese JS et al. (2022). Diagnostic and public health investigation of *Mycobacterium tuberculosis* infection in a dog in Ontario, Canada. *J Vet Diagn Invest,* 34(2), 292-297.

Public Health England (2013). Qualitative assessment of the risk that cats infected with Mycobacterium bovis present to human health. UK Government report.

Jordan HL, Cohn LA, Armstrong PJ (1994). Disseminated *Mycobacterium avium* complex infection in three Siamese cats. *J Am Vet Med Assoc* 204(1), 90-93.

Lalor SM, Mellanby RJ, Friend EJ et al. (2012). Domesticated cats with active mycobacterial infections have low serum vitamin D (25(OH)D) concentrations. *Transbound Emerg Dis,* 59(3), 279-281.

Major A, O'Halloran C, Holmes A et al. (2018). Use of computed tomography imaging during long-term follow-up of nine feline tuberculosis cases. *J Feline Med Surg,* 20(2), 189-199.

Malik R, Hughes MS, James G et al. (2002). Feline leprosy: two different clinical syndromes. *J Feline Med Surg,* 4(1), 43-59.

Manou M, Milgram J, Kelly P et al. (2021). *Mycobacterium bovis* BCG Danish strain 1331 isolated from a periarticular lesion in a domestic cat. *J Small Anim Pract,* 62(10), 924-928.

Mitchell JL, Wilson C, Alexander JE et al. (2023). Development of an enzyme-linked immunosorbent assay for the diagnosis of feline tuberculosis. *Vet Immunol Immunopathol,* 255, 110538.

Murray A, Dineen A, Kelly P et al. (2015). Nosocomial spread of *Mycobacterium bovis* in domestic cats. *J Feline Med Surg,* 17(2), 173-180.

O'Brien CR, Malik R, Globan M et al. (2017a). Feline leprosy due to *Mycobacterium lepraemurium*. *J Feline Med Surg,* 19(7), 737-746.

O'Brien CR, Malik R, Globan M et al. (2017b). Feline leprosy due to Candidatus '*Mycobacterium tarwinense*': Further clinical and molecular characterisation of 15 previously reported cases and an additional 27 cases. *J Feline Med Surg,* 19(5), 498-512.

O'Brien CR, Malik R, Globan M et al. (2017c). Feline leprosy due to Candidatus '*Mycobacterium lepraefelis*': Further clinical and molecular characterisation of eight previously reported cases and an additional 30 cases. *J Feline Med Surg,* 19(9), 919-932.

O'Connor CM, Abid M, Walsh AL et al. (2019). Cat-to-human transmission of *Mycobacterium bovis*, United Kingdom. *Emerg Infect Dis,* 25(12), 2284-2286.

O'Halloran C, Burr P, Gunn-Moore DA, Hope JC (2025). Comparative performance of ante-mortem diagnostic assays for identification of *Mycobacterium bovis*-infected domestic dogs (*Canis lupus familiaris*). *Pathogens,* 14(1), 28.

O'Halloran C, Gunn-Moore DA (2017). Mycobacteria in cats: An update. *In Pract,* 39(9), 399-406.

O'Halloran C, Ioannidi O, Reed N et al. (2019). Tuberculosis due to *Mycobacterium bovis* in pet cats associated with feeding a commercial raw food diet. *J Feline Med Surg,* 21(8), 667-681.

Palmer MV, Stoffregen WC, Carpenter JG, Stabel JR. (2005). Isolation of *Mycobacterium avium* subsp paratuberculosis (Map) from feral cats on a dairy farm with Map-infected cattle. *J Wildl Dis,* 41(3), 629-635.

Pekkarinen H, Airas N, Savolainen LE et al. (2018). Non-tuberculous *Mycobacteria* can cause disseminated mycobacteriosis in cats. *J Comp Pathol,* 160, 1-9.

Phan TA, Relic J (2010). Sporotrichoid *Mycobacterium marinum* infection of the face following a cat scratch. *Australas J Dermatol,* 51(1), 45-48.

Posthaus H, Bodmer T, Alves L et al. (2011). Accidental infection of veterinary personnel with *Mycobacterium tuberculosis* at necropsy: a case study. *Vet Microbiol,* 149(3–4), 374-380.

Public Health News and Reports (2014). Cat-to-human transmission of bovine TB: risk to public 'very low'. *Vet Rec,* 174(14), 337.

Ramdas KE, Lyashchenko KP, Greenwald R et al. (2015). *Mycobacterium bovis* infection in humans and cats in same household, Texas, USA, 2012. *Emerg Infect Dis,* 21(3), 480-483.

Shah R, Shah S, Lyon PR et al. (2023). Nontuberculous mycobacterial infection following cat scratch in the setting of topical steroid use. *Cureus,* 15(5), e38901.

Stavinohova R, O'Halloran C, Newton JR et al. (2019). Feline ocular mycobacteriosis: Clinical presentation, histopathological features, and outcome. *Vet Pathol,* 56(5), 749-760.

Sykes JE (2025). Cutaneous mycobacterioses of cats and dogs. *Vet Clin Small Anim Pract,* 55(2), 237-249.

Van Veterinary Journal

https://dergipark.org.tr/tr/pub/vanvetj

ISSN: 2149-3359 **Corrigendum (Yazar Düzeltmesi)** e-ISSN: 2149-8644

Histopathological and Immunohistochemical Investigation on Effects of Boric Acid Used in Treatment of Rats with Knee Osteoartritis on Kidney Tissues (2024). Van Vet J, 35 (3), 145-151.

Kübra Asena TERİM KAPAKİN[1] İsmail BOLAT[1,*] Esra MANAVOĞLU KİRMAN[1]
Gülşah GÜNDOĞDU[2] Köksal GÜNDOĞDU[3] Fatma DEMİRKAYA MİLOĞLU[4]
Şeymanur YILMAZ TAŞÇI[4]

[1] *Atatürk University, Faculty of Veterinary Medicine, Department of Pathology, Erzurum, Türkiye*
[2] *Pamukkale University, Faculty of Medicine, Department of Physiology, Denizli, Türkiye*
[3] *Denizli State Hospital Orthopedics and Traumatology, Denizli, Türkiye*
[4] *University of Health Sciences, Hamidiye International School of Medicine, Department of Physiology, İstanbul, Türkiye*

Corrigendum:

The article titled "***Histopathological and Immunohistochemical Investigation on Effects of Boric Acid Used in Treatment of Rats with Knee Osteoartritis on Kidney Tissues***" published on pages 145-151 of 2024-year, Volume 35, Issue 3 of the Van Veterinary Journal, the institutional affiliation of the author Şeymanur Yılmaz Taşcı was inadvertently reported incorrectly by the authors. The author has corrected this error with the corrigendum text provided below.

Orijinal Makale URL: https://dergipark.org.tr/en/download/article-file/3901321
Orijinal Makale DOI: https://doi.org/10.36483/vanvetj.1477410

Diz Osteoartritli Sıçanların Tedavisinde Kullanılan Borik Asitin Böbrek Dokuları Üzerindeki Etkilerinin Histopatolojik ve İmmünohistokimyasal Olarak Araştırılması (2024). Van Vet J, 35 (3), 145-151.

Düzeltme:

Van Veterinary Journal dergisinin 2024 yılı 35. cilt 3. sayısının 145-151. sayfalarında yayımlanan "***Diz Osteoartritli Sıçanların Tedavisinde Kullanılan Borik Asitin Böbrek Dokuları Üzerindeki Etkilerinin Histopatolojik ve İmmünohistokimyasal Olarak Araştırılması***" başlıklı makalede Şeymanur Yılmaz Taşcı adlı yazarın kurum bilgisi, yazar tarafından sehven hatalı bildirilmiştir. Bu hata, yazar tarafından aşağıda verilen düzeltme metni ile düzeltilmiştir.

Original Article URL: https://dergipark.org.tr/en/download/article-file/3901321
Original Article DOI: https://doi.org/10.36483/vanvetj.1477410

CORRIGENDUM TEXT

Corrected Affiliation:

Şeymanur Yılmaz Taşcı, University of Health Sciences, Hamidiye International School of Medicine, Department of Physiology, Istanbul, Türkiye.

✉ *Corresponding author: ismail.bolat@atauni.edu.tr